final report

DEPLOYABLE ANTENNA PHASE A STUDY

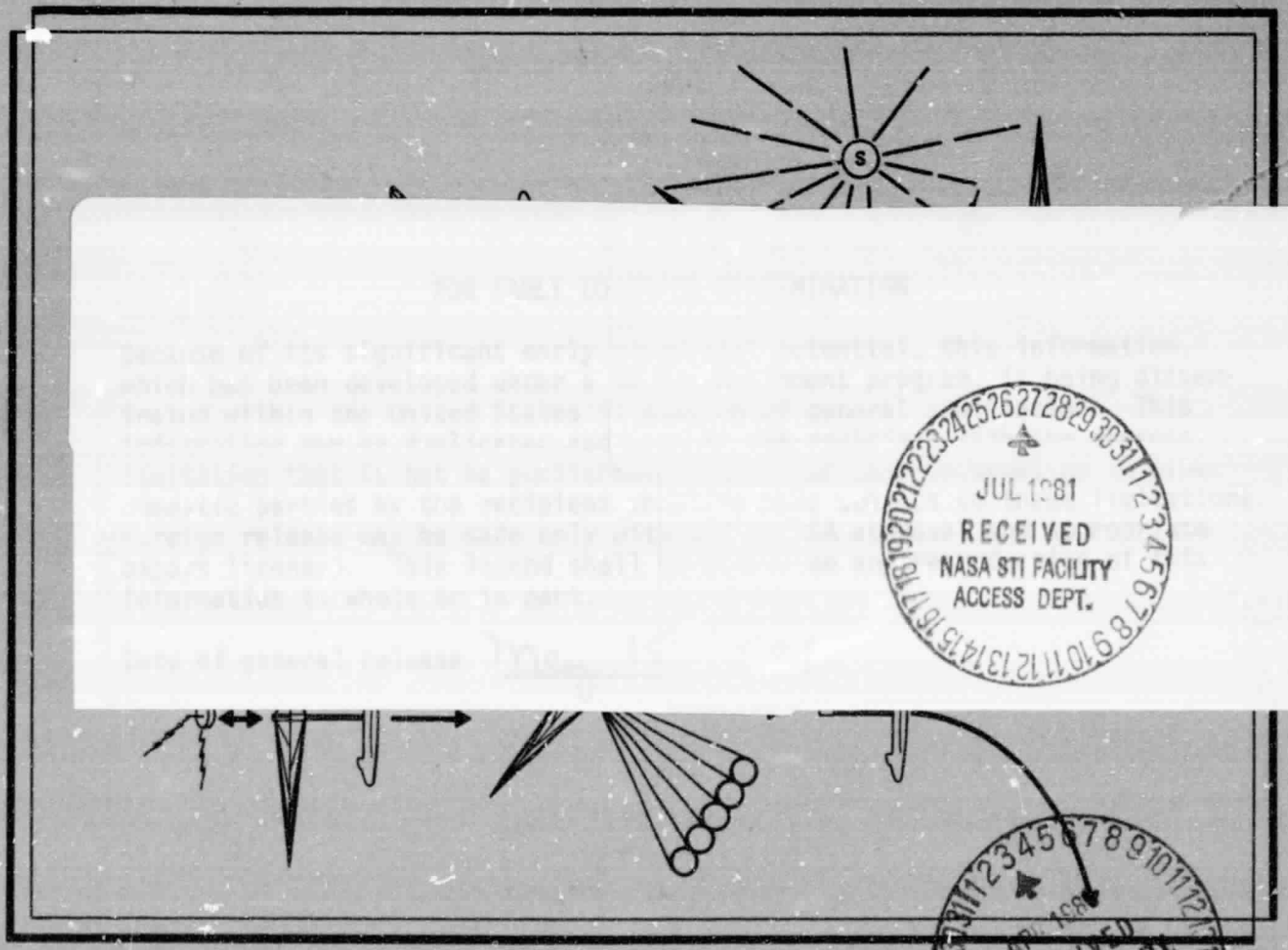

GRUMMAN AEROSPACE CORPORATION

final report

DEPLOYABLE ANTENNA PHASE A STUDY

prepared for

National Aeronautics and Space Administration

NAS8-32394

Authors: J. Schultz, J. Bernstein,
G. Fischer, G. Jacobson, I. Kadar,
R. Marshall, G. Pflugel, J. Valentine

prepared by

Grumman Aerospace Corp.
Bethpage, N.Y. 11714

MSFC Contracting Officer's Representative

PS/04 Wilbur E. Thompson

Report covers period 1 May 1978 - 31 March 1979

15 May 1979

CONTENTS

CONTENTS (Contd)

ILLUSTRATIONS

ILLUSTRATIONS (Contd)

ILLUSTRATIONS (Contd)

ILLUSTRATIONS (Contd)

1 - SCOPE AND SUMMARY

This is the final report for the Deployable Antenna Phase A study (FY-78 study), conducted by the Grumman Aerospace Corporation under NASA Contract NAS8-32394 for the Marshall Flight Space Center. The FY-78 study was conducted as a follow-on to a previous study by Grumman on the same subject (FY-77 study).

The purpose of the FY-77 study was to define a shuttle transportation system (STS) flight experiment for the demonstration of a large (50 to 200 meters) deployable antenna system.

The objectives of the FY-78 study, covered by this report, were:

- Re-examine the applications for large deployable antennas
- Define flight demonstration objectives
- Make a preliminary design of the flight article
- Define the flight program and ground development program, including the support equipment
- Refine the programmatics.

1.1 BACKGROUND

Several flight demonstration options had been defined in the FY-77 study, as shown in Fig. 1-1. The first, and least expensive, option was a single flight to demonstrate the lightweight deployable antenna, which could be a parabolic reflector or a space-fed phased array. Since the demonstration antenna defined for the single flight option was refurlable (and could, therefore, be flown again with configuration change from parabolic reflector to phased array), the second option was to plan more than one flight demonstration. Further options included reflight of the antenna with the addition of test electronics systems for limited mission demonstrations of radar, communication or radiometry. These demonstrations would measure performance parameters critical to the application, but the demonstration would test antenna performance only and would not be an application system per se. The option of a free-flying system was also included.

The results of the FY-77 study were broad in scope, surveying a large number of applications, antenna configurations, and flight program options (Ref. 1-1). The FY-78 study examined fewer options in greater depth; the relationships between these two efforts is shown in Fig. 1-2.

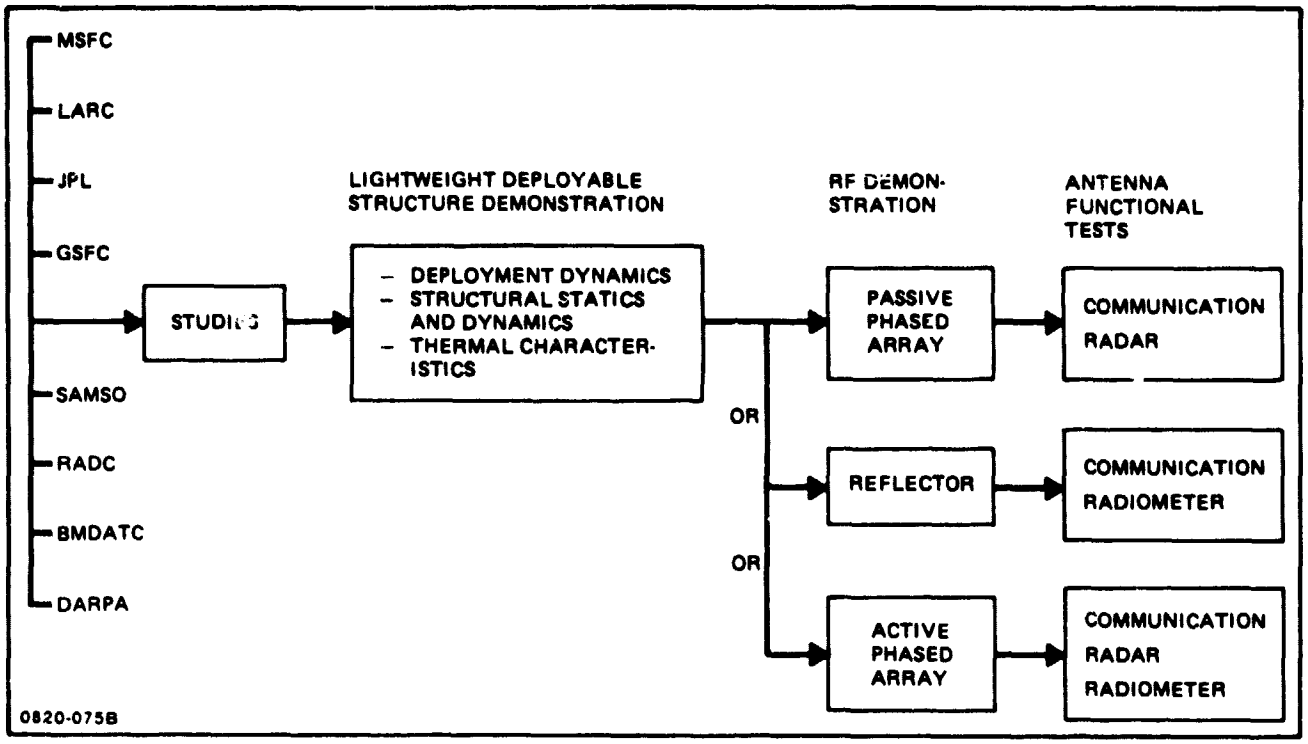

Fig. 1-1 Deployable Antenna Program Options

FY-77 STUDY RESULTS (RESULTS DOCUMENTED IN REF 1-1)	FY-78 STUDY OBJECTIVES (RESULTS IN THIS REPORT)
• MISSION ASSESSMENT LARGE LIGHTWEIGHT DEPLOYABLE ANTENNAS HAVE MANY POTENTIAL APPLICATIONS	• REVISE/UPDATE MISSION ASSESSMENT WITH EMPHASIS ON PERFORMANCE REQUIREMENTS FOR LIMITED MISSION APPLICATION EXPERIMENTS
• ANTENNA CONCEPT EVALUATION THERE IS NO BEST ANT. CONFIGURATION FOR ALL APPLICATIONS. THEREFORE, DEMONSTRATION SHOULD SUPPORT MULTIPLE ANTENNA TYPES	• PRELIMINARY DESIGN OF FLIGHT ARTICLE AND INTERFACE WITH ORBITER
• FLIGHT CONFIGURATION DEFINITION DESIGN DEVELOPED APPLICABLE TO – ANT. TYPES – PARABOLOID, LENS/ARRAY – SIZE – 50 TO 200 m – FREQ – UP TO 146 GHz PAYLOAD RETRIEVABLE FOR RECONFIGURATION BETWEEN FLTS	• DEVELOP DESIGNS IN MORE DETAIL. SUPPORT WITH SPECIAL ANALYSIS ACTIVITIES, TO INCLUDE: – STRUCTURAL (TOLERANCES) – RF (PATTERN ANALYSIS) – RELIABILITY (FMEA) – ATTITUDE CONTROL DYNAMICS DURING DEPLOYED TESTS
• ORBITAL TEST AND OPS ANALYSIS IDENTIFIED TEST OBJECTIVES AND ORBITALS REQUIRED TO SATISFY OBJECTIVES (INCLUDING MEASUREMENT TECHNIQUES)	• DEFINE GSE
	• EXPAND MISSION OPS DEFINITION IN THE FORM OF DESIGN REFERENCE MISSIONS & TIMELINES
• PROGRAMMATICS DATA DEVELOPED FOR A NUMBER OF FLIGHT PROGRAM OPTIONS	• REVISE PROGRAMMATIC DATA

0820-074B

Fig. 1-2 Relationship of the FY-78 Study Effort to the FY-77 Study Results

1.2 STUDY OBJECTIVF AND TASKS

The FY-78 stud, had as its ove:all objective a complete Phase A project definition of selected Deployable Antenna missions. The study was performed in four tasks, with some interaction, as desc ribed below (Fig. 1-3).

- Task 1 - Performance Requirements Analysis - revised and expanded definition of performance requirements for free-flight mission systems with emphasis placed on requirements of specific radar, radiometry and communications missions
- Task 2 - System Definition and Design - provided a complete Antenna System preliminary design, including shuttle interfaces and support, with expanded design activities including structural, RF system and reliability analyses
- Task 3 - Orbital Operations Analysis - defined design reference missions for antenna development flights which support multiple utility requirements of future application missions
- Task 4 - Programmatics Analysis - prepared programmatic data (cost and schedules) and development plans for all space and ground equipment necessary to accomplish the objective demonstration missions.

1.3 SUMMARY OF RESULTS

The principle result of the study was a preliminary design of a deployable-antenna flight article. This design was the basis for definition of the following items:

- Interface structure in the orbiter p"load bay to launch, operate and retract the deployable structure
- Overall size, weight of the flight article
- Instrumentation for development, pre-flight and on-orbit tests
- Estimates of the flight time required for structural testing, RF testing, and refurling of the baseline antenna system in the shuttle-attached mode
- Support equipment requirements
- Ground development program for all of the above
- Baseline program cost and schedule
- Preliminary definition of functional testing of the deployed antenna to obtain results that can be extrapolated to the needs of application systems

FOLDOUT FRAME

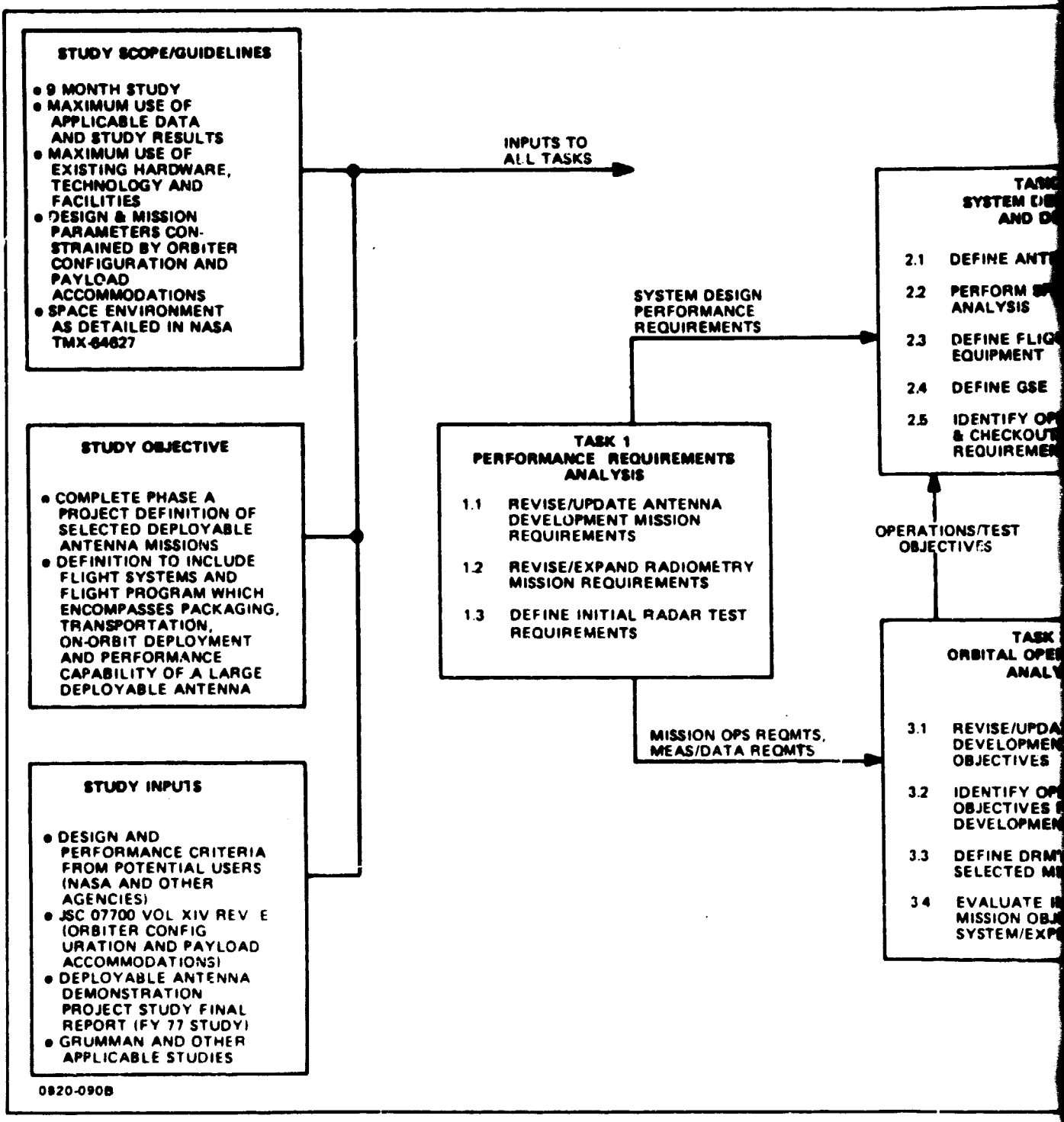

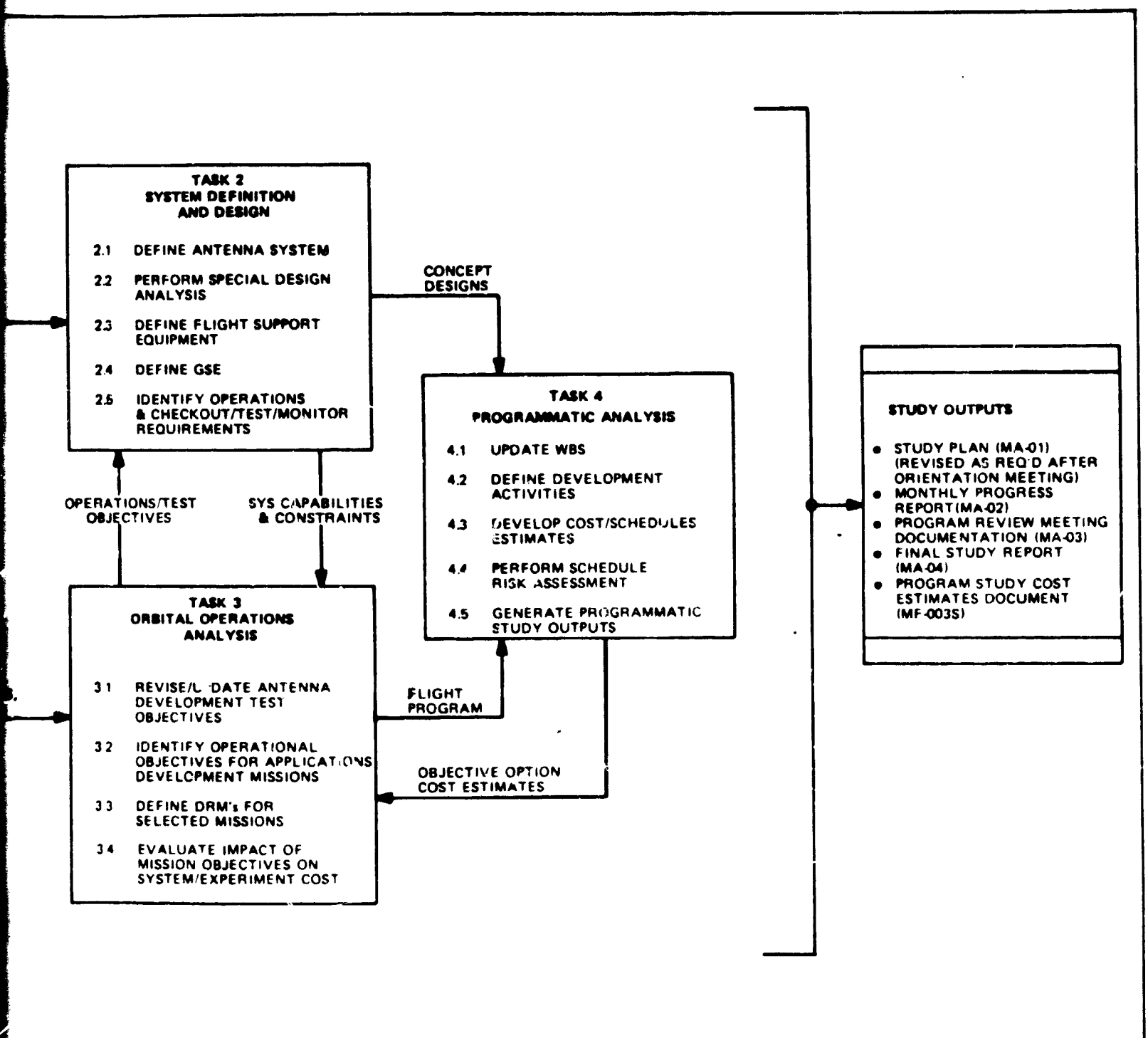

Fig. 1-3 Study Flow Diagram

- Structural analysis of the shuttle-attached deployed antenna and mast during attitude control
- Reliability analysis of the flight experiment.

The performance requirements analysis was based on previous studies of space systems that need antennas in a diameter range of 30 to 300 meters and in a frequency range of 200 MHz to 14 GHz. The flight demonstration system is expected to be in the range of 50 to 200 meters. The applicability to future systems of deployable antennas was considered, whether or not the prior studies anticipated deployable antennas. The major systems considered were communication, radar and radiometry. It is expected that these systems will be revolutionized by large deployable antennas and that the deployment demonstration will spur their development.

1.3.1 FLIGHT ARTICLE

The preliminary design of the deployable flight article uses a structure that is capable of supporting either a flat-faced phased array or a paraboloidal reflector. The phased array configuration, with instantaneous beam steering, is required for radar and beam-hopping communication satellites. The reflector can be used for fixed-beam communication and radiometry satellites. The phased array system is important to the potential of a NASA/DoD joint demonstration mission, and was viewed as the most probable configuration option for the first flight experiment. If this option is selected, the baseline experiment will measure the performance of the structure and phased array antenna system, and the results can be used to predict the performance of the deployable paraboloid. Since the deployable structure is refurbable and re-usable, the option would then exist to modify the antenna to a deployable multi-cone approximation to a paraboloid (for which a preliminary design was made in the FY-77 study) for a second flight demonstration.

The phased array antenna system used in the flight article design is a passive lens. It forms a beam by focusing energy radiated from an antenna feed near the focus. The lens action results from phasing of the antenna elements by RF transmission lines in the array. The lines are of fixed lengths that are adjusted during construction of the array. The lengths are set modulo one wavelength; the result is a zoned lens that will operate at a fixed frequency, a fixed focal length and a fixed off-boresight beam direction.

The passive phased array avoids the need for RF modules, which would add considerably to the cost. One or more antenna beams can be generated by one or more feeds, simultaneously or sequentially, provided the feeds are not displaced from the focal point by more than ten beamwidths.

1.3.2 SIZE AND WEIGHT

The analysis and programmatics were based on the 100-meter deployed-diameter design (Fig. 1-4). The parameters of a 50-meter diameter flight article, which would be less expensive and less cost-uncertain than the 100-meter antenna is also shown in Fig. 1-4. It was planned that the phased-array lens would use 16-dipole subarrays and be designed to operate in L-band (1300 to 1400 MHz). The 100-meter antenna will require 18,000 subarrays. Higher frequency or fewer dipoles per subarray will increase the number of subarrays, the weight of the system and the manufacturing costs.

1.3.3 INSTRUMENTATION

The instrumentation for on-orbit tests will consist of electro-optical distance measuring equipment (E-O DME) for precise static measurement of the positions of structural nodes, photogrammetic cameras for dynamic measurement of the vibration modes of the structure, and thin-film thermocouples, strain gages, and accelerometers. There will be an interface with the orbiter data management system (DMS). There will be a quick-look system for on-board verification of data acquisition, but the primary data reduction will be post flight.

Similar instrumentation will be used for development and preflight testing, including preflight testing of the instruments themselves.

1.3.4 FLIGHT-TIME, REFERENCE MISSION

The first cut at a schedule of orbital operations is shown in Fig. 1-5. The baseline tests are scheduled in detail (4 days), while time available for limited mission testing (3 days) is indicated. More accurate scheduling of the limited mission testing awaits further definition of user test requirements (see subsection 3.4).

1.3.5 SUPPORT EQUIPMENT REQUIREMENTS

Several items of support equipment were defined. The new unique items are a shipping container to handle and protect the flight article, and a payload specialist's station to be used in flight.

1.3.6 GROUND DEVELOPMENT PROGRAM

Figure 1-6 lists the development activities to acquire data for design of the flight system, to run tests to verify the design, and for acceptance testing.

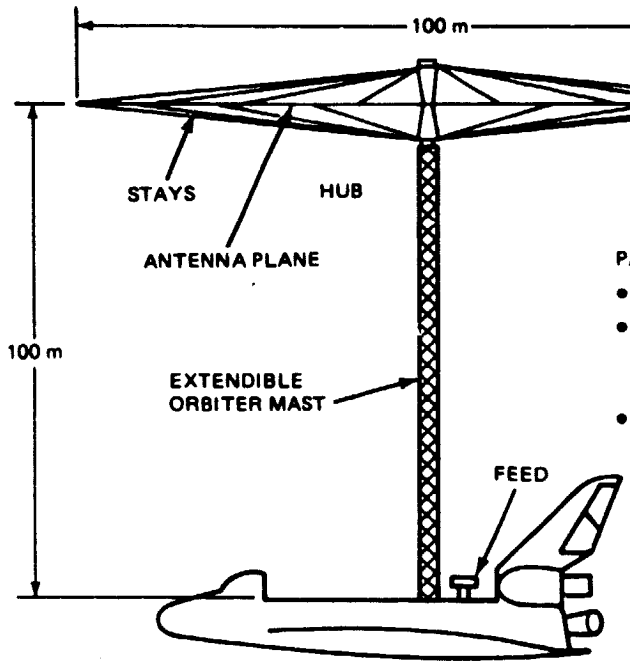

PAYLOAD PARAMETERS

• DEPLOYED SIZE	50 m	100 m
• LAUNCH DIMENSIONS		
LENGTH	8.6 m	12.7 m
DIAMETER	1.32 m	1.7 m
• ELECTRICAL CONFIG:	PASSIVE PHASED ARRAY	

NOTE: SKETCH DEPICTS 100 M CONFIGURATION

WEIGHT BREAKDOWN

COMPONENT	WEIGHT (LB)	
	50 m ARRAY	100 m ARRAY
GORE ASSEMBLY (3 PLANES)	617	2470
RIM MEMBERS (TUBES & HINGES)	176	221
STAY SYS (STAYS, REELS, MOTORS)	40	77
HUB	134	279
STAY PLATFORMS	21	31
DRUM ASSEMBLY	235	442
GORE TENSIONING SYS	46	77
ANTENNA SUBTOTAL	1269	3597
ORBITER MAST	312	625
MAST CANISTER (INCLUDES DEPLOYMENT MECH CLAMPS & RINGS)	110	115
JETTISON SUPPORT MECH & ANT MOUNT	20	30
FWD SUPPORT STRUCTURE	146	294
AFT SUPPORT & ANT PIVOT	310	622
RF SUBSATELLITE (INCL SPIN TABLE)	180	180
INSTRUMENTATION	215	215
UMBILICAL WIRE	150	300
TOTAL PAYLOAD	2712	5978

0820-001B

Fig. 1-4 Flight Configuration

EVENT	GRD ELAPSED TIME HR:MIN	ΔT HR:MIN	ORBITER ATTITUDE	REMARKS
LIFT-OFF	00:00			
STAGE SRBs	00:02			
MECO	00:08			
OMS-1	00:09			
OMS-2	00:52			
ORBITER & PAYLOAD C/O	01:40	00:15		
OPEN PAYLOAD DOORS	01:55	00:05		
SUBSAT TURN ON & C/O	02:00	00:10		
ESTABLISH SUBSAT DEPLOY ATT	02:10	00:05	Y-POP; −X VERT	
SUBSAT SPIN UP & DEPLOY	02:15	00:10	Y-POP; −X VERT	ORBITER BACKS AWAY FROM SUBSAT
ESTABLISH SUBSAT TRACK	02:25	00:05		
MEAL	02:30	01:00		
SPACE ACCLIMATION	03:30	05:30		
MEAL	09:00	01:00		
FREE TIME	10:00	02:15		
PRE SLEEP ACTIVITIES	12:15	00:45		
SLEEP	13:00	08:00		
POST SLEEP ACTIVITIES	21:00	00:45		
MEAL	21:45	00:45		
ESTABLISH ORBITER ANT ERECTION ATTITUDE	22:30	00:05	Y-POP; −X VERT	
DEPLOY RM-1 WITH TV CAMERA	22:35	00:10	Y-POP; −X VERT	
C/O & START ANT. STRUCT/THERMAL DATA ACQ	22:45	00:10+	Y-POP; −X VERT	DATA ACQUISITION CONTINUOUS FOR MISSION DURATION
ERECT ANT. PACKAGE IN PAYLOAD BAY & VERIFY	22:55	00:20	Y-POP; −X VERT	RM-2 ERECTS ANT.; ANT. SENSORS VERIFY ANT. PACKAGE IS PROPERLY ERECTED AND LOCKED IN POSITION FOR REMAINDER OF DEPLOYMENT SEQUENCE
DEPLOY RM-2 WITH TV CAMERA	23:15	00:10	Y-POP; −X VERT	RM-1 & -2 ARE POSITIONED FOR OPTIMUM VIEWING
HOLD ACTIVITIES FOR SUNLIGHT	23:25	00:35	Y-POP; −X VERT	SUNLIGHT REQD FOR DEPLOYMENT VIEWING
DEPLOY ANTENNA MAST	24:00	00:30	Y-POP; −X VERT	
VERIFY MAST DEPLOYMENT	24:30	00:20	Y-POP; −X VERT	SENSOR DATA REVIEWED TO ASCERTAIN PROPER MAST DEPLOYMENT
HOLD ACTIVITIES FOR SUNLIGHT	24:50	00:40	Y-POP; −X VERT	SUNLIGHT REQD FOR DEPLOYMENT VIEWING
DEPLOY ANTENNA	25:30	00:40	Y-POP; −X VERT	
VERIFY DEPLOYMENT	26:10	00:45	Y-POP; −X VERT	
ESTABLISH MINIMUM DISTURBANCE ATTITUDE	26:55	00:05	Y-POP; −X VERT	
ACTIVATE E-ODME & START MEASUREMENT SEQUENCE	27:00	00:45		
EXPOSE PHOTOGRAMMETRIC PLATES	27:15			
EXPOSE PHOTOGRAMMETRIC PLATES	27:30	00:30		
EXPOSE PHOTOGRAMMETRIC PLATES	27:45			
MEAL	27:50	00:40		

0820-050B(1)

Fig. 1-5 Deployable Antenna Demo DRM Timeline (Sheet 1 of 4)

EVENT	GRD ELAPSED TIME HR:MIN	ΔT HR:MIN	ORBITER ATTITUDE	REMARKS
ESTABLISH FULL SUN ATTITUDE	28:30	00:05		
CONTINUE E-ODME MEASUREMENT SEQUENCE	28:35	00:45		FULL SUN STRUCT/THERMAL MEASUREMENTS
EXPOSE PHOTOGRAMMETRIC PLATES	28:40			
EXPOSE PHOTOGRAMMETRIC PLATES	29:00	00:35		
EXPOSE PHOTOGRAMMETRIC PLATES	29:10			
ESTABLISH EDGE SUN ATTITUDE	29:15	00:05		
CONTINUE E-ODME MEASUREMENT SEQUENCE	29:20	01:10		
EXPOSE PHOTOGRAMMETRIC PLATES	29:25			EDGE SUN STRUCT/THERMAL MEASUREMENTS
EXPOSE PHOTOGRAMMETRIC PLATES	30:00	01:10		
EXPOSE PHOTOGRAMMETRIC PLATES	30:30			
ESTABLISH 45° SUN ATTITUDE	30:35	00:05		
CONTINUE E-ODME MEASUREMENT SEQUENCE	30:40	01:05		
EXPOSE PHOTOGRAMMETRIC PLATES	30:45			45° SUN STRUCT/THERMAL MEASUREMENTS
EXPOSE PHOTOGRAMMETRIC PLATES	31:00			
EXPOSE PHOTOGRAMMETRIC PLATES	31:15	01:00		
EXPOSE PHOTOGRAMMETRIC PLATES	31:30			
EXPOSE PHOTOGRAMMETRIC PLATES	31:45			
ESTABLISH DYNAMIC DISTURBANCE ATTITUDE	31:50	00:05		
CONTINUE E-ODME MEASUREMENT SEQUENCE	31:55			DYNAMIC MEASUREMENTS
FIRE - Z THRUSTERS	32:00			
	32:30	01:00		
	33:00			
EXPOSE PHOTOGRAMMETRIC PLATES	32:00			
PLATES	32:30	01:00		
	33:00			
MEAL	33:30	01:00		
FREE TIME	34:30	02:00		
PRE-SLEEP ACTIVITIES	36:30	00:30		
SLEEP	37:00	08:00		
POST-SLEEP ACTIVITIES	45:00	00:30		
MEAL	45:30	00:45		
ESTABLISH PATTERN MEASUREMENT ATTITUDE	46:15	00:15	X-POP	
ESTABLISH & VERIFY SUBSAT/ORBITER PATTERN MEASURING EQUIP INTERFACE	46:30	01:30		X-POP PATTERN MEASUREMENTS
PATTERN DATA ACQUISITION	48:00	03:30		
MEAL	51:30	01:00		
ESTABLISH PATTERN MEASUREMENT ATTITUDE	52:30	00:15	Y-POP	
VERIFY SUBSAT/ORBITER PATTERN MEASURING EQUIP INTERFACE	52:45	00:15		Y-POP PATTERN MEASUREMENTS
PATTERN DATA ACQUISITION	53:00	03:00		
FREE TIME	56:00	01:00		
MEAL	57:00	01:00		
FREE TIME	58:00	02:30		
PRE-SLEEP ACTIVITIES	60:30	00:30		

0820-050B(2)

Fig. 1-5 Deployable Antenna Demo DRM Timeline (Sheet 2 of 4)

EVENT	GRD ELAPSED TIME HR:MIN	ΔT HR:MIN	ORBITER ATTITUDE	REMARKS
SLEEP	61:00	08:00		
POST-SLEEP ACTIVITIES	69:00	00:30		
MEAL	69:30	00:45		
ESTABLISH COMM EXP ATTITUDE	70:15	00:15	Y-POP; –X VERT	
ESTABLISH & VERIFY SUBSAT/ORBITER COMM EXP MEASURING EQUIP INTERFACE	70:30	01:15	Y-POP; –X VERT	
COMMUNICATIONS EXP DATA ACQUISITION	71:45	03:45	Y-POP; –X VERT	
MEAL	75:30	01:00		
COMMUNICATIONS EXP DATA ACQUISITION	76:30	02:00	Y-POP; –X VERT	
RECONFIGURE ANTENNA ELECTRONIC CONFIG FOR RADAR EXP	78:30	01:30		
FREE TIME	80:00	01:00		
MEAL	81:00	01:00		
FREE TIME	82:00	02:30		
PRE-SLEEP ACTIVITIES	84:30	00:30		
SLEEP	85:00	08:00		
POST-SLEEP ACTIVITIES	93:00	00:30		
MEAL	93:30	00:45		
ESTABLISH RADAR EXP ATTITUDE	94:15	00:15		
VERIFY RADAR ELECT EQUIP	94:30	00:30		
RADAR CLUTTER EXP DATA ACQUISITION	95:00	04:00		
QUICK LOOK CLUTTER DATA EVALUATION	96:00	03:00		
MEAL	99:00	01:00		
RADAR COOPERATIVE TARGET EXP DATA ACQUISITION	100:00	05:00		
QUICK LOOK CO-OP TARGET DATA EVALUATION	101:00	04:00		
MEAL	105:00	01:00		
FREE TIME	106:00	02:30		
PRE-SLEEP ACTIVITIES	108:30	00:30		
SLEEP	109:00	08:00		
POST-SLEEP ACTIVITIES	117:00	00:45		
MEAL	117:45	00:45		
ESTABLISH ATTITUDE FOR ANTENNA RETRACTION	118:30	00:10	Y-POP; –X VERT	
POSITION RMs WITH TV CAMERAS FOR OPTIMUM VIEWING	118:40	00:20	Y-POP; –X VERT	
ACQUIRE E-ODME RIM MEMBER TARGET	119:00	00:10	Y-POP; –X VERT	
HOLD FOR SUNLIGHT	119:10	00:50	Y-POP; –X VERT	SUNLIGHT REQD FOR VIEWING
RETRACT ANTENNA	120:00	00:40	Y-POP; –X VERT	
VERIFY RETRACTION	120:40	00:10	Y-POP; –X VERT	
HOLD FOR SUNLIGHT	120:50	00:40	Y-POP; –X VERT	SUNLIGHT REQD FOR VIEWING
RETRACT MAST	121:30	00:30	Y-POP; –X VERT	
VERIFY RETRACTION	122:00	00:10	Y-POP; –X VERT	
STOW ONE RM TV CAMERA	122:10	00:10	Y-POP; –X VERT	

0820-050B(3)

Fig. 1-5 Deployable Antenna Demo DRM Timeline (Sheet 3 of 4)

EVENT	GRD ELAPSED TIME HR:MIN	ΔT HR:MIN	ORBITER ATTITUDE	REMARKS
HOLD FOR SUNLIGHT	122:20	00:40	Y-POP; –X VERT	SUNLIGHT REQD FOR VIEWING
LOWER ANTENNA PACKAGE INTO PAYLOAD BAY & SECURE	123:00	00:20	Y-POP; –X VERT	
VERIFY ANTENNA PACKAGE STOWAGE	123:20	00:30	Y-POP; –X VERT	
STOW RMs & TV CAMERA	123:50	00:10	Y-POP; –X VERT	
MEAL	124:00	01:00		
CLOSE OUT ANTENNA EXP & ORBITER	125:00	04:00		
MEAL	129:00	01:00		
FREE TIME	130:00	02:30		
PRE-SLEEP ACTIVITIES	132:30	00:30		
SLEEP	133:00	08:00		
POST-SLEEP ACTIVITIES	141:00	00:45		
MEAL	141:45	00:45		
DE-ORBIT & LAND	142:30			

0820-050B(4)

Fig. 1-5 Deployable Antenna Demo DRM Timeline (Sheet 4 of 4)

1.3.7 PROGRAMMATICS

Figure 1-7 is a schedule of activities leading to a baseline deployable antenna demonstration test. If functional tests are included, the added test equipment must be made available early enough to support this schedule. The items in the ground development program will also be scheduled to match the overall program schedule.

1.3.8 FUNCTIONAL TESTING

The fact that the interface between RF electronics and the antenna is through space from the antenna feed introduces the concept of guest experimenters, who would provide test electronics to be flown with the baseline antenna system. The guest experimenters would provide the feeds and associated electronics for communication, radar or radiometry experiments, which would be conducted after the baseline deployable antenna flight article had been used for the deployment demonstration and structural static, dynamic and thermal tests. For any of the future applications the flight demonstration is an antenna test; the guest experimenters would conduct limited mission demonstrations which are tests only of the suitability of the antenna for the missions.

1.3.8.1 Communication Applications

Examples of guest experimenter tests which would be conducted in communications include:

- Baseline antenna pattern measurements, mainlobe and sidelobes to show resistance to interfering signals or jamming
- Demonstration of isolation of one antenna beam from the effects of sidelobes of multiple additional beams in the same antenna
- Measurement of the power level that the antenna can handle before the onset of intermodulation (IM) crosstalk between multiple communication channels, by plotting the third-order IM levels as a function of power level of two fundamental signals.

For the beam-hopping communication system applications, it will not be possible to demonstrate electronic beam steering, if the fixed passive zoned lens antenna is used. The baseline experiment, however, will show that the phase shifters, properly adjusted, form a good antenna pattern at the desired angle off boresight. It is not necessary, therefore, to demonstrate beam hopping as part of the antenna flight test. Laboratory tests of diode phase shifters, amplifiers and digital logic can be used to demonstrate that application systems can have electronic beam steering.

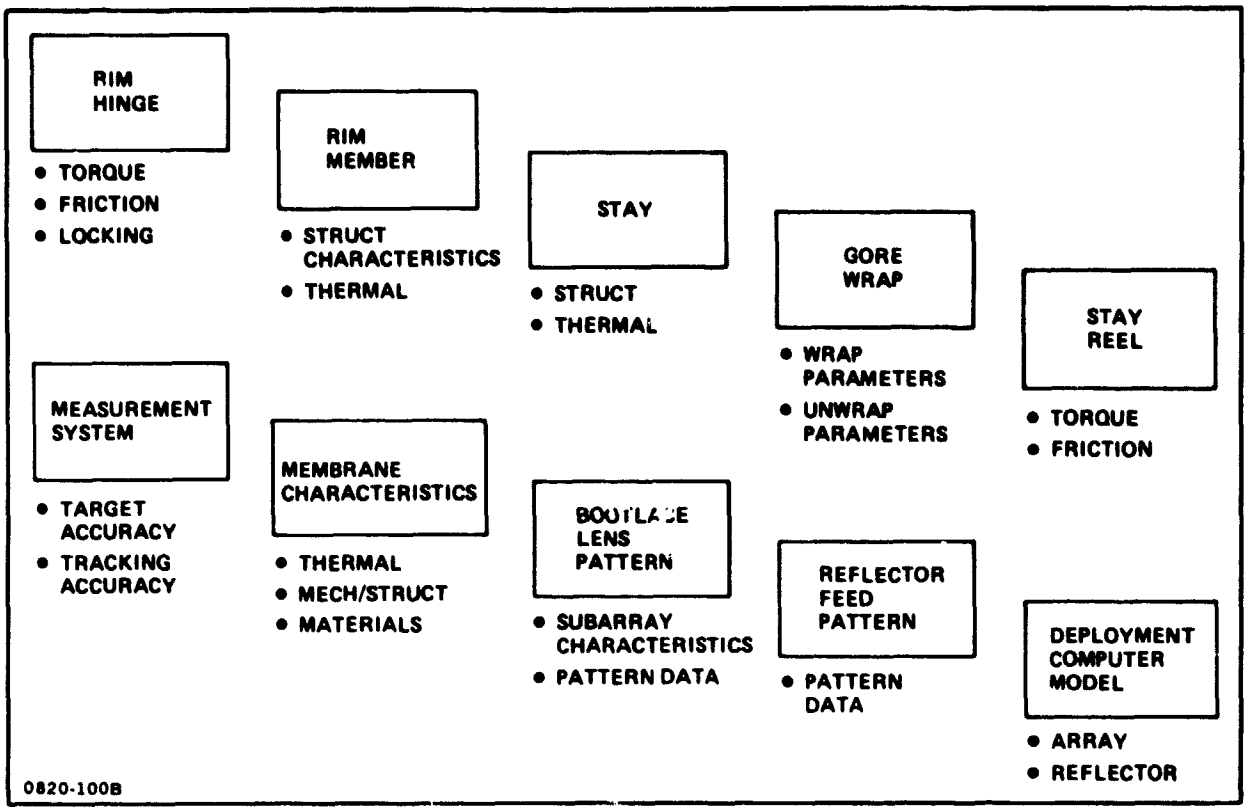

Fig. 1-6 Ground Development

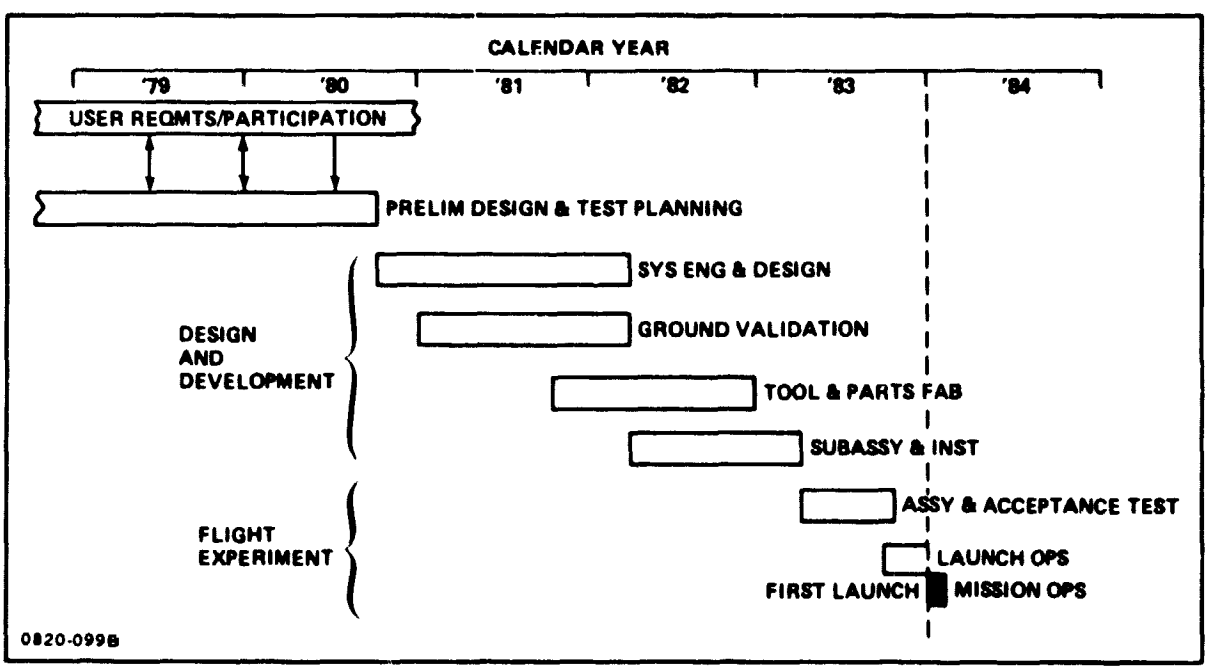

Fig. 1-7 Schedule

1.3.8.2 Radar Application

For radar applications, the guest experimenter tests would include:

- Baseline antenna pattern measurements as for the communication application. These measurements will be made using the free-flying signal generator and will determine the sidelobe levels as a starting point for the subsequent radar-oriented measurements
- Measurements to demonstrate that ground clutter integrated over the sidelobes is negligible compared to ground clutter in the main lobe and targets in the main lobe. These tests will compare clutter returns received while the beam is earth pointing with clutter returns received while the beam is pointed above the horizon
- Measurements to determine that a multiple element feed system and an adaptive cancellation loop can form deep sidelobe-cancellation nulls in the antenna pattern. These tests will use the free-flying signal generator as a signal source. The experimenter will supply the feed system to mount in the orbiter payload bay, and will have the option of recording signals for post-flight sidelobe cancellation or of doing in-flight sidelobe cancellation if he has suitable flight equipment for that purpose.

In the radar tests, since a radar transmitter and receiver will be used for the clutter tests, an opportunity exists to obtain, as a dividend, measurements of ground return (radar clutter) from space, where a few orbits of data collection will provide wider earth coverage than has been obtained in years of measurements from aircraft. The opportunity exists to provide a radar transmitting and receiving system with a wide dynamic range to gather data such as the amplitude of very strong clutter peaks that have often been lost in prior measurements from aircraft. The radar experiment would also gather Doppler bandwidth data on ground clutter, necessary to the design of and prediction of the performance of the future radar Doppler filter systems. For this purpose it is necessary that the spectrum be measured to or below the -60 dB point, as compared to existing data that go only to about -30 dB. Data from various kinds of land, ocean sea states, arctic terrain, snow and ice at various grazing angles, would be recorded by the radar experimenter and would be reduced post flight by various signal processing algorithms, not necessarily in real time. If the experimenter were to arrange a flight of a known aircraft target to intersect the footprint of the antenna beam on one or more orbits, post flight data reduction would demonstrate detection of the known target. An in-flight display would also be provided to verify that good data were being recorded. Of course, many unplanned aircraft detections will occur as the orbiter passes the air-traffic areas of the earth.

1.3.8.3 Radiometer Applications

In addition to antenna pattern measurements to calculate the antenna beam efficiency, the real losses in the antenna are important. The guest experimenter would provide test equipment to inject a known signal after the antenna to calibrate the receiver. The antenna will then be pointed at a quiet area of the sky while the total receiver noise level is measured. These measurements together can be used to derive the antenna noise temperature and losses, which can be compared with predictions. The results can be used to calculate the performance of proposed future radiometry antenna configurations.

1.3.9 MULTI-MISSION TESTS

There is, further, an opportunity to combine the limited mission demonstrations: the radar transmitter and receiver could be designed to serve the communication demonstration, and the radar receiver could serve the radiometer, if such an arrangement were planned in advance.

The limited mission demonstration tests will be done following the baseline deployable antenna demonstration. The baseline lightweight deployable antenna demonstration would be a single flight experiment that would produce results with the least complex test program. It would include the passive phased array antenna, laser instrumentation to survey the deployed structure, photogrammetric cameras to observe the dynamic response of the deployed structure, and a system to measure antenna patterns in flight. The orbiter will provide attitude control electrical power, and data management; the on-board personnel will monitor the experiment via TV cameras on two RMS, and the personnel can take action if anything appears to be going wrong during depioyment. Thus the manned orbiter itself is an important part of the baseline experiment. In addition, it will be used to set a series of fixed sun angles for thermal tests, to impulse the deployed antenna structure to excite the several lowest frequency vibration modes for dynamic tests, to provide angular rotation of the antenna for pattern measurements, and to position the antenna beams for the limited mission experiments.

1.4 REFERENCES AND BIBLIOGRAPHY

1-1 J. Schultz et al, Grumman Aerospace Corporation, Deployable Antenna Demonstration Project Final Report, NAS8-32394, March 24, 1978

2 - PERFORMANCE REQUIREMENTS ANALYSIS (TASK 1)

2.1 INTRODUCTION

The performance requirements analysis task was scoped to provide a technical definition of the antenna capabilities and specifications projected for future applications. These technical requirements are the basis for the definition of a flight article for a large, lightweight deployable antenna flight test. In the FY-77 study we considered the antenna requirements of a large number of applications systems (the list is shown in Fig. 2-1) as the basis for definition of test objectives of a deployable antenna 50 to 200 meters in diameter. As an example on which to base antenna flight tests, we also defined the parameters of a mission reference system for each class of application.

The FY-78 study concentrated on communication, radar, and radiometry applications. The objective was to define firm requirements for functional test of the antenna, as opposed to system test requirements for application systems. Some antenna tests are common to all applications, while some are unique to a particular application.

2.2 THE LITERATURE OF FUTURE LARGE-ANTENNA SYSTEMS

The systems considered in the study were proposed in previous studies (see bibliography) of systems that need large antennas. In the frequency range (0.24 to 14 GHz) and size range (50 to 300+ meters) of interest, the largest antenna is 700 meters for soil moisture radiometry (Ref. 2-1) at about 0.6 GHz, the second largest is space based radar at 300 meters (Ref. 2-2), while the majority are in the 30 to 100 meter range. The system studies contemplate various approaches to large antenna structures: assembly in space of large antennas built of structural elements launched from the ground, assembly of structural elements built in space, and deployable reflectors and lenses. With few exceptions the system studies do not treat the structural analysis, expected deformations, or the tolerance budget of the envisioned antenna systems beyond the requirement to avoid loss of gain by more than one dB. It will be shown in Section 3 that although low sidelobes and low gain loss go together, it is the sidelobe requirement that sets the structural tolerances. Even where one-dB gain loss can be tolerated in the power budget, for satisfactory sidelobe performance the gain loss must be limited to approximately 0.02 dB. Thus, some of the system studies may be somewhat optimistic in their antenna performance expectations, as will be discussed in subsection 2.3.

	SYSTEM CHARACTERISTICS								ANTENNA CHARACTERISTICS							
APPLICATION	FREC	ORBIT	NO OF BEAMS	FOV OR SCAN ∠, BEAM COV	RF BAND WIDTH	NO CHNLS PER BEAM	S/C RADIATED RF PWR	USER RF POWER	CONF TYPE	DIA	F/D	1ST SL	TOLERANCE	GAIN dB	BEAM-WIDTH (DEG)	REMARKS
COMMUNICATIONS																
MOBILE COMM	885-890 MHz	GSO	200	100 MILES	5 MHZ (4 MHz UP, 4 MHz DWN)	50 FDX	.1 W/CHNL	0.13W	ON-AXIS PARABOLIC REFLECTOR	70m (234λ)	0.5	−25dB	λ/25 (0.5 IN.)	52	0.3	ALTERNATE BIFOCAL DUAL REFLECTOR 10,000 FDX CHNLS, 200,000 USERS POINTING ACC = .03 DEG ·10 DB SCAN
MOBILE COMM	885-890 MHz	GSO	72	200 MILES	5 MHz (4 MHz UP, 4 MHz DWN)	50 FDX	.3 W/CHNL	0.37W	ON-AXIS PARABOLIC REFLECTOR	47m (133λ)	0.5	−25dB	0.5 IN.	47	0.5	ALTERNATE BIFOCAL DUAL REFLECTOR 3000 FULL DPLX CHN 20 KHZ/CHNL 60,000 USERS, PHASED ARRAY FEED FREQ. REUSE, EVERY 4TH BEAM ·10 DB SCAN
MILITARY COMM	225-400 MHz	GSO	MULTIPLE BEAMS	·9°	30 MHz	TBD	CLASS.	CLASS	BOOTLACE LENS*	80-100m* (100λ)	1.5-2*	−30dB	1 IN.	[illegible]	TBD	*GAC ESTIMATE
PUBLIC SERVICE PLATFORM	S-BAND	GSO	255	CONUS	33 MHz	1000	100W/BEAM	.625W	BOOTLACE LENS	61m (487λ)	1		10CM AXIAL 3.75CM RADIAL	53.2	0.18	
ORBITING DSN	S-BAND X-BAND K-BAND	GSO		HEMISPHERE	1 MHz	3	N/A RCV ONLY		ON-AXIS PARABOLIC REFLECTOR	45m (300λ S-BAND)	0.424	25dB	λ/25 (0.2 IN.)	70dB		RIGID RIB ANT DUAL REFLECTOR REC TWO LINKS SIMULT, T = 11.5K
MOBILE COMM	823 MHZ, UP 868 MHZ, DWN	GSO	MULTIPLE BEAMS						BOOTLACE LENS	120m (329λ)					0.2-10	
RADAR																
SPACE BASED RADAR (NEAR TERM)	L-BAND 1280MHz	POLAR LEO	1	·35°	INSTANT 2.5 MHz* (200 MHz)	1	5 kw	N/A	PHASED ARRAY LENS	61m (354λ)	1.5	−17/32dB **	0.1 IN. RMS (37 FT. CORR DIST)	56dB	0.28	*2.5 MHZ BANDWIDTH TUNABLE OVER 200 MHZ **17 TRANSMIT 32 RECEIVE
SPACE BASED RADAR (FAR TERM)	L-BAND 1280MHz	GSO	8	·10°	INSTANT 2.5 MHz* (200 MHz)	1	12.7 kw	N/A	PHASED ARRAY LENS	100m (750λ)	2.5	−17/32dB **	0.1 IN. RMS (34 FT. CORR DIST)	67dB	.088	
SPACE BASED RADAR	S-BAND 3300 MHz	GSO	1	·6.5°		1	15.2 kw	N/A	CASSEGRAIN	98.2m (720λ)		λ/16 (.57cm)			0.262	LINEAR POLARIZATION

Fig. 2-1 FY-77 Study Mission Applications Listing (Sheet 1 of 5)

	SYSTEM CHARACTERISTICS								ANTENNA CHARACTERISTICS							
APPLICATION	FREQ	ORBIT	NO. OF BEAMS	FOV OR SCAN ∠, BEAM COV	RF BAND WIDTH	NO CHNLS PER BEAM	S/C RADIATED RF PWR	USER RF POWER	CONF TYPE	DIA	F/D	1ST SL	TOLERANCE	GAIN dB	BEAM WIDTH (DEG)	REMARKS
EARTH OBSERVATIONS																
RADIOMETRY	1.4-40 GHz (8 FREQ)	SUN SYNC (400 KM)		±70°, 88m TO 481m			N/A	N/A	OFFSET PARABOLIC REFLECTOR (CASSEGRAIN)	100m (467λ AT 1.4 GHz)	0.25		λ/32 (.25 IN.)	74dB (88m DIA AT 5.4 GHz)	.013 TO 0.14	BEAM EFF > 65% V&H POL POINTING ACC. .005 DEG (3σ) SENS .05°K (10-S INT TIME) CONICAL & SPIRAL SCANS ±5 SW SCAN
RADIOMETRY	2.5 GHz	LEO (362 KM)		515m (5mi)			N/A	N/A	ON-AXIS PARABOLIC REFLECTOR	~100m (333λ)	0.5		λ/80 (.25 IN.)		.004	OCDA FAB
RADIOMETRY	1.4-5 GHz	LEO		1 km			N/A	N/A	REFLECTOR	30-300m	0.5-5		.03 IN. AT 5GHz	65dB (30m AT 5GHz)	0.110 (30m AT 5 GHz)	50-200 KM SWATH WITH .5-6° K, REFLECTOR CONFIG NOT DEFINED
INTERFEROMETRY (COASTAL MONITORING)	401 MHZ	LEO (45° INCL)							CROSS ARRAY	50-200m						
RADIOMETRY	0.5 - 1.4 GHz	LEO							PHASED ARRAY	100-300m						
RADIOMETRY	S-BAND	LEO							PARABOLIC REFLECTOR	100m						

Fig. 2-1 FY-77 Study Mission Applications Listing (Sheet 2 of 5)

	SYSTEM CHARACTERISTICS								ANTENNA CHARACTERISTICS							
APPLICATION	FREQ (GHz)	ORBIT	NO. OF BEAMS	FOV OR SCAN ϕ, BEAM COV.	RF BAND-WIDTH (MHz)	NO CHNLS PER BEAM	S/C RADIATED RF PWR	USER RF POWER	CONF TYPE	DIA	F/D	1ST SL	TOLER-ANCE	GAIN dB	BEAM-WIDTH (DEG)	REMARKS
COMMUNICATIONS																
BUSH VOICE	2.5/2.5	GSO														47-56dBw EIRP
CB/AMATEUR	24/24	GSO														30dBw EIRP
INTERSATEL-LITE	55/55	GSO	2						REFLECTOR	1.3m						52dBw EIRP
STD. TIME/ FREQ/DISAS	14/0.4	GSO	1	GLOBAL												20dBw EIRP
NAVIGATION	1.6/46	GSO	1	GLOBAL												30dBw EIRP
METEOROLOGY	14/17	GSO	1	GLOBAL												44dBw EIRP
EARTH EXPLORATION	14/8	GSO	1	SPOT												50dBw EIRP
TLM/TRFING/ CNTRL	14/4	GSO	2	GLOBAL												7 dBw EIRP
PBCS	14/11	GSO	4	REGIONAL	100/30/10		100W		REFLECTOR	0.6X1.3m				32.9*	2.8 X 1.8*	*TRANSMIT ALL
	14/11	GSO	3	ALAS/HAW/ CAR	100/30/10		30W		REFLECTOR	1.8m			2 mm	37.9	1.2	
	14/11	GSO	2	SPOTS	100/30/10		30/100		REFLECTOR	1.8m			2 mm	38.4	1.2	
	14/11	GSO	1	CONUS	100/30/10		30		REFLECTOR	0.6X0.2m				27.3	3.0 X 8.0	
	14/11	GSO	1	PACIFIC	100/30/10		30		REFLECTOR	0.15X0.15m				22.0	7.0 X .0	
	14/11	GSO	2	ECH	100/30/10		30/100		HORN	0.1X0 1m				15.0	20 X 20	
	823/886	GSO	1	CONUS			300		REFLECTOR	7X3.1m				26.1	3.8 X 6.8	
	823/886	GSO	1	CONUS			50		REFLECTOR	3.1X3.1m				22.6	6.8 X 6.8	
RADAR																
LONG RANGE SENSOR	S-BAND 3000 MHz	GSO	1	±11.25°/ 6.3NM	1 MHz* (200 MHz)	1	5 KW	N/A	PHASED ARRAY LENS	305m	2.5	22 dB	0.1 IN. RMS (15 FT CORR DIST)	70dB	.023	
SOLAR POWER SATELLITE																
SPS TARGET –	2.45 GHz	GSO	1	TBD	TBD	1	N/A	TBD	PLANAR ARRAY	350m						
SUNLIGHT REFLECTOR	0.4 – 0.7 μm	LEO 2000 KM, 0° INCL	1		N/A		N/A	N/A	PLANAR SURFACE	700m						TYPICAL, 7 REFL. REQ 500 Km² EA

Fig. 2-1 FY-77 Study Mission Applications Listing (Sheet 3 of 5)

	SYSTEM CHARACTERISTICS								ANTENNA CHARACTERISTICS							
APPLICATION	FREQ (GHz)	ORBIT	NO. OF BEAMS	FOV OR SCAN & BEAM COV	RF BAND-WIDTH (MHz)	NO CHNLS PER BEAM	S/C RADIATED RF PWR	USER RF POWER	CONF TYPE	DIA	F/D	1ST SL	TOLER-ANCE	GAIN dB	BEAM-WIDTH (DEG)	REMARKS
COMMUNICATIONS																
FIXED COMMUNICATIONS	8/4	GSO	1	CONUS	250		2-40W		ELIPSOIDAL REFLECTOR	0.7X2m						2 ANTS
	8/4		40		250		40-.25W		REFLECTOR	30m						MULTIPLE FEEDS, OFFSET
	14/12		40	200KM	500		40-4W		REFLECTOR	12m						MULTIPLE FEEDS
	14/12		4		500		4-4W		REFLECTOR	4.8m						4 ANTS
	30/20		1		1C		1-2KW		HORN							
	30/20		10	CONUS	[illegible]		10-4W		REFLECTOR	2.0m						MULTIPLE FEEDS
	2.6/2.6		1	CONUS	[illegible]		2-100W		REFLECTOR	1X3m						
MOBILE	1.6/1.6	GSO	4	OCEANIC	4.0		200W		REFLECTOR	3m						MARISAT, 4 ANTS
	128/132		1	GLOBAL	.55		100W		REFLECTOR	10m						AEROSAT
	1.6/1.6		1	GLOBAL	15		100W		REFLECTOR	1m						AEROSAT
	800-900		4	CONUS TIME ZONES	6		4-80W		REFLECTOR	12m						MOBILE, 4 ANTS
BROADCAST	2.536-2.655	GSO	1	CONUS	120		400		REFLECTOR	1X3m						
	12.2-12.5		1	CONUS	300		500		HORN	0.3X.6m						
	12.2-12.5		3	CONUS	300				HORN	1.8m						3 ANTS
INTERCONTIN-ENTAL TRUNKING	14/11	GSO	6	SHARED	480	800-1000	2.5W		REFLECTOR	10m 6m						2 ANTS, 30-50 dBw EIRP
REGIONAL AND DOMESTIC TRUNKING	30/20	GSO	14	SPOT	4000	100,000	1W		REFLECTOR	10m						60dBw EIRP
REGIONAL AND DOMESTIC NETWORKS	8/4	GSO														43dBw EIRP
BUSINESS NETWORKS	14/12	GSO	2	CONUS	60		1W		REFLECTOR	3m						50-56dBw EIRP
MARITIME SERVICES	1.6/1.5	GSO	1	GLOBAL	10				HELIX ARRAY							40dBw EIRP
AERONAUTIC SERVICES	1.6/1.5	GSO	1	GLOBAL					HELIX ARRAY							43dBw EIRP
TV/DISTRIBUTION	14/12	GSO														
TV/BROADCAST	14/UHF	GSO	3	SHAPED					HELIX ARRAY							75dBw EIRP
EDUCATIONAL TV	14/2.5	GSO	1	CONUS	20	1	100W		REFLECTOR	4X8 FT				30		53-55dBw EIRP

Fig. 2-1 FY-77 Study Mission Applications Listing (Sheet 4 of 5)

	SYSTEM CHARACTERISTICS								ANTENNA CHARACTERISTICS							
APPLICATION	FREQ	ORBIT	NO. OF BEAMS	FOR OR SCAN (), BEAM COV	RF BAND-WIDTH	NO CHNLS PER BEAM	S/C RADIATED RF PWR	USER RF POWER	CONF TYPE	DIA	F/D	1ST SL	TOLER-ANCE	GAIN dB	BEAM-WIDTH (DEG)	REMARKS
SCIENCE																
ORBITING VLBI	1.4 24 GHz	LEO 400-5000 KM ~45° INCL		FULL HEMISPHERE	2 MHz 56 MHz		N/A	N/A	ON-AXIS PARABOLIC REFLECTOR	30m	.3-.5		λ/16			RCV ONLY CASSEGRAIN, POINTING 5-10 SEC (1σ)
SUBMILLIMETER RADIO ASTRONOMY	1000 GHz	LEO		FULL HEMISPHERE			N/A	N/A	ON-AXIS PARABOLIC REFLECTOR	30m	.5		λ/16	98	^2.1 SEC	CASSEGRAIN, POINTING .4 SEC
EARTH OBSERVATIONS																
ACTIVE RADAR	15 GHz 10 GHz 3 GHz	LEO 800KM							TRAVELLING WAVE	8m 12m 40m						MULTIPLE RECEIVING BEAMS
RADIOMETRY	L-BAND 1.42 GHz	NEAR POLAR 1000 KM	61	±14.88°, 1,071 KM	24 MHz	1	N/A	N/A	PARABOLIC TORUS	575m (2721.7λ)	1.16		λ/33	75.81		BEAM EFFICIENCY > 99% 1.07°K RESOLUTION ALTERNATE PHASED ARRAY ANT

Fig. 2-1 FY-77 Study Mission Applications Listing (Sheet 5 of 5)

2.2.1 COMMUNICATION APPLICATIONS

Small antennas generate wide beams, large antennas generate narrow beams, the beamwidth in radians being approximately the reciprocal of the diameter in wavelengths. Communications satellites that use antennas small enough to fit the shroud of the launch vehicle generate beams that cover whole continents. When these small antennas are used on communication satellites, as at present, any ground station within the ground spot can receive signals from the satellite. One consequence is that a large amount of RF power must be radiated by the communication satellite because a very small fraction of the power is captured by the earth antenna. Another consequence is that large antennas are needed at the earth station to allow it to produce a small spot in the sky. Unless the earth station produces a small spot in the sky (geostationary orbit), signals from other communication satellites will interfere with the signals from the desired satellite. Furthermore, it is necessary that communication satellites maintain sufficient spacing in orbit that they do not enter another's territory; individual orbital parking places are required and assigned. The satellite can use a single frequency band only once, because it has no way to discriminate among signals arriving from different ground stations.

Large antennas on communications satellites will change the picture. With large antennas the earth spots will be small, as small as 30 nautical miles in diameter. The satellite will be able to direct its beam toward the desired ground station; it will transmit and receive signals only with ground stations within the small earth spot, but it can produce other earth spots and it can re-use the same frequency band again in each of its earth spots. Earth stations on the same frequency must maintain a two-spot spacing on earth, but there is no requirement on the spot in the sky because the satellite antennas discriminate between ground stations. Thus the earth stations may use small antennas, the satellite and the earth station can use lower RF power, and the frequency bands can be re-used hundreds of times.

At present, earth stations number in the hundreds. Forecasts of future communication requirements envision tens of thousands of earth stations. For the reasons cited above, the world has run out of orbital parking spaces and frequency allocations to handle the projected satellite communication traffic.

A very important part of the solution to breaking through these present barriers to the growth of satellite communication is the development of large deployable antennas for communication satellites. The large antenna in space reduces the required RF power, antenna

size and cost of the ground stations, permits closer orbital spacing of communication satellites, increases the amount of communication traffic that can be carried, and greatly reduces the overall communication system acquisition and operating cost.

Two options are covered in the literature. One option is to build a scanning beam satellite that will produce a single narrow beam that can be electronically steered from ground station to ground station to interchange signals. The other option is to build large satellites that produce simultaneous multiple beams directed at the ground stations (subscribers). One type of scanning beam system (Ref 2-5) for the 12/14 GHz communication band uses time division multiple access (TDMA) with a phase-steered array antenna capable of being pointed at any of 100 contiguous spots in the continential United States. In this system the satellite antenna beam is successively directed at earth stations to transmit and receive signals from each and to interchange signals between them. It accommodates the whole 500 MHz bandwidth of the 12/14 GHz satellite communication band. It has a large antenna (ten times the diameter of an equivalent wide-beam satellite), requires only one percent of the radiated power, yet it suffers no loss of communication capacity compared to the small-antenna wide-beam satellite. As mentioned in Ref. 2-5, the satellite antenna illumination can be tapered to produce low sidelobes. Thus other scanning spot-beam satellites could be used in the same frequency band. With reasonable scheduling of beam pointing to avoid simultaneous illumination of the same earth spot, a very large frequency re-use factor could be achieved.

A larger (30 meters, 4 GHz) scanning-spot-beam satellite system (Ref. 2-6) could use a narrow bandwidth transponder to interchange computer data between a very large number of small earth terminals. This system produces a similar saving of transmitter power in the uplink and downlink, and requires no internal message switching system in the satellite because it uses TDMA and switching is achieved by beam steering. The small earth spots also permit other satellites to share the same frequency band. The concept is easily adaptable to remote area mobile communications applications (aircraft, ground vehicles, or small fixed stations) (Ref. 2-32 and 2-33).

For very high density communication traffic between fixed earth stations, many studies of multibeam communication satellites are available (Ref 2-7 through 2-23). Although most of these studies have been directed at satellite systems that produce overlapping beams, and enough beams to fill the earth area (such as CONUS) that they serve, this configuration is not necessarily optimum; a smaller-than-full number of spots will probably suffice because the dense traffic originates and terminates in the most densely populated areas.

In addition to message traffic and computer data, an important communication satellite application is educational and entertainment broadcasting. There is world-wide interest in future systems to handle television and voice radio signals, either for networking or for direct-to-home broadcasting. In the last few years 1400 receive-only ground stations have been installed in the United States for satellite inputs to CATV and PBS systems. Frequency congestion and orbital congestion are bound to develop also in broadcasting, which can be relieved only by large satellites. Less literature is available on broadcast satellites than on message-communication satellites (Ref 2-24 through 2-26), but the subject has been debated extensively in the United Nations (Ref. 2-27). It is clear that part of the debate is caused by the perception that small earth spots and low sidelobes are not possible. Flight demonstration will change this perception, and should lead eventually to frequency allocation for, and commercialization of, direct broadcast satellites worldwide.

The specification requirements of communication antennas are summarized below.

2.2.1.1 Communication Antenna Parameters

The range of parameters in the source documentation for communication satellites, excluding antennas smaller than the orbiter payload bay and frequencies higher than 14 GHz, are listed below. The antenna flight experiment should be designed to produce results that can reasonably be extrapolated to a variety of future systems.

- Frequency — 150 MHz to 14 GHz
- Wavelength — 2 m to 2 cm
- Radiated power — 1 w to 2 kW
- Antenna diameter — 7 m to 300 m
- Antenna beams — 1 to 1000
- Sidelobes, near — -20 dB to -30 dB
- Sidelobes, far — 0 dB to -10 dBi
- Signal bandwidth — 24 kHz to 500 MHz
- Tunable bandwidth — up to 29%
- Intermodulation — -200 dBw/Hz
- Beam switching time — 20 nsec to 1 μsec
- Angular coverage — 3.5 deg to 8.6 deg
- Polarization — single, dual, circular

2.2.2 RADAR APPLICATIONS

Radar systems transmit signals and receive echoes. Search radars transmit signals to a series of points and look for targets in the echoes. Tracking radars transmit signals toward a target repeatedly and update the target's changing position. The functions can be combined, as in search-track radars that time-share transmitted signals between the two modes, and in track-while-scan radars. The transmitted signal power required of a search or tracking radar is proportional to the fourth power of antenna size, other things (target size, range, frequency, receiver sensitivity) being held constant. The work that can be done by a search radar (area searched per unit time) is proportional to the product of power times aperture area of the antenna (power-diameter squared), while the work that can be done by a tracking radar (number of target updates per unit time) is proportional to the power-aperture-gain product (power times diameter to the fourth). Thus the key to space-based radar is large antenna diameter, for which there is no reasonable substitute.

Applications of space based radar include weather radar (Ref. 2-28 and 2-29) air traffic control (Ref. 2-32), coastal zone monitoring (Ref. 2-33), and military (Ref. 2-34 through 2-36). In all cases, in addition to requiring large antennas for practical detection of the target (such as raindrops in weather radar), large antennas are required to produce narrow beamwidths to discriminate between targets and to allow accurate angle tracking of targets. Space based radar studies to date have largely concentrated on search-track radars that use electronic beam switching to direct the beam quickly from pointing angle to pointing angle. Mechanical scanning of a single-beam antenna is too slow for any reasonable target update time (revisit time). Thus another key antenna requirement for space based radar is phased-array electronic beam steering. Because the required transmitter power is large, antenna efficiency is also important.

2.2.2.1 Radar Antenna Parameters

Radar systems in the literature for weather, soil moisture, and military applications have parameters in the range listed below.

- Frequency — 400 MHz to 16 GHz
- Wavelength — 75 cm to 1.8 cm
- Radiated power, peak — up to 1 MW
- Radiated power, average — up to 5 kW
- Antenna diameter — 30 m to 300 m
- Antenna beams — 1
- Sidelobes, near — -20 dB to -30 dB
- Sidelobes, far — 0 dBi to -10 dBi

• Sidelobe nulling	required
• Signal bandwidth	up to 10 MHz
• Tunable bandwidth	10%
• Intermodulation	-40 dB (harmonics)
• Beam switching time	20 n sec to 1 μ sec
• Angular coverage	8.6 degrees to 30 degrees
• Polarization	single, dual, circular

2.2.3 RADIOMETRY APPLICATIONS

Microwave radiometers measure temperature at a distance. They work by measuring the level of thermal noise radiated by the target at which the antenna beam is pointed. The noise is proportional to the product of the absolute temperature and the (microwave) emissivity of the target. The measured temperature is the area-average temperature of all objects within the beam spot.

Soil moisture can be estimated from microwave radiometer measurements because the emissivity of soil varies rapidly with soil moisture. For example, very dry soil at 300° K (80.6° F) will measure nearly 300° K, while very wet soil will measure 250° K (-9.4° F). The depth of soil moisture measurement is about one-tenth of the wavelength. To measure to a depth of one inch requires a wavelength of 10 inches (25.4 cm), corresponding to a frequency of 1200 MHz. But the radiometer frequency must be selected to avoid man-made radio signals. The frequencies reserved for radio astronomy are also available for radiometry, the nearest one being 1400 MHz (21 cm wavelength). At this wavelength a spot diameter of one nautical mile from an orbit altitude of 500 nautical miles requires an antenna diameter of 140 meters. Although a one-nautical mile diameter spot is larger than would be desired, it will produce useful data over many large agricultural areas.

The soil-moisture radiometer requires multiple beams. Two rows of feeds are used, to project two rows of spots on the earth. Two rows of spots, one behind the other, are needed because it is not possible to place antenna feeds closely enough together to produce overlapping spots in a single row. A single satellite at 500 nautical miles altitude and 60 degrees inclination, with a swath width of 300 one-mile spots, can measure the whole earth in approximately 6 days. Two such satellites are needed to get the desired 3-day revisit time.

A key antenna requirement for radiometry is the ability to produce multiple beams, while for satisfactory operation the sidelobes must be low, the antenna power losses must be small, and the bandwidth must be large. This kind of performance is very difficult

to achieve with parabolic reflectors or with lens antennas, except by using a very large focal length, such as f 4.5, where the length of the mast or feed support must be 4.5 times the antenna diameter (see Section 3).

Radiometer studies by GSFC (Ref. 2-28), LaRC (Ref. 2-28), and JPL (Ref. 2-29) have produced antenna designs in a size range from 10 meters to 700 meters. The GSFC design of a 10-meter phased array radiometer at 1400 MHz, (Ref. 2-28) was proposed as an early flight demonstration that would provide soil moisture data as a useful input to the global weather model. Other GSFC studies (Ref. 2-28) have considered phased array antennas up to 100 meters. The LaRC studies are based on airborne radiometer experiments that have shown important radiometer capability to measure not only soil moisture but also ocean water pollution. Scaling the airborne antenna size to orbital altitude (in such scaling the antenna diameter must be increased directly with altitude) has resulted in forecasts by LaRC of antennas as large as 700 meters. The JPL studies have considered multiple-wavelength radio-meters. The JPL concept is a hybrid earth observation facility, from low earth orbit, that also includes radar sensing. Radar and radiometric observations from a 400 kilometer altitude are accomplished on a time shared basis. Radiometric observations are made at 6 frequencies (1.4, 6.6, 10.69, 18, 21, 37 GHz) and are time shared with 18 and 37 GHz radars.

The antenna configuration previously proposed by JPL is an offset parabolic reflector (F/D = 0.25, offset Cassegrain configuration) having a 100-meter diameter collecting aperture which produces footprints on the earth's surface of 88 to 991 meter diameter at nadir. The collecting aperture of the antenna is offset from the feeds, subreflector, and the electronic equipment assemblies. Tilting and rotating of the subreflector permits fine pointing variations within ±5 beamwidths of the central RF axis. The inner portion of the aperture is used for high frequency operation and the lower frequencies use portions of the aperture up to the full dimension. A surface contour accuracy of $\lambda/32$ is a design goal. For multiple frequency operation of the sensors, multiple diameters of the collecting aperture can be illuminated simultaneously.

Clearly all radiometer studies to date are somewhat conjectural and subject to revision to higher orbit altitudes for acceptable air drag, larger focal lengths for acceptable sidelobe performance and large diameters for usable spot resolution. Although the design tradeoffs are difficult, performance measurements as part of a deployable antenna demonstration are relatively easy, and the data are critically necessary to operational system design.

2.2.3.1 Radiometer Antenna Parameters

Microwave radiometers are covered by the parameters listed below for all systems requiring antennas larger than the payload bay.

• Frequency GHz	0.611	1.4	3	10	19	22
• Wavelength cm	50	21	10	3	1.6	1.4
• Antenna diameter m	700	100	49	25	17	10
• Absolute temperature accuracy			1° K			
• Delta temperature resolution			1° K			
• Beam efficiency			90%			
• Sidelobes, near			-30 dB			
• Sidelobes, far			-10 dBi			
• Signal bandwidth			50 MHz			
• Angular coverage			30 deg			
• Polarization			single, dual, circular			

2.3 KEY ANTENNA CONFIGURATIONS

The majority of projected space systems use either phased arrays or offset parabolic reflectors. Although on-axis parabolic reflectors are used in large ground antennas to produce low-sidelobe antenna patterns, it is not practical merely to use the same configuration in space. For low sidelobes in multi-beam space antennas, it is necessary to use high F/D numbers (F/D = 1 or larger) as opposed to the low F/D numbers (F/D = 0.5 or smaller) that are convenient for single-beam antennas. The large focal length requires a large feed in front of the parabola for each beam, and the beam blockage produced by multiple feeds becomes prohibitive. Fortunately, the offset parabola (Fig. 2-2) can produce sidelobe performance nearly equal to the on-axis parabola, and it avoids the beam blockage problem, as does the space-fed phased-array lens (Fig. 2-3).

There are several types of phased-array lenses: passive, active, and electronically steered. For a discussion of the capabilities and limitations of offset parabolas and the several phased array configurations, see Fig. 2-4.

2.4 DEPLOYABLE ANTENNA TEST REQUIREMENTS

Tests to measure antenna characteristics that are common to all applications are envisioned as a baseline antenna flight experiment. Antenna requirements that are unique to specific applications are envisioned as additional tests that could be performed on the same flight or a later flight.

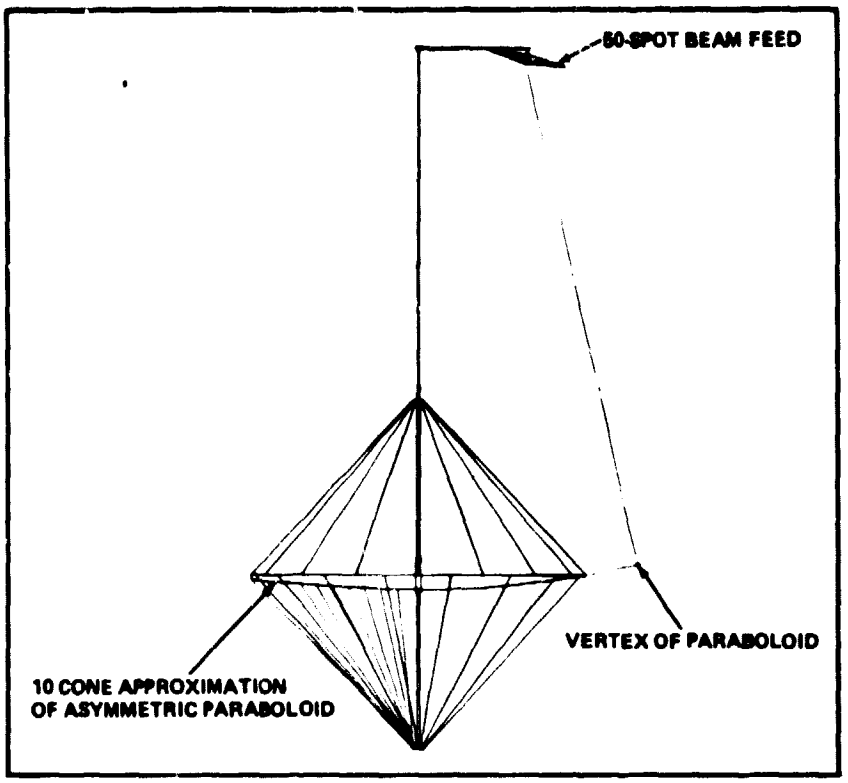

Fig. 2-2 Offset Parabola Configuration

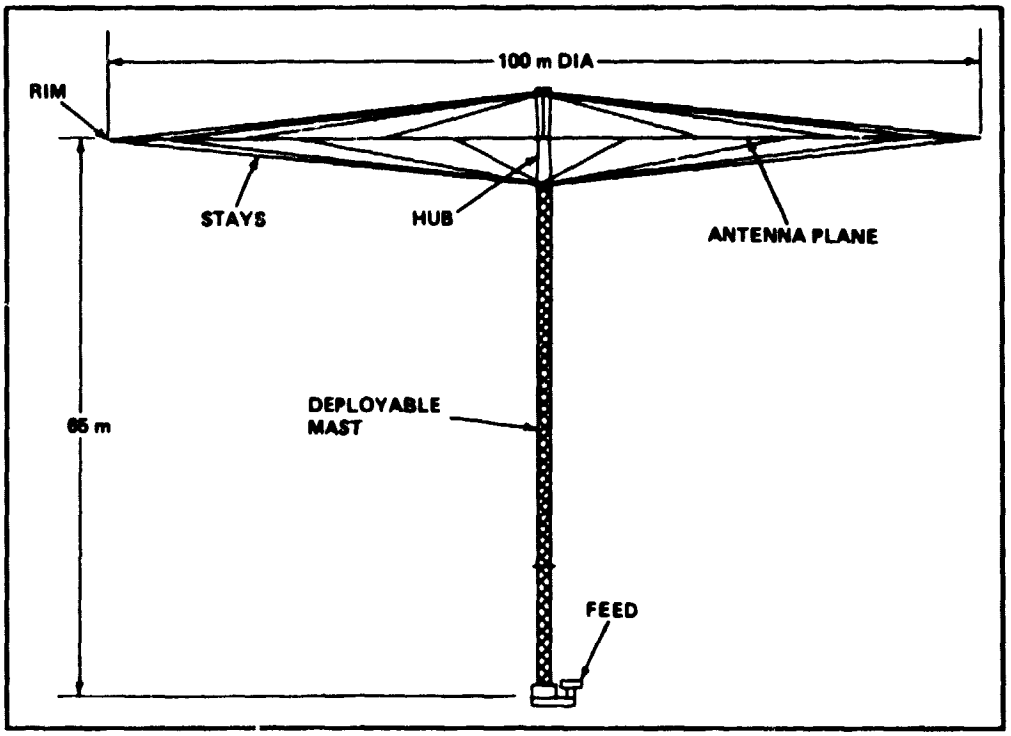

Fig. 2-3 Phased Array (Lens) Configuration

PRIMARY APERTURE	FEED SYSTEM	CAPABILITIES	LIMITATIONS	APPLICATIONS (WITHIN LIMITATIONS)
• OFFSET PARABOLOID	CLUSTER OF HORNS OR OR FEED SUBARRAYS	FREQUENCY BANDWIDTH A REFLECTOR HAS A BROADBAND BEAM-FORMING CAPABILITY. IT IS CAPABLE OF COVERING THE FULL BANDWIDTH ALLOCATED TO ANY OF THE SERVICES. ANGULAR COVERAGE A REFLECTOR IS CAPABLE OF FORMING BEAMS OFF BORESIGHT BY AS MUCH AS 8.5 DEGREES REQUIRED FOR FULL-EARTH COVERAGE FROM GEOSTATIONARY ORBIT. SEE FIGURE 3-61 FOR EARTH LOOKING RADIOMETERS, A REFLECTOR WITH SPECIAL FEEDS (SEE SUBSECTION 3-XX) SHOULD BE CAPABLE OF PRODUCING BEAMS 17 DEGREES OFF BORESIGHT, REQUIRED FOR 6-DAY EARTH COVERAGE FROM 500-NAUTICAL MILE ALTITUDE.	BEAM SPOTS FOR LOW SIDELOBES THE ILLUMINATION OF THE PARABOLOID MUST BE TAPERED, BY FEED DESIGN, TO A LOW LEVEL AT THE EDGE OF THE APERTURE. THE REQUIRED FEED SIZE PRECLUDES PLACING THE INDIVIDUAL FEEDS CLOSE TOGETHER; THE CROSSOVER BETWEEN BEAMS WILL BE 5.7 dB BELOW THE PEAK OF THE BEAM, REQUIRING 5.7 dB (3.7 TIMES) HIGHER RF POWER TO COMMUNICATE WITH GROUND STATIONS LOCATED AT THE BEAM CROSSOVER POINTS. FREQUENCY BANDWIDTH THE BANDWIDTH IS LIMITED NOT BY THE REFLECTOR, BUT BY THE FEED SYSTEM. THE INSTANTANEOUS AND TUNABLE BANDWIDTH CAN BE AS HIGH AS +29 PERCENT OF THE GEOMETRIC MEAN FREQUENCY. OF COURSE THE ALLOWABLE BANDWIDTH IS LIMITED BY REGULATORY FREQUENCY ALLOCATIONS. WITH ONE EXCEPTION (240 TO 400 MHz) THE ALLOCATIONS ARE ±5 PERCENT AND CAN BE COVERED BY BROADBAND HORN OR SUBARRAY FEED DESIGNS. THE UPPER USABLE FREQUENCY OF A REFLECTOR IS SET BY THE SIDELOBE REQUIREMENTS AND IS LIMITED BY THE SURFACE ACCURACY. RANDOM SURFACE ERRORS MAY HAVE A ONE-SIGMA TOLERANCE OF ONE THIRTIETH OF A WAVELENGTH, BUT NONRANDOM LARGE-AREA SURFACE ERRORS MUST BE HELD MORE CLOSELY (ONE HUNDREDTH OF A WAVELENGTH). SIDELOBES FOR ALL SPACE APPLICATIONS, SIDELOBES ARE THE CONTROLLING LIMITATION. WITH TAPER OF APERTURE ILLUMINATION THE FIRST SIDELOBES CAN BE 30 dB BELOW THE MAIN BEAM. WITHOUT TAPER (UNIFORM ILLUMINATION) THE FIRST SIDELOBES ARE 17 dB BELOW THE MAIN BEAM. IN EITHER CASE, WITH CLOSELY HELD SURFACE TOLERANCES, THE ULTIMATE SIDELOBES WILL BE BELOW ISOTROPIC (DOWN FROM THE PEAK OF THE BEAM BY MORE THAN THE ANTENNA GAIN).	1) MULTIBEAM COMMUNICATION 2) MULTIBEAM RADIOMETER. THE RADIOMETER CAN OVERCOME THE BEAM CROSSOVER LIMITATION BY USING A DOUBLE ROW OF FEEDS, STAGGERED BY HALF THE SPACING OF THE FEEDS IN EACH ROW
0820-095B(1)				

Fig. 2-4 Deployable Antenna Key Antenna Configurations and Application (Sheet 1 of 4)

PRIMARY APERTURE	FEED SYSTEM	CAPABILITIES	LIMITATIONS	APPLICATIONS (WITHIN LIMITATIONS)
• OFFSET PARABOLOID	CLUSTER OF HORNS OR FEED SUBARRAYS		SCANNING BEAM SCANNING IS NOT POSSIBLE EXCEPT BY THREE-AXIS STEERING OF THE SATELLITE, OR BY RF SWITCHING BETWEEN FEEDS. LOSSES THERE IS A SPILLOVER LOSS BETWEEN THE FEED AND THE DISH (LESS THAN 1dB WITH TAPERED ILLUMINATION, AND 3 dB WITH UNIFORM ILLUMINATION), AND SOME POWER LOSS IN THE REFLECTOR MESH SURFACE (LESS THAN 0.5 dB).	
• OFFSET PARABOLOID	PHASED ARRAY	FREQUENCY BANDWIDTH SAME AS ABOVE ANGULAR COVERAGE SAME AS ABOVE, PLUS A SINGLE BEAM CAN BE PHASE SCANNED OVER A WIDE ANGLE (± 8.6 DEGREES). A SINGLE SCANNING BEAM CAN BE POINTED EXACTLY AT THE DESIRED POINT' AVOIDING THE BEAM-CROSSOVER LOSS OF MULTIBEAM SYSTEMS.	SAME AS ABOVE	BEAM HOPPING COMMUNICATION
• PASSIVE SPACE-FED PHASED-ARRAY LENS; A FULL BOOTLACE ARRAY WITH FULL TIME DELAY BEAM FORMING, VIA FULL-LENGTH TRANSMISSION LINES INTERCONNECTING THE TWO SIDES OF A FLAT-FACED ARRAY CONSISTING OF TWO ANTENNA PLANES SEPARATED BY A GROUND PLANE (FIGURE 3-61) 0820-095B(2)	CLUSTER OF HORNS OR FEED SUBARRAYS	FREQUENCY BANDWIDTH A FULL BOOTLACE ARRAY HAS A BROADBAND BEAM-FORMING CAPABILITY. ANGULAR COVERAGE CAPABLE OF AS MUCH AS 8.5 DEGREES OF BORESIGHT (SEE FIGURE 3-XX, WHICH APPLIES TO PARABOLOIDS OR LENSES) SIDELOBES SAME AS PARABOLOID	FREQUENCY BANDWIDTH THE BANDWIDTH IS LIMITED BY THE FEED. IT IS ALSO LIMITED BY THE BANDWIDTH OF THE ELEMENTS (SUBARRAYS) USED IN THE PRIMARY APERTURE. IT IS CAPABLE OF ±29% INSTANTANEOUS OR TUNABLE BANDWIDTH. LOSSES FOR LARGE APERTURES, THE REQUIRED LENGTH OF INTERCONNECTING TRANSMISSION LINES IS LARGE, PRODUCING A ONE-WAY POWER LOSS AS LARGE AS 6 dB, IN ADDITION TO SPILLOVER LOSSES	LOW-COST TEST CONFIGURATION

Fig. 2-4 Deployable Antenna Key Antenna Configurations and Application (Sheet 2 of 4)

PRIMARY APEPTURE	FEED SYSTEM	CAPABILITIES	LIMITATIONS	APPLICATIONS (WITHIN LIMITATIONS)
• PASSIVE SPACE-FED ZONED LENS, SAME AS ABOVE EXCEPT USING MODULO 2-pi TRANSMISSION LINES TO INTER-CONNECT THE ANTENNA PLANES (FIGURE 3-61)	SAME AS ABOVE	FREQUENCY BANDWIDTH INVERSELY PROPORTIONAL TO DIAMETER	FREQUENCY BANDWIDTH THE INSTANTANEOUS BANDWIDTH IS LIMITED BY PATH LENGTH DIFFERENCES ACROSS THE APERTURE TO ABOUT THE VELOCITY OF LIGHT DIVIDED BY THE DIAM-ETER. FOR EXAMPLE, A 100-METER ZONED LENS HAS A BANDWIDTH OF $\frac{\text{300 M PER MICROSECOND}}{\text{100 M DIA}}$ = 300 MHz	LOW COST TEST CONFIGURATION
• PASSIVE SPACE-FED ZONED LENS WITH DIODE-SWITCHED PHASE SHIFTERS	SAME AS ABOVE OR SINGLE FEED	FREQUENCY BANDWIDTH INSTANTANEOUS BANDWIDTH SAME AS ABOVE. TUNABLE BAND-WIDTH CAN BE ±29% OF CENTER FREQUENCY BECAUSE PHASE CAN BE ADJUSTED TO TUNE THE ARRAY AND STEER THE BEAM. WITH A SINGLE FEED, THE ARRAY CAN BE DESIGNED TO COVER 20 DEGREES OFF BORESIGHT. MULTIPLE BEAM STABILIZATION A CLUSTER OF BEAMS CAN BE STEERED OVER A NARROW ANGLE (±5 DEGREES) FOR STABILIZATION, ALLEVIATING THE PROBLEM OF 3-AXIS STABILIZATION OF THE SPACECRAFT AND ANTENNA.	FREQUENCY BANDWIDTH INSTANTANEOUS BANDWIDTH LIMITED AS ABOVE. TUNABLE BANDWIDTH LIMITED BY BANDWIDTH OF FEED AND BANDWIDTH OF SUBARRAYS. ANGULAR COVERAGE LIMITED TO THE BEAMWIDTH OF THE SUB-ARRAYS IN THE PRIMARY APERTURE. LARGE SUBARRAYS (4 X 4 = 16 DIPOLES) CAN COVER 8.5 DEGREES OFF BORESIGHT. SMALLER SUB-ARRAYS (2 X 2 = 4 DIPOLES) CAN COVER 20 DEGREES. ONE PHASE SHIFTER IS REQUIRED PER SUBARRAY. THIS WORKS OUT TO A NEED FOR AS MANY SUBARRAYS AS THERE ARE BEAMWIDTHS IN THE SOLID-ANGLE COVERAGE OF THE ARRAY. PHASE SHIFTERS REQUIRED WITH A SINGLE FEED AND 8.5 DEGREES SCAN CAPABILITY, A 30-METER ARRAY AT 4 GHz REQUIRES 14,000 PHASE SHIFTERS. THIS NUMBER SCALES UP AND DOWN WITH ANTENNA AREA AND SOLID ANGULAR COVERAGE.	HOPPING BEAM COMMUNICATION

0820-095B(3)

Fig. 2-4 Deployable Antenna Key Antenna Configurations and Application (Sheet 3 of 4)

PRIMARY APERTURE	FEED SYSTEM	CAPABILITIES	LIMITATIONS	APPLICATIONS (WITHIN LIMITATIONS)
• ACTIVE SPACE-FED ZONED LENS; SAME AS ABOVE WITH RF AMPLIFIERS. ONE LOW NOISE AMPLIFIER FOR RECEIVE, AND ONE LOW POWER AMPLIFIER FOR TRANSMIT, PER PHASE SHIFTER.	ARRAY OF FEEDS OR SINGLE FEED	FREQUENCY BANDWIDTH, BEAM STABILIZATION, SIDELOBES AND ANGULAR COVERAGE. SAME AS ABOVE EFFICIENCY HIGH BECAUSE LOSSES THAT ENTER INTO PERFORMANCE CAPABILITY ARE ONLY THOSE FOLLOWING THE TRANSMITTER AMPLIFIERS OR PRECEDING THE RECEIVER AMPLIFIERS	SAME AS ABOVE LOSSES WITH REASONABLE GAIN (15 TO [illegible], THE LOSSES THAT ENTER INTO THE POWER BUDGET AND NOISE FIGURE BUDGET ARE LESS THAN 0.3 dB. COST THE NEED FOR LARGE NUMBERS (10^4 TO 10^5) OF RF MODULES (RF AMPLIFIERS, PHASE SHIFTERS AND LOGIC CHIPS) WILL LEAD TO HIGH COST UNTIL PRODUCTION DESIGN AND AUTOMATIC MANUFACTURE BRINGS THE MODULE COST TO AN AFFORDABLE LEVEL (TARGET $10 TO $100).	1) HOPPING BEAM COMMUNICATION 2) MULTIBEAM COMMUNICATION 3) RADIOMETER 4) RADAR
0820-095B(4)				

Fig. 2-4 Deployable Antenna Key Antenna Configurations and Application (Sheet 4 of 4)

2.4.1 BASELINE REQUIREMENTS

2.4.1.1 Deployability

The first requirement is that the antenna be deployable. It is desirable to have a large ratio between the deployed and launch diameters and to minimize the length of the launch configuration. For the flight experiment, and for certain applications, it is necessary that the antenna be capable of being retracted, or furled, for return to earth in the orbiter payload bay for modification and reuse in later flight experiments.

A key requirement on deployability is that the primary deployable structure be able to deploy reflectors (doubly-curved surfaces) as well as phased arrays which use flat three-layer surfaces. The mesh material used in reflectors can be gathered into a compact volume at launch, but the material used in phased arrays cannot be gathered, but must be rolled up on a cylindrical or double-conical drum.

For large deployable antennas it is necessary that the deployment sequence be slow. It is not acceptable to release a mechanism and allow it to pop open; in large antenna sizes such a procedure is likely to cause structural failures. A demonstration requirement is provision for visual monitoring, via TV cameras with zoom lenses, of the deployment sequence. Part of this requirement is to obtain sun illumination for satisfactory visibility.

The deployability and tolerance-holding properties of large deployable antennas need demonstration, and can only be demonstrated in zero gravity.

2.4.1.2 Loads, Temperatures, and Structural Deformations

The baseline tests should measure the deployed dimensions under conditions that simulate, or exceed, the expected static and dynamic conditions of the projected application systems. It is assumed here that the deployed configuration is a thick structure, one that uses compression members and tension members to maintain the structural figure in three dimensions. Thin structures, including those that have doubly-curved surfaces, will not maintain reasonable tolerances because differential heating causes large bending.

The expected static structural deformations are 3 to 6 milimeters, and the static measurement accuracy should be better than 0.5 millimeter. The dynamic and static deformations are to be measured. In the free flying mission systems, dynamic deflections resulting from RCS thruster impulses are usually smaller than the thermally caused static deformations, but in the shuttle attached demonstration system the orbiter RCS thrusters can be used to excite large amplitudes which can be observed photogrammetrically.

For projection of measured results to larger and smaller sizes, the measurements must include confirmation of the structural vibration analysis by checking the several lowest-frequency vibration modes.

Temperatures and loads must be recorded from thin-film thermocouples and load cells.

2.4.1.3 Antenna Patterns

The RF beam-forming properties of the antenna should be measured, including the beamwidth, level of the near-in sidelobes, and a sufficiently large survey of the far-out sidelobes to confirm the RF uniformity of the primary aperture. These measurements should include off-boresight antenna beams at the scan limit.

2.4.1.4 Efficiency

The beam efficiency (the fraction of the radiated power in the main beam) and the power losses (the fraction of the RF input power dissipated in the antenna) should be measured by: integration over the measured pattern, comparison with a gain-standard antenna and measurement of the noise temperature of the antenna.

2.4.1.5 Intermodulation Interference

The ability to receive signals while transmitting signals is limited by intermodulation products, which result from the simultaneous use of two or more transmitter carriers. Very small non-linearities in conductivity of the antenna and associated structure will cause measurable interference, and the importance of these effects requires that they be measured in the baseline antenna tests. The effects are very sensitive to power level, and should be measured over the expected range of application system power levels.

These measurements are primarily applicable to multibeam frequency re-use communication satellite antennas. Radar and beam-hopping TDMA communication satellites are less vulnerable to intermodulation because they do not transmit and receive simultaneously, and of course there is no problem with receive-only radiometric satellites.

2.4.2 MISSION SPECIFIC ANTENNA TEST REQUIREMENTS

Many of the mission-specific antenna requirements can be, and therefore should be, measured in ground tests. Some, however, cannot be measured or extrapolated from ground tests. In any case, the tests considered are functional tests of the antenna. These tests have the purpose of characterizing the antenna as a component of the system, not to test the application system per se.

2.4.2.1 Communication Antenna Functional Test Requirements

The unique requirements of multibeam communication antennas are beam isolation and the associated requirement for low intermodulation interference, both to allow frequency reuse. The intermodulation is a baseline test. The multibeam performance would be measured by providing a cluster of feeds connected to separate receivers, each of which would be used to record antenna patterns. Thus the signal isolation between separate feeds and the pattern degradation of off-axis feeds would be observed, and littile additional test time would be required.

The unique requirements of a hopping-beam communication antenna are that the beam pointing can be switched quickly (approximately 20 n sec), that off-boresight beam angles can be achieved (up to 8.6 degrees) without excessive grating lobes and that the RF transmit-receive modules will perform reliability. A simple on-axis feed is used; multiple feeds are not required. The system alternately transmits and receives; intermodulation is not a problem. The baseline antenna flight tests are all that are required, because the unique requirements of the hopping-beam antenna can be measured by laboratory ground tests of RF modules. Given the RF modules, the electronic beam-steering capabilities of space-fed phased arrays are known from development of the several large ground systems that are in operational use.

2.4.2.2 Radar Antenna Functional Test Requirements

The beam-steering radar requirements are, like the hopping-beam communication antenna, completely predictable from the baseline antenna flight tests coupled with ground tests of RF modules. The unique requirements of radar antennas are:

- Ground clutter generated by antenna sidelobes must be negligible in comparison to mainlobe targets and mainlobe ground clutter (the mainlobe clutter must be Doppler filtered and is not affected by the antenna)
- The antenna sidelobes must have sufficient amplitude and phase stability to allow adaptive nulling of jamming
- The RF losses in the antenna plane must be low, and known.

These measurement requirements and procedures will be the subject of a later supplement to this final report.

2.4.2.3 Radiometer Antenna Functional Test Requirements

The baseline antenna tests include all measurements required for extrapolation to operational radiometer systems, although uniess the baseline antenna is specifically designed (feeds, focal length, losses, efficiency) for radiometry the flight article would not be directly usable. The antenna noise temperature is more important in a radiometer antenna than for other systems, because a noisy antenna will dilute the noise-measuring capability of the system. Measurement of antenna noise temperature, requiring a low-noise receiver, is part of the baseline tests, however, because it provides a measurement of antenna losses for all applications. Further, the offset parabola or the modulo 2-pi lens are the only low-cost configurations that permit good loss measurements to be made.

2.5 REFERENCES AND BIBLIOGRAPHY

2-1 GAC-MSFC Visit to LaRC on August 23, 1977.

2-2 BMDATC Long Range Sensor Study, Final Technical Report, (Secret), March 15, 1977

2-3 Grumman Aerospace Corporation, Long Range Sensor Study Final Report, Contract DASG 60-77-C-0051, April 1978.

2-4 F. Austin, et al "Dynamic Structural Analysis of 100 Meter Deployable Antenna", Grumman Aerospace Corporation, Memorandum TO-EG-STME-MO-78-66.

2-5 D. O. Reudink et al, "A Scanning Spot-Beam Satellite System", BSTJ, October 1977

2-6 Grumman Aerospace Corporation, CTR/176-469, Adaptive Multibeam Phased Array (AMPA), Proposal in Response to GSFC RFP 5-92174-256, January 23, 1976.

2-7 Aerospace Corporation Report ATR-76 (7365)-1 Vol. IV, Advanced Space System Concepts and Their Orbital Support Needs (1980-2000).

2-8 F. E. Bond, Aerospace Corporation Report ATR-78 (7730)-1, Vol. II, Geo-stationary Platform Feasibility Study, September 29, 1978.

2-9 S. Fordyce, A New Concept for Communications Satellites - "The Switchboard in the Sky," NASA Headquarters.

2-10 Edelson & Morgan, "Orbital Antenna Farms," AIAA, September 1977

2-11 SAMSO, General Purpose Satellite Communications System, ASCVG 2788 G-3503, June 7, 1977, (Secret)

2-12 Microwave Performance Characterization of Large Space Antennas, JPL Publication 77-21, May 15, 1977

2-13 SAMSO, Final Report for Advanced General Purpose Forces Satellite Antenna Study, TR No. 74-71, December 1973

2-14 JPL, Large Space Antenna Configuration Studies, May 18, 1977

2-15 RCA, Multiple Beam Isolation Study (IS-379), March 1973

2-16 J. Ruze, "Lateral-Feed Displacement in a Paraboloid," IEEE Trans. A&P, September 1965

2-17 NASA CR-2894, AAFE Large Deployable Antenna Development Program, Executive Summary, October 1977

2-18 NASA CR-145397 Large Furlable Antenna Study, LMSC, January 20, 1975

2-19 Large Deployable Antenna Shuttle Experiment, (LDASE), AAS 21st Meeting, Paper No. AAS 75-253

2-20 General Dynamics/Convair, Report No. GDC DCL 67-002, "Feasibility Study of Large Space Erectable Antennas."

2-21 A. W. Lowe, "A Brief History of Reflector Antennas," IEEE Professional Group on Antennas and Propagation, Los Angeles Chapter Meeting, January 15, 1976

2-22 I. Bekey, "Integrating Space Developments 1980-95," Astronautics and Aeronautics, February 1978

2-23 J. L. Schultz, "The Space Fed Lens: An Antenna for Space," Paper 5/1, 1979 Electro Professional Program, April 24, 1979

2-24 K. G. Schroeder, "Direct-to-Home TV Broadcast Satellites for the Pacific U.S.," AIAA 7th Comm Symposium, April 24, 1978

2-25 E. Henderson et al, "Visual Teleconferencing Experiments via a 14/12 GHz Satellite System," AIAA 7th Comm Symposium, April 24, 1978

2-26 J. L. Schultz et al, "A Frequency Reuse Direct-to-Home TV Broadcast Satellite System," 7th AIAA Communication Satellite Systems Conference, April 1978

2-27 G. P. Skall et al, "Direct International and Domestic Television Broadcasting by Satellite - A. Myth or Potential Reality," AIAA 7th Comm Symposium, April 24, 1978

2-28 Wilbur Thompson, GSFC Inputs via Telecon of October 10, 1977

2-29 David Atlas, et al, GSFC, "Visions of the Future Operational Meteorological Satellite System," Eascon 1978 Conference, September 25, 1978

2-30 F. T. Veaby et al, GSFC, "Microwave Remote Sensing of Soil Moisture," NASA Earth Resources Survey Symposium, JSC June, 1975

2-31 V. R. Baker et al, U of Texas, "Flood Hazard Studies in Central Texas Using Orbital and Suborbital Remote Sensing Imagery," NASA Earth Resources Survey Symposium, JSC, June 1975

2-32 W. T. Brandon, A. G. Cameron, et al, MITRE Corporation, "An Air Traffic Control System Employing a Ground-Controlled Satellite-Borne Phased Array Antenna," AIAA Comm System Conference, April 6, 1970

2-33 Robert Freitag, NASA, "Overview of Future Programs - USA," Future Programs Session, 15th Space Conference, Cocoa Beach, Florida, April 27, 1978

2-34 SAMSO, Space Based Radar Vol. III Technical, Report No. TR-77-78 (Secret), May 20, 1978

2-35 TRW, Space Based Radar Surveillance Study, Final Report, Report 28086-6021-TR01 (Secret), February 28, 1977

2-36 Woods & Wade, "On the Design of Self-Deploying, Extremely Large Parabolic Antennas and Arrays", IEEE, Mechanical Engineering in Radar, 1977.

2-37 B. P. Miller, "Economic Factors of Outer Space Production," Section 4.2 Land Mobile Communication Services, American Association for the Advancement of Science, 145th National Meeting, January 3-8, 1979.

3 - SYSTEM DESIGN AND DEFINITION (TASK 2)

The definitions of flight system and ground support hardware for selected payload options are described in this section. Following an overview of the configurations examined (subsection 3.1), the three primary activities of Task 2 are addressed:

- Antenna system definition - description of designs with emphasis on structural/mechanical aspects of the deployable antenna (subsection 3.2)
- Design analysis - results of static/dynamic, RF and reliability analyses which support the system design (subsection 3.3)
- Mission experiment payload definition - description of potential radar, communications and radiometry payloads (subsection 3.4).

Additional elements required to complete the system are presented in subsequent subsections including flight support equipment (subsection 3.5) and ground support equipment (GSE) (subsection 3.6).

3.1 PAYLOAD CONFIGURATION SUMMARY

Design efforts during this study phase focused on a detailed definition of a baseline system to provide demonstration of basic, large deployable antenna technology. The payload defined includes both a deployable antenna and supporting equipment required to satisfy a set of baseline test objectives as defined in Section 4. Characteristics of the payload are summarized in Fig. 3-1. The antenna as shown is configured as a passive phased array. While this configuration has been selected for the baseline system, the antenna is designed to be retrievable, thereby retaining the capability for multiple flights with different antenna configurations as described in Ref. 1-1.

Design details presented in this section are based on a reference 100-meter diameter antenna operating at L-band (1.4 GHz). The structure has been specified with the design goal of satisfying error tolerances for a 120-meter antenna operating up to 14 GHz (Fig. 3-2). As indicated, an instrumentation measurement accuracy of 3 millimeters has been estimated for the demonstration system. Therefore, as a practical consideration, assuming the measurement error cannot be substantially reduced, the antenna should be of a size consistent with the allowable and measurement errors; (e.g., the expected deformation should be around 3 millimeters but less than 5 millimeters). An antenna size between 50 and 100 meters meets

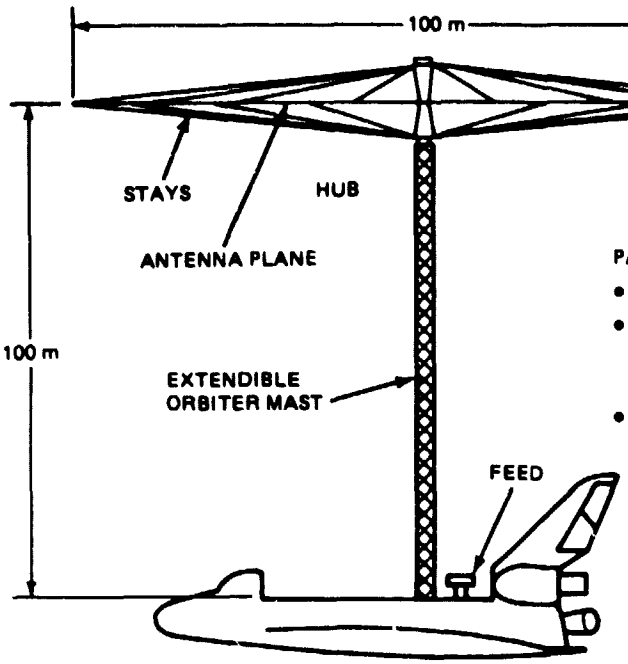

PAYLOAD PARAMETERS

• DEPLOYED SIZE	50 m	100 m
• LAUNCH DIMENSIONS		
LENGTH	8.6 m	12.7 m
DIAMETER	1.32 m	1.7 m
• ELECTRICAL CONFIG:	PASSIVE PHASED ARRAY	

NOTE: SKETCH DEPICTS 100 M CONFIGURATION

WEIGHT BREAKDOWN

COMPONENT	WEIGHT (LB)	
	50 m ARRAY	100 m ARRAY
GORE ASSEMBLY (3 PLANES)	617	2470
RIM MEMBERS (TUBES & HINGES)	176	221
STAY SYS (STAYS, REELS, MOTORS)	40	77
HUB	134	279
STAY PLATFORMS	21	31
DRUM ASSEMBLY	235	442
GORE TENSIONING SYS	46	77
ANTENNA SUBTOTAL	1269	3597
ORBITER MAST	312	625
MAST CANISTER (INCLUDES DEPLOYMENT MECH CLAMPS & RINGS)	110	115
JETTISON SUPPORT MECH & ANT MOUNT	20	30
FWD SUPPORT STRUCTURE	146	294
AFT SUPPORT & ANT PIVOT	310	622
RF SUBSATELLITE (INCL SPIN TABLE)	180	180
INSTRUMENTATION	215	215
UMBILICAL WIRE	150	300
TOTAL PAYLOAD	2712	5978

0820-001B

Fig. 3-1 Flight Configuration

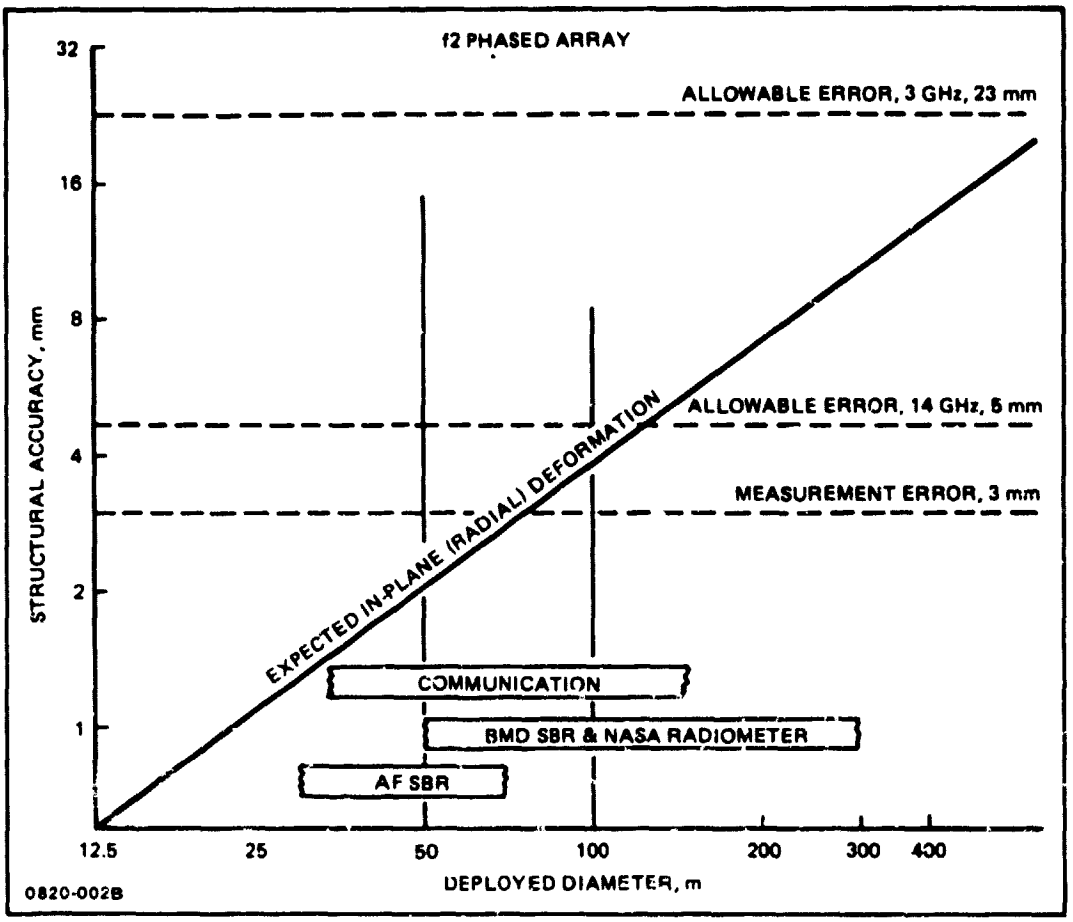

Fig. 3-2 Flight Article Structural Accuracy

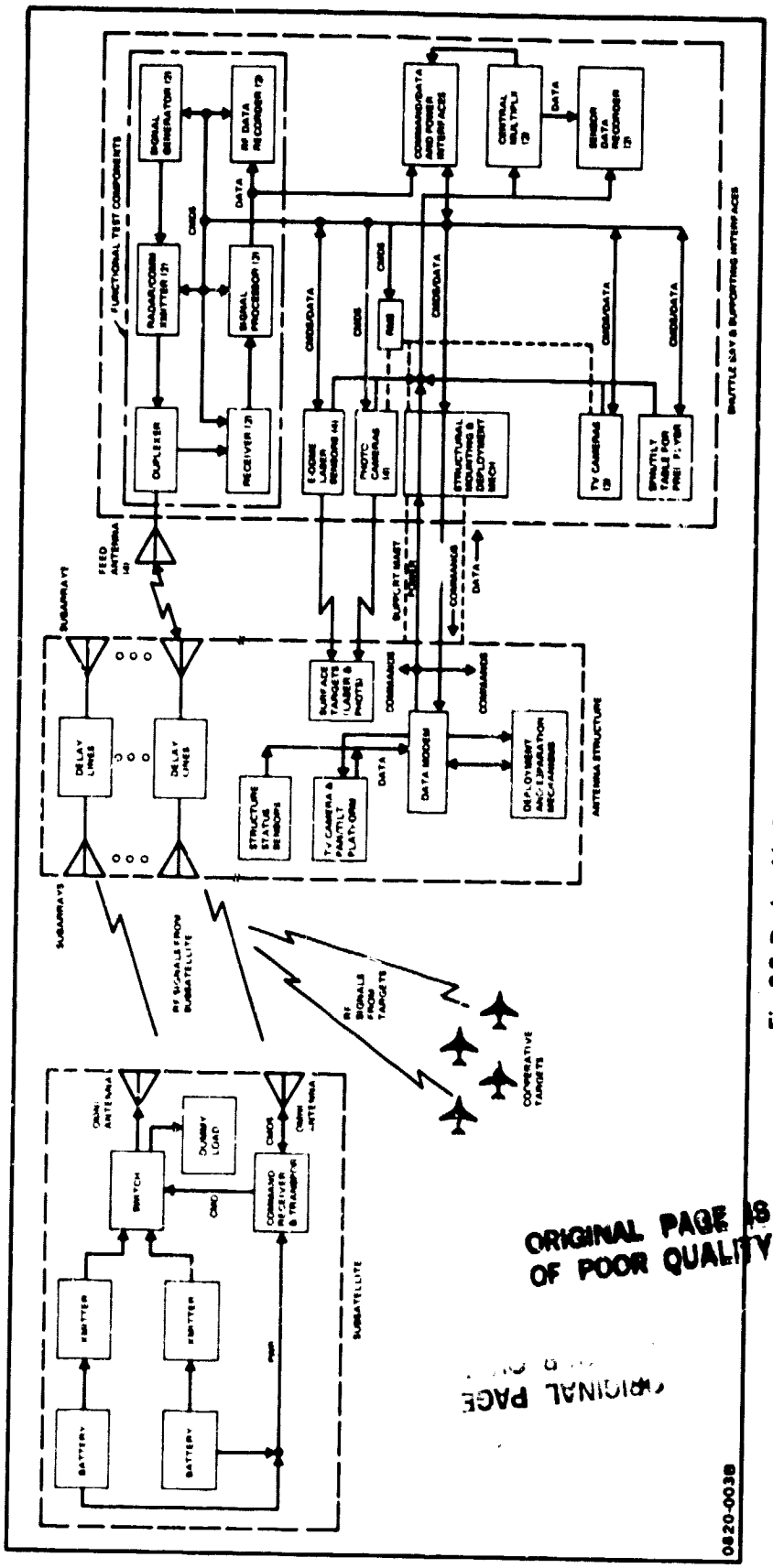

Fig. 3-3 Deployable Antenna Test Block Diagram

this criterion and falls within the band of potential applications. Payload characteristics for a 50-meter antenna are included in Fig. 3-1 as a typical size option.

Potential user requirements will have a greater influence on frequency selection. The initial baseline work assumed 1.4 GHz because this frequency is used for soil moisture radiometry and L-band radar applications. Recent inputs from the radar community indicate the S-band might be a more useful frequency. Changing our design to 3.0 GHz would require modification of design details of the gore assembly and supporting RF electronics with some cost impact on the gore manufacturing complexity.

In summary, the baseline design presented in this section is readily adaptable to a range of size and frequency options. Final selection of these parameters will be based on at least three factors: potential user requirements, confidence in the validity of scaling results up and down to cover the range of applications, and a better understanding of cost and risk drivers. A functional block diagram showing the general location of major components and interfaces is presented for the baseline demonstration as a reference for the detailed design discussions (Fig. 3-3).

The baseline flight test of this system will verify technology parameters applicable to missions in all of the user areas we evaluated. Orbital operations described in Section 4 will:

- Verify lightweight deployment techniques applicable to a variety of antenna types
- Measure the capability of the structure to hold tolerances within specified limits under a variety of environmental conditions
- Verify antenna gain and low sidelobe properties by measurement of RF patterns.

Other parameters which may also be derived from the antenna pattern data include beam efficiency (for radiometry) and sidelobe stability (for radar).

In order to satisfy other unique mission-related test objectives, additional payload hardware may be provided by guest experimenters.

Since user participation in the demonstration program is anticipated, additional payload options, singly and in combination, have been defined. Characteristics of possible experiment implementations are summarized in Fig. 3-4 and described in detail in subsection 3.4. These experiments are only representative of what might be useful payloads based on our assessment of mission requirements in Task 1. Final selection/definition will require additional interface with those users interested in a joint demonstration program to ensure experiment results which support their requirements. Since the primary interface

between antenna and mission experiment is RF, payload development activities will be simplified.

3.2 ANTENNA SYSTEM DEFINITION

Grumman's design of the primary antenna structure uses a deployable wire-wheel configuration described in Ref. 1-1. In the deployed configuration (Fig. 3-5), force is transmitted from the hub to the rim by tension stays. The segmented rim is composed of tubes and hinges (rim nodes). Distortion of the rim is resisted by tension in individual stays, and rim position is controlled by stay stiffness and length. A primary feature of this configuration is the ability of the structure to obtain a predictable shape after deployment and to maintain this shape within predictable tolerance in the operational space environment.

The phased array antenna plane is formed by stretching a number (N) of triangular gore members between N rim members and the hub, with tension supplied by springs at the hub. The deployed gores form a flat surface in the plane of the rim, filling the area between rim and hub.

In the stowed (launch) configuration, shown in Fig. 3-6, the N gores are wound around a tapered drum. The rim tubes form a cylindrical annulus outside the drum.

A partially-deployed configuration is also shown in Fig. 3-6. Energy for deployment is stored in spring systems within the rim tubes near each rim node. Torque from the spring system forces simultaneous rotation and radial translation of the rim tubes since the rim tubes must move outward to permit tube rotation. A mechanism is used at each rim tube end-fitting to ensure that each rim tube rotates through the same angle relative to a rim node and that the rim node attitude remains constant during deployment. A stay is attached to each rim node. Radial motion of each rim tube is restrained by tension in the stay. Stay reel motions are locked together and synchronized with drum rotation (which controls the rate of gore unwinding). Thus, the rate of antenna deployment is controlled by regulating the payout rate of the stays.

During deployment, the rim nodes are constrained by the stays to lie on the surface of a sphere (at any particular instant). When deployment is symmetric, the rim nodes are equally spaced above and below a plane which bisects the hub. The stability of a partially deployed configuration can be visualized most easily when the angle between adjacent rim tubes exceeds 120 degrees. For this condition, it seems clear that the axial displacement of the rim node relative to the others will not impede the rim from reaching the flat (180-degree) position. As the other rim hinges open to flatter angles, they pull the displaced node toward the symmetric position.

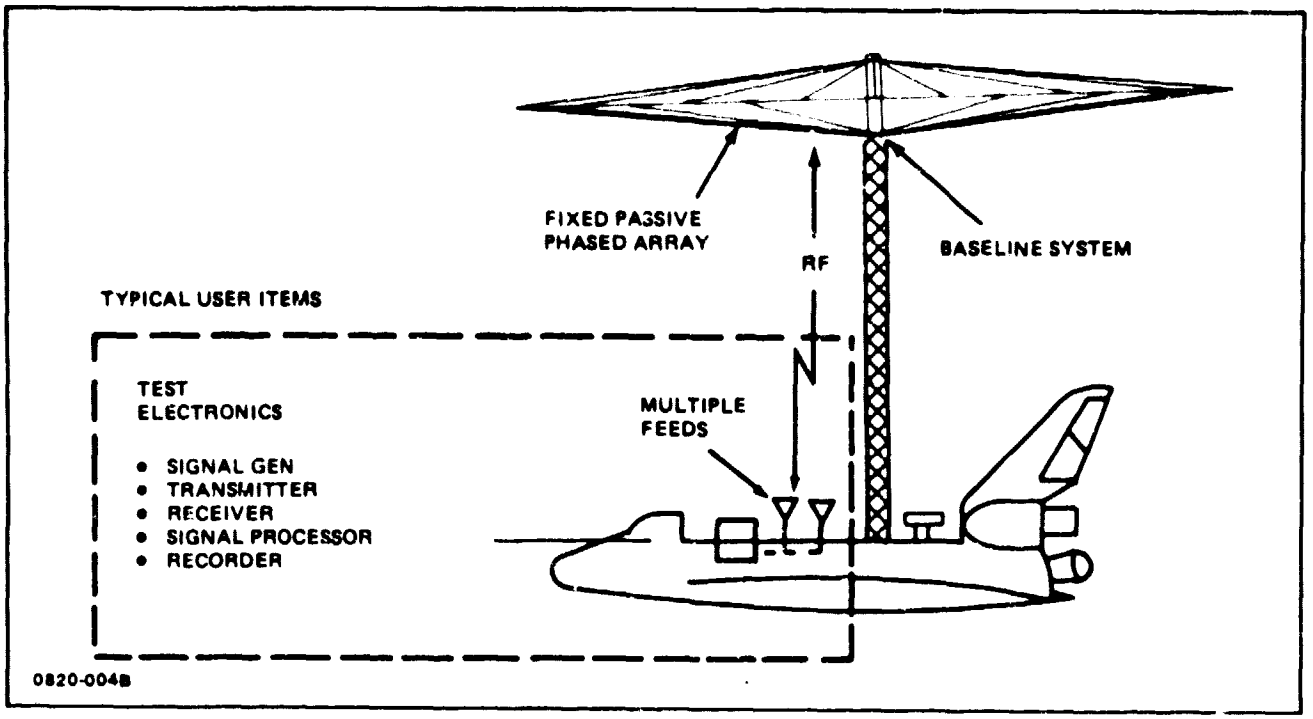

Fig. 3-4 Potential Joint Program

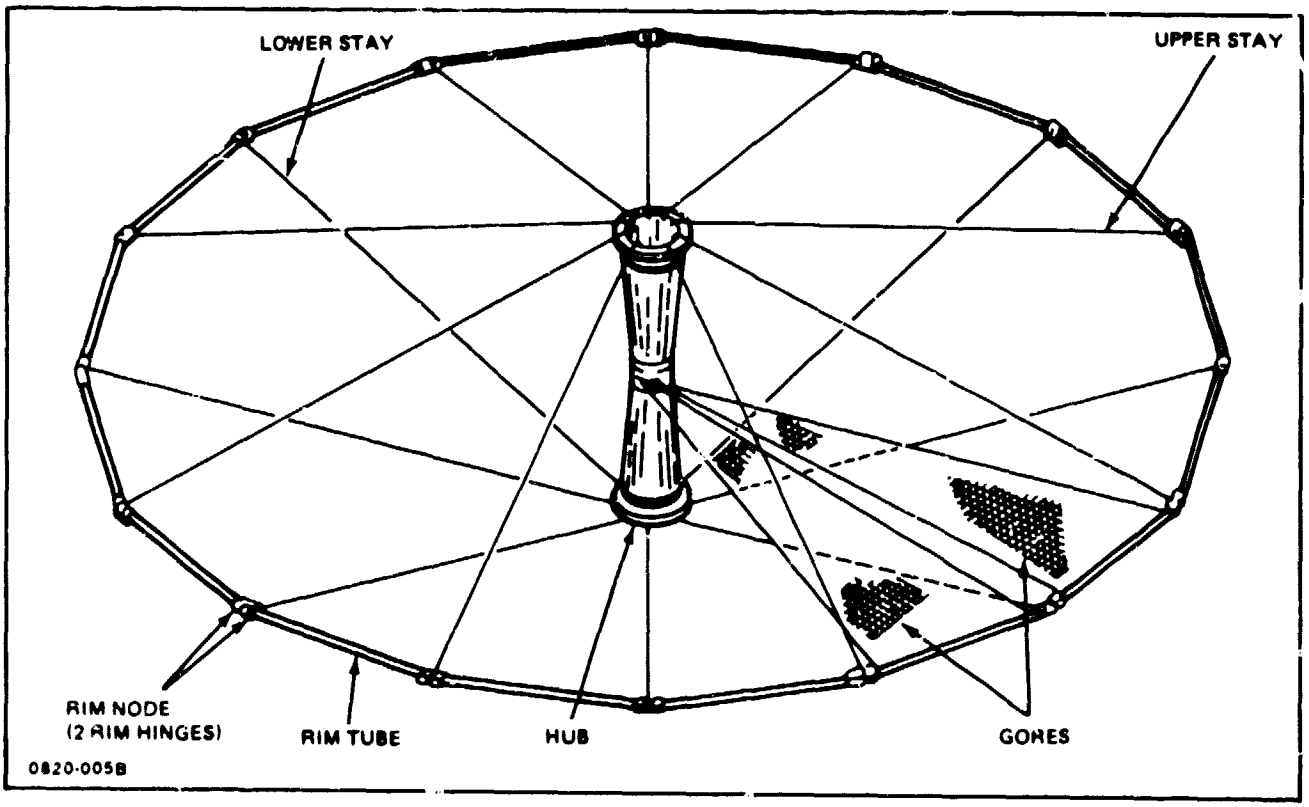

Fig. 3-5 Wire Wheel Schematic – Deployed

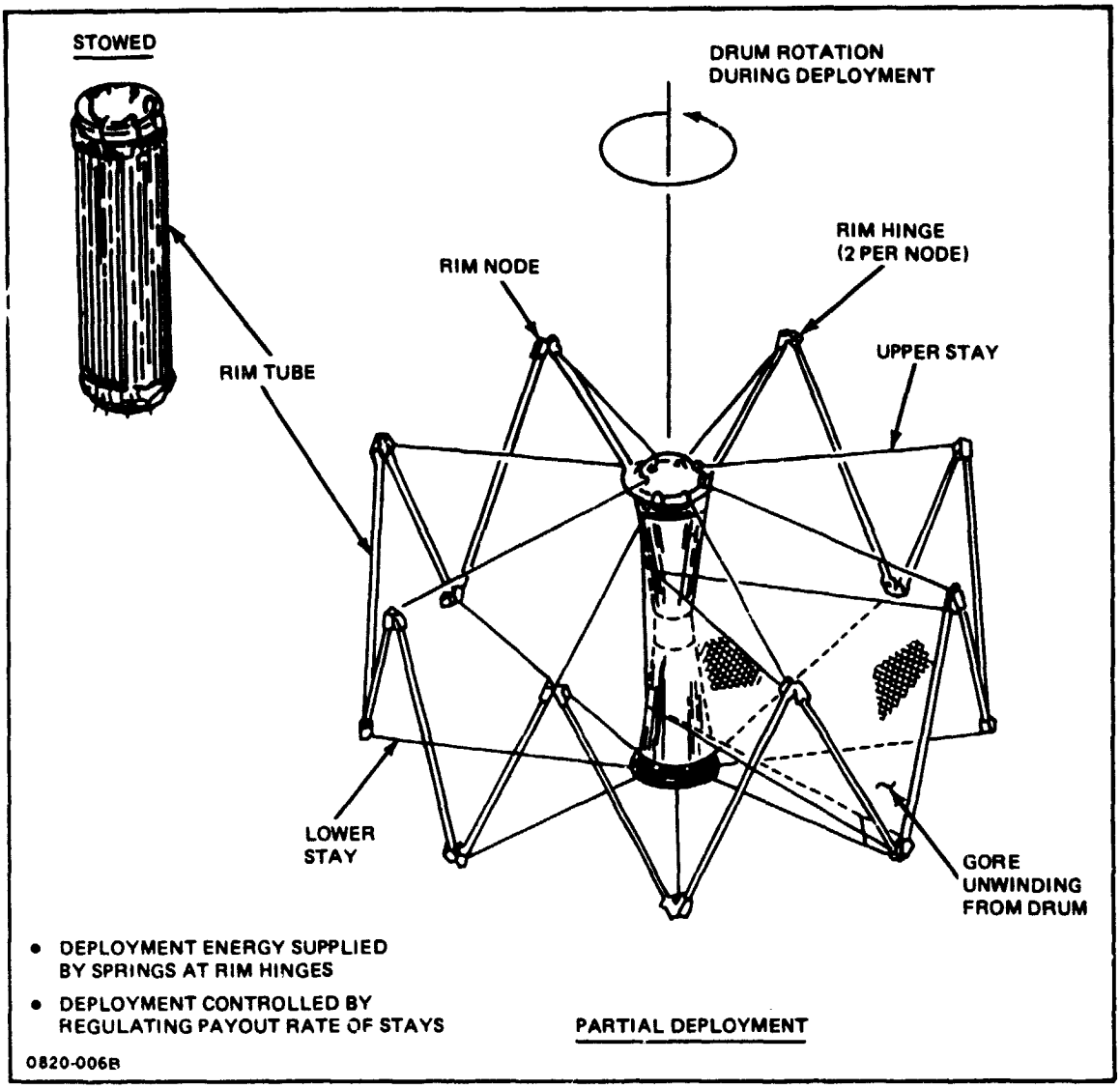

Fig. 3-6 Wire Wheel Schematic – Deployment

To retrieve (furl) the antenna, stay tension is increased until the rim bending moment at a hinge exceeds the torque developed by the deployment spring system. Since gores are attached to rim tubes, they rotate through 90 degrees during retrieval. To initiate retrieval, the gores are rotated 90 degrees by a mechanism at the hub before being wound on the drum.

Designs for each of the major antenna structure components is described in the paragraphs which follow. During this study effort, we have worked on simplification of details to reduce complexity and manufacturing cost. Two key areas examined are the construction of deployable gores and rim hinges.

3.2.1 HUB AND DRUM ASSEMBLIES (Fig. 3-7)

The antenna hub is the primary structural member which supports the stowed and deployed antenna. It has a circular cross section and is fastened at each end to a stay platform. The design is a semi-monocoque consisting of aluminum frames, skin and stringers. The hub can be constructed using standard aircraft manufacturing methods. Aluminum alloys are used as the structural material because the thermal expansion or contraction of the hub is not critical to antenna operation. Special hub frames distribute loads imposed by the drum during launch and deployment. These loads are transferred through bearings supported by the drum. The hub provides stowage space for the mast structure which is secured at one end to an internal frame. External brackets fastened to the hub support the two drum drive motors.

The drum is made in two conical sections joined together by a circular fitting that houses the gore rotating mechanism (see Fig. 3-7). The slight taper of the conical sections provide a level wrap for the triangular gores. The drum is a semi-monocoque structure consisting of aluminum alloy skins, frames and stringers. One frame near each end supports a ring gear that engages the motor driven gear on the hub. This drive system ensures a controlled tension on the gores during deployment and stowage and is synchronized with the stay reel rotation. Tension springs contained in the drum allow movement of the gores dictated by thermal gradients when deployed. Bearings at each end of the drum transmit longitudinal loads into the stay platforms. These bearings also guide the drum during rotation. Bearings mounted on drum frames transmit lateral loads from the drum to the hub. Lock pins at each end prevent the drum from rotating prior to deployment and resist loads in a lateral direction. These pins are driven by actuators so the drum may be re-locked prior to re-entry.

FOLDOUT FRAME

ORIGINAL PAGE IS
OF POOR QUALITY

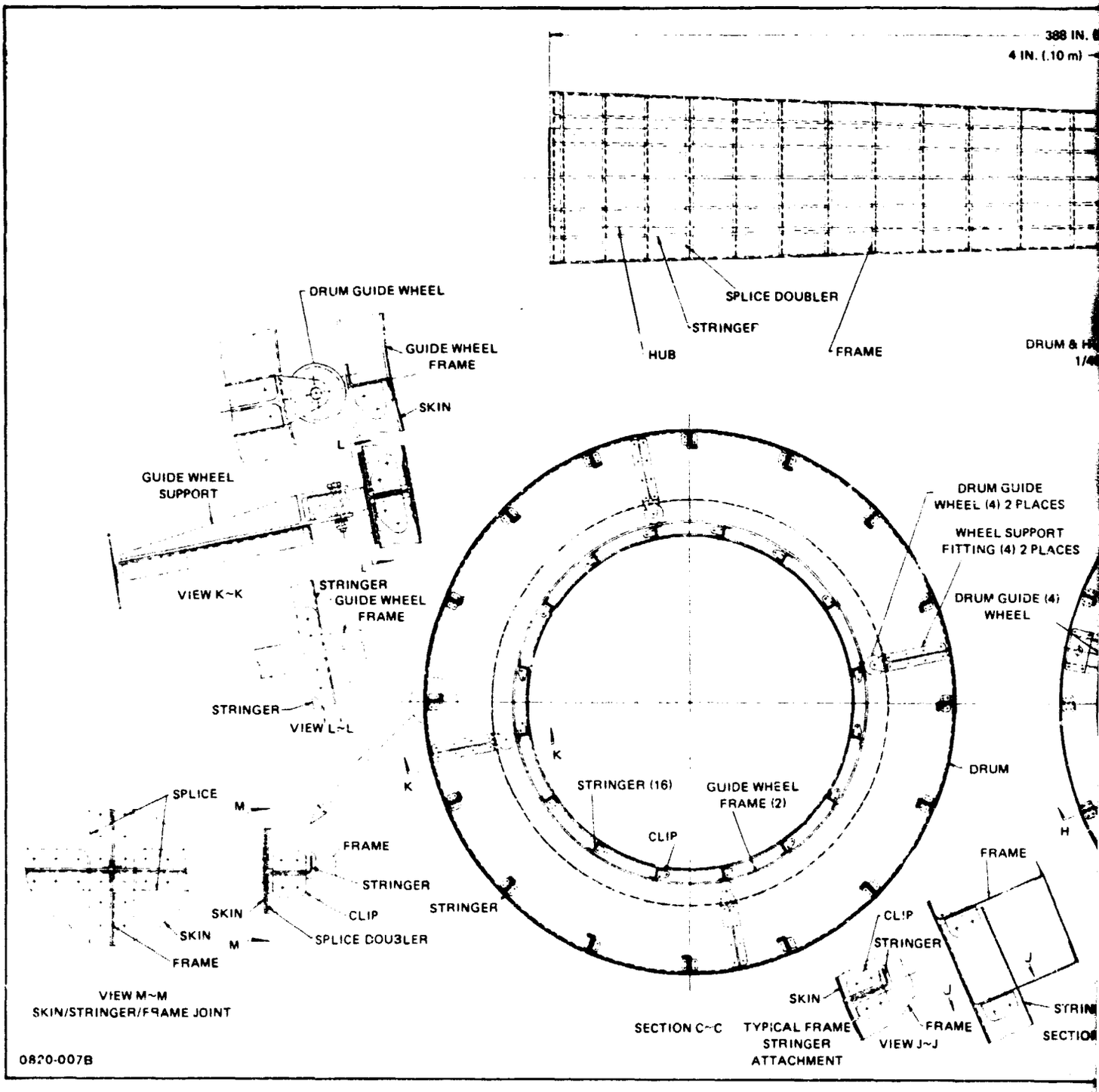

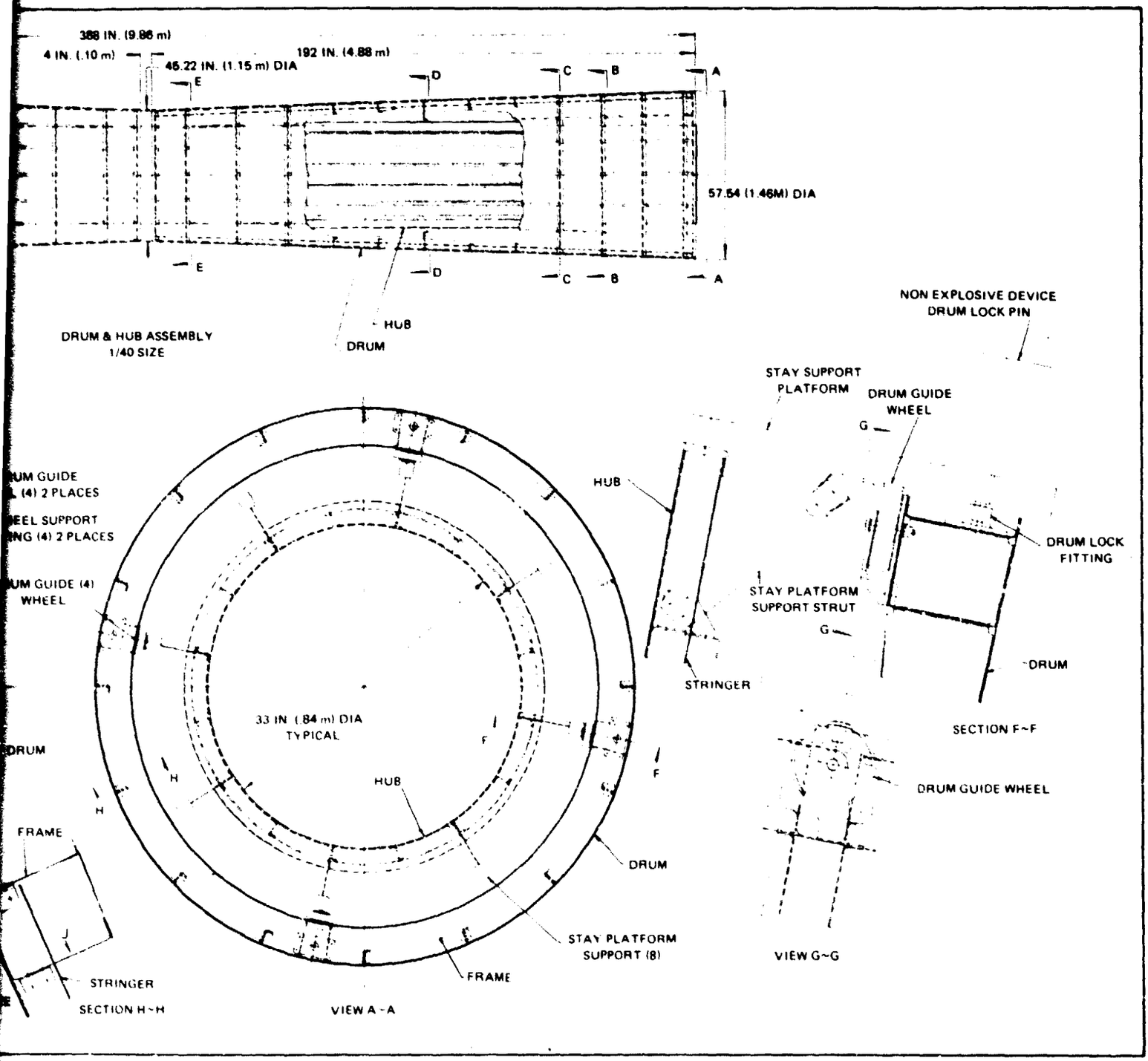

Fig. 3-7 Hub & Drum Assemblies (Sheet 1 of 2)

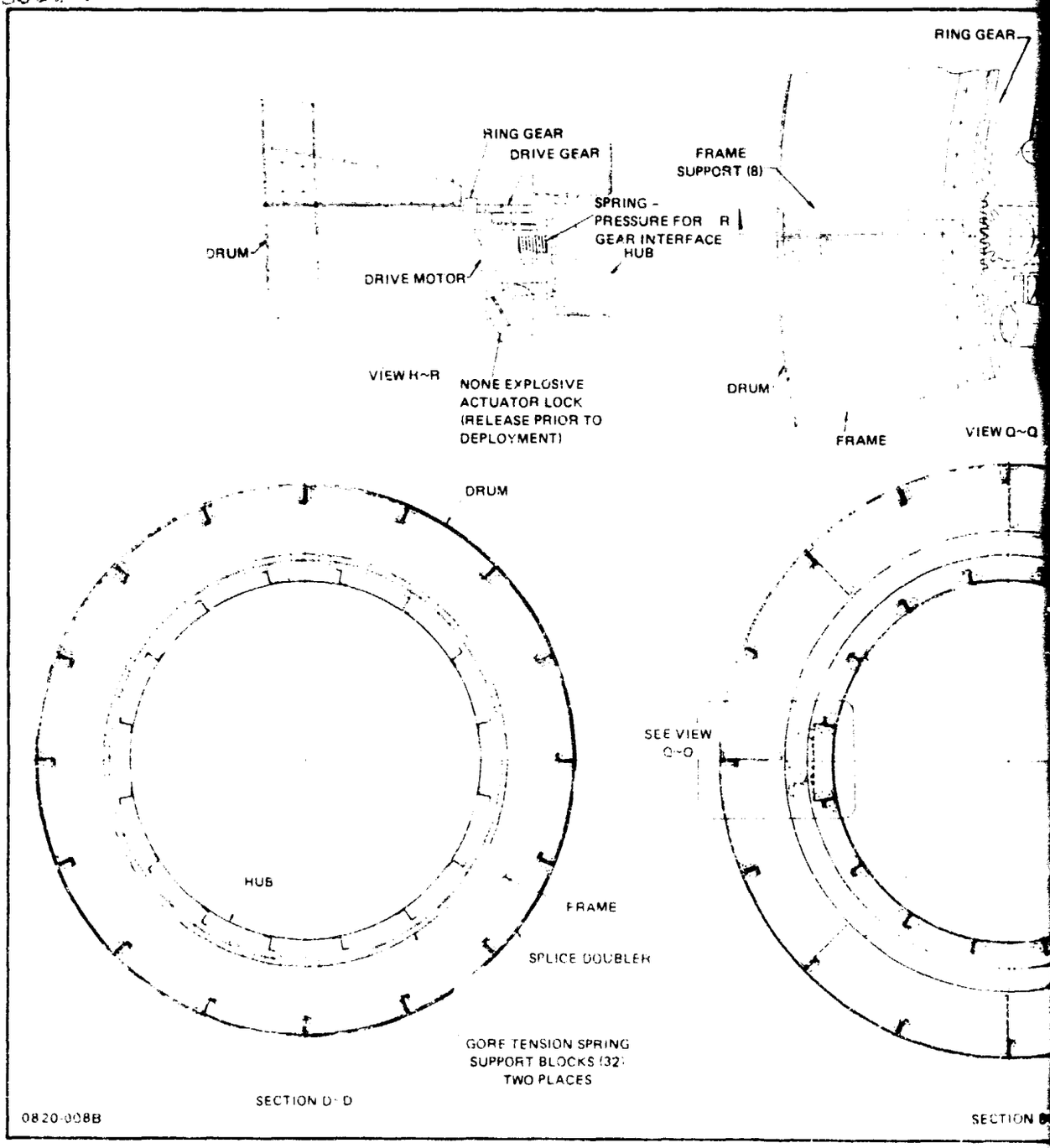

2 FOLDOUT FRAME

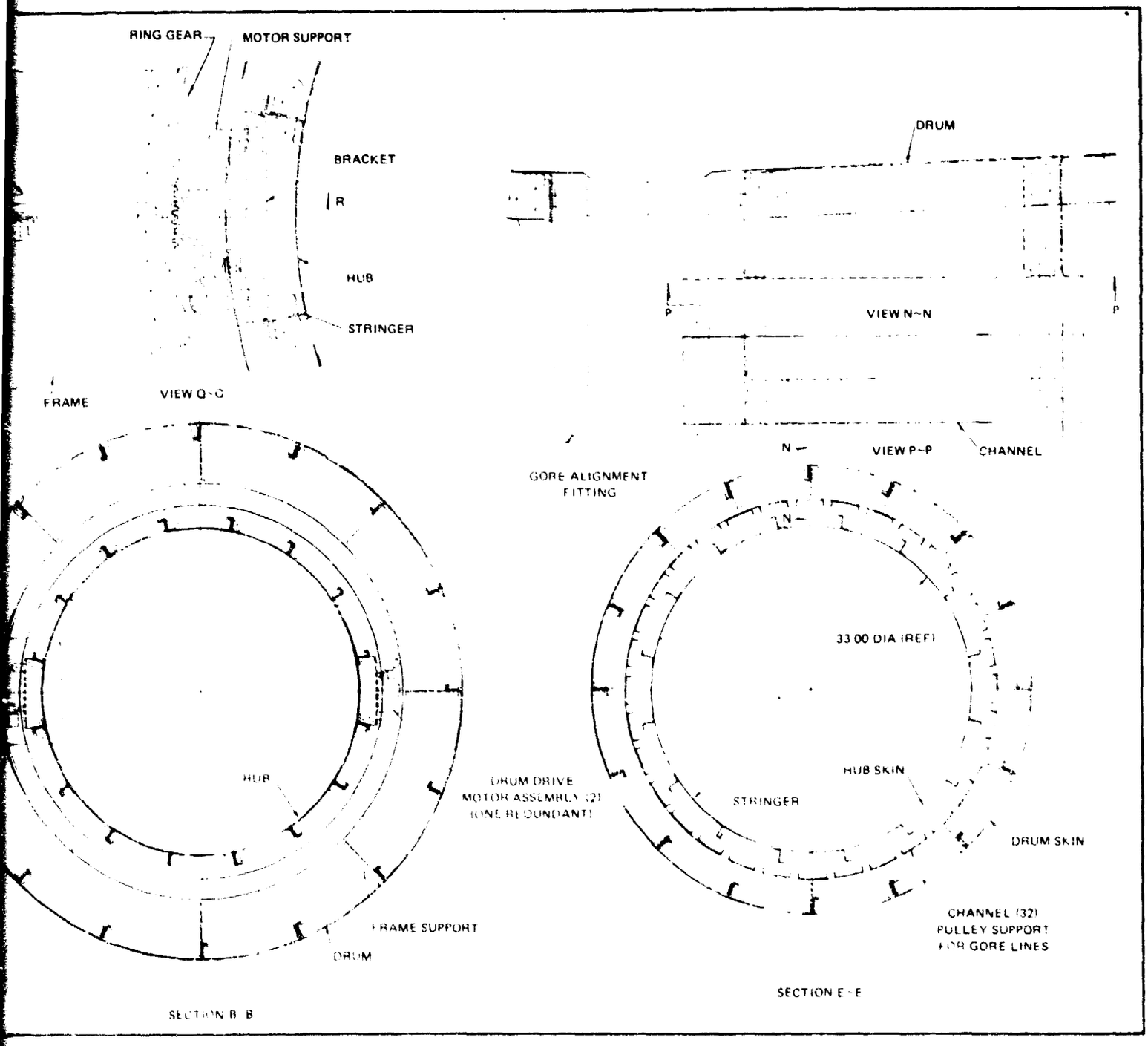

Fig. 3-7 Hub & Drum Assemblies (Sheet 2 of 2)

3.2.2 STAY SYSTEM (Fig. 3-8)

A stay platform is fastened to each end of the hub. It is an aluminum alloy honeycomb structure and supports the stay reel, stay reel drive assembly, stay guide pulleys and the rim members. The stay reel is an aluminum spool on which is wound 16 stays. The stays are 0.005- x 0.375-inch tapes fabricated from graphite/epoxy. Each stay is secured at one end to the reel inside diameter and at the other end to a rim node. Tension in the stays hold the rim members into support fittings which are mounted on the stay platform. These fittings take longitudinal and tangential loads during launch. Rotation of the reel allows the rim members to move radially from the hub to the deployed position at a controlled rate. Opposite rotation pulls the rim members back to the stowed position. The stay reel is driven through a ring gear by a motor assembly. Pulleys mounted on the stay platform align the pay-out and pay-in of each stay. A pin pull mechanism prevents stay reel rotation prior to deployment.

3.2.3 RIM MEMBERS

The 100-meter diameter antenna employs 32 rim members which support the gores at the periphery. The rim members consist of a graphite/epoxy tube 4.25 inches in diameter with a 0.015-inch wall thickness, and with node assemblies at each end. The node assemblies contain the hinge fitting, stay tie fitting, rim equalizing segments and the drive springs. The hinge fitting, stay tie fitting and rim equalizing segments are made of aluminum alloy. The rims are linked together by the hinge fittings (Fig. 3-9), and bending moments in the plane of the rim; tube torsion and compression loads are transferred from tube to node by shear across the hinge pins. Energy for deployment is stored in spring systems within the rim tubes near each rim node. Torque from the system forces simultaneous rotation and radial translation of the rim members since the tubes must move outward to permit tube rotation. A cable running on a pulley in each tube connects the springs together. Tension in the cable provided by the springs produces a torque output of 60-inch-pounds in the stowed position and 30-inch-pounds in the deployed position. A stop on the stay tie fitting limits each rim member to a 90-degree rotation. This rotation is evenly controlled by the equalizing segments.

3.2.4 GORE SYSTEMS

The gore system (radiating membrane) previously reported for space-fed phased array applications is made up of a three-layer structure consisting of two antenna planes on the exterior surface with a ground plane between. Both antenna planes contain an array of antenna elements (dipoles). Arrays on the feed side are electrically connected to subarrays

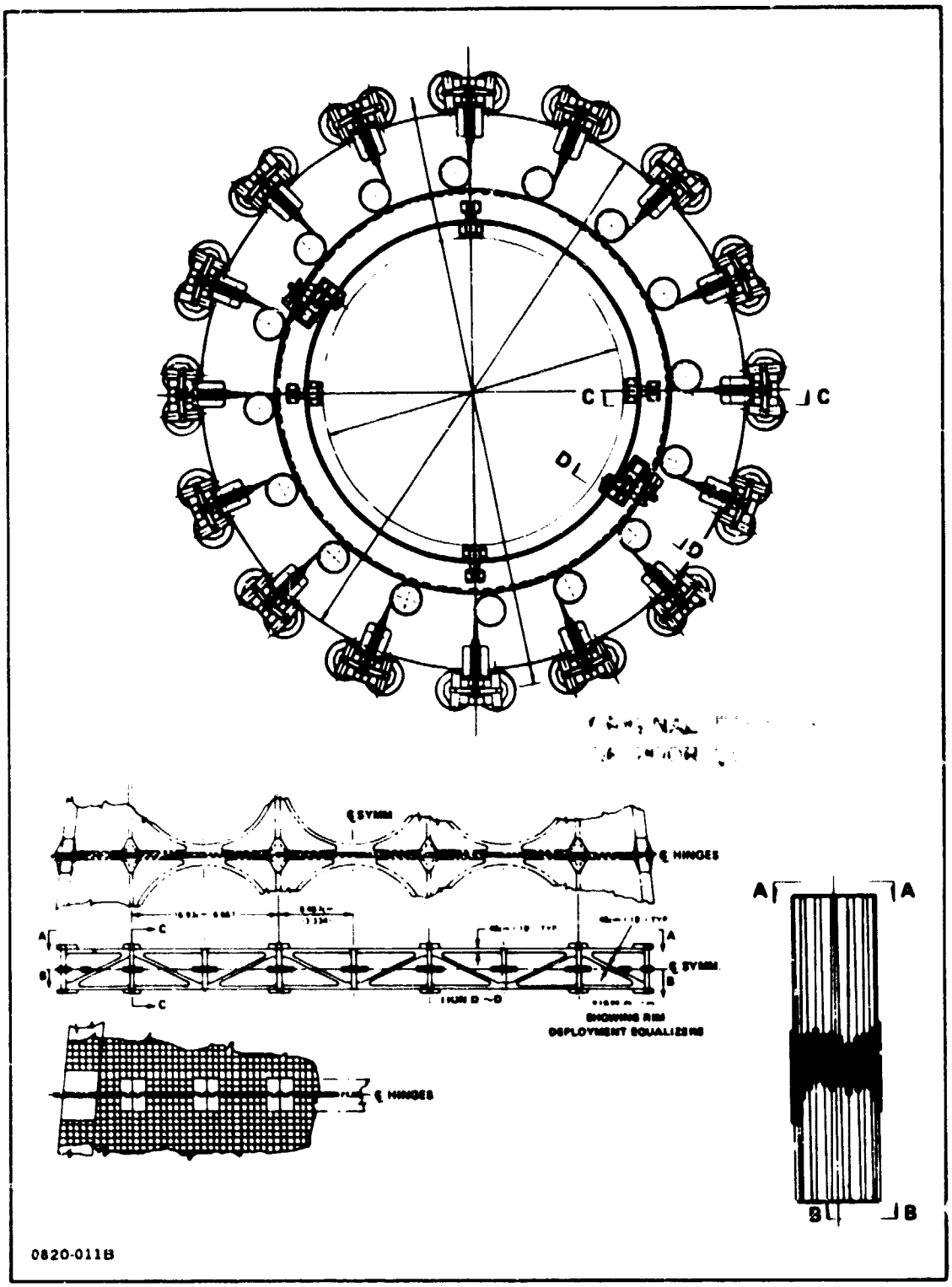

Fig. 3-8 Stay Reel Assembly

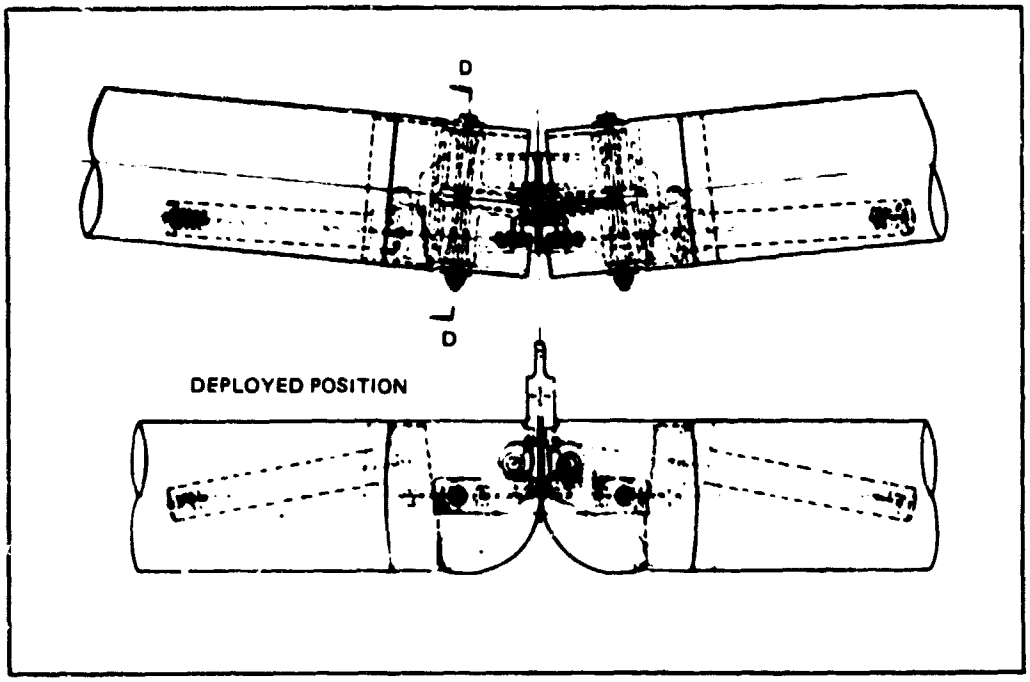

Fig. 3-9 Rim Hinge

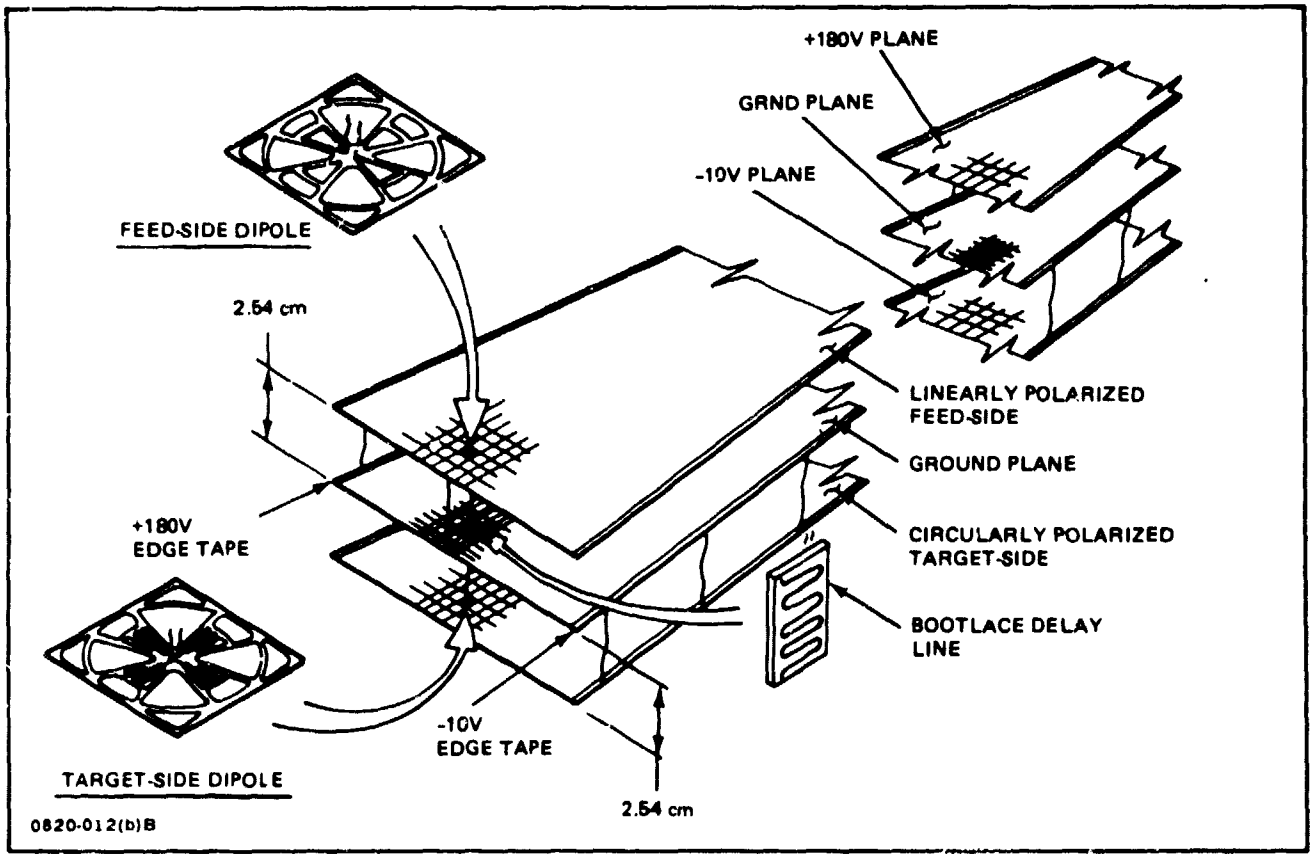

Fig. 3-10 Typical Gore Panel Assembly

on the target side by delay lines as shown in Fig. 3-10. Structural details of the resulting passive phased array configuration are described in Ref. 1-1. The gore is the most complex structural component of the antenna. The three layers, the hinge beams, the springs in the antenna planes and small material gauges used, impose burdens on both design and manufacturing activities. Therefore, we have considered two gore alternatives during the current phase of the study with the objective of simplifying the design. Both designs use slot arrays instead of dipoles and eliminate the requirement for minihinges between planes.

3.2.4.1 Aluminum Foil Three-Plane Gore

The main view of Fig. 3-11 shows a portion of the radiating surface of a phased array antenna. Parts of three gore sectors are shown near the hub region, with the upper portion of the hub removed for clarity. Tension lines, attached to the interior of the drum, pull against the inner portion of each gore sector. The outer regions of each gore sector are attached to the rim (not shown). The continuous aluminum foil surface of each antenna plane is interrupted by a series of dumbbell shaped slots, the radiating elements of this antenna. The slots are arranged in a rectangular pattern, .7λ by .7λ (5.9 by 5.9 inches), wherever enough material exists on a gore sector to provide a complete slot. Approximately 340,000 slots fill a 100-meter diameter antenna. The patterns are parallel for all gore sectors. On the center gore sector of the view shown, the slot pattern is parallel to the centerline (axis of symmetry) of the gore. As the gore sector widens, additional lines of slots are added, leaving a wide strip of continuous aluminum foil on either side of the central line of slots. These strips provide a load path from the hub area to the rim for this gore sector. However, for the gore sector which is at a 45-degree angle to the center gore sector, there are no continuous foil strips to carry tension from the hub region to the rim. Consequently, aluminum edge strips are provided on all gore sectors as the primary tension path. The lowest cost edge-strip arrangement utilizes a straight edge line from hub to rim. However, the edge lines of Fig. 3-11 are a series of intersecting straight lines which approximate the shape of the widest possible gore sector (for a separation distance between antenna planes of 2.5 inches). This was done to display the maximum number of slots within the confines of this drawing; i.e., to minimize the number of slots which are lost because they intersect an edge. To utilize this edge shape, compression carrying members (battens) are required between the symmetric edge kick points. The splice strips shown on the main view of Fig. 3-11 do not perform this function. They are only a manufacturing aid. The splice strips are shown as discontinuous to reinforce the viewpoint that the deployed shape of a gore sector is determined by the interaction of environmental effects and tension in the edge members. Edge-member strain induces tensile strain in the 0.0005-inch thick

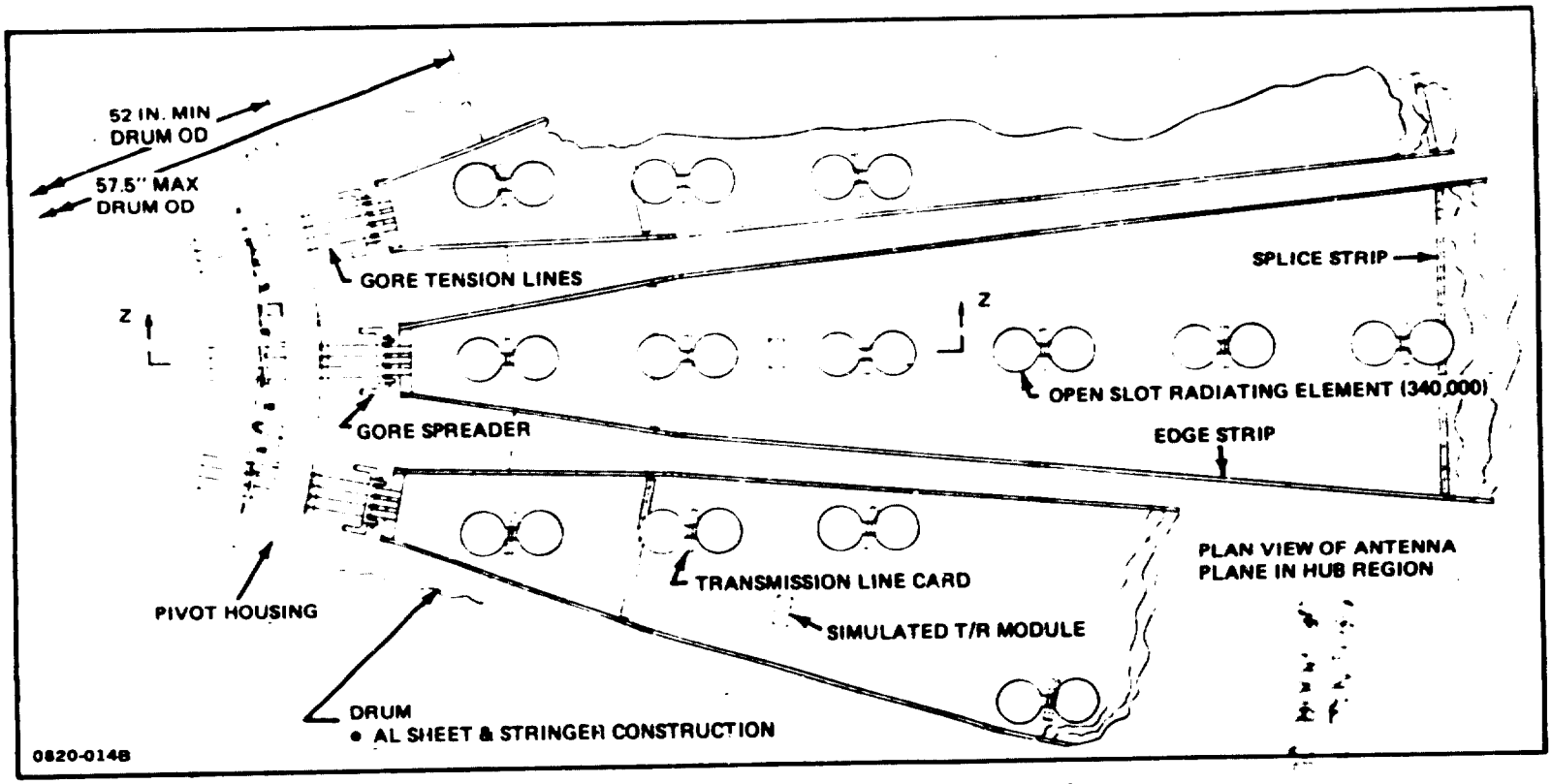

Fig. 3-11 Aluminum Foil Three-Plane Gore (Sheet 1 of 3)

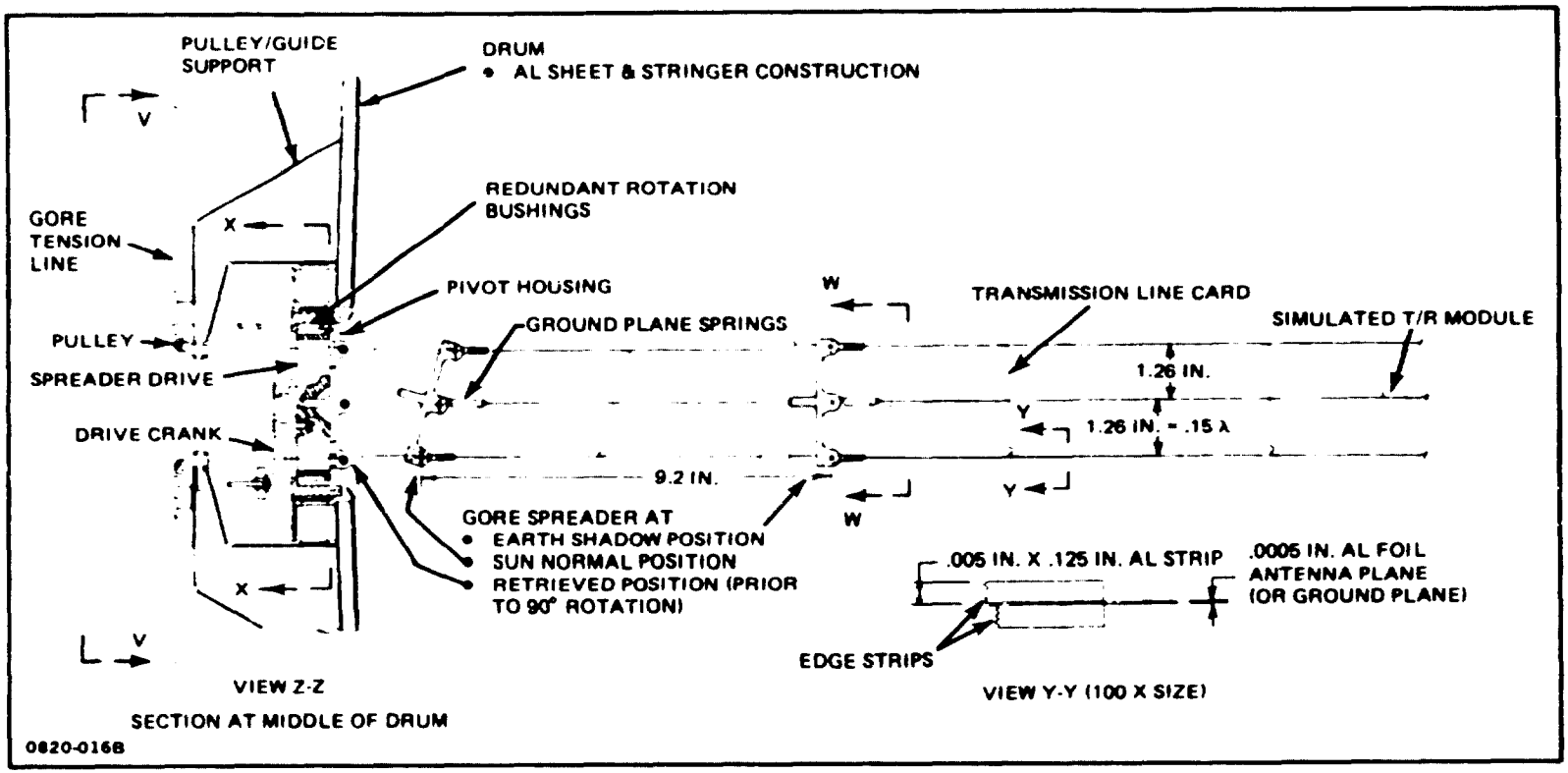

Fig. 3-11 Aluminum Foil Three-Plane Gore (Sheet 2 of 3)

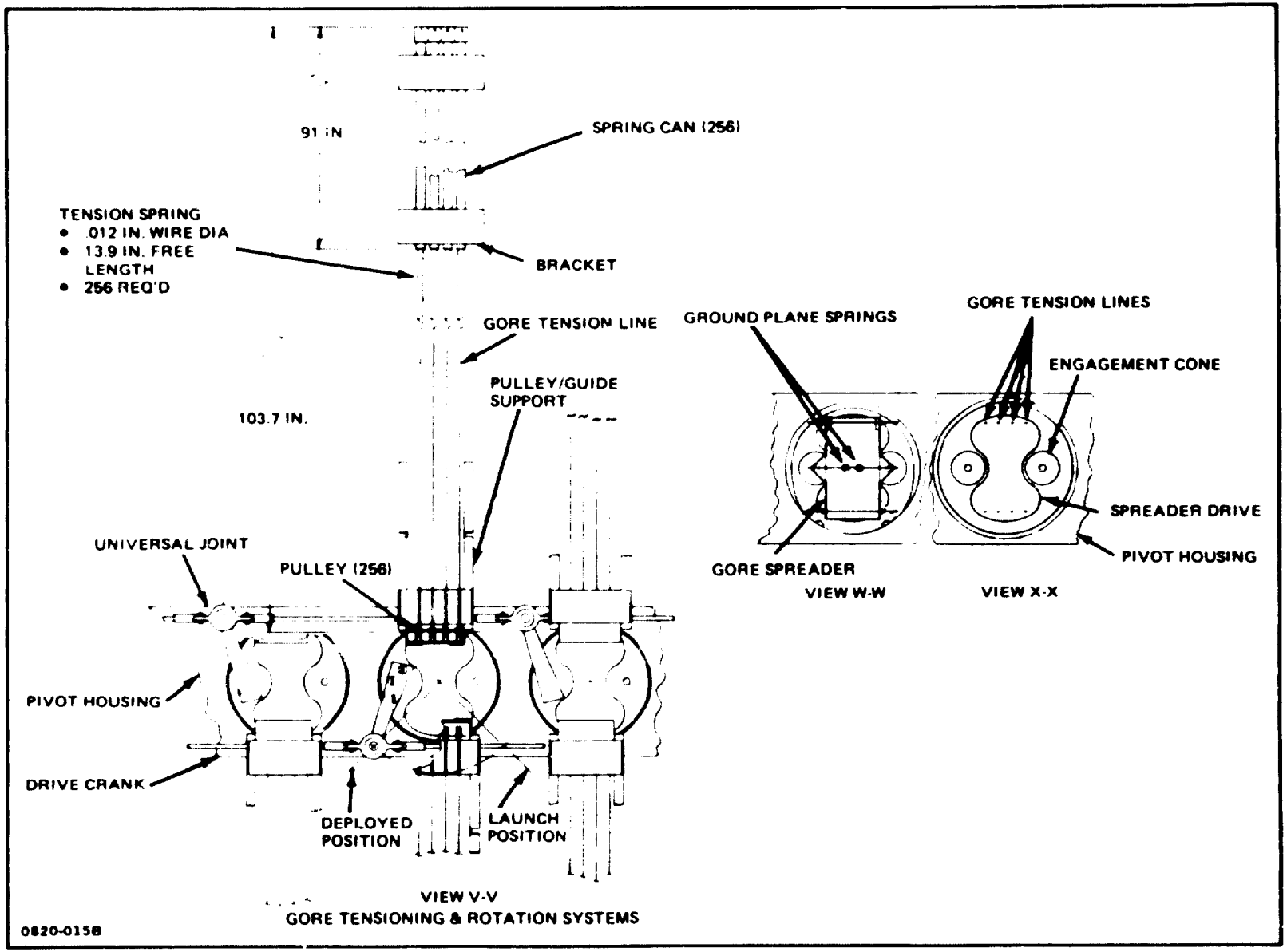

Fig. 3-11 Aluminum Foil Three-Plane Gore (Sheet 3 of 3)

foil surfaces, which has no significant compression carrying capability. Since compression cannot be carried in the foil, it will wrinkle. The expected static shape is analogous to a tension field beam, with diagonal tension in the foil pulling against the edge strips, causing them to bow inward in the plane of the antenna. This expected deviation from a flat surface is seen as acceptable when tolerance requirements are considered. The average (1 sigma) tolerances permitted on the location of a slot (for the more stringent radiometry and radar applications), at an operating frequency of 1.4 GHz, are ±0.26 inches radial and ±2.6 inches axial. Another argument which points to the conclusion that antenna plane surface wrinkles are benign is that, for a constant level of tension in the surface, the position-changes which result from tension wrinkling are constant bias errors. If they become significant, they can be compensated for in a variety of ways. The weight of the three aluminum foil planes, with transmission line cards, splice strips, edge strips and simulated T/R modules, is approximately 2500 pounds.

The drum diameters shown in the main view of Fig. 3-11 are typical of the smallest diameters possible for an antenna of this type. The smallest wrapping circumference (52-inch drum diameter) is based upon choices made for the following parameters: number of gore sectors, axial clearance between adjacent wrapped gore sectors, width of gore edge strips and the separation distance between deployed antenna planes. The largest diameter on the tapered drum (57.5 inches) is determined by the minimum drum diameter, average gore thickness and the maximum diameter of the deployed antenna. Average gore thickness is strongly influenced by the thickness, width and number of T/R modules. This design assumed a 2 by 2 subarray arrangement and a T/R module thickness of 0.125 inches.

View Z-Z (Fig. 3-11) shows some of the gore tensioning and deployment mechanisms attached to the middle of the drum as well as several different positions of the inner portion of a gore. The upper and lower planes of the three layer gore are antenna planes with dumbbell shaped slots. The central gound plane is solid aluminum foil (0.0005 inches thick) and supports the simulated T/R modules. (The T/R modules are not needed for a passive bootlace array. However, simulated modules have been included to reproduce dynamic behavior of an active phased array and to simulate actual packaging during gore wrapping on a drum). The corresponding slots in each antenna plane are connected by a Z-shaped transmission line card which is similar to the one described for the two-plane gore configuration (subsection 3.2.4.2). The top and bottom tabs of the Kapton Z are bonded to the antenna planes. This provides an RF coupling path between the copper transmission lines and the centers of the dumbbell slots. A rectangular hole is provided in the ground plane to permit a transmission line card to pass through without shorting an RF signal. In the main view of Fig. 3-11, the

orientations of transmission line cards are perpendicular to the axis of symmetry (C_L) of each gore sector, and not perpendicular to the axis of symmetry of the dumbbell slots. For a gore sector at 90 degrees to the central one in Fig. 3-11, each tab on the Z is slit down the center. One half tab on both top and bottom are folded 180 degrees before bonding to form a shape that resembles an I-beam cross-section. This is done to maintain an RF coupling at the centers of the dumbbell slots while permitting the cards to offer minimum stiffness and apparent thickness during wrapping on the drum. The transmission line cards also perform a secondary structural function. During orbital operations, all surfaces of a gore will have the same electrostatic charge polarity. Consequently, repulsive forces on the order of 10^{-7} psi are expected. The cards are relatively stiff in tension, and aid in maintaining gore flatness.

The principal technique for maintaining gore shape is tension applied through a gore spreader. The inner end of each antenna plane is attached to a gore spreader with three end fittings which are capable of rotating about their connecting pin (Fig. 3-11, main view). In view Z-Z, the gore spreader is shown slightly rotated at the "sun normal position." In this position, the sun has heated the lower antenna plane to about 68° F. The upper plane is heated by the earth and radiation from the ground plane to about 37° F. The gore spreader has rotated to accommodate the length differences between the two antenna planes. Length changes in the ground plane are compensated by a pair of ground plane springs (view W-W). The largest gore length change occurs when the antenna is immersed in earth shadow and a gravity vector is parallel to the antenna plane. Under these conditions, all three planes are at the same temperature (-300° F), and the lower antenna plane has moved 9.2 inches to the earth shadow position shown in view Z-Z.

To retrieve (refurl) a deployed antenna, stay forces are increased until the rim tubes rotate about their pivots and the entire rim moves radially inward. The gores are maintained under tension by a long-stroke, low spring-rate spring system on the inside of the drum (view V-V). The springs restrict operational gore tension variations to 10%. They have been sized to apply a total of 5 pounds of force to each gore sector. As retrieval progresses from the "earth shadow" position, the two probes on each end of a gore spreader (see main view) encounter two conical surfaces (engagement cones) on a spreader drive (see views Z-Z and X-X). The spreader drive probes are forced into the engagement cones by the geometry of gore tension lines; the shape of the opening in the spreader drive (see view X-X - the kidney shaped opening) which is shown is schematic only. Four tension lines are used for each antenna plane, for redundancy. In the event of failure of one tension line it is important to have at least one remaining gore tension line on each side of the gore

centerline. As the rim continues to move radially inward, the gore spreader is pulled into its retrieved position within the spreader drive (see view Z-Z), and the gore becomes slack. A gore rotation drive, consisting of redundant electric motors, three gear meshes and two power transmission paths composed of pushrods and drive cranks, is used to rotate the gore spreaders 90 degrees. Part of the power transmission path is shown in view V-V (Fig. 3-11). Drive cranks are fastened to each spreader drive. The upper pushrods and universal joints connect every other spreader drive until a closed loop is formed around the drum for 16 spreader drives. A similar closed loop is formed of the lower pushrods and universal joints. For retrieval, both the upper and lower loops move to the right (in view V-V, from deployed position to launch position). This produces opposite-sensed rotation on adjacent gores (to correspond with the opposite-sensed rotation of adjacent rim members) as the spreader drives rotate within the pivot housing. Redundant rotation bushings (view Z-Z) are used to accommodate this rotation. After completion of the 90-degree rotation, the drum is rotated about its centerline until the edges of the gores are made taut by the stationary rim. As this occurs, the antenna planes and ground plane rotate 90 degrees with respect to the gore spreader and lie flat against one another. Rim retrieval and drum rotation are resumed with tension in gore edge strips. The tapered surface of the aluminum drum (view Z-Z) is completely covered with a thin (e.g., 0.002 inches) adhesive transfer tape (e.g., silicone, acrylic neoprene). As the tapered gore sectors are wound on the tapered drum, the inner (upper in view Z-Z) surface of all edge strips on all antenna planes and ground planes adhere to the drum. This adhesive attachment of edge strips to the drum is the load path for gore loads during launch and re-entry. An adhesive with 90-psi shear strength permits this attachment technique to withstand 100-g and higher launch accelerations. By designing small clearances (e.g., 1/8 inch) between wrapped edge strips, the foil surfaces of the gores are prevented from contacting the adhesive drum surface. The peel strength of these adhesives is approximately 85 ounces per inch of width. This implies that gore tension of approximately 4 pounds will be required to deploy the antenna from the launch configuration.

3.2.4.2 Graphite/Epoxy Two-Plane Gore

Figure 3-12 shows a different technique for implementing a bootlace phased array antenna at 1.4 GHz. The main view displays part of an antenna plane whose radiating elements are rectangular slots in a continuous RF conducting surface. The slots are arranged in the same rectangular pattern as the antenna, (Fig. 3-11), 5.9 inches by 5.9 inches. The gore is composed of only two planes. Both are antenna planes. One receives energy from the feed and the other radiates energy to the target. The principle RF connection between the two planes is a transmission line card. A distinctive feature of this

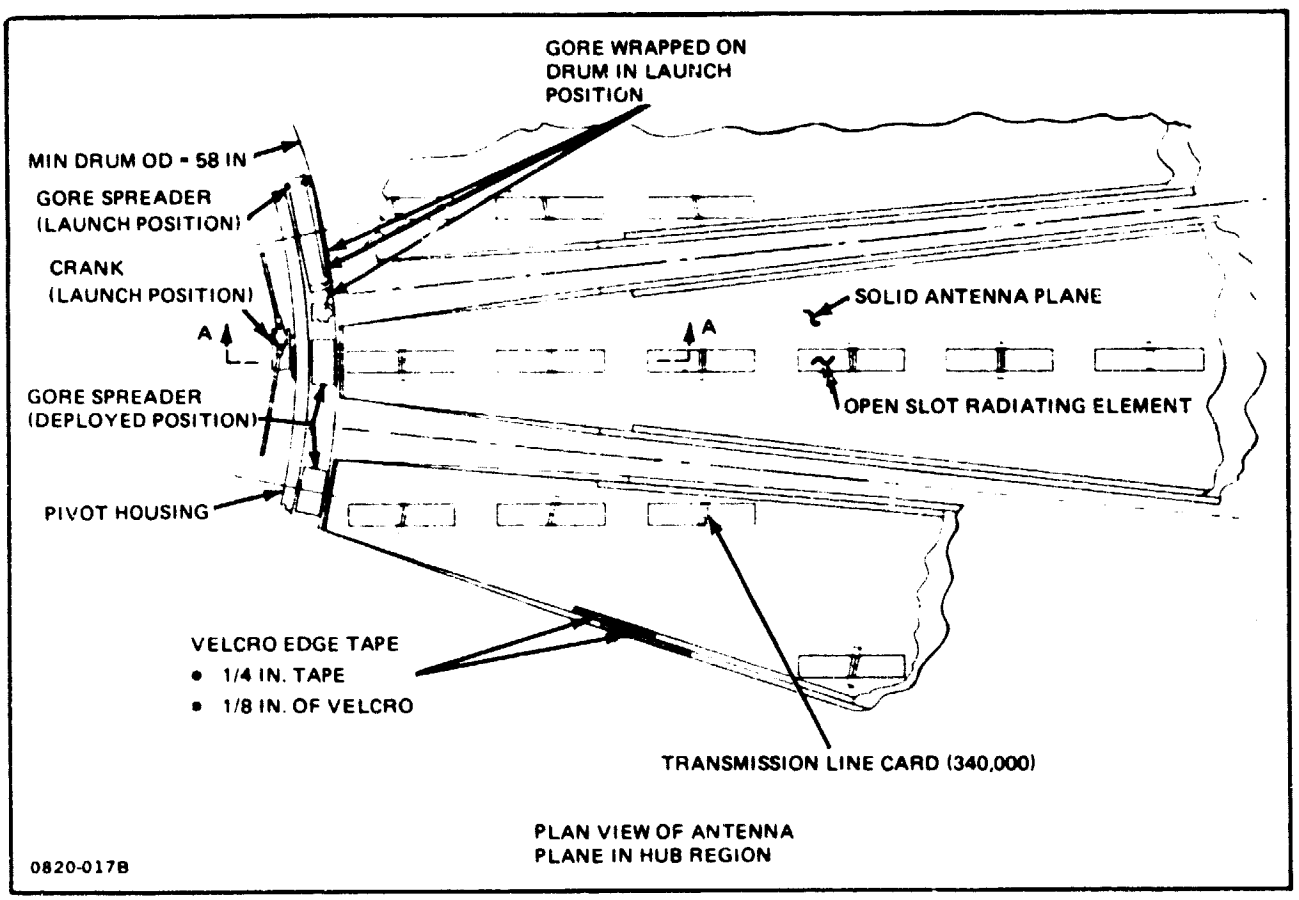

Fig. 3-12 Graphite Epoxy Two Plane Gore (Sheet 1 of 3)

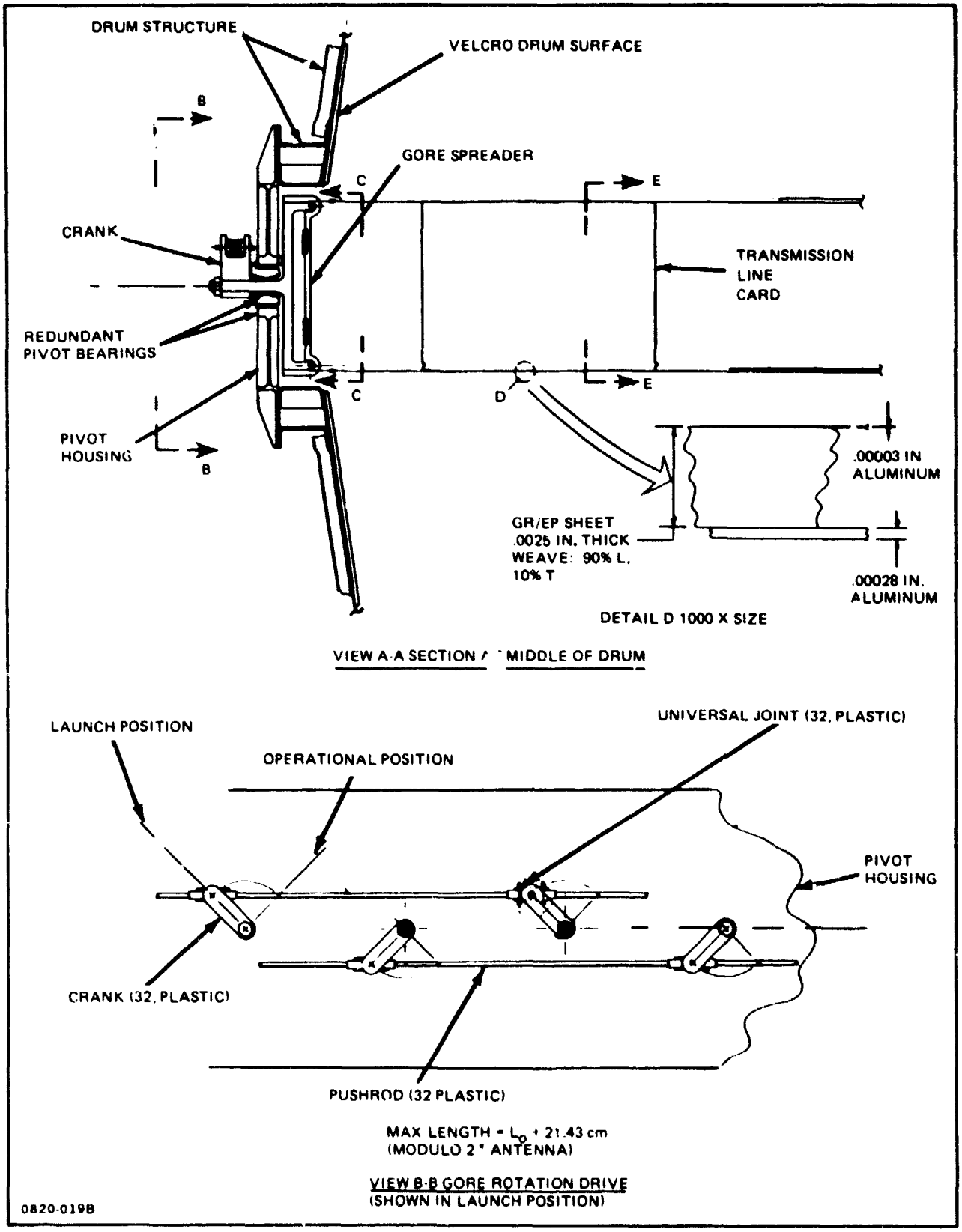

Fig. 3-12 Graphite Epoxy Two Plane Gore (Sheet 2 of 3)

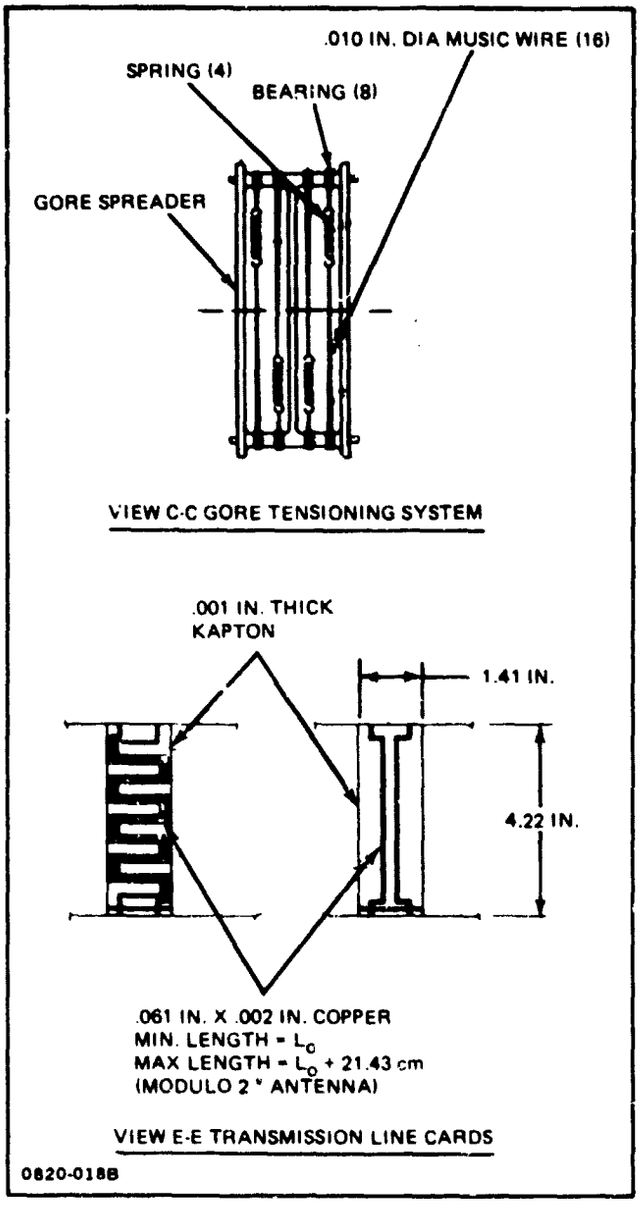

Fig. 3-12 Graphite Epoxy Two Plane Gore (Sheet 3 of 3)

design is the absence of a ground plane, whose normal function is to isolate the radiated energy of one plane from the other. A powerful technique for isolating the feed and target sides is to build the two antenna planes with their slot patterns at 90 degrees to each other. Thus, the polarized energy from a feed slot would not excite the oppositely polarized target slot. A disadvantage of having the two slot patterns orthogonal is that it increases the number of slots whose shape extends beyond the edge of a gore sector (see main view of Fig. 3-12). This reduces the number of radiating elements and may disturb the radiation pattern.

The principle structure of the antenna surface is a woven and cured graphite epoxy (GR/EP) cloth (see detail D, Fig. 3-12). Ninety percent of the graphite fibers are longitudinal. The remaining 10% are in the transverse direction (i.e., perpendicular to the gore). The inside surface has a thin film of aluminum (on the order of 3×10^{-5} inches) to protect the GR/EP from the degradation produced by ultra violet light. To conduct RF energy, the outer radiating surface thickness is chosen as 3 skin thicknesses. For 1.4 GHz energy, this implies an aluminum thickness of 0.00028 inches. Consequently, a likely outer surface is 0.3-mil aluminum sheet, bonded to the GR/EP substrate. The GR/EP cloth is fabricated in 36-inch widths. An overlap joint 1/8-inch wide, will be used to form the gore sectors (which are 32 feet wide at the rim). The upper edges of each plane (view Z-Z) are bonded to Velcro edge tapes. These tapes provide a load path to the drum, which is covered with a Velcro surface, during launch and re-entry. The rectangular holes (slots) go completely through each antenna plane. They produce the only region of unprotected GR/EP (the perimeter of the slot) on the antenna. The weight of the two GR/EP planes, including edge tapes and transmission line cards, is approximately 4000 pounds. The cost of purchasing and curing the graphite epoxy material is approximately $320,000 per antenna (assuming a quantity price of $80 per pound, and allowing for wastage).

Tension is maintained in each gore sector by four springs which fit inside the gore spreader (views A-A and C-C, Fig. 3-12). Compact, low-rate springs are possible because the extremely low thermal expansion characteristics of the GR/EP cloth restrict the contraction of the gore to 0.11 inches. When rim position changes are considered, the maximum motion of the inner (hub) end of a gore sector from operational temperature changes is 0.06 inches. This points out a significant advantage of GR/EP gores for antennas with stringent tolerances on the radial position of radiating elements. For this 1.4 GHz design, an advantage of GR/EP is a very simple gore tensioning and rotation system. The gore spreader is permanently attached to the pivot housing (view A-A), with freedom of rotation provided by a bearing (and a bushing as a backup). A crank is fastened to the gore spreader. The same system of motors, gears, pushrods and universal joints (view B-B) is used to

produce 90-degree gore rotations as was described for the 3-layer aluminum gore. The upper left region of the main view of Fig. 3-12 shows how the gores wrap over the gore spreaders and other gores during retrieval after the drum has started rotating.

The arrangements of two different transmission lines are displayed in view E-E Fig. 3-12. The length of transmission line required for a card is a function of the card's radial distance from the centerline of the antenna, since that radius determines the RF path length from feed to slot. For these Modulo 2 antennas, any radial location is selected for the minimum length transmission line (L_0), and a reference RF path length is determined by the difference between the RF path length at this location and the reference path length, divided by the operating wavelength (λ). This produces a quotient, N·n where N is an integer and n is the fractional part of a wavelength. To produce an in-phase planar wavefront, the length of transmission line required at this location is ($n\lambda + L_0$). The longest length of transmission line (approximately $L_0 + \lambda$) is shown on the left side of view E-E. Each path is formed of 2-mil copper, 1/16 inch wide. The two paths on each card are separated by a 1/16-inch wide gap. The structure which supports and isolates these paths is 1-mil Kapton, bent into a Z shape. The weight of 340,000 of these transmission line cards is approximately 260 pounds.

As the gore sectors are wrapped around the drum, the interior antenna planes on each gore sector lose tension and become slack between the drum and rim while the exterior antenna planes are under constant tension. This occurs because the exterior planes are always wrapped over a larger diameter - the drum diameter plus the thickness of the interior plane and transmission line cards. For a given amount of drum rotation, the larger diameter creates a longer circumference. Consequently, the quantity of "excess" interior antenna plane progressively increases with the number of drum revolutions required for retrieval. Tension in the exterior plane forces the Velcro edge strips on the interior plane to adhere to the Velcro covered drum during retrieval in space. For ground preparation prior to launch, tension can be manually applied to the interior planes. The effect of buckling of the "excess" interior planes is shown in Fig. 3-13. The elastically buckled interior plane applies a load on the order of 2.25 pounds to its attachment fitting on the rim tube. The buckled shape is trapped between the tensioned exterior plane of its gore sector and that of an adjacent gore sector.

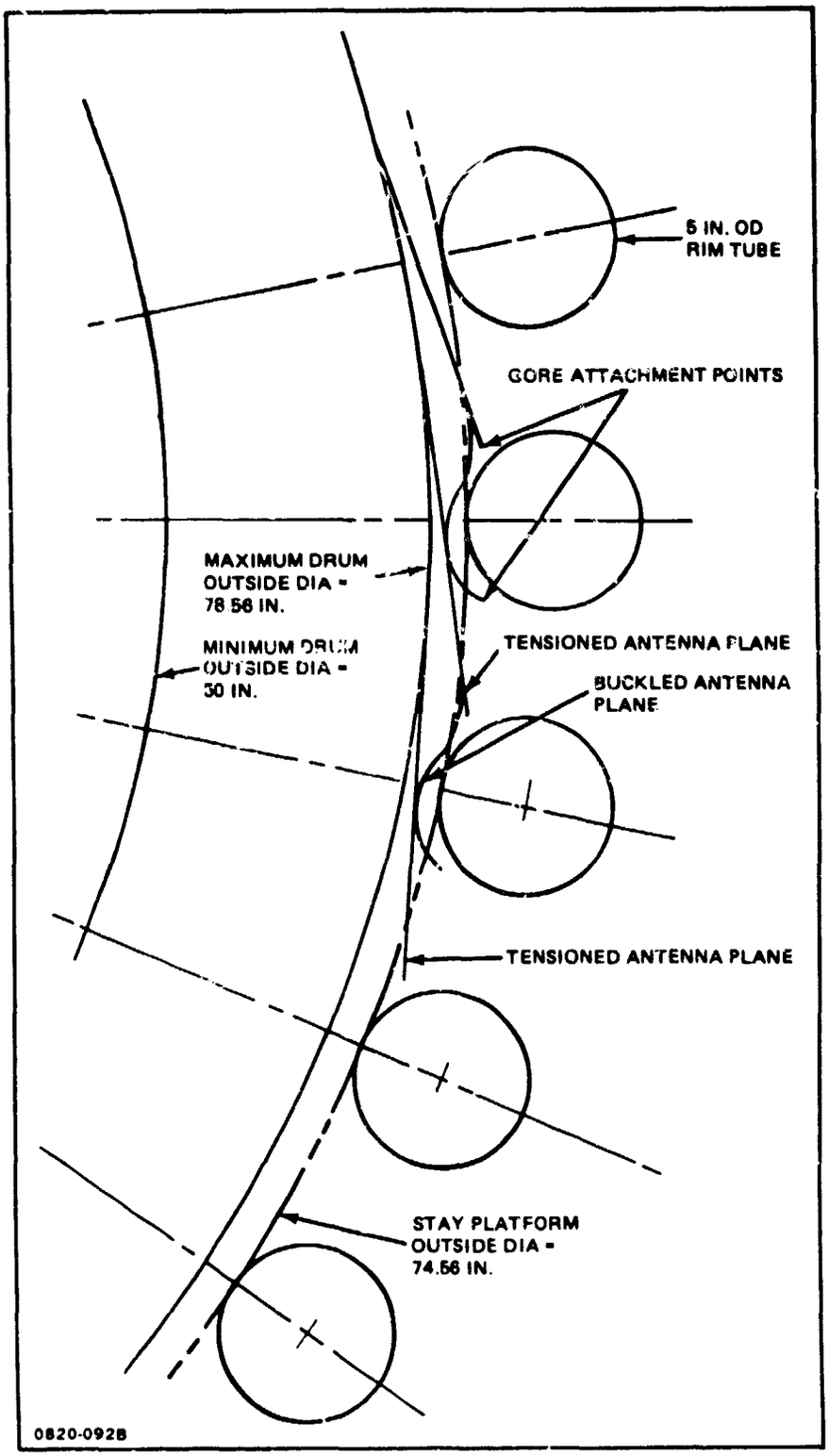

Fig. 3-13 Two Plane Gr/Ep Gore – Drum/Gore/Rim Interface at Launch

3.3 DESIGN ANALYSES

3.3.1 STATIC/DYNAMIC ANALYSIS

In a previous activity, a structural analysis was conducted of a free-flying 100-meter diameter lens antenna at geostationary orbit (Ref. 3-1 and 3-2). Static, buckling, modal vibrations and thermal stress analyses indicated that the structural design would satisfy performance requirements in the zero-gravity space environment. In addition, dynamic analysis was conducted to determine the impact of disturbance torques on structural performance. The major disturbances were varying solar pressure and the satellite's attitude control system. The antenna structure was modeled using a finite element system to describe the reference structures for gores, rim, hub, and extendible feed mast. The largest computed dynamic motions are summarized in Fig. 3-14. Gore errors are very small when compared with allowable errors at 1.4 GHz (approximately 0.25 inch rms in the radial direction and 2.5 inches rms in the axial direction). Feed position errors at the end of a 250-meter long mast are also trivial.

As part of this study, these analyses were expanded in two areas. First, static analyses of the antenna were conducted for the two alternative gore configurations described in subsection 3.2.4. (The original analysis assumed the baseline three-layer gore structure). Results obtained indicated that pre-tension loads in both configurations had to be increased to achieve the desired frequency for the lowest mode. Second, the dynamic behavior of the shuttle-attached antenna was studied. As a result of this initial analysis it was determined that the antenna could be controlled within required pointing accuracies for different maneuvers by using the vernier thrusters available on the orbiter without exciting severe mechanical vibration. It was assumed that orbiter thruster firing logic could be reprogrammed to accomplish this task. As an additional result of the analysis, information was derived to size the mast.

3.3.1.1 Static Analysis

Two different gore configurations for the 100-meter diameter antenna were considered. The first consisted of three planes, all made of aluminum, and the second utilized two planes made of graphite epoxy. For both, 32 triangular sectors made up the full circular gore.

A finite element model was used for the analysis of the three-plane aluminum gore. Stresses due to the pre-tension loads were determined as well as natural frequencies and mode shapes. Hand computations were used to check the lowest bending mode. For the graphite epoxy gore, only hand computations were employed to obtain the natural frequencies.

The analyses indicated that the pre-tension loads in both configurations had to be increased to obtain the desired frequency for the lowest mode.

Three-Plane Aluminum Gore - The three planes of this design are structurally identical. They are made of 0.0005-inch aluminum sheet bounded by edge tapes, as shown in Fig. 3-15. Simulated modules are placed on the middle plane (ground plane), which greatly increase the weight of this plane. The three planes act independently since there are no minihinges interconnecting the planes as in other designs. There are only the transmission lines connecting the planes which are not considered structural.

The pre-tension loads are applied at the apex of each triangular sector as shown in Fig. 3-15. These loads provide the out-of-plane stiffness of the triangular membranes. The finite element model which was used in both the static and vibration analyses is shown in the top part of Fig. 3-16. Quadrilateral and triangular membrane elements were used to model the triangular sector, with bar elements along the edges to model the edge tapes. The average radial and tangential stresses in the ground plane with a 3-pound tension load at the apex are shown in Fig. 3-17. The results obtained with edge tapes having cross-sectional area five times larger are also plotted. Note that there is some oscillation in the tangential stress near the apex of the sector. This oscillation is due to the coarse finite element grid in this area.

In order to obtain the frequencies and mode shapes of the ground plane under the pre-tension load, the mass of the structure must be computed. This is made up of the weight of the aluminum sheet and edge tapes which is equal to 19.08 pounds, and the weight of the 10,625 simulated modules, each of which weighs 0.012 pounds, giving a total weight of 146.58 pounds. Assuming this mass to be uniformly distributed on the ground plane sector, the two lowest frequencies and mode shapes are shown in Fig. 3-16. Note that the lowest mode involves twisting of the sector while the second is a bending mode, and that the frequencies are close.

A similar analysis was performed for the dipole plane. Here the weight is the weight of the aluminum sheet and edge tapes only, and a tension load of 1.5 pounds at the apex was used. The two lowest modes are shown in Fig. 3-18. The modes are the same as those for the ground plane but have frequencies about double those of the ground plane.

Hand computations can be used to check the frequency of the bending mode, by employing the formula for the first frequency of a string with uniform mass:

$$f = \sqrt{\frac{T}{\rho}} \left(\frac{1}{2L}\right)$$

- TRANSIENT RESPONSE RESULTS USING FINITE ELEMENT MODEL
- CONFIGURATION: 100 m DIA LENS, SINGLE FEED, F/D = 2.8
- ORBIT: GEOSTATIONARY AT SOLSTICE, EARTH POINTING, FREE FLYING
- REF CONFIG USED FOR GORES & RIM

IN PLANE OF ANTENNA (⊥ TO GRAVITY VECTOR)	MAX GORE DISPLACEMENT	0.0005 IN.
	MAX RIM NODE DISPLACEMENT	0.0006 IN.
IN AXIAL DIRECTION (∥ TO GRAVITY VECTOR)	MAX RIM NODE DISPLACEMENT	0.026 IN.
	MAX DISPLACEMENT OF A SINGLE GORE POINT RELATIVE TO HUB MID PLANE	0.40 IN.
FEED MOTION RELATIVE TO ℄ OF LENS	RADIAL DISPLACEMENT	0.175 IN.
	ANGULAR ROTATION	0.0018 DEG

0820-021B

Fig. 3-14 Summary of Dynamic Structural Analysis

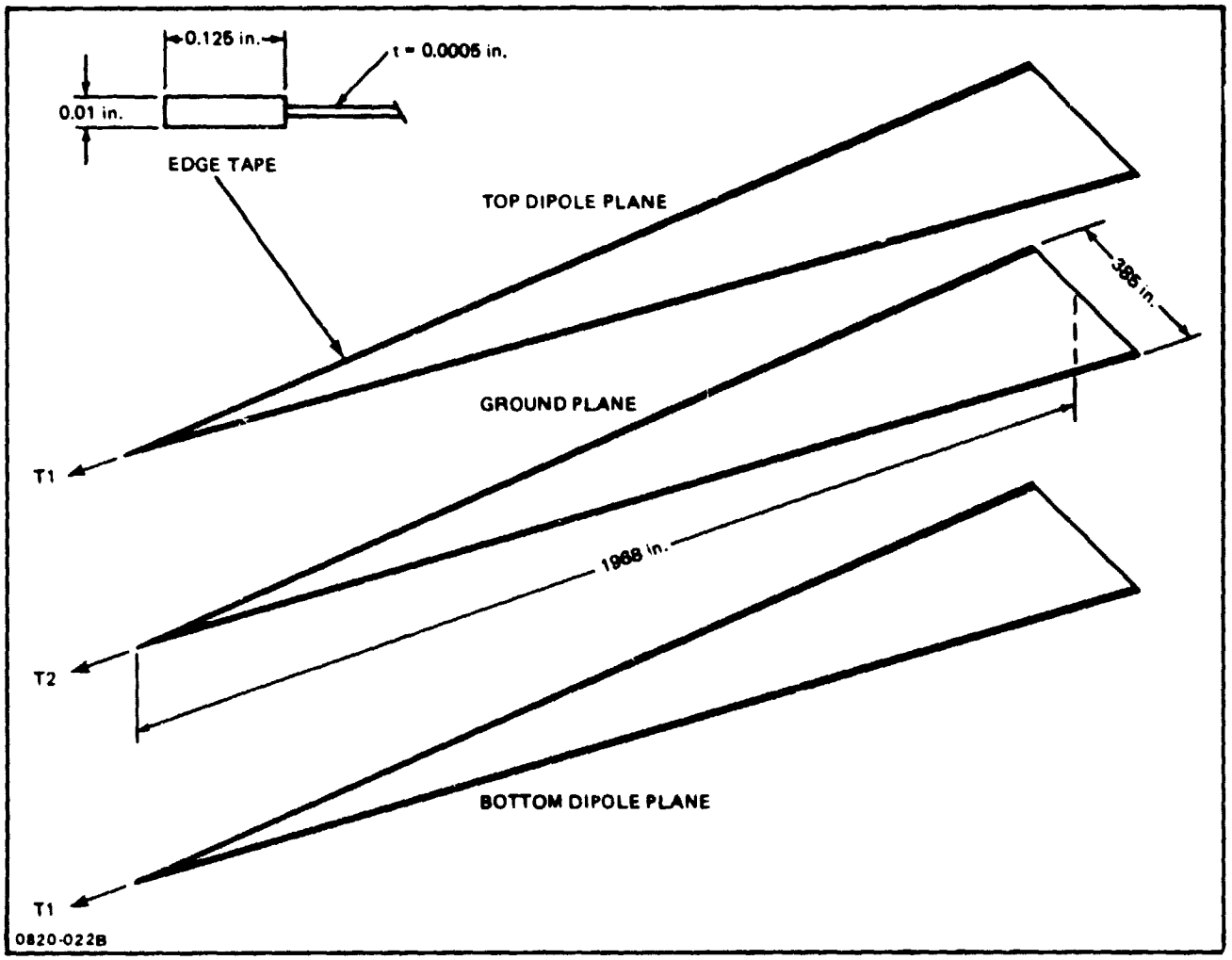

Fig. 3-15 Three Plane Aluminum Gore

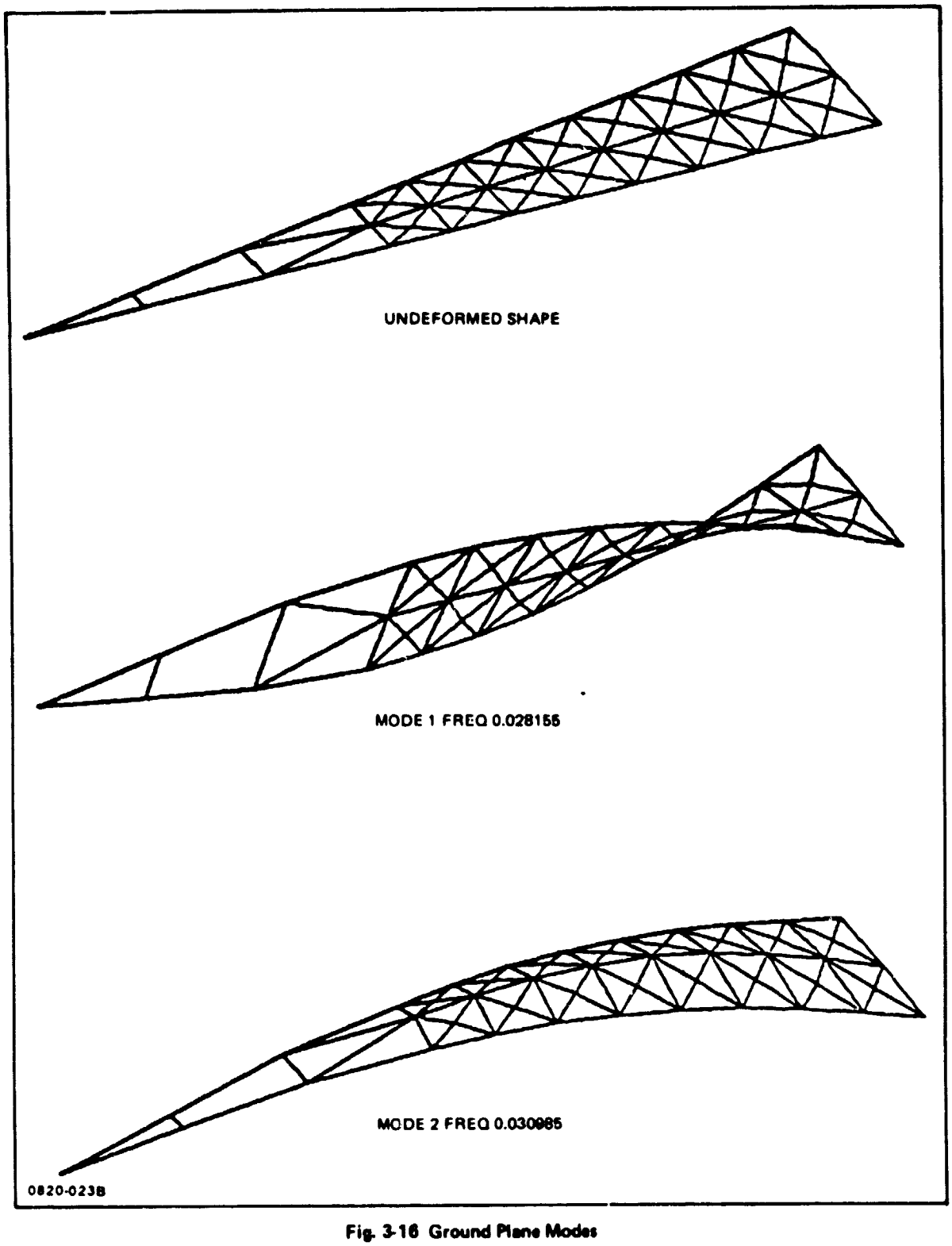

Fig. 3-16 Ground Plane Modes

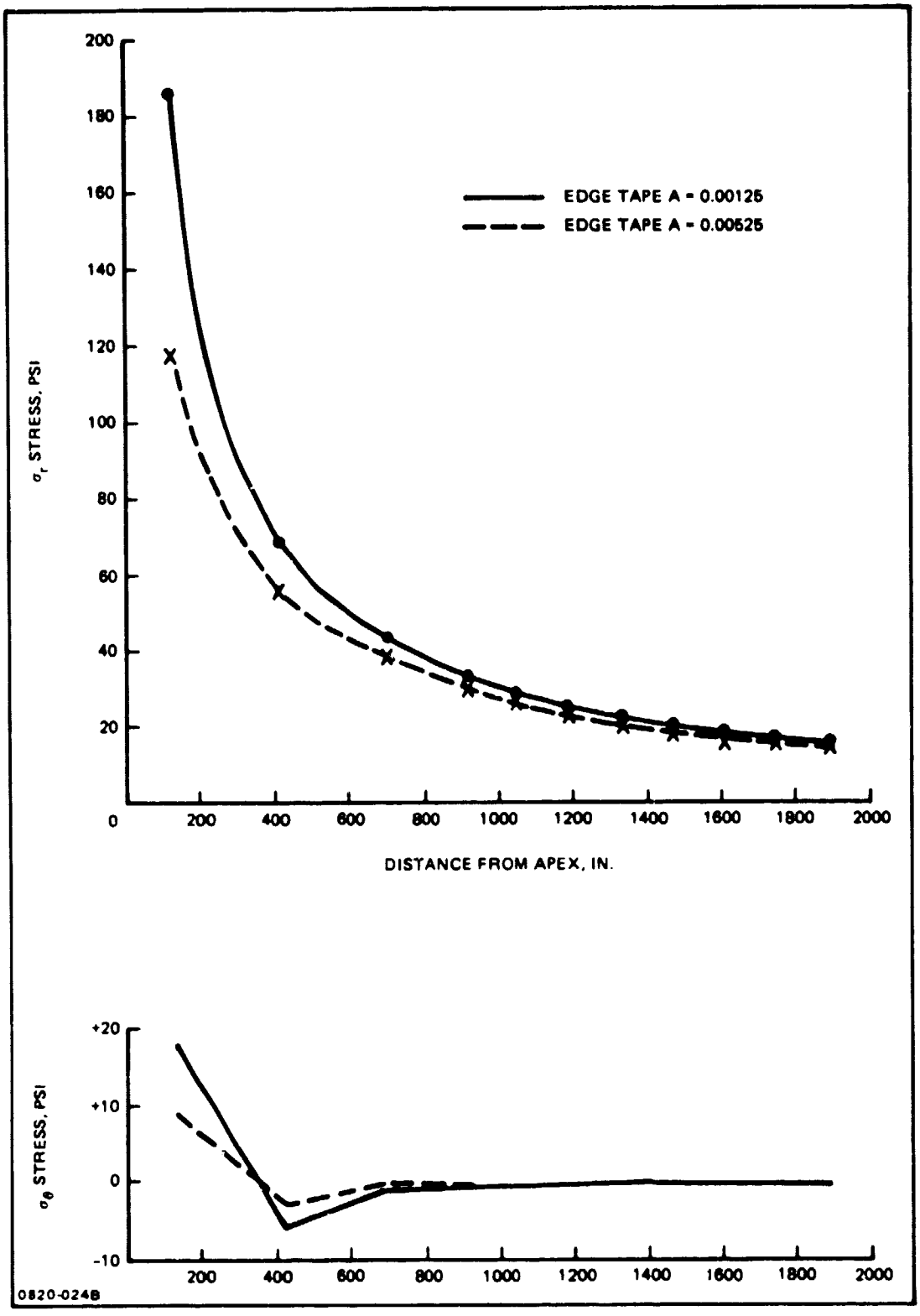

Fig. 3-17 Stresses in Ground Plane

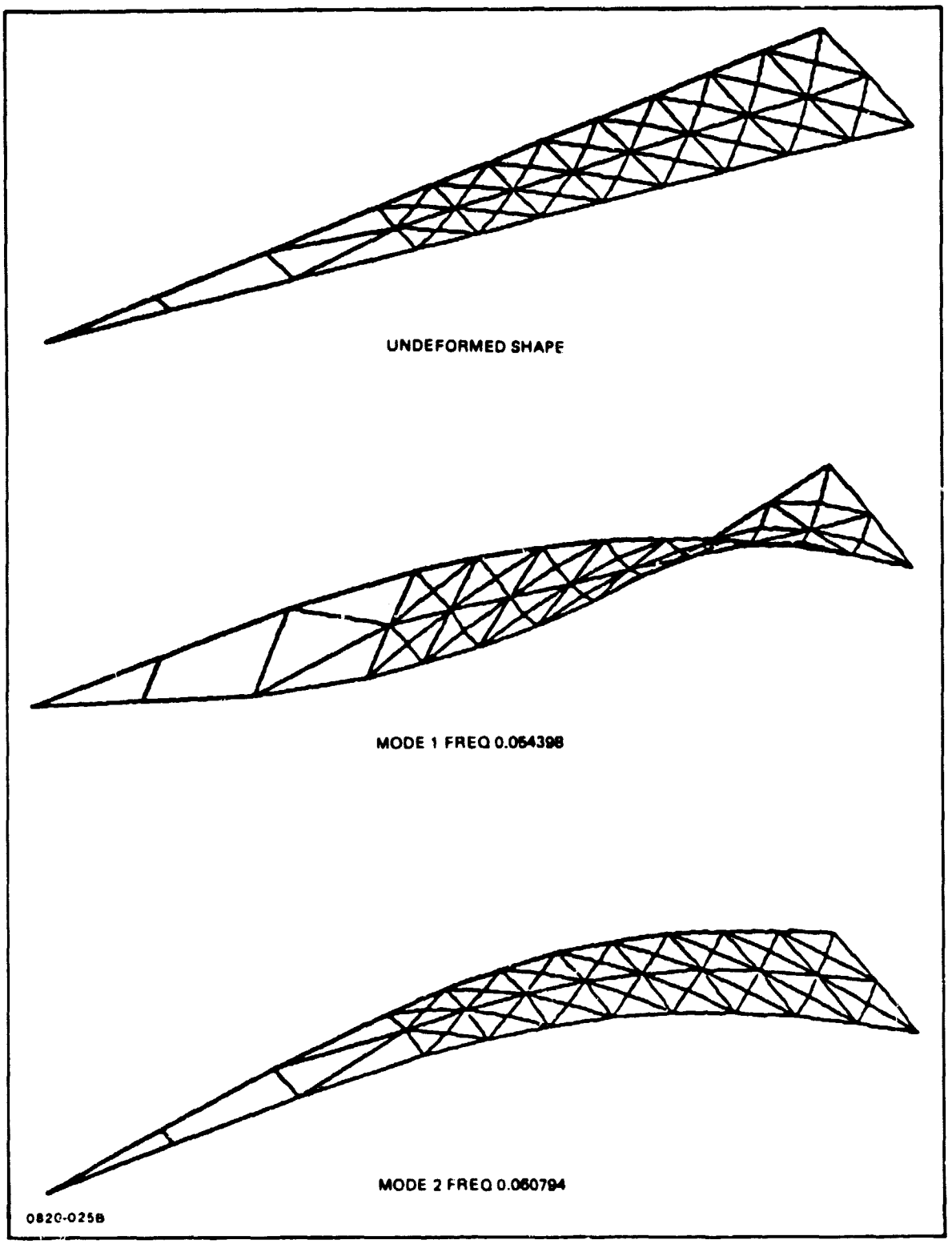

Fig. 3-18 Dipole Plane Modes

where T is the tension, ρ is the mass per unit length and L is the length of the string. Using this formula gives

f = 0.0317 cps for the ground plane

f = 0.0621 cps for the dipole plane

which agree very well with the values obtained from the finite element analysis.

These frequencies are, however, too close to the frequency of the second bending mode of the entire antenna. It is desirable to increase these frequencies of the ground plane and the dipole planes to 0.1 cps. This can be accomplished by increasing the tension in the ground plane to 30 pounds and the tension in the dipole plane to 6 pounds. This would increase the compression load in the rim of the antenna which would cause the rim to buckle if it exceeded the critical load. The compressive load in the rim due to the gore tensions is:

$$P = \frac{(2\ (6) + 30)}{385} \times 1968 = 214 \text{ lb}$$

Considering the rim to be a ring on an elastic foundation (stays), the critical load is given by

$$P_{cr} = 2\sqrt{kEI}$$

The rim and the stays have the following properties:

Rim	Stays
D = 4.25 in.	A = 0.01
t = 0.005 in.	$E = 16 \times 10^6$ in.^{2}
$E = 16 \times 10^6$ psi	L = 1980 in.
$I = 0.3$ in.^{4}	$k = \frac{AE}{L} = 81$
	$kz = 81 (\sin 5.25°)^2 = 0.7$
	$\frac{kz}{385} = 0.0018$

$$P_{cr} = 2\sqrt{18 \times 16 \times 10^6 \times 0.3} = 186 \text{ lb}$$

Since the compressive load in the rim exceeds the critical load, the rim would buckle. By increasing the rim thickness and the cross-sectional area of the stays, P_{cr} could be increased substantially so that the rim would be stable. For example doubling both the rim thickness and the stay cross-sectional area would double P_{cr}.

Two-Plane Graphite Epoxy Gore - The two-plane graphite epoxy gore consists of two structurally independent and identical planes. The construction is actually a sandwich with a 0.0025-inch GR/EP core bounded by a 0.00003-inch aluminum layer on one side and a 0.00028-inch aluminum layer on the other. There are no simulated modules on this design, hence the weight is due only to the structure which is 63.5 pounds. Assuming a 2-pound tension load applied at the apex and using the formula for the vibrations of a uniform string, gives

$$f = 0.039 \text{ cps}$$

which again is too low. It is necessary to raise the tension load to 13 pounds in each plane to attain a frequency of 0.1 cps. This would result in a compressive load of 133 pounds in the rim.

3.3.1.2 Dynamic Analysis

Description of the Problem - The 100-meter diameter antenna is attached to the space transportation system (STS) by a relatively flexible deployable mast as shown in Fig. 3-19. The first problem selected for study was the dynamic response of the system while it is maintaining a constant inertial attitude (within an allowable error of ±5 degrees) in the first quarter of the 350-nautical mile orbit as shown in Fig. 3-20. The aerodynamic, gravity-gradient and solar-radiation pressure torques are additive in this quarter of the orbit; therefore, the total environmental torque reaches its maximum value in this region. The STS attitude thrusters do not fire in couples, and the largest control torque exerted by the vernier thruster is 39,800 inch-pounds developed when the two 25-pound forward thrusters fire to counteract the environmental torque. This control torque is over 60 times as large as the maximum environmental torque of 649 inch-pounds. For these reasons, the pulsing of the forward pitch jets is expected to result in the most severe vibration in the indicated quarter of the orbit.

To simplify the investigation, only motion in the plane of the orbit was considered. While the investigation does not address some of the complex questions concerned with out-of-plane motion, it does treat the basic control/vibration problem for the region and attitude orientation in which the loads are a maximum. It would appear that if the mast is sized for this condition, it will be adequate for the other required maneuvers.

The second problem selected for study was to point the boresight toward a desired position near a target satellite located down-range so that far-field pattern measurements could be made. The desired position changes uniformly with time at the rate of 10

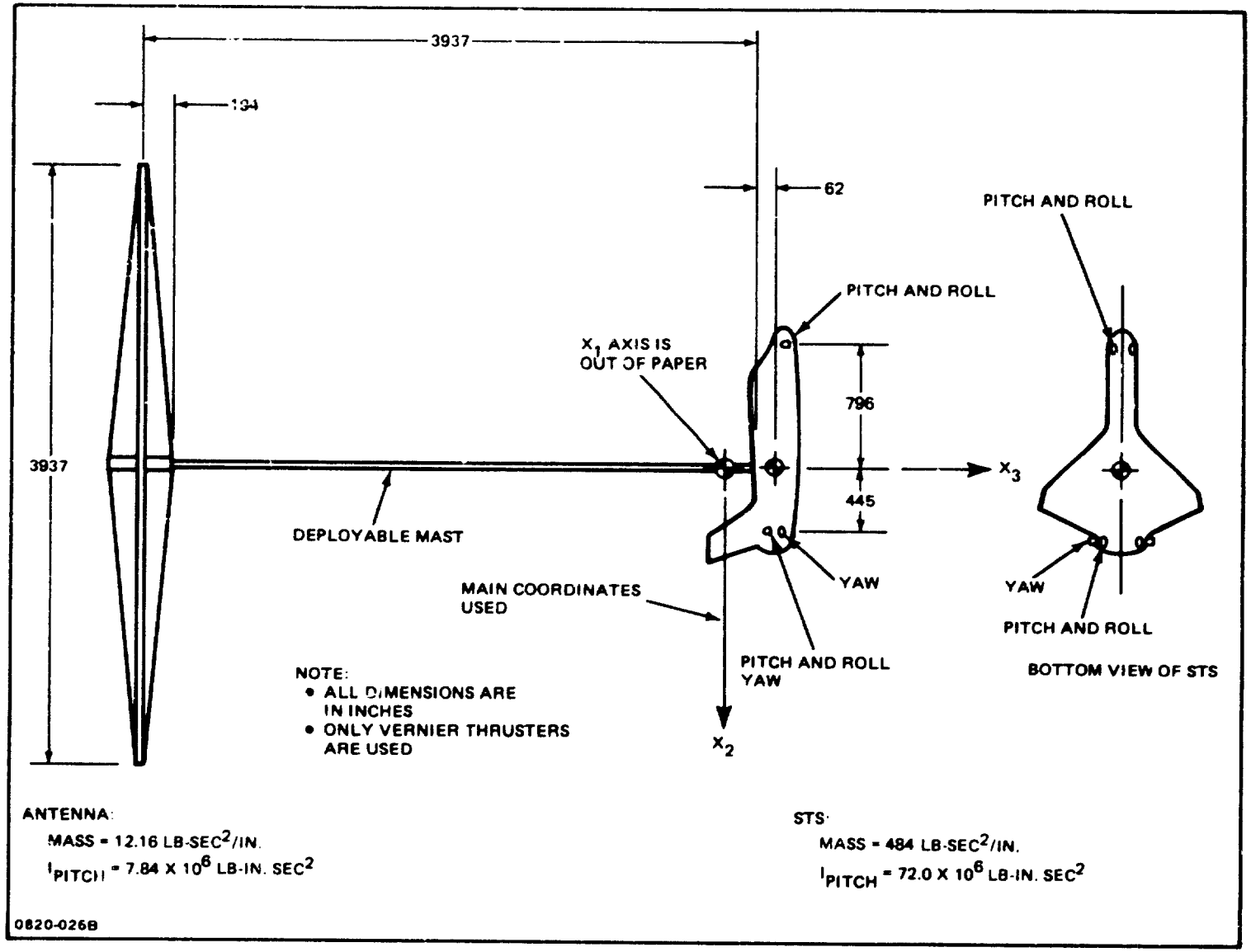

Fig. 3-19 Configuration & Mass Properties

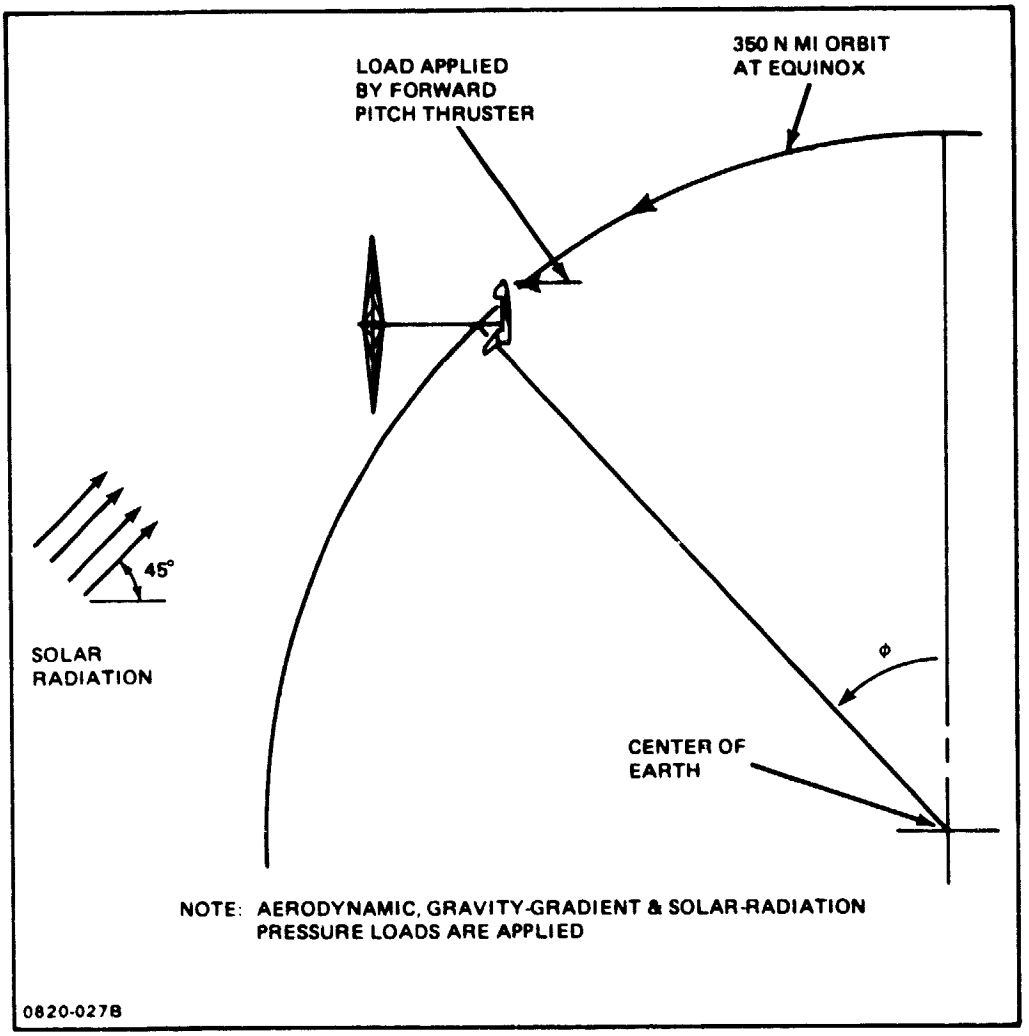

Fig. 3-20 Satellite in Orbit

beamwidths (1.47 degrees) per quarter orbit, and the desired pointing accuracy was a maximum total peak-to-peak oscillation of one beamwidth (0.147 degree). This maneuver was designed to demonstrate the ability to perform precision pointing while slewing. As in the previous problem, only motion in the plane of the orbit was considered.

Summary - The results of this study are based on an idealization which employed a rigid antenna and STS connected by a flexible mast. The study was conducted for the inertial attitude-hold phase of the mission and for a maneuver that combined precision pointing with slewing.

The cap members of the deployable mast were sized to withstand the stresses resulting from vibration excited by the control thrusters. The mast is graphite/epoxy; it has three longerons located at the vertices of its triangular cross section, 14.75 inches from the cross-section center. The longerons are tubes with a 0.442-inch OD and a 0.081-inch wall.

In the first simulation of the attitude-hold maneuver, control pulses that were obtained from a rigid-body control analysis were applied to the STS as a function of time. The maximum pointing error (e_p in Fig. 3-21) was 1.2 degrees from the desired attitude, which was well within the ±5-degree requirement. The maximum deflection δ in Fig. 3-21 was 90 inches. While this may seem large, the mast was not overstressed. The longeron cross-section, specified above, was designed to prevent local buckling during these vibrations with a safety factor of two, and in addition, to provide the desired mast cross-sectional moment of inertia ($I = 30$ in.^{4}).

Next, a control law was developed to simultaneously control the attitude and the flexible vibrations. This control law is a function of the predetermined vibration modes of the system. A coupled control-system flexible-vehicle simulation indicated that during the attitude-hold maneuver, the pointing error could be reduced to 0.24 degree from the desired position, and the maximum excursion δ could be reduced to 15 inches. Further performance improvements may be achievable by optimizing the parameters of the control law; however, because of budget and schedule limitations, it was not possible to do this under the present contract.

A simulation was then conducted to demonstrate precision pointing while slewing, using the combined attitude/vibration control law. The total peak-to-peak pointing error was only 0.028 degree, which was well within the desired value of 0.147 degree. The maximum elastic deflection of the feed relative to the drum centerline was 1.7 inches.

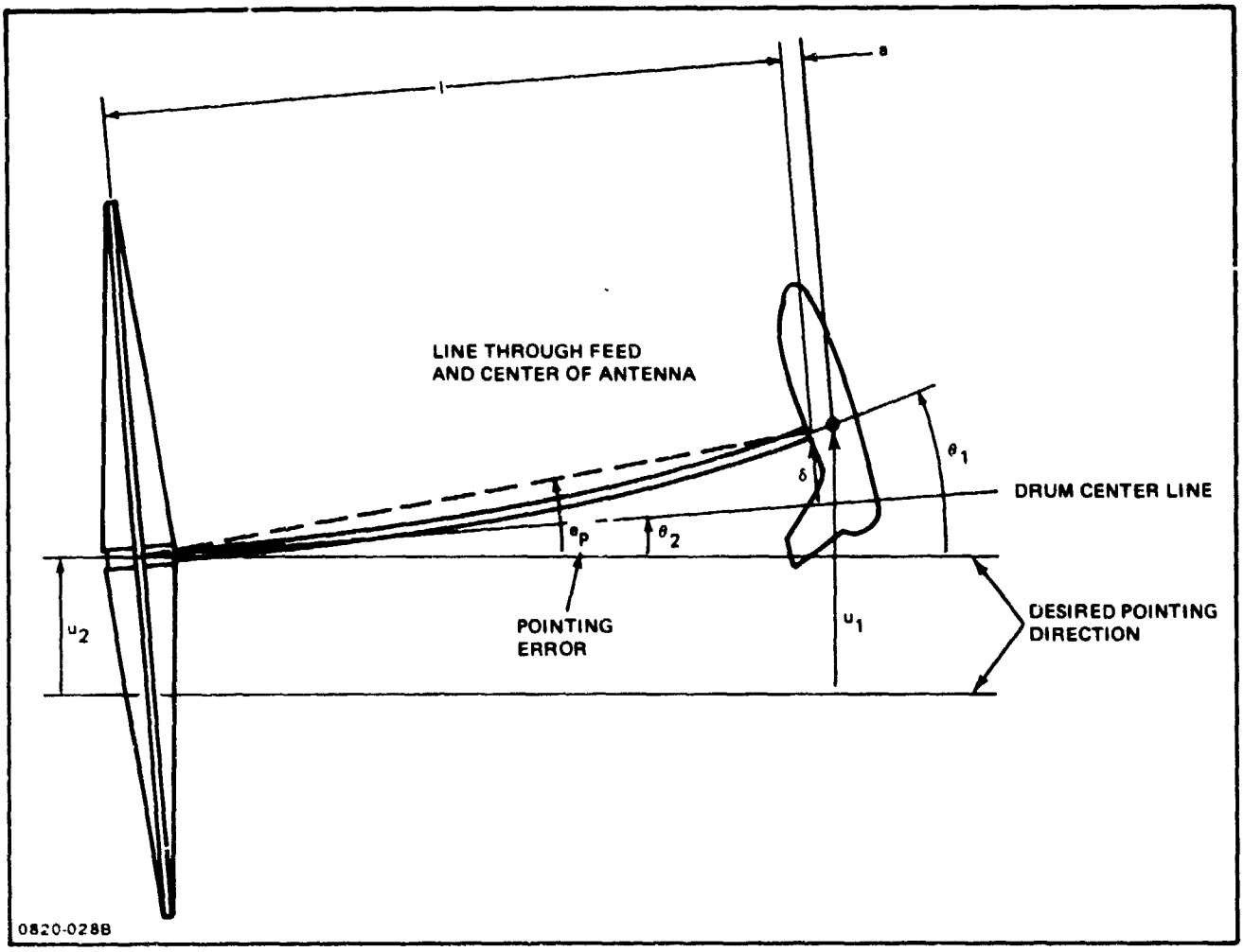

Fig. 3-21 System Shown in Deformed Position

While only the 100-meter diameter antenna was studied, the 50-meter diameter antenna system should be even easier to control since it should be more rigid, (i.e., it would have a higher fundamental vibration frequency), and the environmental loads on the smaller system would be substantially lower.

Configuration and Idealization - The configuration and mass properties used are shown in Fig. 3-19. The antenna and STS, when unattached by the deployable mast, are expected to be relatively rigid; i.e., they are expected to have natural vibration frequencies that are high relative to the first two bending-mode frequencies of the coupled structure. Consequently, in this first investigation, the antenna and STS are assumed to be rigid bodies while the mast is assumed to be flexible. Also, since the mass of the mast is small relative to the masses of the antenna and STS, the mass of the mast is neglected.

The STS contains the vernier thrusters shown in Fig. 3-19. Each thruster can apply a force of 25 pounds. These thrusters do not apply couples to the vehicle; e.g., to pitch the nose up, both forward pitch thrusters fire in the X_3 direction producing the desired rotation as well as an undesired translation in the $-X_3$ direction. The yaw thrusters are located only in the aft section of the STS and produce roll in addition to yaw and translation because they are not located in a plane containing two principle axes of the combined system. However, this first study is confined to a pitch-plane analysis only; consequently three-axis coupling is not addressed.

Vibration Modes - It can be shown that the eigenvalue problem for the free vibrations can be written so that ω^2/EI is the eigenvalue, where ω is the vibration frequency, E is the modulus of elasticity and I is the cross-sectional moment of inertia of the mast. Furthermore, E and I do not appear elsehwere in the equations. Consequently, ω^2/EI is a constant for each mode (j), regardless of the stiffness EI of the mast, and the mode shapes are also independent of EI. This simplification occurs because the tip masses (STS and antenna) are assumed to be rigid.

The mast is assumed to be graphite/epoxy with a modulus of $E = 16 \times 10^6$ psi. Then the bending frequencies are

$$\omega_1 = 0.01480 \sqrt{I} \text{ rad/sec} \quad (1)$$

$$\omega_2 = 0.05364 \sqrt{I} \text{ rad/sec} \quad (2)$$

where I is expressed in in.^4. The bending mode shapes are tabulated in Fig. 3-22. These mode shapes and the coefficients in equations (1) and (2) were obtained from a NASTRAN modal analysis for a system with $I = 1.494$ in.^4 and were then validated for a system with $I = 100.0$ in.^4.

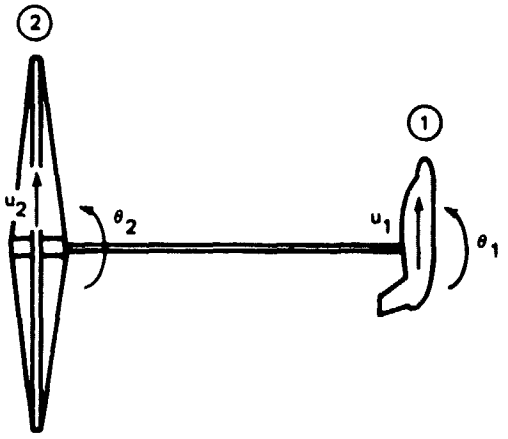

COORDINATE	MODE SHAPE		
	RIGID-BODY ROTATION	FIRST BENDING	SECOND BENDING
u_1	5.970×10^{-3}	3.218×10^{-3}	2.155×10^{-3}
θ_1	6.091×10^{-5}	-9.856×10^{-5}	-2.156×10^{-5}
u_2	-0.2376	-0.1281	-0.08578
θ_2	6.091×10^{-5}	1.107×10^{-4}	-3.340×10^{-4}
NOTE: MODE SHAPES ARE NORMALIZED TO UNIT MODAL MASS			

0820-029B

Fig. 3-22 Bending Mode Shapes

Environmental Loads - A subroutine was prepared to generate the aerodynamic, gravity-gradient and solar-radiation forces and torques on the antenna and the STS. Equations for both the aerodynamic lift and drag were based on Ref. 3-3 and 3-4. The density used was 5.6×10^{-15} slugs/ft^3 which includes the maximum deviation listed in Ref. 3-5 for the 350-nautical mile orbit.

Equations for the solar-pressure normal and shear stresses were based on Ref. 3-6. Perfectly diffuse emission was assumed. This condition occurs when the rays are reflected by dull surfaces and results in the highest shear stress.

Equations for the gravity-gradient forces and torques were extracted from Ref. 3-7. These equations also include the effect of orbital rotation.

The variation of the environmental torques with time is shown in Fig. 3-23 for the satellite in the fixed inertial attitude indicated in Fig. 3-20. The solar torque is not shown since it remains constant. The largest values are

aerodynamic	-440 inch-pounds
gravity gradient	-200 inch-pounds
solar radiation	-16.0 inch-pounds

These values occur at different times. The largest total environmental torque is -649 inch-pounds.

Rigid-Body Control Law - A common control law for on-off thrusters is based on switching curves as shown in Fig. 3-24. In this illustration there is no disturbance torque. The error e is the difference between the actual attitude of the vehicle and the desired attitude, and the curves shown are the vehicle performance in the error, error-rate phase plane. In the right-hand region a negative control torque is exerted. Since the control torque is constant, motion with constant angular acceleration occurs and the e versus $\dot{e}$ curve is parabola. As soon as the right switching curve is reached, the thrusters are turned off, and the system drifts through the dead band. The switching curves are parabolas that are programmed into the control law. When the left switching curve is reached, other thrusters are turned on to exert a positive control torque. As the control continues, the error and error rate spiral into the origin.

Figure 3-25, view A indicates the performance in the presence of the environmental torque for small errors. Since the environmental torque varies little during one control-system oscillation, it may be regarded as a constant for the present discussion. The trajectories of Fig. 25, view A are therefore parabolas, and they spiral into the point on

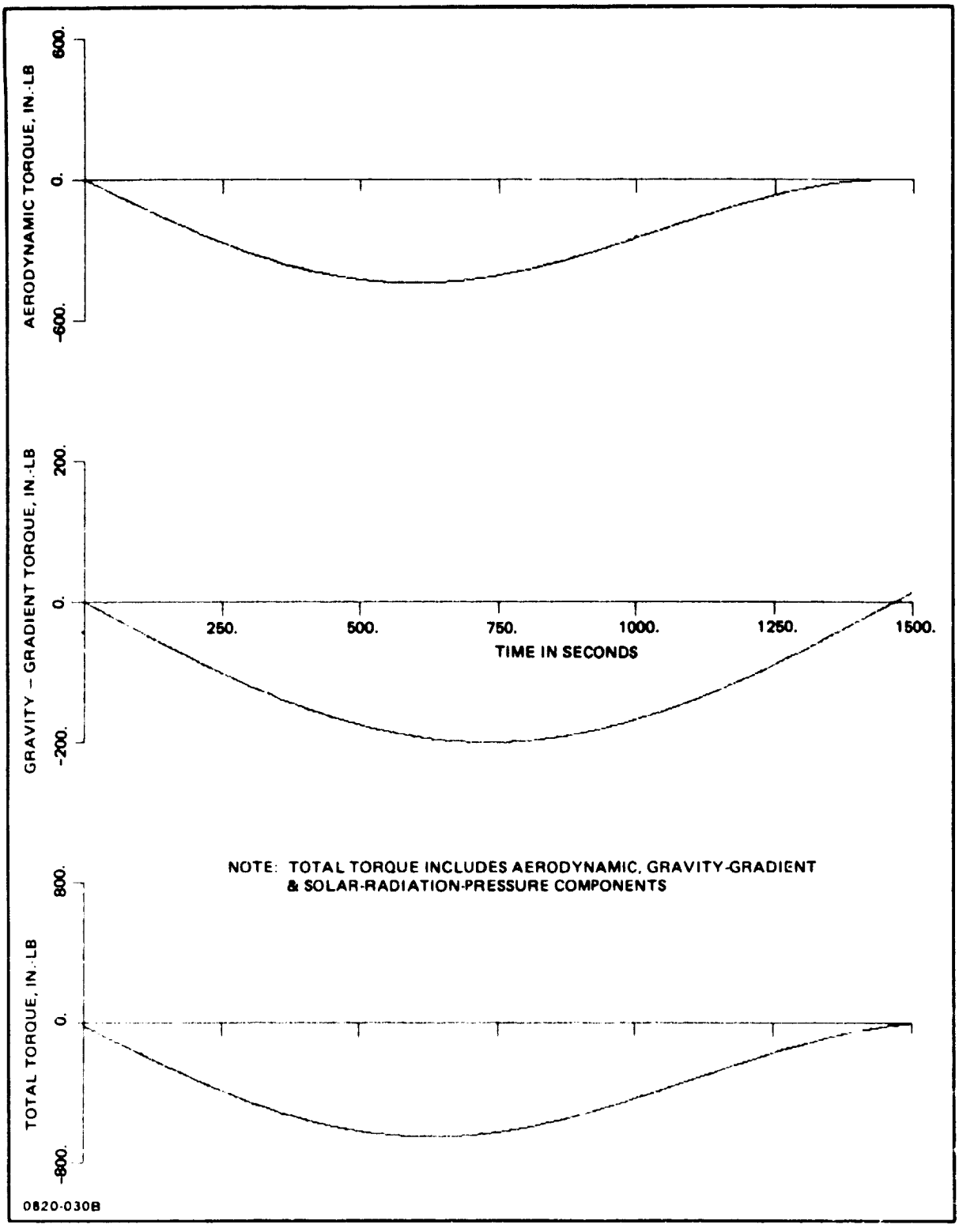

Fig. 3-23 Environmental Torques During First Quarter of Orbit When System is in the Contant Inertial Attitude Shown in Fig. 3-20

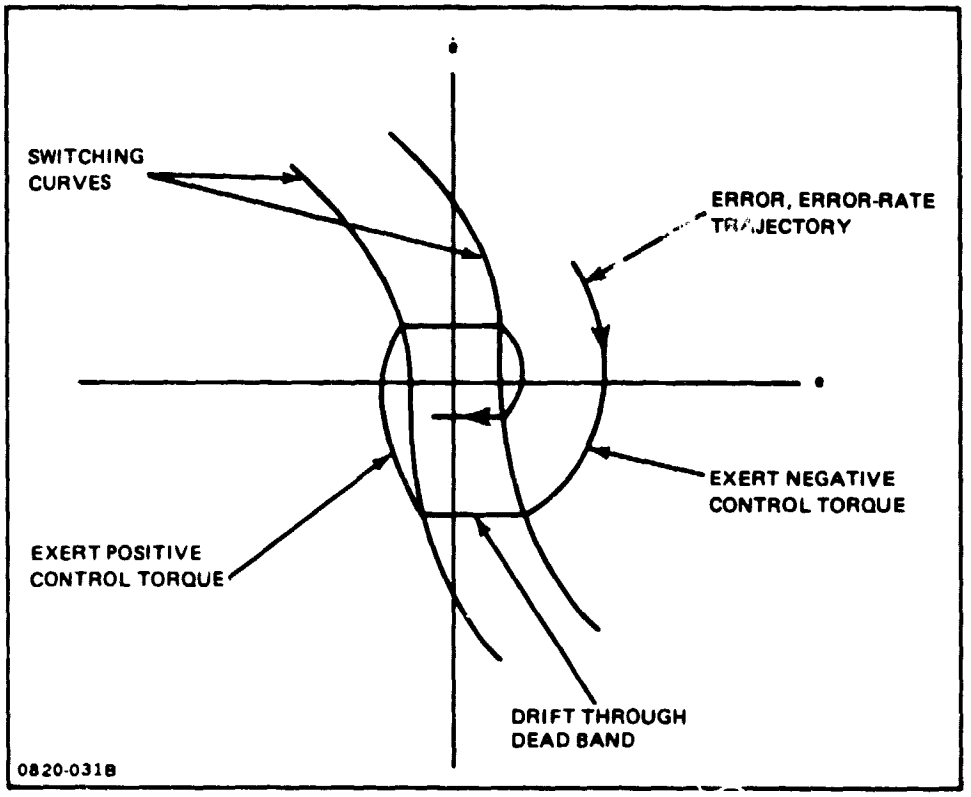

Fig. 3-24 Performance of Rigid-Body Control Law in Absence of Disturbance Torque

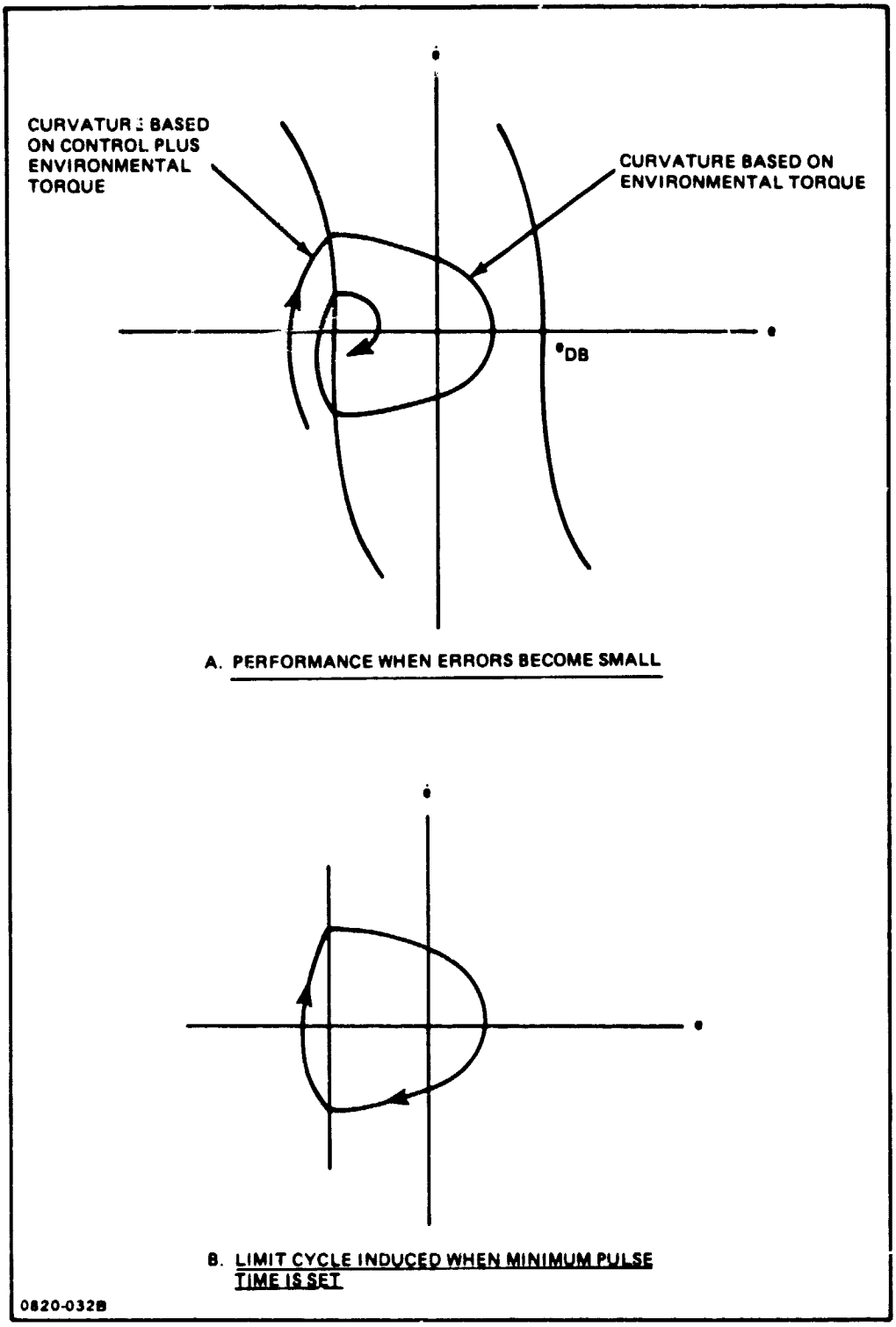

Fig. 3-25 Performance of Rigid-Body Control Law in Presence of Environmental Torque

the left dead band where $e = -e_{DB}$ and $\dot{e} = 0$. The period of oscillation is given very closely by the equation*

$$\tau = -\frac{T_C}{T_E} t_p \tag{3}$$

where T_C is the control torque, T_E is the environmental torque, and t_p is the pulse time. The negative sign is needed because T_E and T_C are of opposite sign. When the spirals become smaller, t_p, and therefore τ, becomes smaller and the frequency becomes larger and larger. Consequently, to prevent exciting structural instability resulting in severe elastic vibrations, it is necessary to limit the control frequency so that it remains sufficiently lower than the first vibration frequency. A simple way of accomplishing this is by introducing a minimum pulse time. The phase plane curves will then spiral into the limit cycle shown in Fig. 3-25, view B.

If the minimum pulse time is set equal to a constant, it must be sized so that the smallest control period (which, in accordance with equation (3), occurs when $|T_E|$ is at its maximum value) is significantly longer than the period of the lowest-frequency vibration mode. In this way coupling with the elastic modes, leading to large vibration and possible instability, is avoided. However, when $|T_E|$ is lower than the maximum, τ increases, and the rigid-body oscillations into the dead-band region also increase. Consequently, a larger dead band is required, or a significant amount of inefficient pulsing will occur to rotate the vehicle back and forth across the dead band. To reduce the oscillations, and thereby avoid this situation, it is assumed that the minimum pulse time is varied in accordance with equation (3) to maintain the control period τ as a constant at its minimum allowable value; i.e., from equation (3)

$$t_p = \text{larger of} \begin{cases} 0.040 \text{ sec} \\ \dfrac{T_E}{T_C} \end{cases} \tag{4}$$

where the 0.040** sec cut off is limited by the STS hardware. This scheme requires the measurement of T_E, or alternatively α_E, the angular acceleration caused by the environmental torque, which is multiplied by the moment of inertia to obtain T_E.

*The equation is exact when the switching curve is a vertical line; therefore, for the parabolic switching curves, the equation becomes more accurate as the spirals become smaller.

**Note: 0.080 sec minimum burn time constraint was identified after analysis was completed.

Selection of Mast - The flexible vibration periods for the first two bending modes were computed from equations (1) and (2) and are presented in Fig. 3-26 as a function of the beam cross-sectional moment of inertia. To limit the control-system coupling with flexible vibration, the control system period (listed in the table as the rigid-body period) was selected as 4.3 times the first-mode bending period. An integer multiple was not selected so that one of the higher harmonics of the Fourier series describing the pulse would not be equal to the first bending period.

A rigid-body control analysis was then performed to determine the maximum total oscillation that would occur in the presence of the total environmental torque shown in Fig. 3-23. To perform this analysis, closed form solutions were developed for the maximum peak-to-peak attitude oscillation, θ_{TOT}, based on the limit cycle shown in Fig. 3-25, view B. A 20% safety margin was added so that the system would not drift across the opposite dead band thereby expending unnecessary fuel. It was assumed that the two 25-pound vernier jets, which exert a control torque T_C of 39,800 inch-pounds, are being pulsed to counteract the environmental torque. The total vehicle moment of inertia about the pitch axis passing through the center of mass is required for the calculations and is 2.70×10^8 pound-inch-sec^2. The results are tabulated as $(1/2)\,\theta_{TOT}$ in Fig. 3-26.

Next, the undamped flexible system response to a single control pulse was computed by obtaining closed-form solutions to the equations of motion. The mast was assumed to be graphite/epoxy with a modulus of elasticity E of 16×10^6 psi. The results include the flexible contribution to the pointing error e_p and the deflection of the feed relative to the drum centerline δ (see Fig. 3-21). The amplitudes of these values in each mode are listed in Fig. 3-26. To obtain the time-varying response, each amplitude must be multipled by $\pm \sin \omega_j t$ and the results must be added, where $\omega_j = 2\tau / \tau_j$, the frequency of the corresponding mode, and τ_j is the tabulated modal period.

The required pointing accuracy for the case studied, attitude hold relative to inertially fixed axes, is ±5 degrees. This value is needed for the thermal experiments. With this requirement in mind, the data of Fig. 3-26 was reviewed, and a mast with an $I = 30$ in.^{4} was selected for further study even though the vibration amplitudes were considerably higher than those for the heavier, stiffer masts.

Flexible Response for Attitude-Hold Maneuver, Using Rigid-Body Control - The flexible response of the vehicle in the inertial attitude-hold position shown in Fig. 3-20 was simulated by numerical integration during the first quarter of the orbit using the NASTRAN computer program. The control dynamics were not coupled with the flexible dynamics in this first simulation; i.e., the pulses based on the rigid-body control law were applied to the

MAST MOMENT OF INERTIA, I ($IN.^4$)	OSCILLATION PERIOD (SEC)			RIGID BODY OSCILLATION AMPLITUDE, $1/2\,\theta_{TOT}$ (DEG)	FLEXIBLE RESPONSE TO LARGEST SINGLE CONTROL PULSE			
	RIGID BODY, τ	FLEXIBLE			CONTRIBUTION TO AMPLITUDE OF POINTING ERROR, e_p (DEG)		BENDING VIBRATION AMPLITUDE, δ (IN.)	
		MODE 1, τ_1	MODE 2, τ_2		MODE 1	MODE 2	MODE 1	MODE 2
10	577	134	37.0	3.43	1.48	0.0532	246	60.1
20	408	94.9	26.2	1.71	0.742	0.0266	123	30.0
30	333	77.5	21.4	1.14	0.495	0.0177	81.9	20.0
40	289	67.1	18.5	0.857	0.371	0.0133	61.5	15.0
50	258	60.0	16.6	0.686	0.297	0.0106	49.2	12.0
60	236	54.8	15.1	0.572	0.247	0.0089	41.0	10.0
70	218	50.7	14.0	0.490	0.212	0.0076	35.1	8.58
80	204	47.5	13.1	0.429	0.186	0.0066	30.7	7.51
90	192	44.8	12.3	0.381	0.165	0.0059	27.3	6.67
100	183	42.5	11.7	0.343	0.148	0.0053	24.6	6.01

0820-033B

Fig. 3-26 Information Used to Select Mast

C-2

flexible vehicle as a function of time. Therefore, rotation of the sensor due to vehicle flexibility is not accounted for. Only the flexible vibration modes were included in the simulation; the rigid-body modes were omitted.

The mast dimensions are shown in Fig. 3-27. Each of the three longeron cap members has an area of 0.092 $in.^2$ and is located on a 14.75-inch radius, providing an I of 30 $in.^4$. The damping used for each flexible mode use 3% of critical damping. Control pulses were applied at 333 sec intervals in accordance with the period indicated in Fig. 3-26; the pulse widths were determined by equation (4) and are listed in Fig. 3-28.

Selected results are shown in Fig. 3-29 through 3-31. Most of the response is attributable to the first bending mode. Fig. 3-29 shows the deflection δ and Fig. 3-30 shows the flexible contribution to the pointing error e_p. Both quantities are defined in Fig. 3-31. The maximum bending stress in the mast occurred at the STS connection, and the variation of this stress with time is shown in Fig. 3-31. The magnitudes of the peak values are:

Deflection δ: 89.9 in.
Flexible contribution to e_p: 0.00799 rad = 0.458 deg
Mast bending stress: 5,130 psi

The overall load required to buckle the mast is 338 pounds while the maximum applied load was only 1.3 pounds. However, if the longerons were solid, they would fail in local buckling. The local buckling load would be 201 pounds compared with a 471-pound maximum applied load. To achieve a safety factor of 2 for local buckling, the area moment of inertia of the longerons was increased by making them hollow tubes with the dimensions shown in Fig. 3-27.

In addition to the above responses caused by the control thrusters, the environmental loads cause some bending of the structure. Since these loads do not vary much during the 78 sec period of the first mode, they may be applied to the structure statically. The NASTRAN inertia relief option was used to compute this additional bending. The contributions to δ and e_p are 1.27 in. and 0.00103 rad (0.059 deg), respectively, at the time when the magnitude of the environmental load is a maximum.

Attitude Control Coupled with Vibration Control - A study was conducted to determine whether the pointing error and elastic vibrations could be reduced by modifying the control law. It was found that substantially better performance could be achieved by introducing the flexibility parameters into the control law.

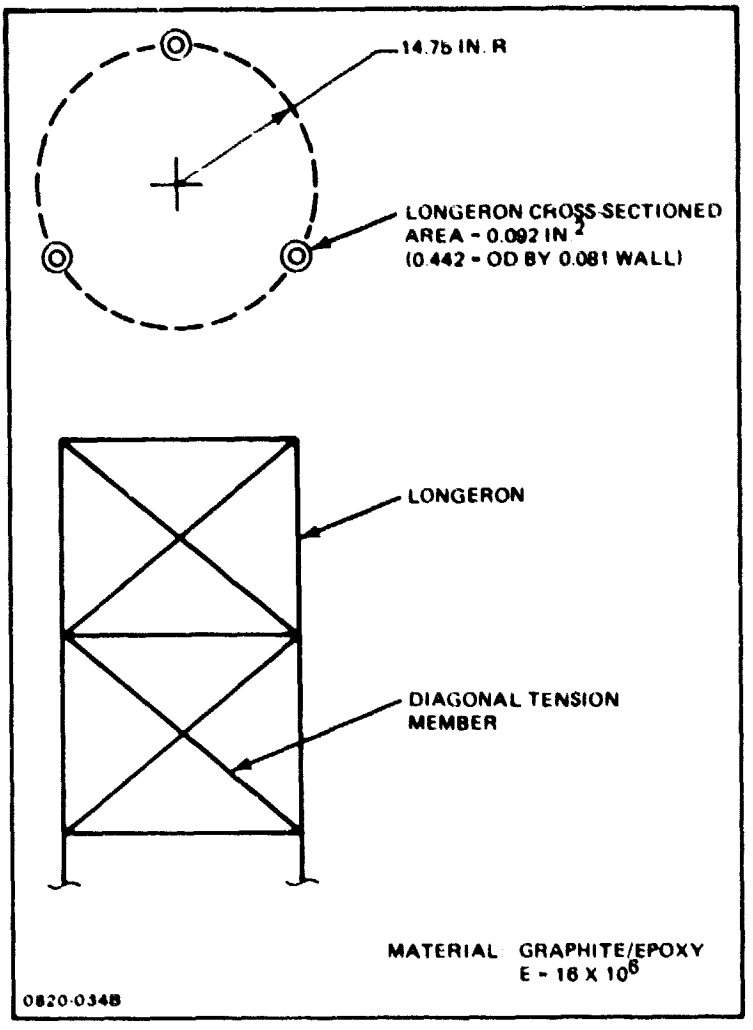

Fig. 3-27 Mast

TIME ON	TIME OFF	PULSE WIDTH, t_p
0	0.04	0.04
333	337.06	4.06
666	671.42	5.42
999	1002.63	3.63
1332	1332.85	0.85

NOTE: PULSES ARE APPLIED BY THE TWO 25-LB VERNIER THRUSTERS IN NOSE OF STS

0820-035B

Fig. 3-28 Pulsing Schedule for Simulation of Attitude-Hold Maneuvers Based on Rigid-Body Control Law

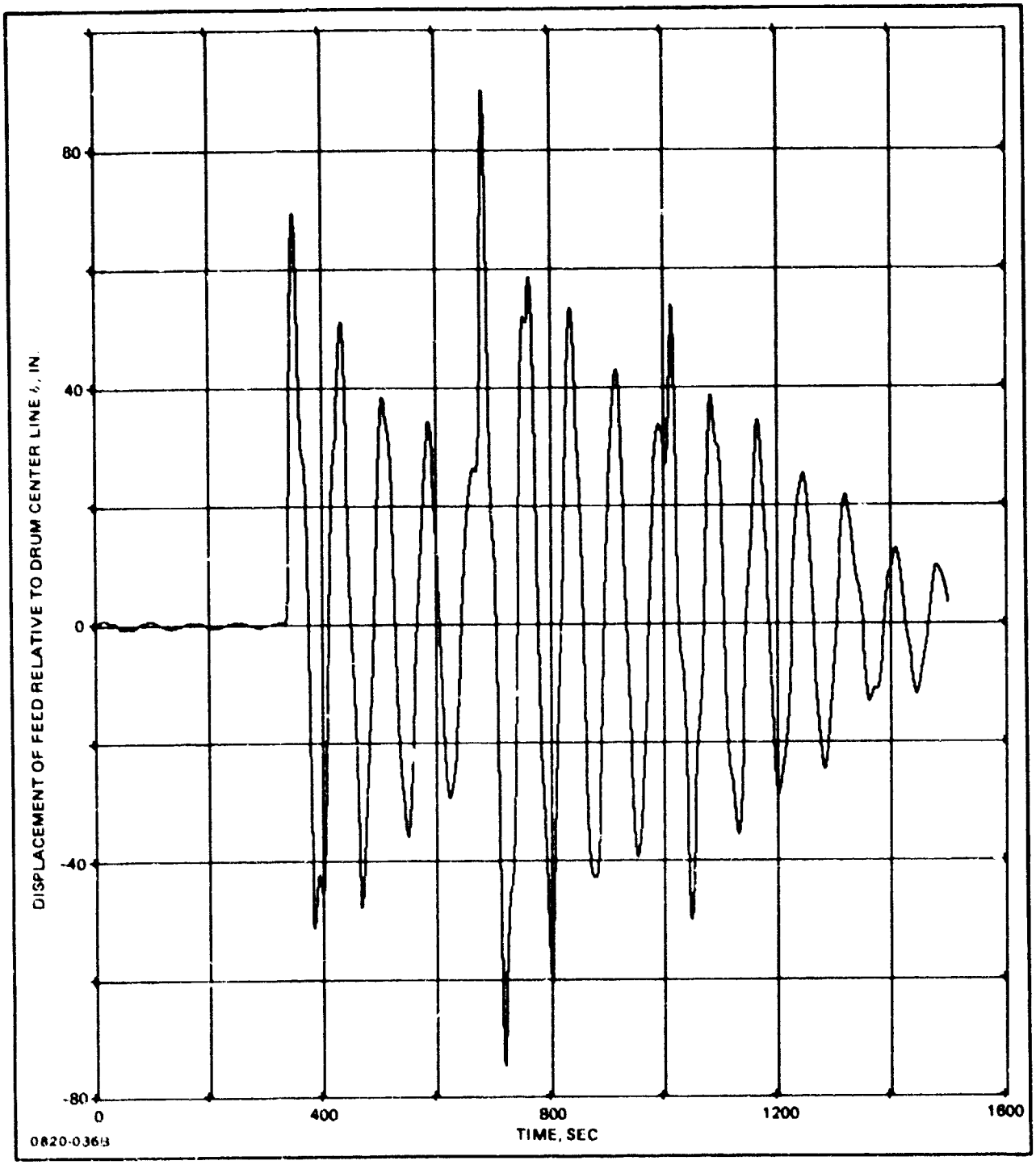

Fig. 3-29 Displacement of Feed Relative to Drum Center Line, Using Rigid-Body Control Law for Attitude-Hold Maneuver

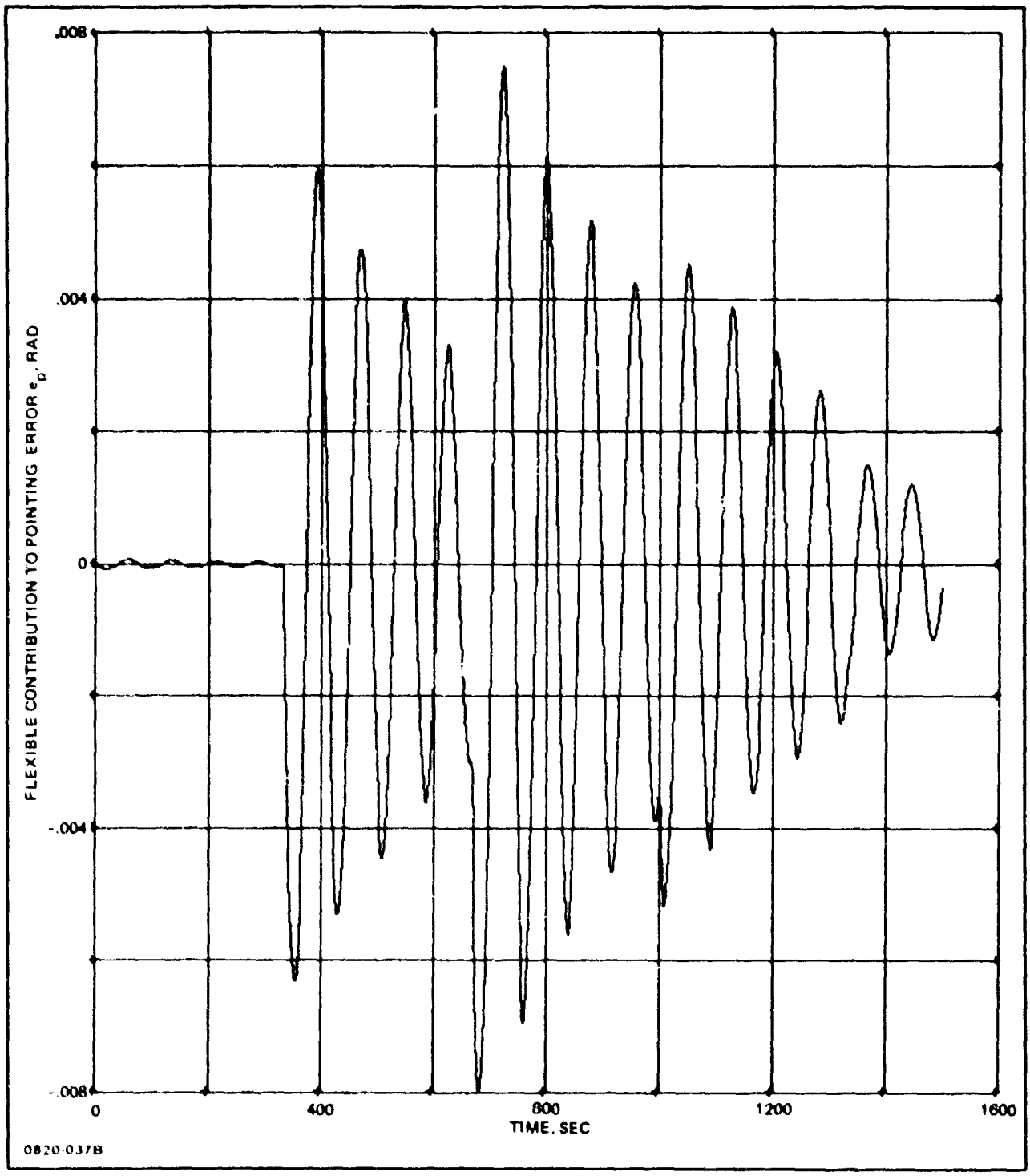

Fig. 3-30 Flexible Contribution to Pointing Error e_p, Using Rigid-Body Control Law For Attitude-Hold Maneuver

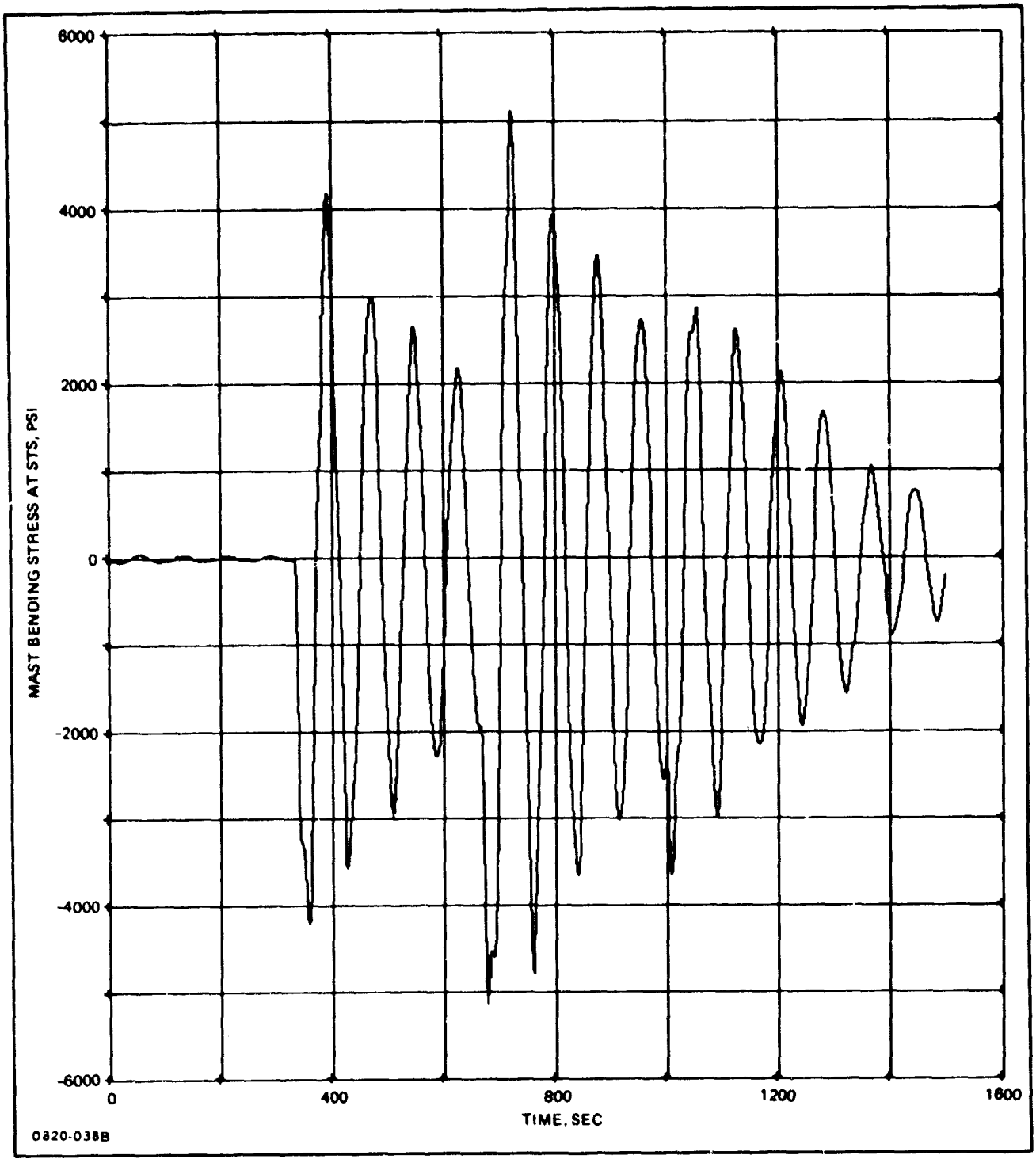

Fig. 3-31 Mast Bending Stress at STS Using Rigid-Body Control Law for Attitude-Hold Maneuver

The control logic is based on minimizing a quantity E, which is the weighted sum of the energy components; i.e.,

$$E = C_R E_R + C_1 E_1 + C_2 E_2 \qquad (5)$$

where E_1 and E_2 are the total (potential plus kinetic) energies associated with the two bending modes, E_R is the potential plus kinetic energy associated with the difference in the error and error rate from their values at the dead band reference point (e.g., the reference point is where $e = -e_{DB}$ and $\dot{e} = 0$ when e and $\dot{e}$ are located to the left of left switching curve of Fig. 25, view A), and C_R, C_1 and C_2 are weighting coefficients that are constants programmed into the control law. The average pulsing period τ is also a constant predetermined control parameter.

To illustrate the control logic, it is assumed that e and $\dot{e}$ are in the region of Fig. 3-24 where a positive control torque must be exerted, and that the current time falls within the n^{th} pulsing interval (e.g., time = t which is between $(n-1)\tau$ and τ, as illustrated in Fig. 3-32, view A. The projected value of E (E following the pulse) is predicted at time t and at future times $t + \Delta t$, $t + 2\Delta t$, . . . between t and $n\tau$ in order to determine whether the current value is a minimum. If the current projected value of E is a minimum, the thrusters are pulsed; otherwise the thrusters are not pulsed, and the projections are repeated at a slightly later time. The pulse widths used in the projections are based on the curves shown in Fig. 3-32, view B. For clarity, only the left switching curve is shown. The lower portion of the switching curve is based on α_C, the angular acceleration due to the control torque, the phase plane trajectory is based on the current value of α_E, the angular acceleration due to the environmental torque, and the upper portion of the switching curve is based on $(1 + \epsilon)\alpha_E$ where ϵ is a small quantity ($\epsilon = 0.05$ was used in the current work). Projected pulse widths are based on the alternative trajectories during pulsing at t, $t = \Delta t$, $t + 2\Delta t$, etc., where Δt is a pre-specified control parameter.

The current values of e and $\dot{e}$ are needed, but are not directly measurable because of the vibrations. In addition, the bending modal displacements ξ_1 and ξ_2 and their derivatives are needed. Simple expressions have been derived to determine these quantities indirectly from measurements of δ, θ_1, $\theta_1 - \theta_2$ (see Fig. 3-21), and the derivatives of these quantities. These expressions as well as the expressions used to project E, are a function of the vibration frequencies (equations (1) and (2)) and the mode shapes (Fig. 3-22). The expressions to project E are also simple and are based on the following assumptions:

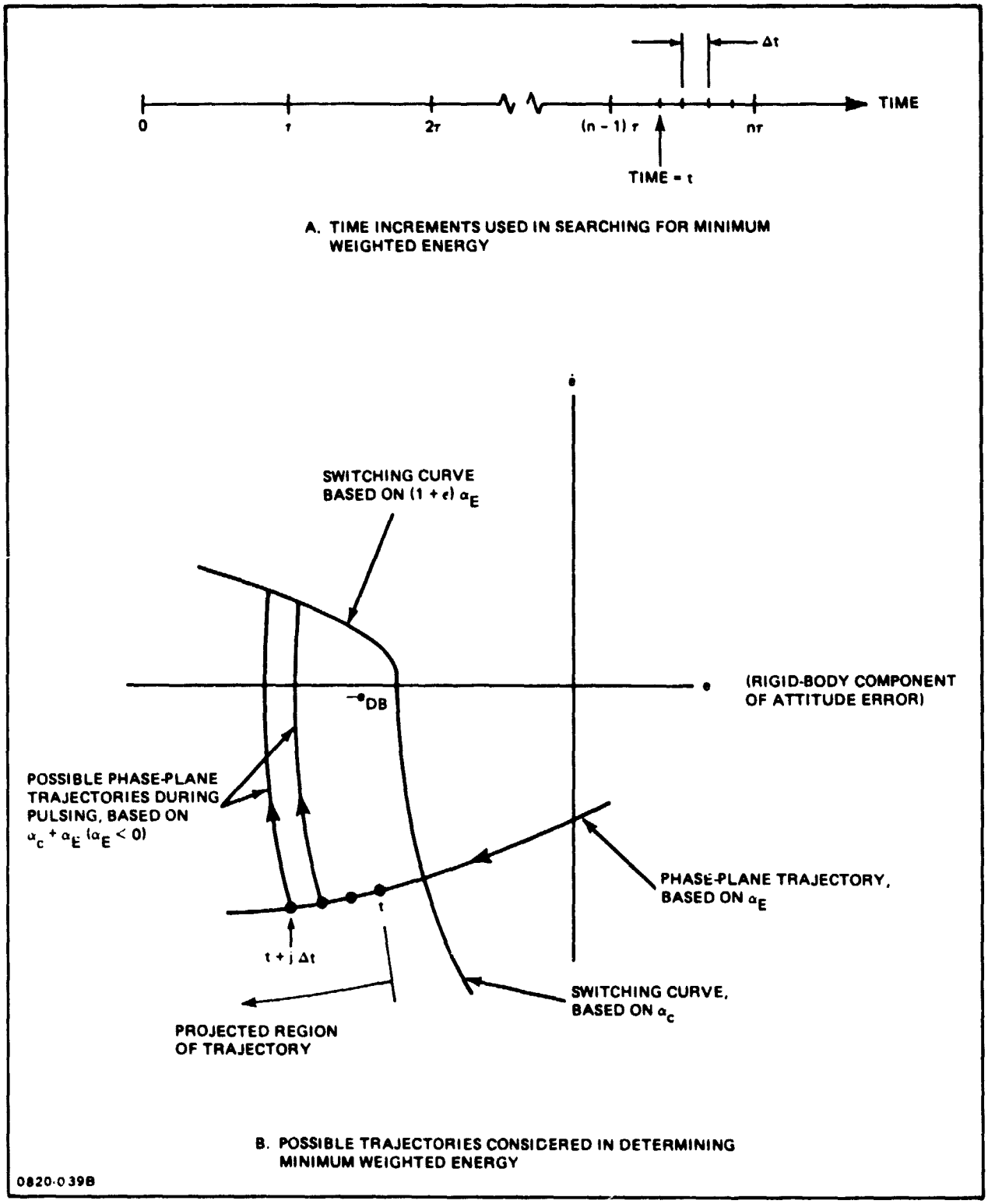

Fig. 3-32 Time Increments & Associated Phase-Plane Trajectories Used in Search for Minimum Weighted Energy for Coupled Attitude-Vibration Control

- Damping is neglected
- The thrusts act as impulses*
- Static deformations caused by the environmental loads are neglected**

The effects of these assumptions are included in the simulations of the motion that will be described.

The main parameters that can be adjusted to tune the control law are τ , C_R, C_1, and C_2. An advantage of this control law is that the average pulsing period τ can be decreased to the period of the first bending mode τ_1, thereby decreasing the pointing error (with the rigid-body, control law $\tau = 4.3\ \tau_1$ was recommended) while minimizing the elastic vibration. A further decrease in τ will result in additional improvement in the pointing accuracy at the expense of additional elastic vibration. However, τ cannot be decreased indefinitely; it must remain well separated from the periods of the higher vibration modes that are not included in the control law. The values of C_R, C_1, and C_2 can also be varied to trade off pointing accuracy (achieved by increasing C_R) with vibration reduction (achieved by increasing C_1 and C_2).

This control law was added to the Grumman SPACE12 Computer Program (Ref. 3-8), and the combined program was checked out. SPACE12 is used to simulate the controlled behavior of satellites of any shape by numerically integrating the equations of motion. The program includes the effects of control-system/elastic-vibration coupling as well as the nonlinear effects of large rotations.

Attitude-Hold Maneuver, Using Coupled Attitude/Vibration Control - The simulation of the attitude-hold maneuver described above was repeated using the coupled attitude-vibration control law. In order to complete the work within the allocated budget and schedule, it was not possible to adequately explore the effects of varying the control parameters. Only two runs were made, one with $\tau = 42$ sec and the other with $\tau = 21$ sec. The other control data used are:

$$C_R = 2.0$$
$$C_1 = 1.0$$
$$C_2 = 1.0$$

*It is not too complicated to change this and include the actual pulse shape; however, the response to impulsive thrusts are an excellent approximation to the actual response in this problem since the pulse widths are very short relative to the vibration periods of the modes being controlled.

**It is possible to modify the control law to include this effect.

$\epsilon = 0.05$

$e_{DB} = 0.0003$ rad

$t_{p_{min}} = 0.04$ sec (minimum pulse time)

$t_{p_{max}} = 1.0$ sec (maximum allowable pulse time)

$t = 2.0$ sec (intervals at which projections of E are made)

The maximum pulse time is included in the control law to limit the magnitude of flexible bending. Since the new control law enables pulsing at a higher frequency, it is possible to use significantly lower pulse widths than those used with the previous control law (see Fig. 3-28). The numerical-integration time interval used was 0.04 sec.*

Selected results are presented in Fig. 3-33 and 3-34 for the run with $\tau = 42$ sec. Fig. 3-33 shows the angular deflection of the STS θ_1 and the deflection δ of the feed relative to the drum centerline (see Fig. 3-21). The rigid-body pointing error e, its rate $\dot{e}$, and the total pointing error e_p are shown in Fig. 3-34. There is a nearly vertical rise in $\dot{e}$ every time a thruster is pulsed; thus verifying the fact that the control loads are nearly impulsive. A history of the thruster pulses is presented in Fig. 3-35. The total thruster impulse expended, which is proportional to the fuel used during the quarter orbit, is 660 pound-sec. The peak values of δ and e_p (converted to degrees) that occurred in this run and the run with $\tau = 21$ sec are summarized in Fig. 3-36. For comparison, the results for the rigid-body control of the previous subsection are also presented. It is seen that the use of coupled attitude-vibration control can substantially decrease both the pointing error and vibration deflection. As was expected, reducing the value of τ improved the pointing accuracy but produced larger elastic vibration. After the effects of varying the control parameters of this method are fully explored, it may be found that even better control can be achieved.

Simulation of Precision Pointing and Slewing, Using Coupled Attitude-Vibration Control - In another maneuver that was considered, the satellite is pointed at a target satellite located down-range (see Fig. 3-37) so that measurements of the radar-beam far-field pattern can be made. It was desired to direct the radar beam within a total (peak-to-peak oscillation) accuracy of one beam width (0.147 deg at 1.4 GHz). Fortunately the aerodynamic and gravity-gradient torques are relatively small with the satellite in this orientation; consequently, it is easier to achieve a higher pointing accuracy. It is also required to slew the satellite approximately ten beamdwidths (or 1.47 degrees) in order to measure the sidelobes.

*In the Runge-Kutta numerical-integration scheme used, the time interval is split in half and both a prediction and a correction are made at the half interval and the final interval. Thus, the 0.04 sec is equivalent to a finer interval for a cruder algorithm.

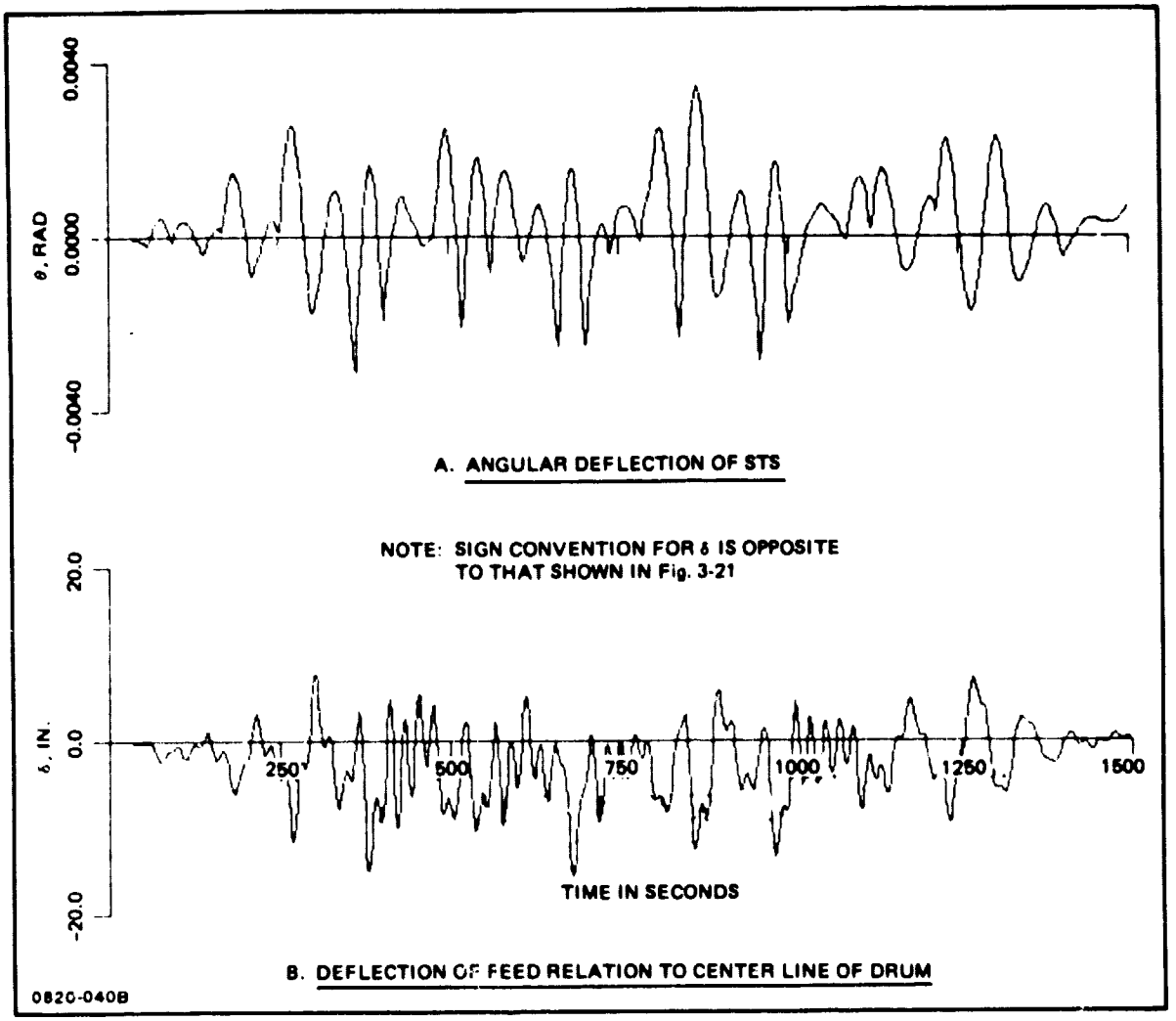

Fig. 3-33 System Vibration During Attitude-Hold Maneuver, Using Combined Attitude-Vibration Control with τ = 42 Seconds

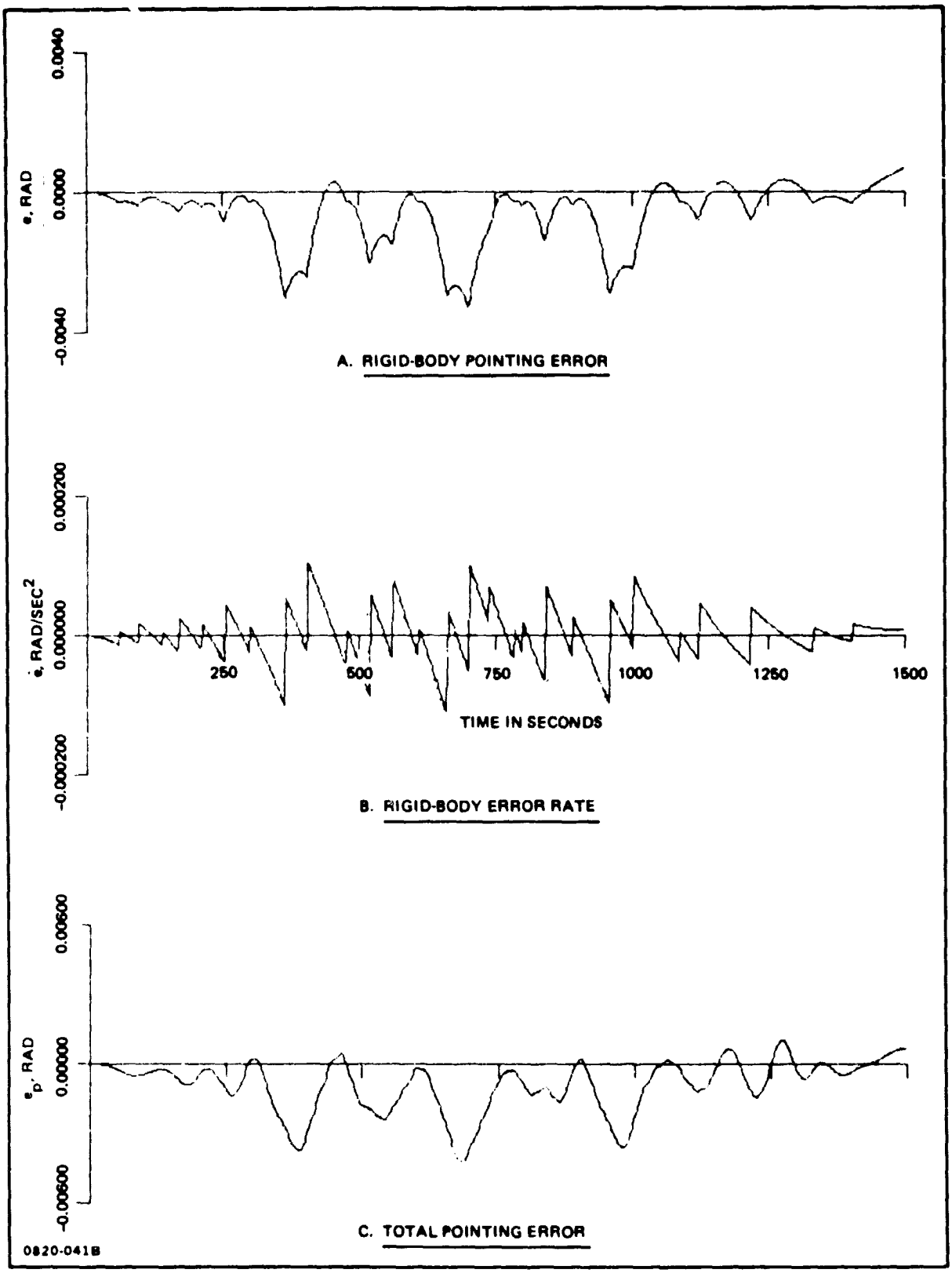

Fig. 3-34 Pointing Accuracy During Attitude-Hold Maneuver, Using Combined Attitude-Vibration Control With τ = 42 Seconds

THRUSTER TURNS ON AT TIME (SEC)	PULSE WIDTH, t_p (SEC)
59	0.096
94	0.150
140	0.114
168	0.320
210	0.274
252	0.541
299	0.183
363	1.000
404	0.827
477	0.369
520	1.000
561	0.766
610	0.229
662	1.000
700	1.000
737	0.322
782	0.238
798	0.314
840	0.952
891	0.348
958	1.000
1000	0.655
1086	0.269
1120	0.474
1217	0.493
1332	0.188
1403	0.079

NOTE: ALL PULSES ARE APPLIED BY THE TWO 25-LB VERNIER PITCH THRUSTERS LOCATED IN THE NOSE OF THE STS

0820-042B

Fig. 3-35 Pulsing History for Attitude-Hold Maneuver, Using Combined Attitude-Vibration Control With τ = 42 Seconds

TYPE OF CONTROL	POINTING ERROR (ϵ_p, DEG)		MAXIMUM DEFLECTION OF FEED RELATIVE TO DRUM CENTER LINE (δ, IN.)	
	MINIMUM	MAXIMUM	MINIMUM	MAXIMUM
COUPLED ATTITUDE-VIBRATION CONTROL WITH τ = 42 SEC	-0.24	0.06	-15	7.5
COUPLED ATTITUDE-VIBRATION CONTROL WITH τ = 21 SEC	-0.12	0.03	-17.5	9.2
RIGID-BODY CONTROL USED FOR FLEXIBLE SYSTEM	-1.2[a]	[b]	-90[c]	75[c]

[a] WAS NOT COMPUTED DIRECTLY. FOR THE PURPOSE OF COMPARISON, THE VALUE WAS ESTIMATED BY TAKING THE ROOT SUM SQUARE OF THE 1.14 DEG RIGID-BODY CONTRIBUTION FROM FIG 3-26 & THE 0.458-DEG FLEXIBLE CONTRIBUTION OBTAINED FROM THE SIMULATION OF THE PREVIOUS SUBSECTION

[b] WAS NOT COMPUTED

[c] ADJUSTED FOR DIFFERENT SIGN CONVENTION IN RUNS

0820-043B

Fig. 3-36 Comparison of Results for Different Types of Control During Attitude-Hold Phase of Mission

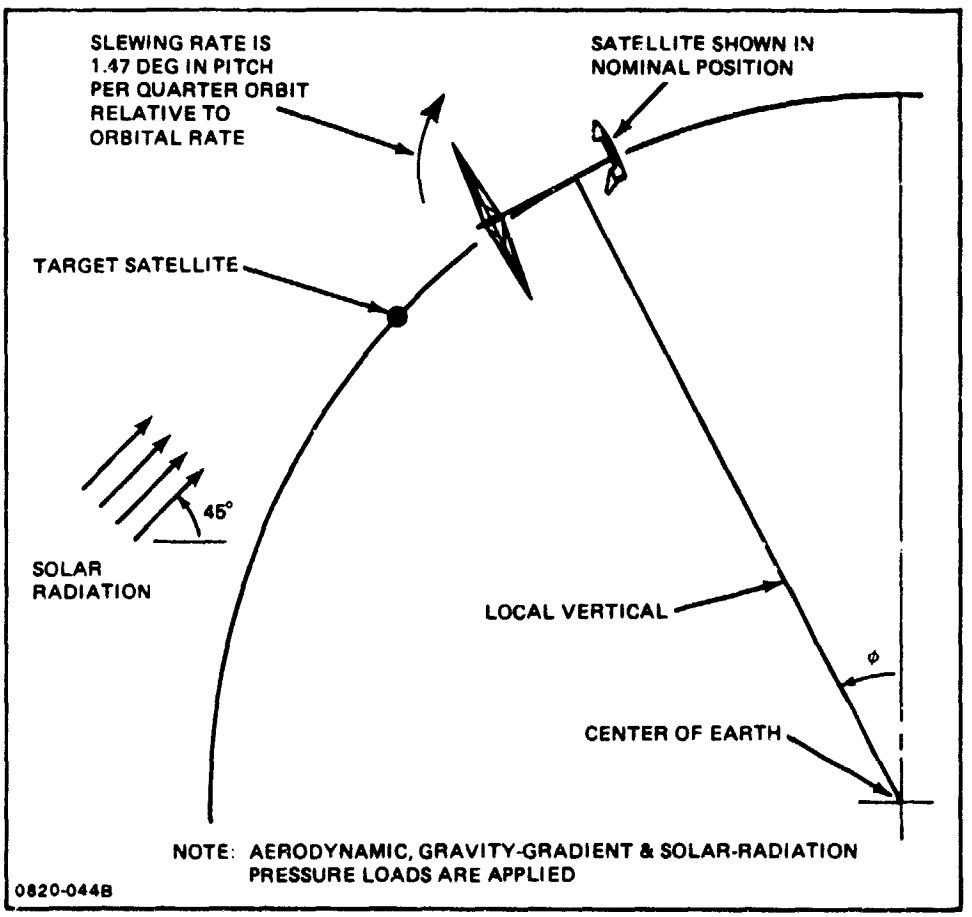

Fig. 3-37 Satellite in Orbit During Precision Pointing While Slewing

To demonstrate the capability of the combined attitude-vibration control law to perform both the precision pointing and slewing functions in a single simulation, the following maneuver was postulated:

- Satellite is initially, and nominally, oriented with the mast perpendicular to the local vertical (see Fig. 3-37); consequently the nominal rotation rate is nose down in pitch at the orbital rate, $\omega_o = 0.001071$ rad/sec
- Satellite is slewed relative to orbital angular velocity at constant nose-up pitch rate of $\dot{\theta}_p = -1.750 \times 10^{-5}$ rad/sec (based on 10 beamwidths per quarter orbit); consequently pitch angle command is $\theta_c = (\omega_o + \dot{\theta}_p)t$
- To demonstrate precision pointing, the allowable deviation from θ_c is one beamwidth (0.147 deg, peak-to-peak). This deviation is e_p in Fig. 3-21.

In the previous simulation, the attitude-hold maneuver, the location of the center of pressure (CP) on the STS was not significant since the aerodynamic torque was predominantly attributable to the pressure exerted on the antenna; however, in the present simulation this contribution to the total torque is nominally zero. Consequently, while the CP on the STS could be (and was) previously assumed to coincide with its CM without introducing any significant error, in the present simulation the location of the CP is significant. It is assumed to be located 200 inches forward of the STS CM, so that a conservatively large environmental torque will be generated. A minimum pulse time of 0.080 sec was used since we were recently notified that this limitation would be a new STS requirement. The value of τ was set at 50 seconds. Except for these values and the attitude orientation command, the control data are the same as the data for the attitude hold maneuvers.

The pulsing history that occurred during the simulation is presented in Fig. 3-38. It is seen that only the minimum pulse width of $t_{p_{min}} = 0.080$ sec occurs. In accordance with the control logic, no pulse is applied unless the theoretical required pulse width is greater than $t_{p_{min}}/2$. When the theoretical pulse width is between $t_{p_{min}}/2$ and $t_{p_{min}}$, a pulse of width $t_{p_{min}}$ is applied. Since the pulse widths are shorter than those of the previous simulation, a smaller numerical integration interval, 0.010 sec, was used.

Figure 3-39 shows the rigid-body error e, its rate $\dot{e}$, and the total pointing error e_p. The total pointing error oscillates between +0.001 deg and -0.027 deg; thus the total peak-to-peak deviation is 0.028 deg which is well within the desired value of 0.147 deg. The vibration of the STS relative to the antenna is illustrated in Fig. 3-40. The maximum linear deflection of the feed relative to the drum centerline is 1.7 inches. Figure 3-41 shows the aerodynamic, gravity-gradient, and total environmental torque components on the satellite.

THRUSTER TURNS ON AT TIME (SEC)	PULSE WIDTH, t_p (SEC)
99	0.080
215	0.080
380	0.080
496	0.080
665	0.080
780	0.080
977	0.080
1094	0.080
1266	0.080
1399	0.080

NOTE ALL PULSES ARE APPLIED BY THE TWO 25-LB VERNIER PITCH THRUSTERS LOCATED IN THE NOSE OF THE STS

0820-045B

Fig. 3-38 Pulsing History for Precision Pointing While Slewing, Using Combined Attitude-Vibration Control

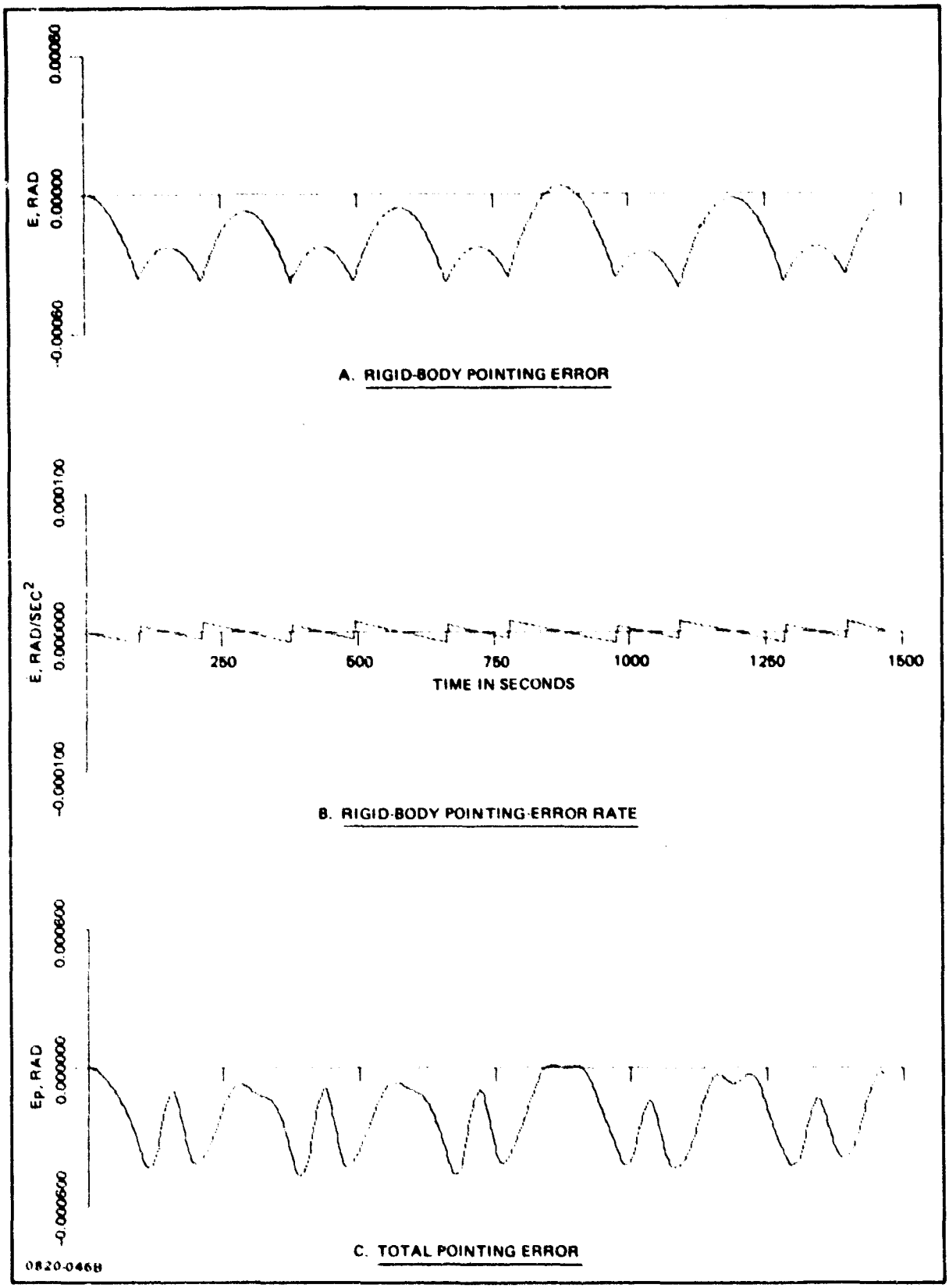

Fig. 3-39 Pointing Accuracy During Precision Pointing and Slewing, Using Combined Attitude-Vibration Control

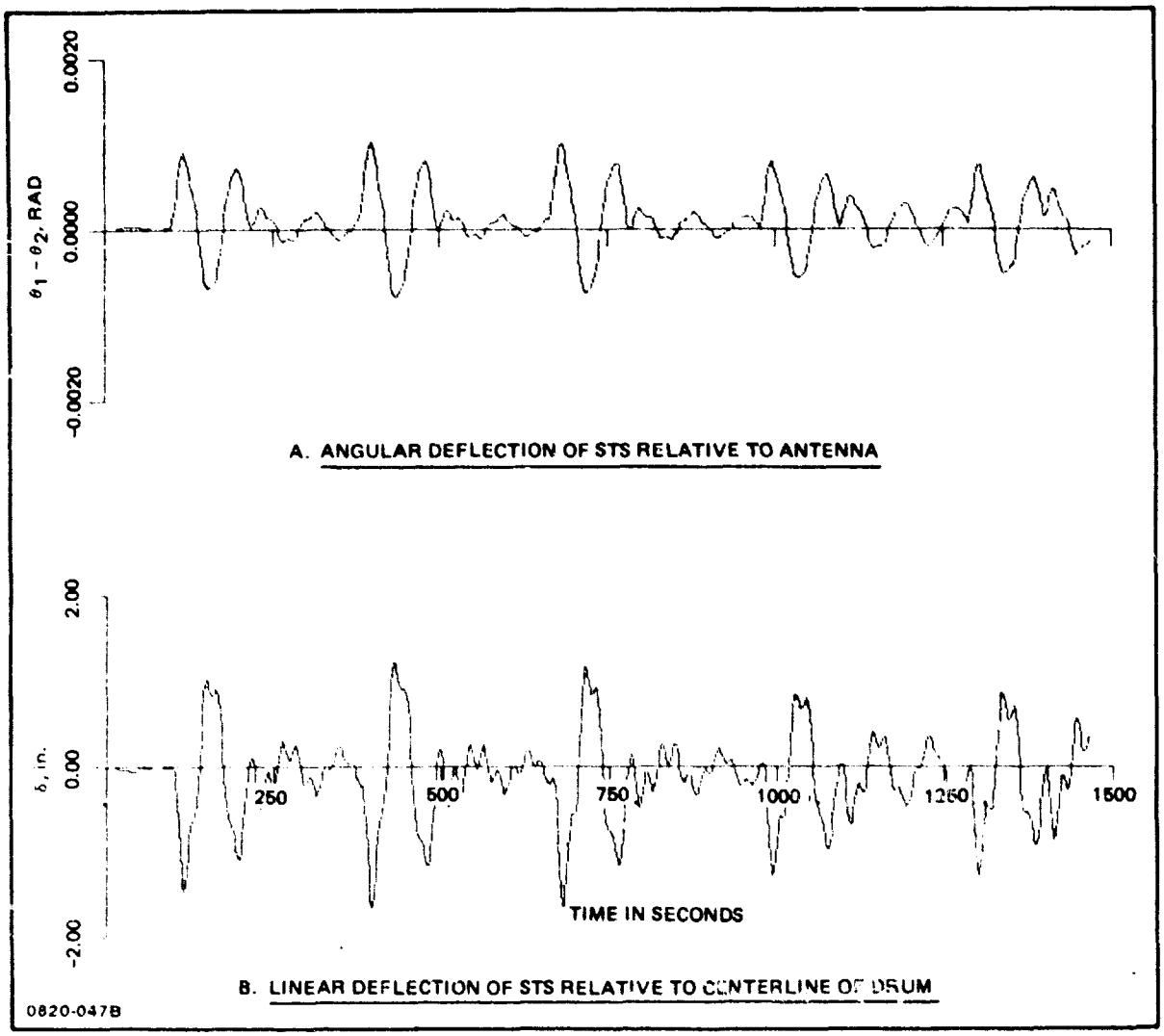

Fig. 3-40 Elastic Vibration During Precision Pointing and Slewing, Using Combined Attitude-Vibration Control

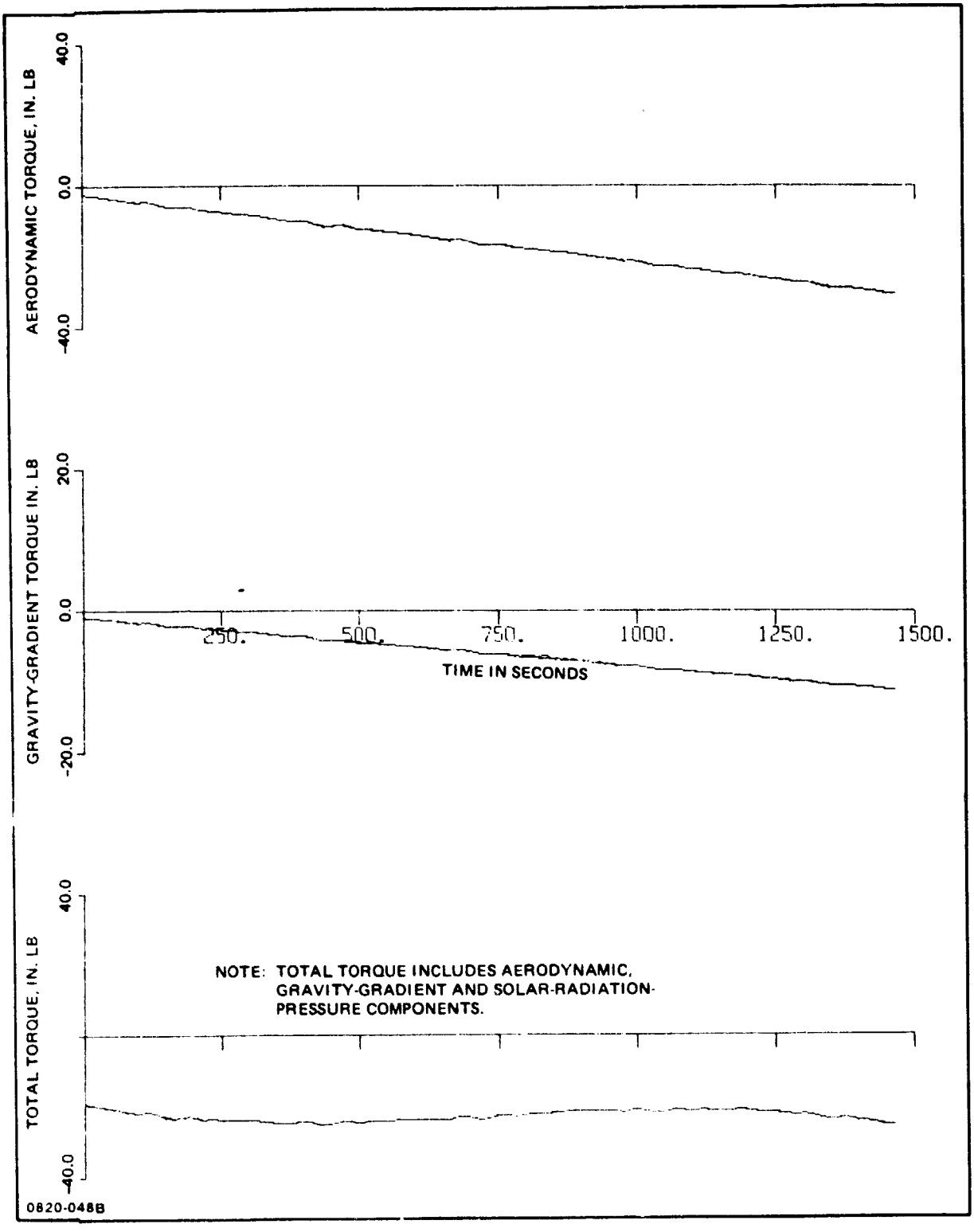

Fig. 3-41 Environmental Torques During Precision Pointing and Slewing Maneuver in First Quarter of Orbit

The total torque also includes the contribution caused by solar radiation pressure. The maximum environmental torque magnitude is only 26 inch-pounds which may be compared with the 649 inch-pounds that occurred during the attitude-hold maneuver. The total thruster impulse expended, which is proportional to the fuel used during the quarter orbit, is 40 pound-seconds. This value is considerably lower than the 660 pound-seconds that was required to counteract the higher torques during the attitude-hold maneuver.

3.3.2 RF ANALYSIS

This part of the study concentrated on the development of analysis tools to predict the performance of antenna systems (reflectors and lenses) for various mission configurations, including the scan limitations of flat-faced, space-fed antenna systems for multi-beam applications. Both the bootlace and zoned lens configurations were evaluated.

It is shown that the scan performance of the systems satisfying the geometric optics approximation is only limited by the feed placement (geometry) and is independent of the primary focus compensation method. However, the system bandwidth is affected by the selected focusing method.

By expanding the aberration function into a power series about the radial direction (in the plane of the lens), both coma and astigmatism scan limits are evaluated. It is shown that coma limits the scan performance for short focal length systems while astigmatism limits the scan performance for long focal length systems. The results are shown to be in agreement with previous work on offset reflectors.

The distorted far-field radiation patterns, due to the significant aberration coefficients, are also evaluated using the principles of Fourier optics (diffraction theory). The gain loss, beam position shift, sidelobe asymmetry and level change are computed as a function of a family of feed positions (scan angles) for a given peak aperture edge phase error.

By adapting and modifying a NASA/Langley reflector antenna computer program (RAPDAT) the far-field radiation patterns of several offset reflector and conventional parabolic reflector geometries were computed. This allowed the comparison of the far-field patterns of various feed configurations and verified the use of the simplified Siedel aberration approximation.

Having evaluated the performance limitations of the system, a design procedure for a compensating feed array is outlined. The feed array is synthesized (i.e., the excitations of a family of nonplanar array elements) such that the projected aperture approximates the desired illumination function in the least square sense. Since the array element excitation

coefficients are dependent on the feed location, criteria for optimum feed loci are established. Even with a complex offset optimum feed, the displacement scan regime of a flat-faced lens will at best asymptotically approach the scan capability of the optimum offset reflector.

3.3.2.1 Summary of Computer Results

There are two sets of systems designs, the reference and limited mission demonstration systems. These systems are further subdivided into radar, communications and radiometer applications. The major differences among the antenna systems is the focal length-to-diameter ratio and the desired scan performance requirements.

The characteristics of the family of antenna systems considered in the study are summarized in Fig. 3-42. The far field radiation patterns associated with the systems are shown in Fig. 3-43. The far-field radiation patterns depicted in Fig. 3-43 for the various mission scenarios utilized a circularly symmetric corrugated horn feed with the electric field vector linearly polarized. The horn size was adjusted in each case to make the first sidelobes of the feed just miss the edge of the reflector.

The off-set feed system far-field radiation patterns show evidence of coma aberration as expected. Coma is particularly evident in the short focal length systems (limited mission flight demonstration). However, the primary purpose of the limited mission demonstration systems is to verify the analytical models by actual measurements. As a matter of fact, the short focal length systems exaggerate the aberrations with minimum displacement steering and provide a suitable test bed for the comparison of theory and experiment.

Based upon the simplified theory of primary (Siedel) aberrations, the number of displacement beam positions allowed for 14 dB sidelobes is approximately six. In comparing Fig. 3-43 (views I and K) for 5 beam positions off-axis, one will note that the first sidelobes in view K are approximately at 15 dB. This result shows good agreement with theory. Similar comparisons can be made for the F/D = 0.5 radiometer system which allows 2.25 times more beam positions.

3.3.2.2 Methodology Used in Calculation of Radiation Patterns

The far-field radiation pattern for the reflector systems (both on-axis fed and offset geometry) were evaluated using a NASA/Langley developed CDC computer program adopted to the Grumman IBM/Time Share environment.

The far field pattern computation program, RADPAT, uses equations of geometrical optics to calculate the reflected electric field using the radiation patterns of the feed and the parameters defining the reflector surface.

REFERENCE SYSTEMS			LIMITED MISSION – FLIGHT DEMONSTRATION		
RADAR	COMMUNICATIONS	RADIOMETER	RADAR	COMMUNICATIONS	RADIOMETER
A) 71 METER DIA FREQ: 1.35 GHz PHASE ARRAY ON-AXIS FEED, PHASED STEERED, FLAT-FACED LENS F1.5. B) 300 METER DIA FREQ: 3 GHz, F1.5.	80 METER DIA FREQ: 0.89 GHz F1.5. OFFSET PARABOLIC REFLECTOR. DISPLACED FEED STEERED, MULTIBEAM SYSTEM	100 METER DIA FREQ: 1.4 GHz F4. OFFSET PARABOLIC REFLECTOR. DISPLACED FEED STEERED, MULTIBEAM PUSH-BROOM SYSTEM.	100 METER DIA FREQ: 1.35 GHz F1. PHASED ARRAY FLAT-FACED LENS BOTH ON-AXIS PHASE AND DISPLACED FEED STEERED.	100 METER DIA FREQ: 1.35 GHz F1. PHASED ARRAY FLAT-FACED LENS BOTH ON-AXIS PHASE AND DISPLACED FEED STEERED.	100 METER DIA FREQ: 1.4 GHz F1.5 OFFSET PARABOLIC REFLECTOR. DISPLACED FEED STEERED.
RADIATION PATTERN ON-AXIS ONLY (FIG. 25) 0820-076B	RADIATION PATTERN ON-AXIS AND 4 DEG OFF-AXIS (16 BW) (FIG. 26, 27 & 28)	RADIATION PATTERN ON-AXIS, 10 DEG OFF-AXIS (80 BW) AND 50 BW (FIG. 29, 30, 31 & 32)	RADIATION PATTERN ON-AXIS AND 0.76 DEG OFF-AXIS (5 BW) (FIG. 33, 34 & 35)		RADIATION PATTERN TWO FEEDS, ON-AXIS AND 1.4 DEG OFF-AXIS (10 BW) FIG. 36, 37, 38 & 39)

Fig. 3-42 Antenna Systems

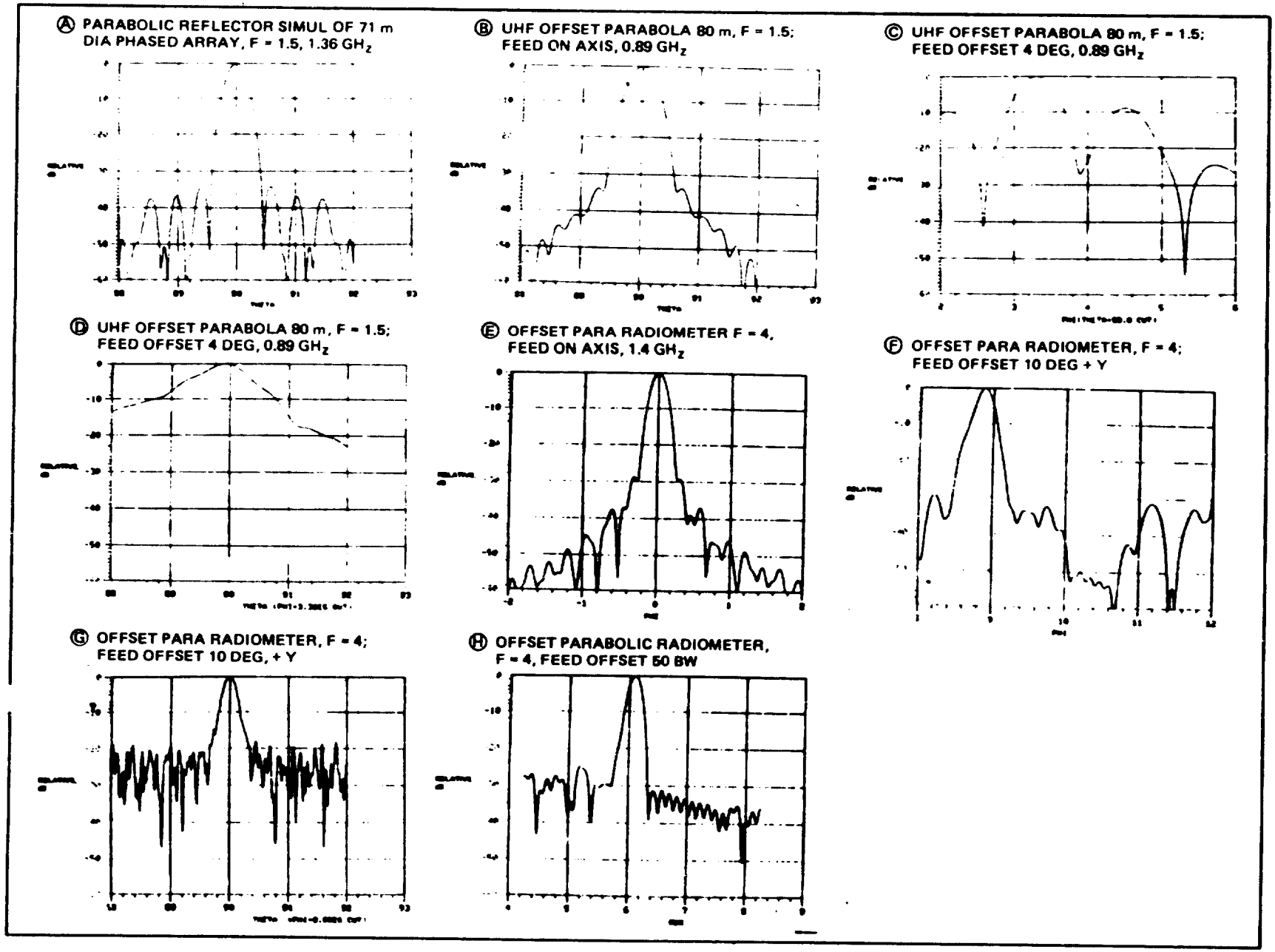

Fig. 3-43 Antenna Systems Field Radiation Patterns (Sheet 1 of 2)

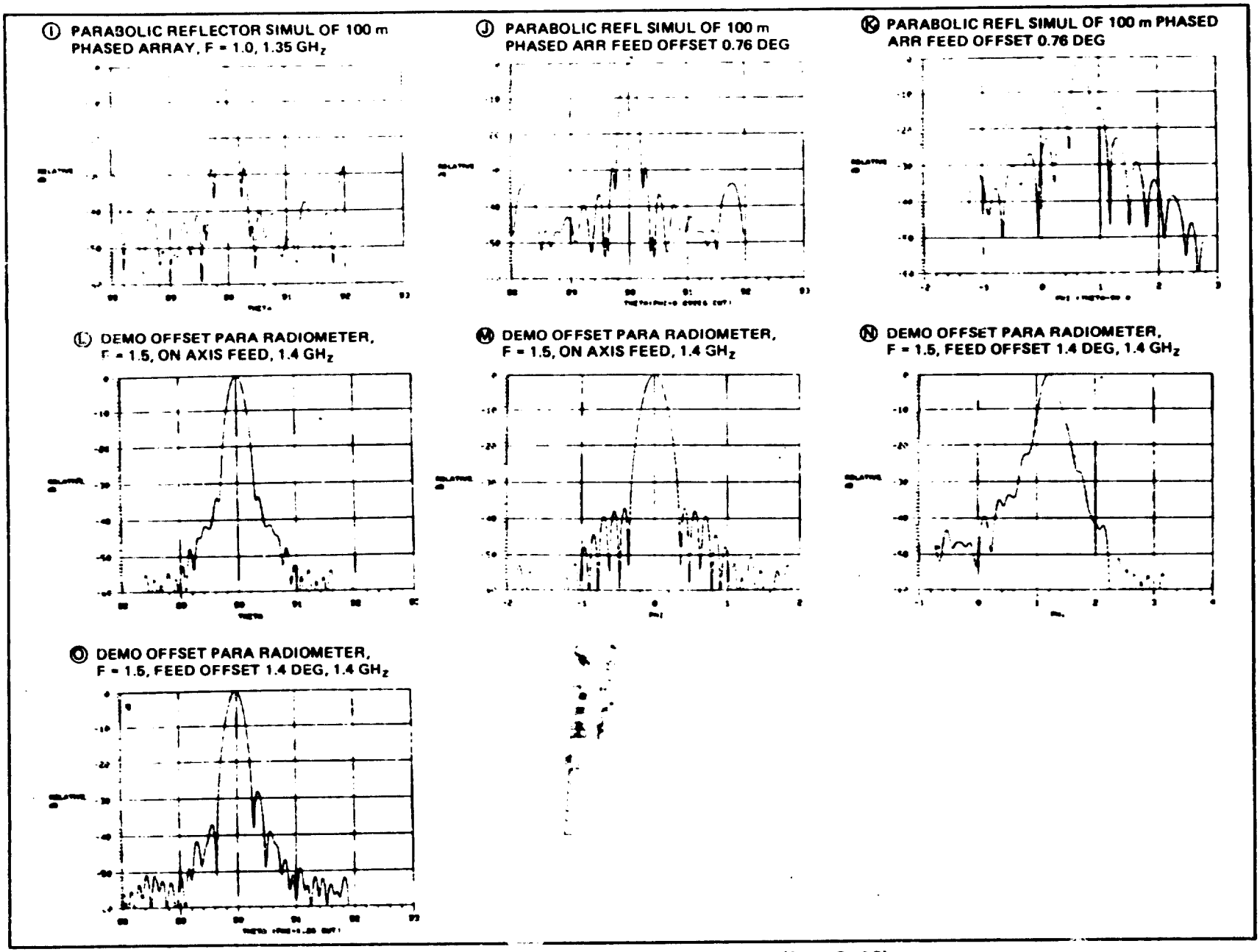

Fig. 3-43 Antenna Systems Field Radiation Patterns (Sheet 2 of 2)

The feed and reflector coordinate systems geometry is depicted in Fig. 3-44. The bundle of rays emanating from the feed is mapped via the reflector into the aperture plane as shown in Fig. 3-45. The reflector can be a paraboloid, an ellipsoid or a sphere. The ray bundles are obtained by specifying the feed radiation pattern to fill the reflector and quantizing the beam into a number of grid spaces of multiple wavelength width in the aperture plane. The quantized feed pattern information is stored in a three-dimensional array (see Fig. 3-46) containing E and H field amplitudes and phase information along with the angular location of the pierce points. The directions of the reflected ray and the point of intersection of the reflected ray with the aperture plane are also obtained. The magnitude and phase of the electric field vector is computed at each pierce point with the family of pierce points comprising the aperture distribution. The resultant aperture distribution is integrated numerically over the aperture plane to yield the far field radiation pattern. The theory of the computer program is described in (Ref. 3-9 and 3-10).

The most commonly used alternative formulation is the current distribution method (Ref. 3-10), where the surface current J_s on the reflector is taken to be $2(\hat{n} \times H_i)$. H_i is the incident magnetic field calculated from the feed pattern using geometrical optics, and $\hat{n}$ is the unit normal to the reflector surface. This current is then integrated over the reflector surface to yield the far-field radiation pattern. Common to both methods of analysis are the following:

- The surface current on the shadow side of the reflector is assumed to be zero
- The discontinuity in the surface current at the edge of the reflector is neglected
- Aperture blockage and direct radiation from the feed are not included. These approximations commonly restrict the accuracy of the calculations using either formulation to the main beam and the close-in sidelobes (Ref. 3-11 and 3-12).

The advantage of the method used here is that the integration over the aperture plane can be performed with equal ease for any feed position and any feed pattern, whereas the integration over the reflector surface is time-consuming and becomes difficult when the feed is placed off-axis or when the feed radiation pattern has no symmetry which can be used to simplify the formulation.

3.3.2.3 Aberration Analysis of the Offset Space-Fed, Constrained, Flat-Faced Lens

A lens is considered fully constrained if the ray paths within the lens are parallel to the lens axis (Ref. 3-13). The initial analysis of the lens depicted in Fig. 3-47 assumed the lens to be fully constrained. However, this limitation may be removed. The additional

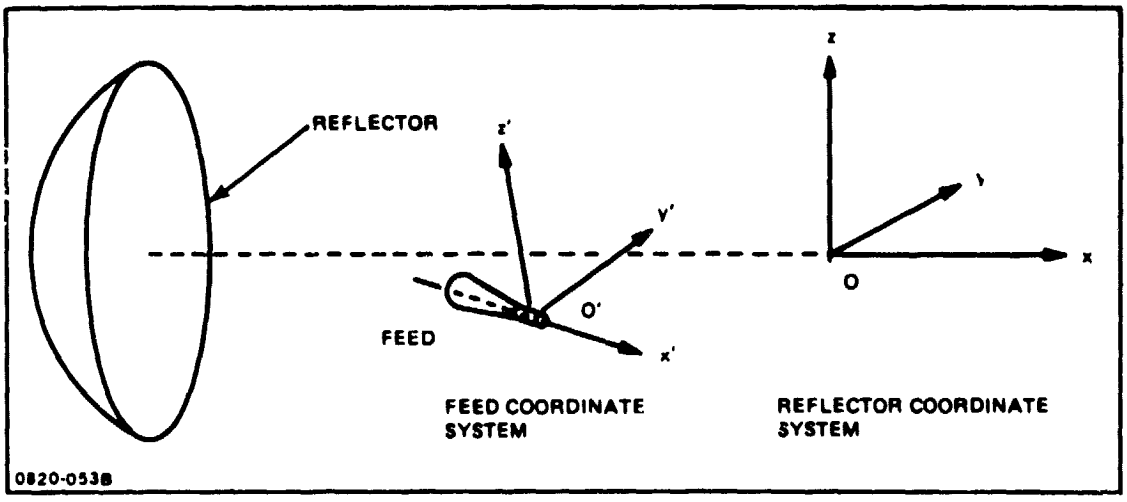

Fig. 3-44 Feed and Reflector Coordinate Systems

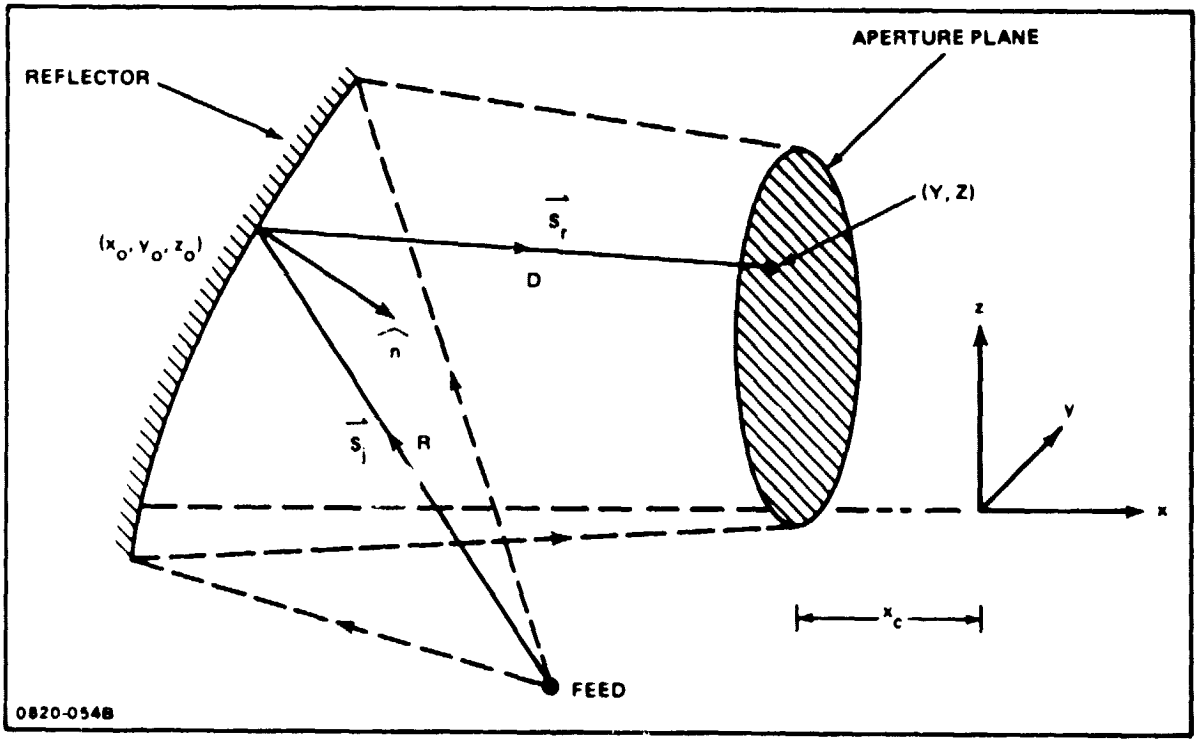

Fig. 3-45 Geometry of the Reflector Antenna

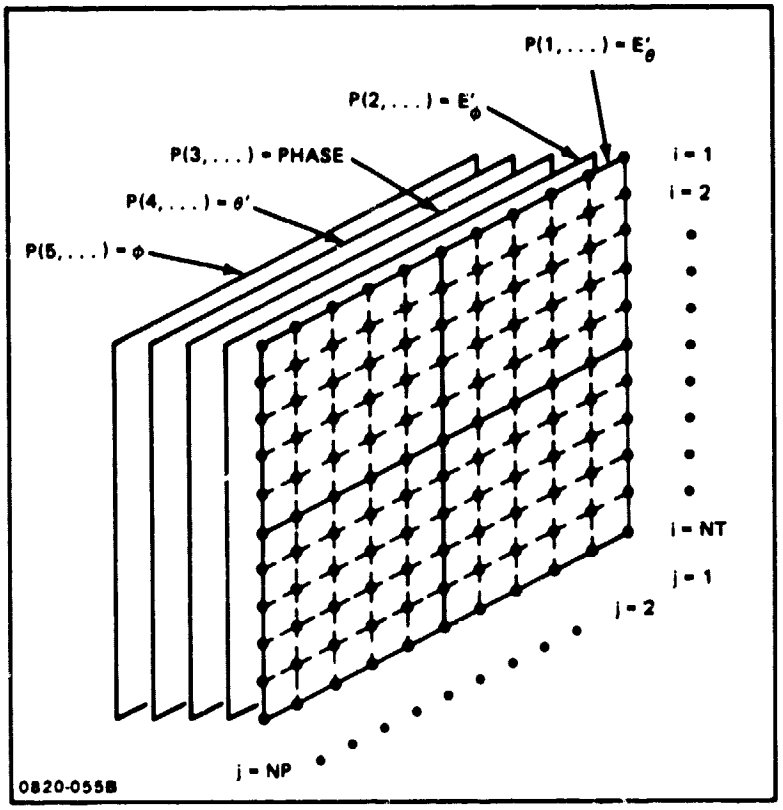

Fig. 3-46 P Array & Feed Pattern Information

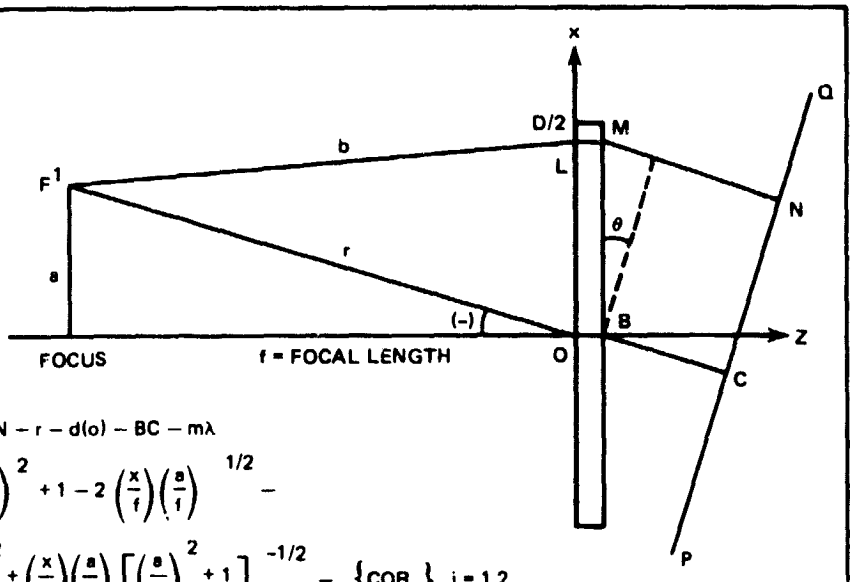

$$E(x) = b + d(x) + MN - r - d(o) - BC - m\lambda$$

$$\frac{E(x)}{f} = \left(\frac{x}{f}\right)^2 + \left(\frac{a}{f}\right)^2 + 1 - 2\left(\frac{x}{f}\right)\left(\frac{a}{f}\right)^{1/2} -$$

$$-\left[\left(\frac{a}{f}\right)^2 + 1\right]^{1/2} + \left(\frac{x}{f}\right)\left(\frac{a}{f}\right)\left[\left(\frac{a}{f}\right)^2 + 1\right]^{-1/2} - \left\{COR_i\right\}, i = 1,2$$

1. $COR_1 = \left[\left(\frac{x}{f}\right)^2 + 1\right]^{1/2} - 1$ (BOOTLACE)

2. $COR_2 = \frac{\lambda}{f} INT\left[\frac{E(x)}{f}\ \frac{f}{\lambda}\right] + COR_1 - \frac{\lambda}{f} INT\left[\frac{f}{\lambda}\ COR_1\right]$ (ZONED)

$$\frac{E(x)}{f} \simeq \frac{x}{f}(SIN\ \theta - COS\ \theta\ TAN\ \theta) + \frac{1}{2}\left(\frac{x}{f}\right)^2\left(COS\ \theta - \frac{TAN^2\theta}{COS^3\theta}\right) + \frac{1}{4}\left(\frac{x}{f}\right)^3 \frac{TAN\ \theta}{COS^3\theta} + H.O.T.$$

WHERE COR = CORRECTION

0920-056B

Fig. 3-47 Offset Feed for a Constrained Lens

degree of freedom then gained could be used to reduce the aberrations due to the flat input and output lens surfaces. The mathematical formulation of the unconstrained flat-faced lens is considered later.

In reference to Fig. 3-47, the condition that the phase should be constant along the line PQ is that the electrical path length LMN should be constant for any possible path through the lens: the emerging rays BC and MN are assumed to make an angle θ with the lens axis, also being the angle FOF[1] (Ref. 3-13). This condition gives

$$F'L + LM + MN = F O + OB + BC + m \tag{1}$$

where the term $m\lambda$ has been added to allow for the possibility of stepping (Ref. 3-13).

From the geometry of Fig. 3-47, we obtain the expression for the path length error (aberration function) when the feed occupies any position F':

$$E(x) = b + d(x) + MN - r - d(o) - BC - m\lambda \tag{2}$$

where d(x) and d(o) are the path lengths due to either a bootlace or modulo λ zoning within the lens (i.e., the refractive index times the lens thickness in a dielectric).

From the geometry of Fig. 3-47 one obtains:

$$\frac{E(x)}{f} = \left[\left(\frac{x}{f}\right)^2 + \left(\frac{a}{f}\right)^2 + 1 - 2\left(\frac{x}{f}\right)\left(\frac{a}{f}\right)\right]^{1/2}$$

$$- \left[\left(\frac{a}{f}\right)^2 + 1\right]^{1/2} + \left(\frac{x}{f}\right)\left(\frac{a}{f}\right)\left[\left(\frac{a}{f}\right)^2 + 1\right]^{1/2} - COR_i, \; i = 1, 2 \tag{3}$$

where COR_i, $i = 1, 2$ refers to a correction of the spherical aberration term for the primary focus, located a distance f (focal length) away from the lens surface. The correction term (COR_i), $i = 1, 2$ can be either real time delay ($i = 1$) making the unscanned lens infinite bandwidth for a point source feed at the primary focus using bootlaces, or using a correction corresponding to modulo λ multiple of a wavelength (or module 2π phase shift) using zoning ($i = 2$) (Ref. 3-13). Since the aberration function is strictly a function of the lens geometry, the aberration properties of the flat-faced lens system are independent of the type of primary focus compensation method (i.e., bootlace or modulo λ compensated).

Returning to the aberration function, (3), the bootlace correction is given by:

$$COR_{i=1} = \left|\left[\left(\frac{x}{f}\right)^2 + 1\right]^{1/2} - 1\right| \tag{4}$$

while the correction for the zoned lens is given as (i = 2)

$$COR_{i=2} = \frac{\lambda}{f} \text{ INT}\left[\frac{E(x)}{f}\frac{f}{\lambda}\right] + COR_{i=1} - \frac{\lambda}{f} \text{ INT}\left[\frac{f}{\lambda} COR_{i=1}\right] \tag{5}$$

In order to examine the significant aberration terms we expand (3) in powers of x:

$$\frac{E(x)}{f} \simeq \frac{x}{f}(\sin\theta - \cos\theta \tan\theta) + \frac{1}{2}\left(\frac{x}{f}\right)^2\left[\cos\theta - \frac{\tan^2\theta}{\cos^3\theta}\right] + \frac{1}{4}\left(\frac{x}{f}\right)\frac{\tan\theta}{\cos^3\theta} + \text{H.O.T.} \tag{6}$$

The second term in equation (6) represents astigmatism and field curvature and the third term represents coma. In order to evaluate the effects of the primary aberrations on the scan limit performance of the lens we examine their effects separately. The amount of aberration that can be tolerated by the system is limited primarily by the sidelobe levels. The relationship between the rms phase error (aberration) and the sidelobe levels in the far field patterns are established (Ref. 3-14). However, before we examine the two primary Siedel aberrations (Ref. 3-14) one by one, we plot the total aberration function (Equation (3)) as a function of the reciprocal of the focal length to diameter ratio with displacement scan angle as a parameter in Fig. 3-48 through 3-52. We note that the aberration function takes on multiple values for large scan angles. As will be shown later, to maintain the desired sidelobe levels (approximately 40 dB down) we have to limit the (E/F) to less than ±0.0001, that is, to systems with (F/D) > 2 for scan angles in the neighborhood of one degree or larger. Of course, this is an oversimplified statement since the scan angle limits are also a function of the number of wavelengths in the aperture.

3.3.2.4 Instantaneous Bandwidth Limitations

The bandwidth of a space-fed zoned lens depends on the optical path length differences. Since the zoned lens only removes modulo λ multiples of the path length difference, the instantaneous bandwidth of the lens is affected by the path length difference (e.g., equation (1)), and by the amount of phase scanning. As a matter of fact, even in the case of the bootlace correction for an on-axis primary feed, the instantaneous bandwidth is reduced when one displacement steers the lens. The instantaneous bandwidth of the zoned lens is given by:

$$W = \frac{8c\,(f/D)}{D\left[1 + 4\left(\frac{f}{d}\right)\sin\theta\right]} \tag{7}$$

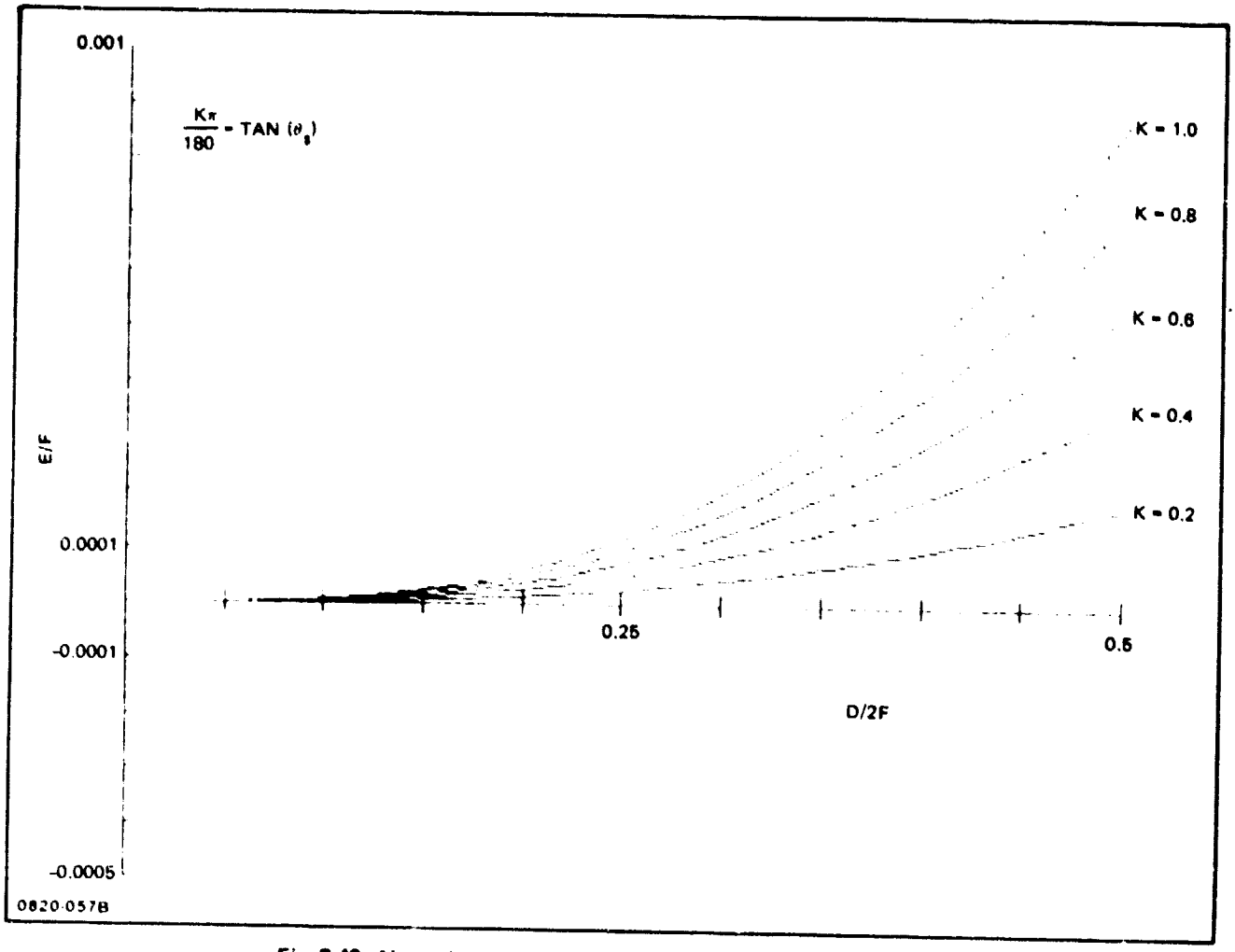

Fig. 3-48 Aberration Function with Feed Location K as a Parameter

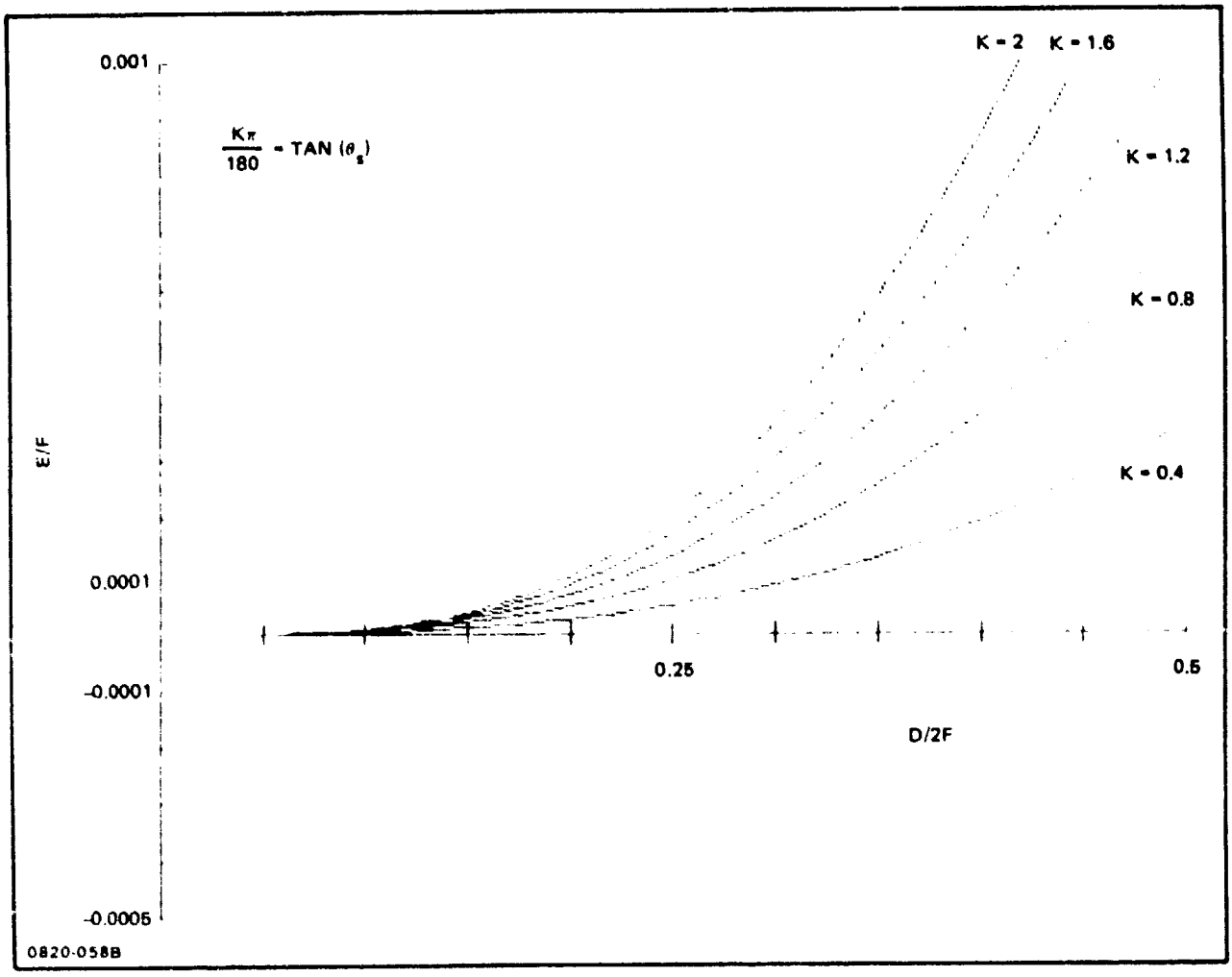

Fig. 3-49 Aberration Function

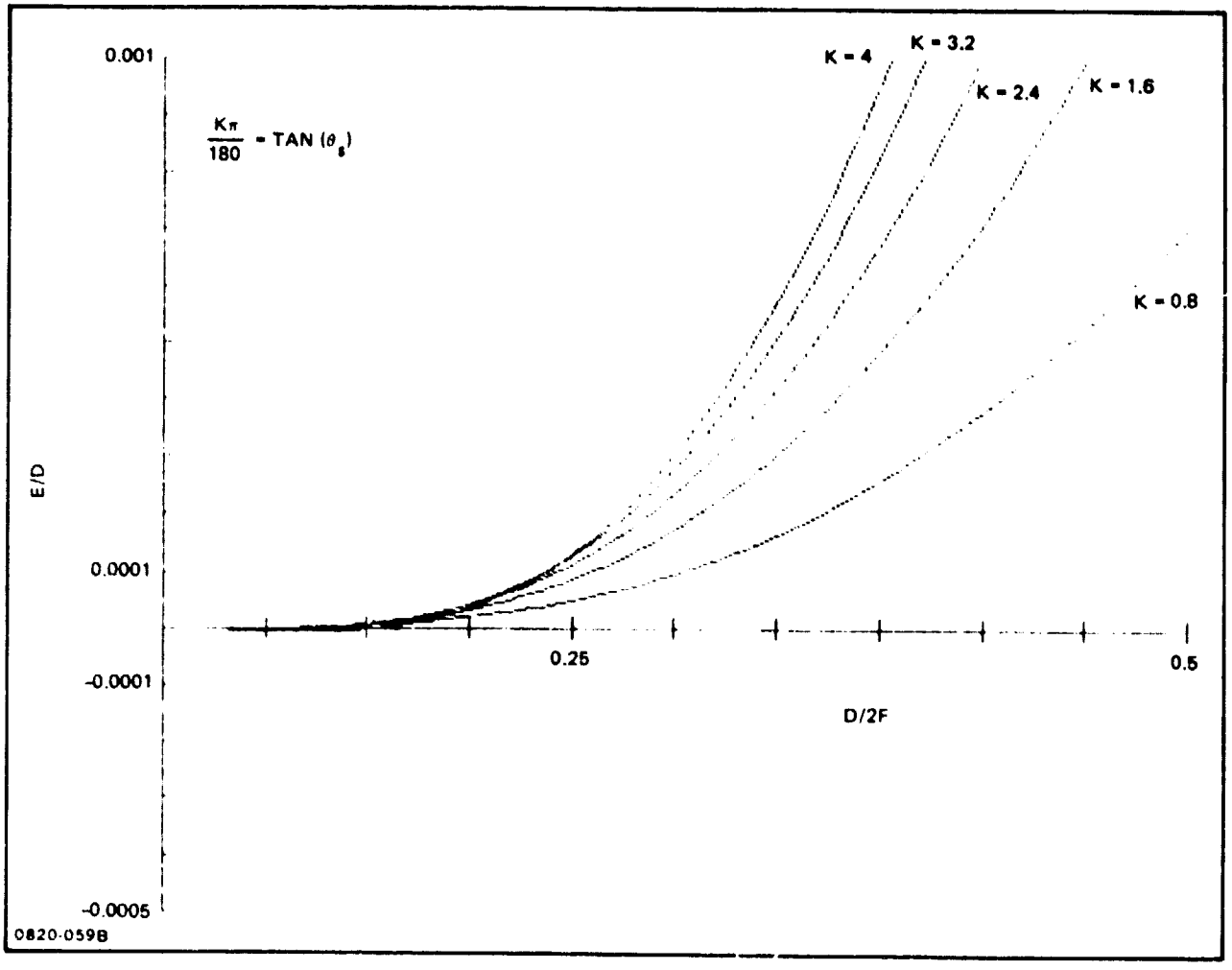

Fig. 3-50 Aberration Function

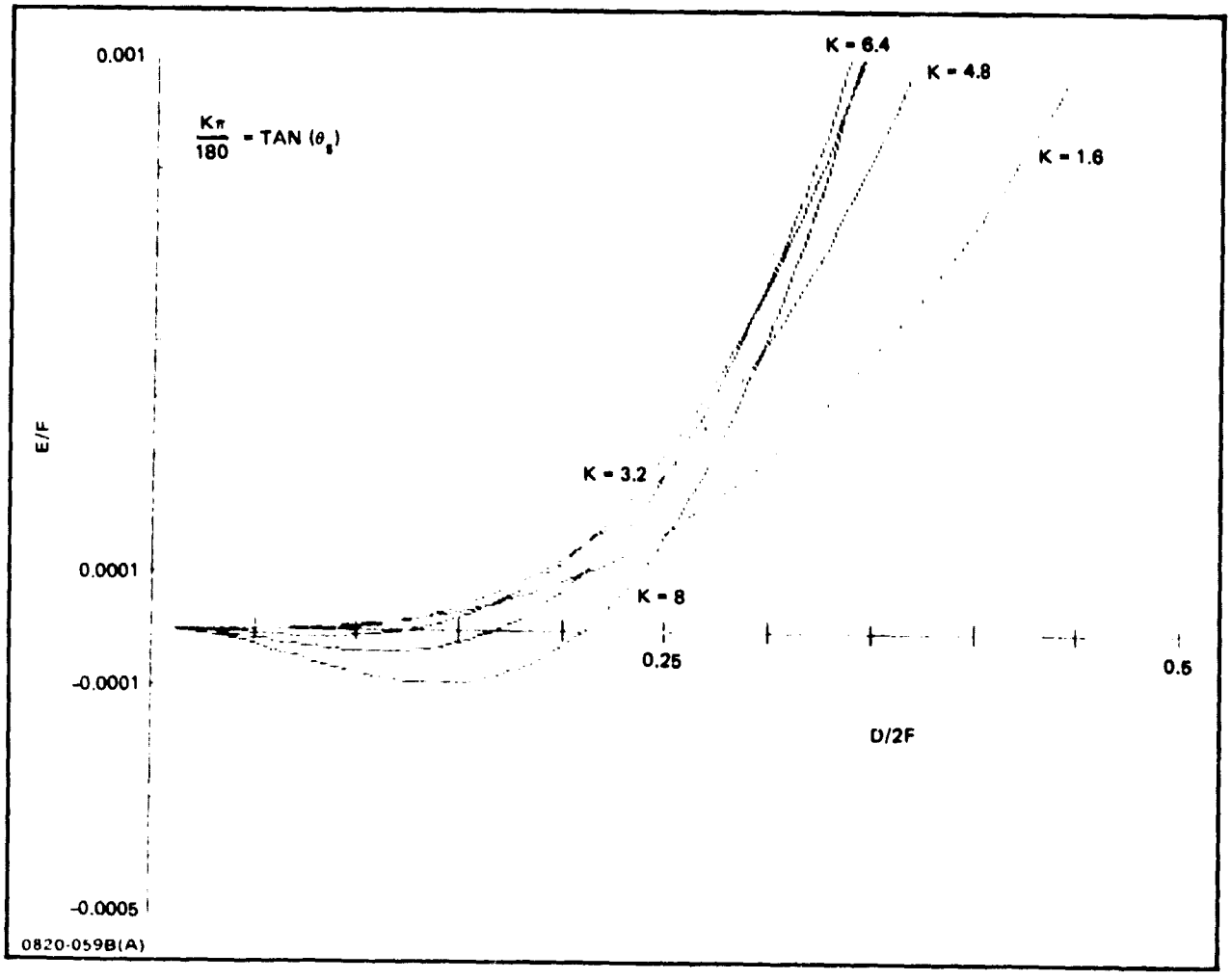

Fig. 3-51 Aberration Function

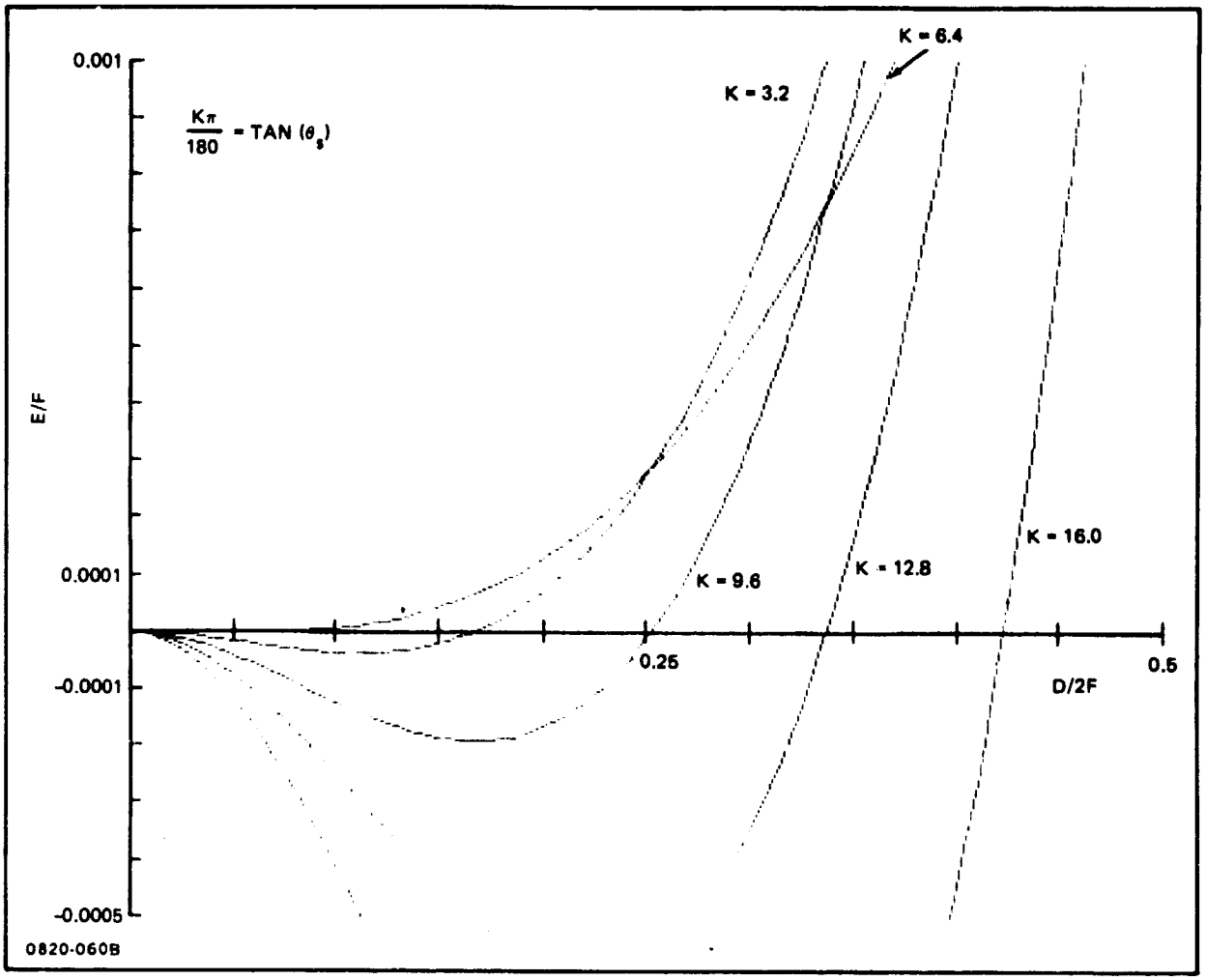

Fig. 3-52 Aberration Function

where, c is the speed of light, f/D is the focal length to diameter ratio and θ is the scan angle.

3.3.2.5 Marechal Tolerance Criterion

In order to estimate the maximum amount of aberration that may be tolerated by a lens, we resort to diffraction theory. Since we are dealing with a microwave lens rather than an optical one, there is a significant difference in the amount of gain loss (light loss in optics) and sidelobe level (high spatial frequency) the microwave system can tolerate. Therefore, it is important to appropriately modify the criterion established for optics to satisfy the more stringent requirements of the microwave lens system.

Therefore, one has to be careful in applying a criterion established for optical systems to low sidelobe lens antennas.

Define the "mean-square deformation" $(\Delta\phi)^2$ of the wavefront either impinging on the aperture or created by the aperture as:

$$(\Delta\phi)^2 = \bar{\phi}^2 - (\bar{\phi}^2)^2. \tag{8}$$

The magnitude squared of the far-field radiation pattern can be shown to be reduced by the phase aberration as

$$|E|^2 \geq 1 - \left(\frac{2\pi}{\lambda}\right)^2 (\Delta\phi)^2 \tag{9}$$

where $\Delta\phi$ is the root mean square departure of the wavefront from the ideal expressed as a fractional part of a wavelength. Marechal's criterion in optics (Ref. 3-13) allows $|E|^2 \geq 0.8$, when $|\Delta\phi| \leq \lambda/14$ and considers an optical system well corrected. In terms of antenna theory, this condition represents a gain loss of 1 dB. Interpreting this for a uniformly illuminated linear aperture, an rms phase error of $\lambda/14$ across the aperture means a peak phase error at the aperture edge of $\sqrt{12}(\lambda/14)$ or approximately one-quarter wavelengths aperture edge error. The corresponding rms sidelobe level is -14 dB. Clearly this level is not acceptable for low sidelobe performance.

A more desirable tolerance is an rms phase error of $\lambda/48$. For uniform illumination the corresponding peak aperture edge phase error is $\sqrt{12}\,\lambda/48$ or approximately $\lambda/14$. In this case the gain loss is 0.015 dB and the rms sidelobe level is -35 dB.

It should be pointed out that using other illumination functions, the rms to peak phase error ratio will be lower than 12.5. Hence, one would expect, on the average, a lower peak sidelobe level with tapered illumination functions.

Using diffraction theory, the effects of the primary Siedel aberrations on the sidelobe levels can also be directly evaluated. If we define aberration in the system as a measure of the departure of the phase from the ideal, then corresponding to each primary aberration term there is a corresponding induced phase error. In the following subsections we examine the effects of square law and cubic phase (coma) variation on the far-field radiation patterns.

3.3.2.6 Effects of Square Law Phase Variation

Assume a uniform amplitude distribution and a square law phase variation $\phi(x) = k x^2$, $-a/2 \leq x < a/2$, over a linear continuous aperture. The far field pattern is given by:

$$F(\theta) = \int_{-a/2}^{a/2} e^{-j\phi(x)} e^{j \cdot \frac{2\pi x \sin\theta}{\lambda}} dx \qquad (10)$$

To evaluate (10), we expand the quadratic phase term in a power series, for $k x^2 < \pi/2$, rather than by the direct use of Fresnel integrals. The exponential terms can be approximated as:

$$e^{-jkx^2} \simeq 1 - jkx^2 - \frac{k^2 x^4}{2} + \ldots \qquad (11)$$

Substituting (11) into (12) and evaluating the resultant integrals term by term one obtains

$$F(\psi) = \frac{\sin\psi}{\psi} - \frac{k^2}{2} B - jk A \qquad (12)$$

where: $\psi = b\frac{a}{2}, b\frac{2\pi}{\lambda} \sin\theta, a = 1$

$$A = \frac{1}{\psi^3}\left[\frac{\psi^2}{4}\sin\psi + \frac{\psi}{2}\cos\psi = \frac{1}{2}\sin\psi\right]$$

$$B = \frac{1}{\psi^2}\left[\frac{\psi}{16}\sin\psi + \frac{1}{4}\cos\psi - 3A\right]$$

The magnitude square of the far field pattern

$$\left|F(\phi)\right|^2 = \left[\frac{\sin\psi}{\psi} - \frac{k^2}{2} B\right]^2 + k^2 A^2 \qquad (13)$$

is plotted in Fig. 3-53 for $k = 0, \pi/2, \pi, 3\pi/2, 2\pi$ which corresponds to aperture edge phase errors of $(0, \frac{\lambda}{16}, \lambda/8, 3\lambda/16, \lambda/4)$ or (0, 22.5°, 45°, 67.5°, 90°). The aperture was normalized to unity length.

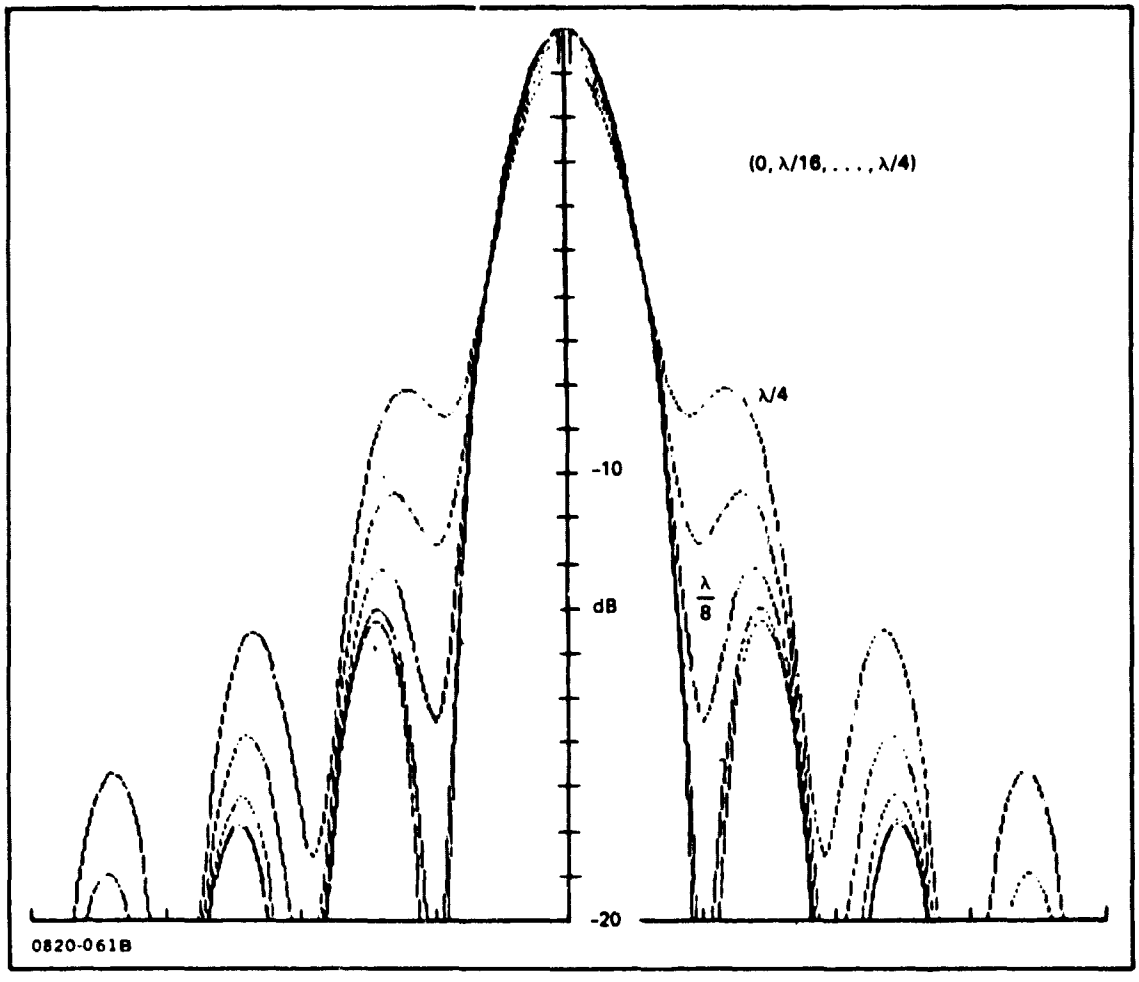

Fig. 3-53 Far Field Pattern with Quadratic Aberration (Aperture Edge Peak Error as a Parameter)

The theoretical curves can be applied to represent important practical problems. These include defocusing effects due to the inexact placing of the primary feed or defocusing of a zoned lens due to operation at a frequency off mid-band.

In addition to providing far-field patterns of apertures with curved wave fronts, (12) provides theoretically the near-field (Fresnel diffraction field) pattern for antennas with plane wavefronts.

The use of the linear aperture to approximate the performance of paraboloidal reflectors or lenses with phase aberrations was found to be satisfactory by computer simulation of the actual systems.

Quadratic aberration has two primary effects on the far field radiation pattern. The gain (directivity) is reduced and the sidelobe levels increase symmetrically. These effects are plotted in Fig. 3-54 and 3-55 respectively, as a function of peak aperture edge error.

3.3.2.7 Effects of Cubic Phase Variations

Assume a uniform amplitude distribution and a cubic phase variation $\phi^c(x) = -k^c x^3$ across the aperture, $-a/2 < x < a/2$. To evaluate the far field pattern, we expand the cubic phase term (exponentiated) in a power series

$$e^{-jk^6 x^3} \simeq \left| - j k^4 x^3 - \frac{k^2 x^6}{2} + \ldots \right. \tag{14}$$

for $kx^3 < \pi/2$. The far-field pattern is obtained by evaluating the integral in (10) with the cubic phase term expansion (14) replacing $e^{-j\phi(x)}$. The resultant far-field pattern is of the form:

$$F(\psi) = \frac{\sin\psi}{\psi} + \frac{k}{8\psi^4}\left[(3\psi^2 - 6)\sin\psi + (6\psi - \psi^3)\cos\psi\right]$$
$$- \frac{k^2}{128\psi^7}\left[(\psi^6 - 30\psi^4 + 360\psi^2 - 720)\sin\psi + \right. \tag{15}$$
$$\left. + (6\psi^5 - 120\psi^3 + 720\psi)\cos\psi\right]$$

where

$$\psi = \frac{ba}{2}\ , \ b = \frac{2\pi}{\lambda}\ \sin\theta\ , \ a = 1.$$

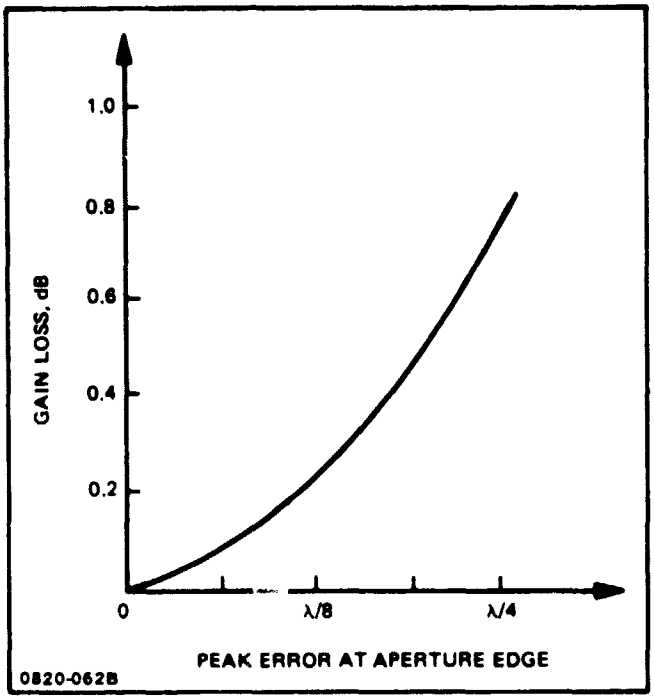

Fig. 3-54 Effects of Quadratic Aberration, Gain Loss

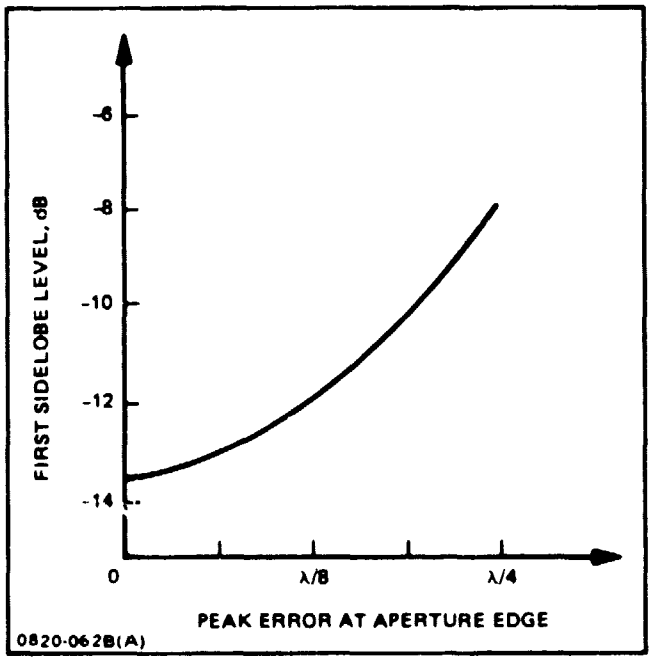

Fig. 3-55 Effects of Quadratic Aberration, Sidelobe Level

Typical far-field patterns are plotted in Fig. 3-56 for $k = 0, \pi, 2\pi, 3\pi, 4\pi$, which corresponds to (0, $\lambda/16$, $\lambda/8$, 3 $\lambda/16$, $\lambda/4$) or (0, 22.5°, 45°, 67.5°, 90°) peak aperture edge phase errors. The aperture was normalized to unity length.

Cubic distortions are found in parctice when reflectors or lenses are illuminated by primary feeds which are off-axis either because of inaccurate alignment or because, off-axis beam(s) are desired. The beam distortion due to cubic phase variation is known in optics as "coma" and the increased unsymmetrical lobe which is particularly evident in Fig. 3-56 is called the "coma lobe," Note also the tilt in beam direction due to "coma aberration" in Fig. 3-56.

The gain loss and sidelobe levels increase as a function of aperture edge peak phase error are plotted in Fig. 3-57 and 3-58, respectively.

The criterion of allowable gain loss and effects on the sidelobe levels are discussed in the scanning limit considerations section.

3.3.2.8 Scan Limits of Primary Aberrations

In examining the entire aberration function we established approximate scan limits (see Fig. 3-48 through 3-52) as a function of the reciprocal of the focal length to diameter ratio. In this section we examine equation (2) with respect to a three-dimensional lens geometry. To facilitate numerical computation of the predominant wavefront errors due to the primary aberrations (astigmatism and coma) we make a small angle approximation, i.e. $\sin\theta \simeq \tan\theta \simeq \theta$, $\cos\theta \simeq 1 - \frac{\theta^2}{2}$. Then we consider each term separately by placing limits on the magnitude of the errors. In order to facilitate numerical comparisons we normalize the data to a unity diameter aperture.

The coma aberration can be bounded as

$$E_3 = \frac{f}{32}\left(\frac{D}{f}\right)^3 \theta_c^3 \leq \frac{\lambda}{n} \quad . \tag{16}$$

Equation (16) can be expressed in terms of scan angle limit as:

$$\theta_c^o \leq \frac{(32)\,(100)\,f^2\lambda}{\pi D^3 n} \tag{17}$$

where, f is the focal length, D is the aperture diameter and n is the reciprocal of the fractional part of the wavelength, $n \geq 1$.

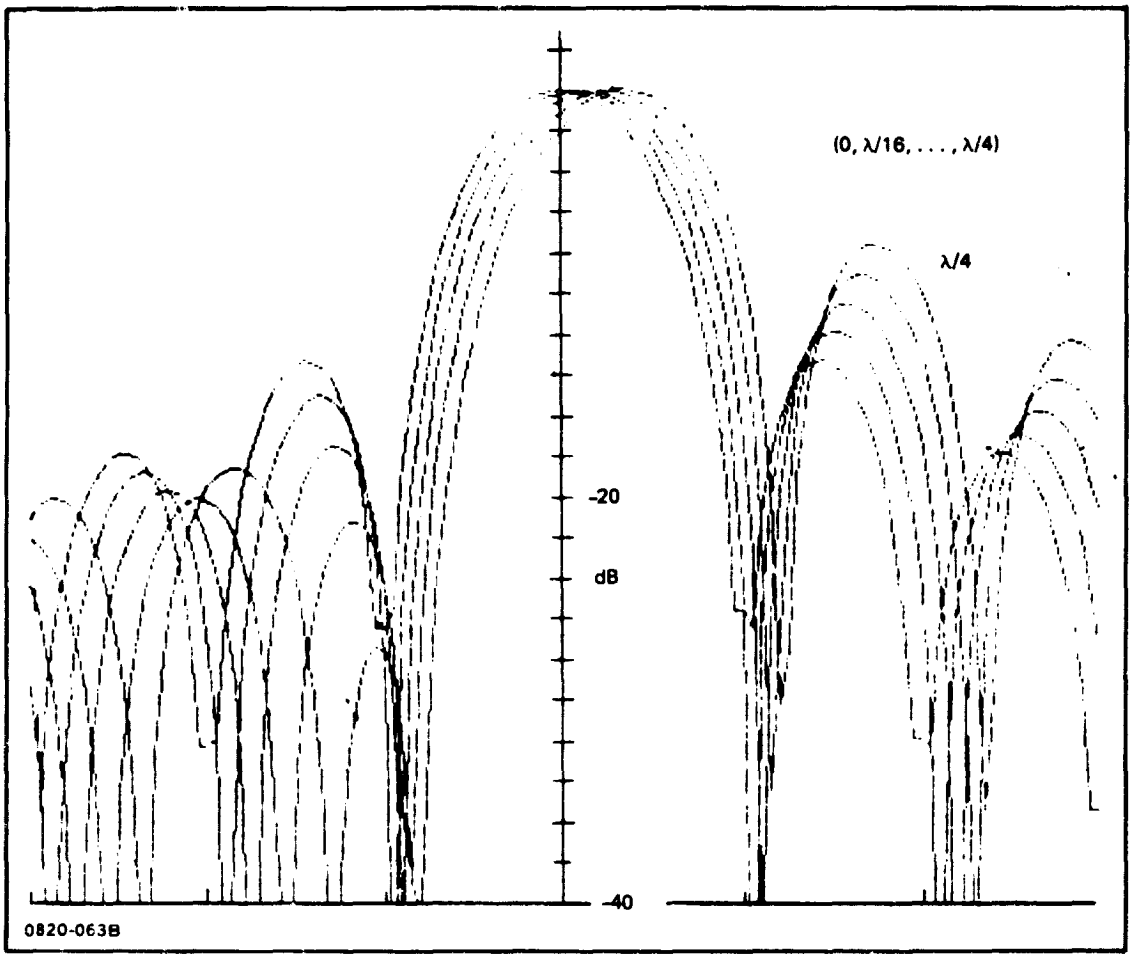

Fig. 3-56 Far Field Pattern with Coma Aberration (Aperture Edge Peak Error as a Parameter)

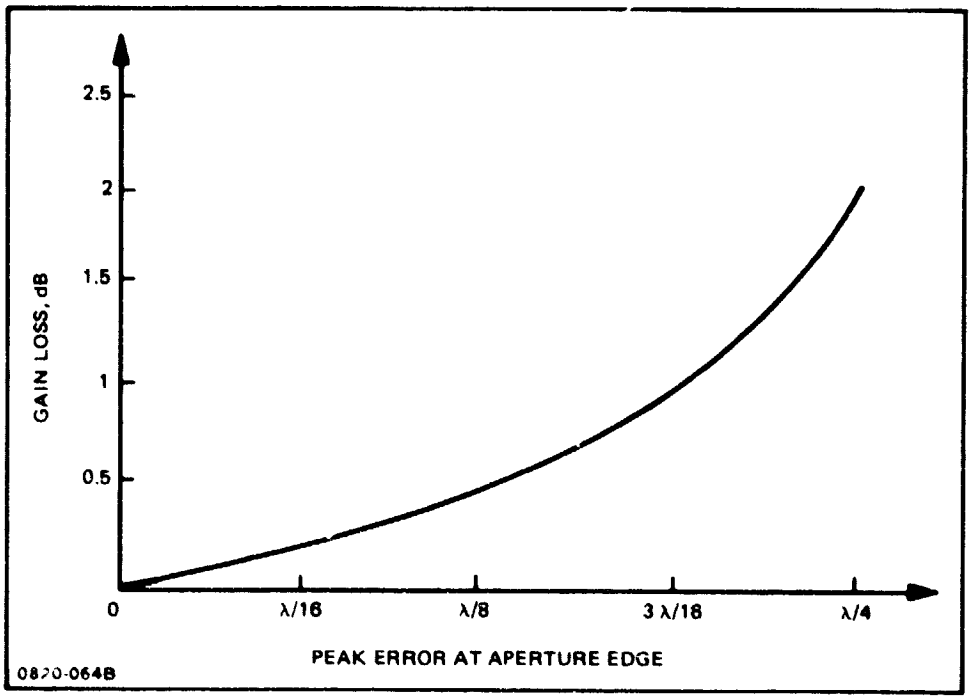

Fig. 3-57 Effects of Coma Aberration, Gain Loss

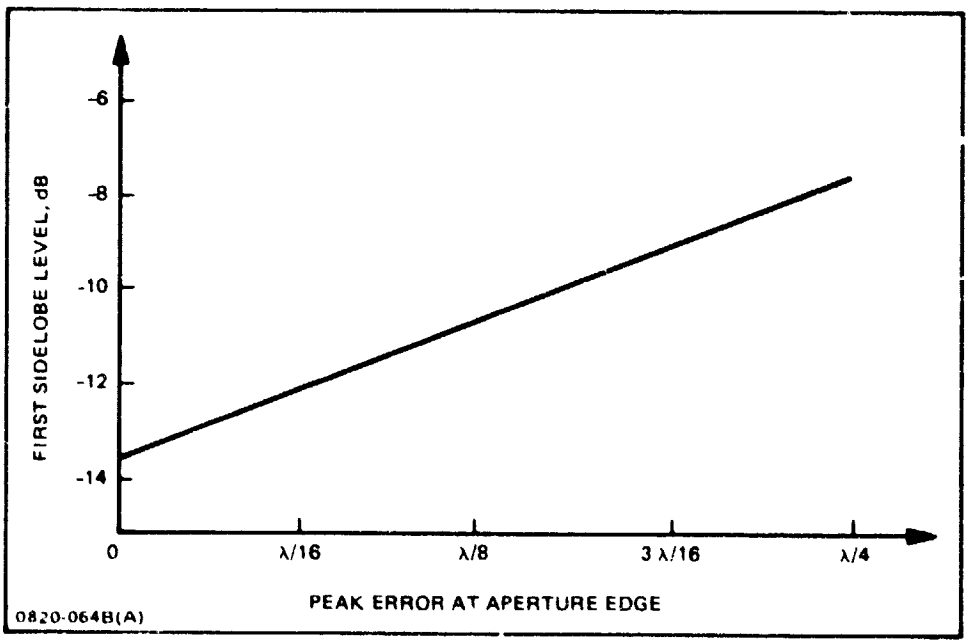

Fig. 3-58 Effects of Coma Aberration, Sidelobe Level

Equation (17) is plotted in Fig. 3-59 through 3-62 for a range of focal lengths, and phase errors as a function of the number of wavelengths in the aperture. Figure 3-59 and 3-60 assumed a peak aperture edge phase error of ($\lambda/4$) which corresponds to a gain loss of 1 dB and an rms sidelobe level of 14 dB for uniform illumination. Figure 3-61 and 3-62 assumed a peak aperture edge phase error of ($\lambda/14$) which corresponds to a gain loss 0.015 dB and an rms sidelobe level of 37 dB for uniform illumination. As expected, the more stringent phase error requirements reduce the allowable displacement scan. Furthermore, by defining the diffraction limited antenna beandwidth as

$$\theta_D \simeq 1.2 \quad \frac{\lambda}{D} \tag{18}$$

we can compute the number of beam positions that can be scanned (due to coma only) by defining $N_B \triangleq \theta_c / \theta_D$ and

$$N_B{}^c \leqslant \pm \frac{80}{3n} \left(\frac{f}{D}\right)^2 \tag{19}$$

However, one has to be careful in applying the above equations to large (f/D) ratios where astigmatism is the limiting term.

Astigmatism can be bounded by:

$$E_2 = \frac{3 D^2 \theta^2 A}{16f} = \frac{\lambda}{n} \tag{20}$$

The scan limit due to astigmatism can be expressed as:

$$\theta^\circ_A \leqslant \frac{180}{\pi} \sqrt{\frac{16 f \lambda}{3 D^2 n}} \tag{21}$$

Equation (21) is plotted in Fig. 3-63 through 3-66 for aperture edge peak phase errors of λ 4 and λ 14 respectively. We note in comparing Fig. 3-59 through 3-62 for the coma aberration case with Fig. 3-63 through 3-66, that for small (f/D) ratios the coma aberration limits the scan while for large (f/D) ratios the astigmatism places an upper limit on the scan.

These results are in agreement with the work of Mrstik (Ref. 3-15) on offset reflector antennas. As a matter of fact, Fig. 3-67 is a plot for 1 dB gain loss for the scan limits of an offset reflector with optimum feed location (Ref. 3-15). We note that our combined results represented by Fig. 3-59, 3-60, 3-63 and 3-64 are in agreement with Fig. 3-67. However, the results shown for the flat-faced lens with non-optimum feed locations are more pessimistic. This result is not unexpected for several reasons. First, the non-optimum

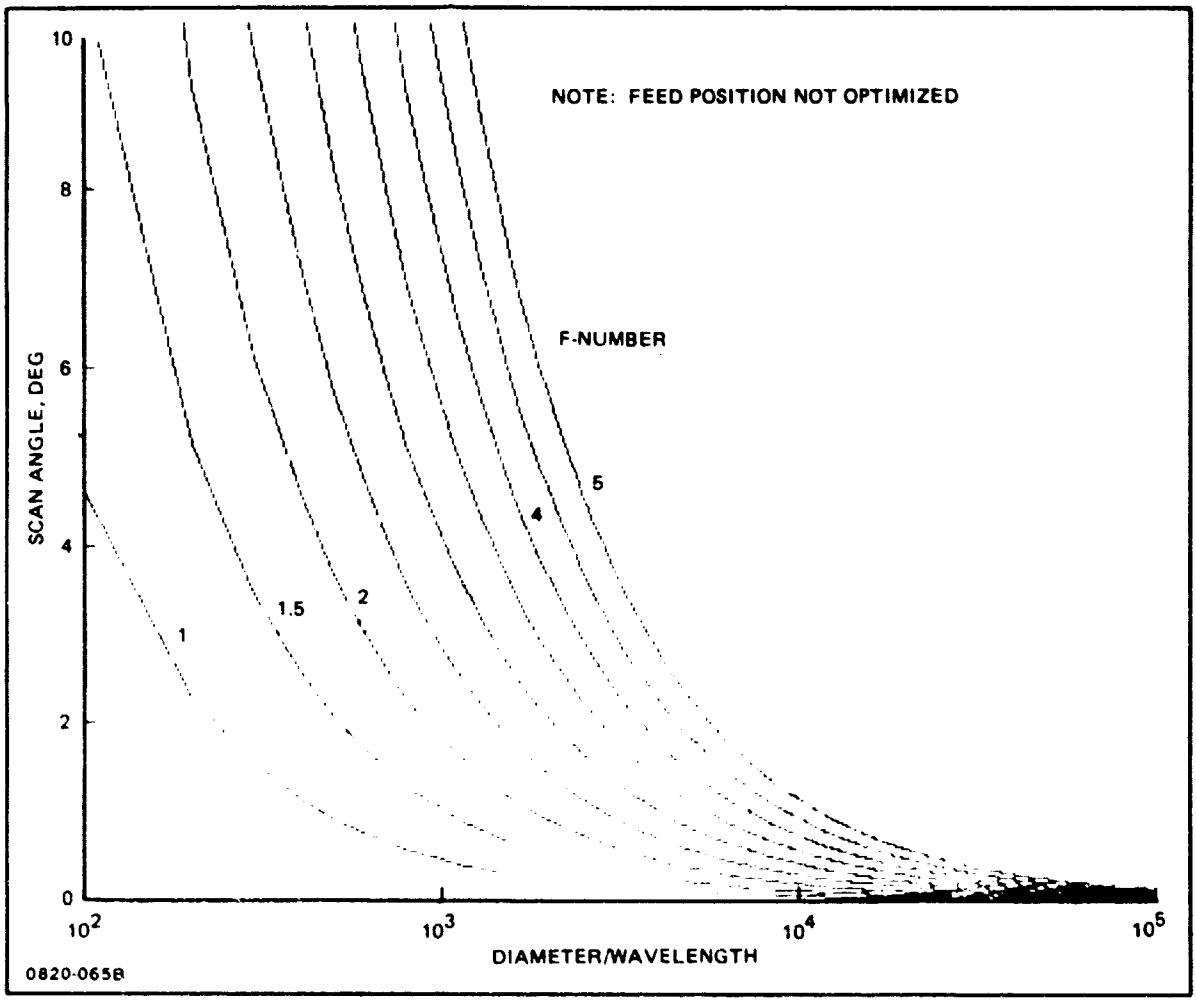

Fig. 3-59 Coma Scan Limits for Displacement Steered Space-Fed Flat-Faced Lens at 1 dB Gain Loss (Uniform Illumination)

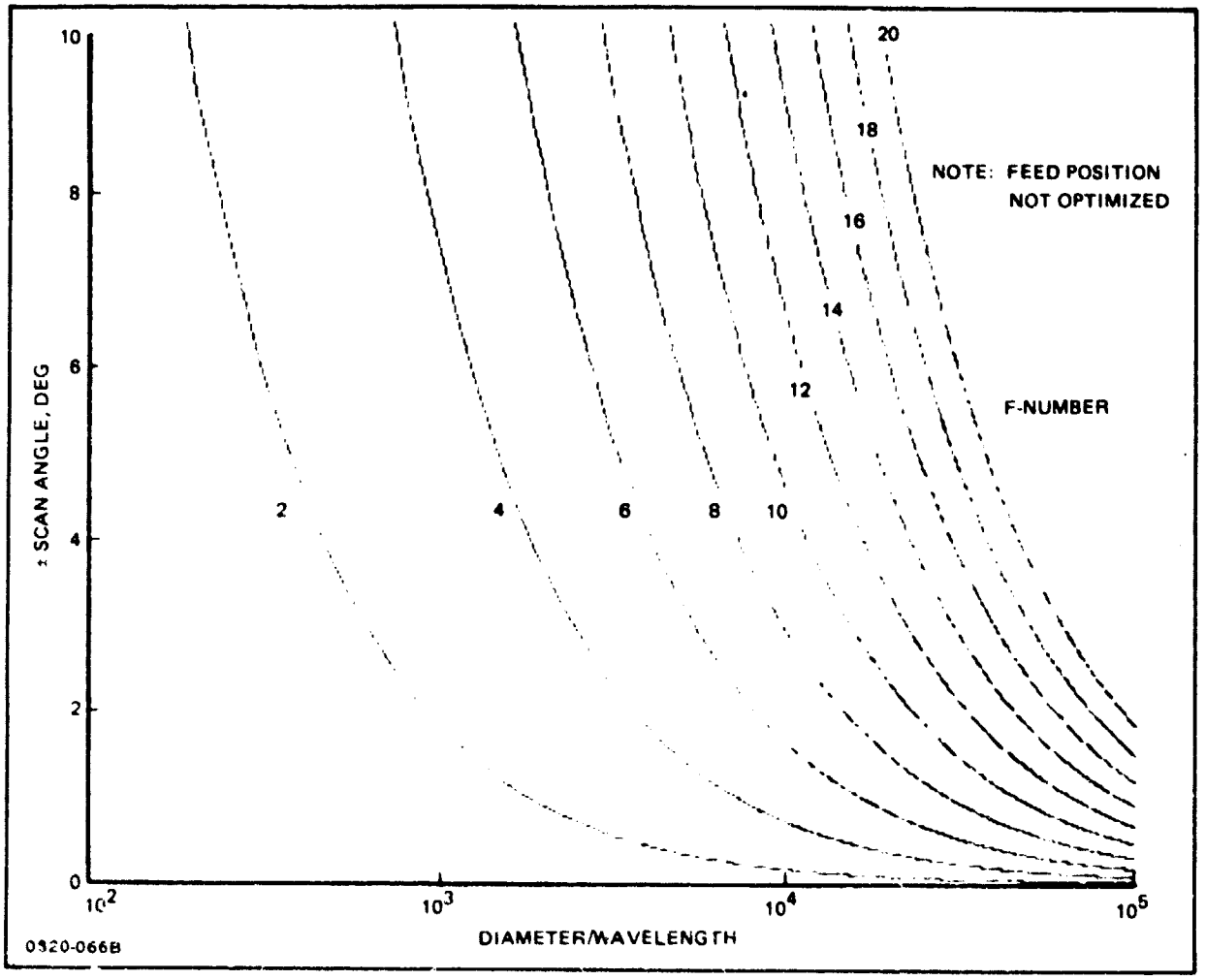

Fig. 3-60 Coma Scan Limits for Displacement Steered Space Fed Flat-Faced Lens at 1 dB Gain Loss (Uniform Illumination)

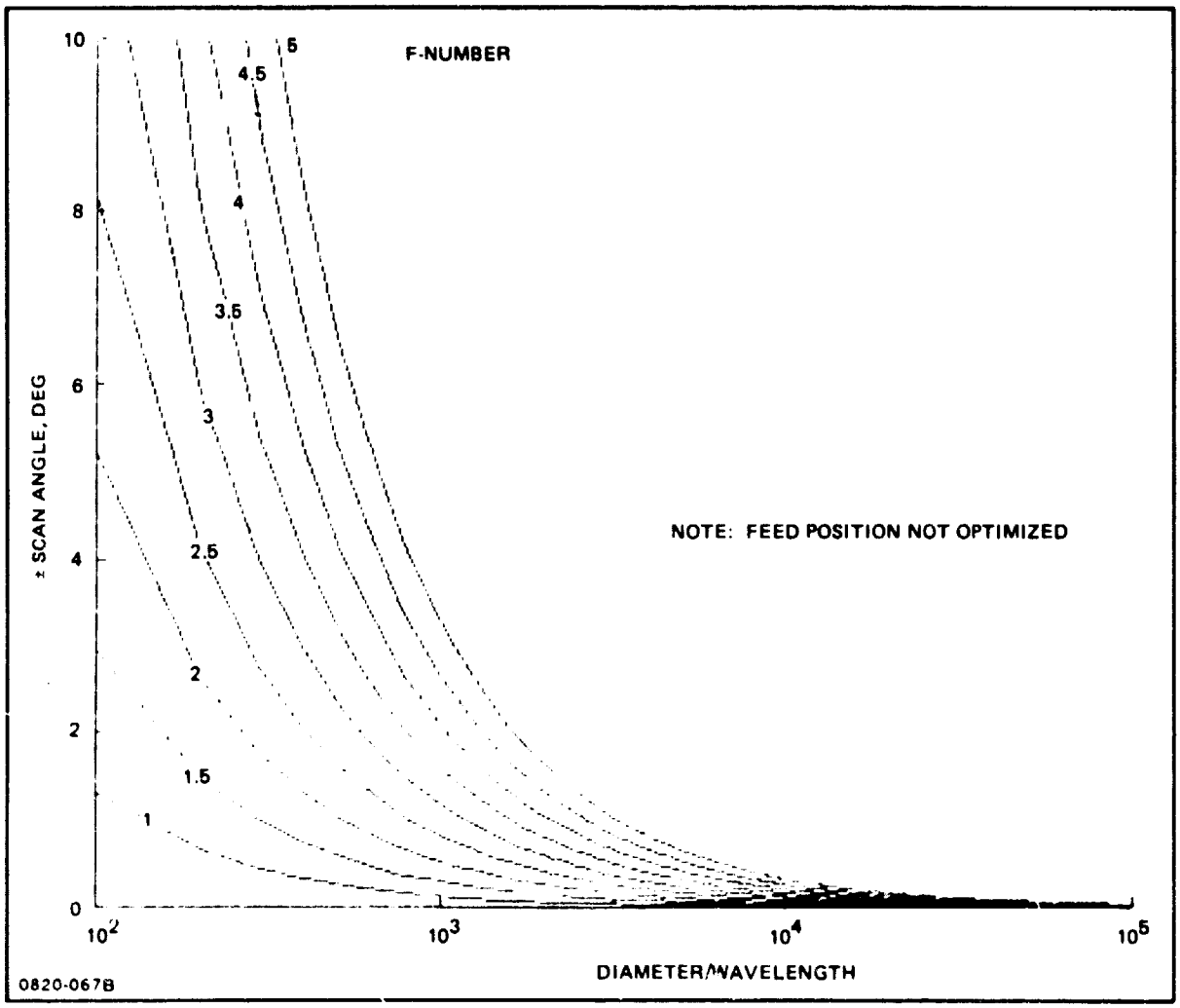

Fig. 3-61 Coma Scan Limits for Displacement Steered Space-Fed Flat-Faced Lens at 0.015 dB Gain Loss (Uniform Illumination)

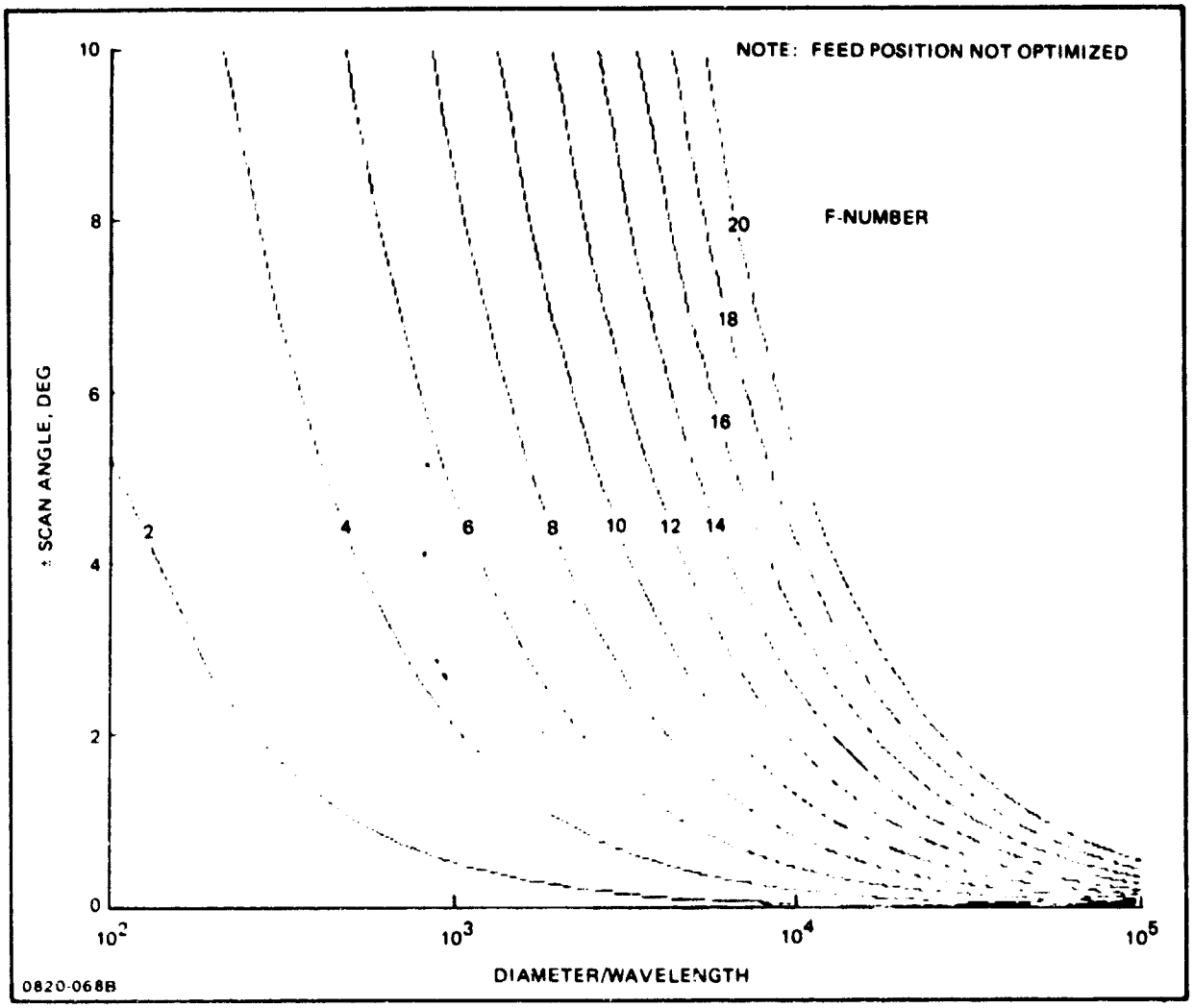

Fig. 3-62 Coma Scan Limits for Displacement Steered Space-Fed Flat-Faced Lens at 0.015 dB Gain Loss (Uniform Illumination)

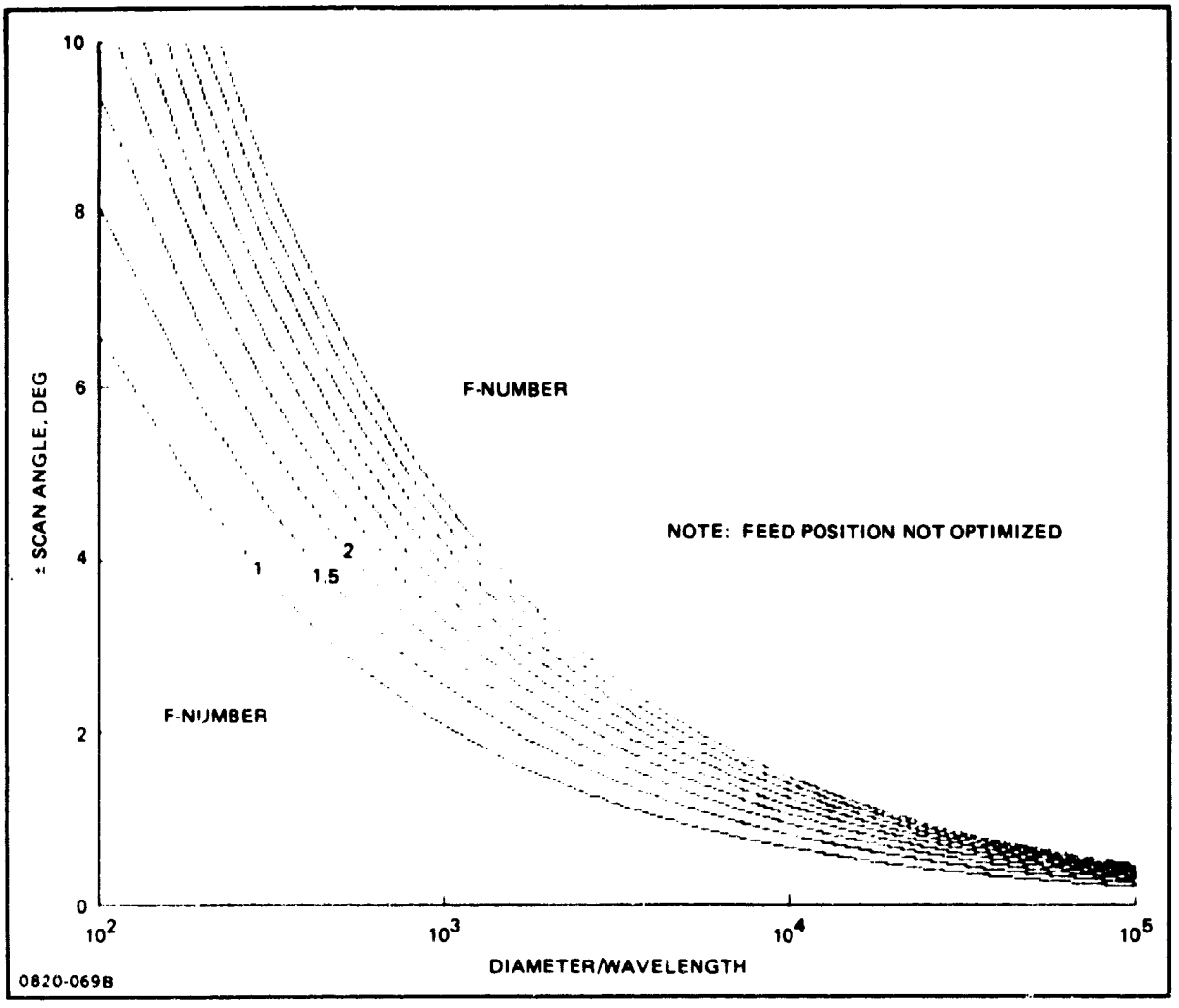

Fig. 3-63 Astigmatism Scan Limits for Displacement Steered Space-Fed Flat-Faced Lens at 1 dB Gain Loss (Uniform Illumination)

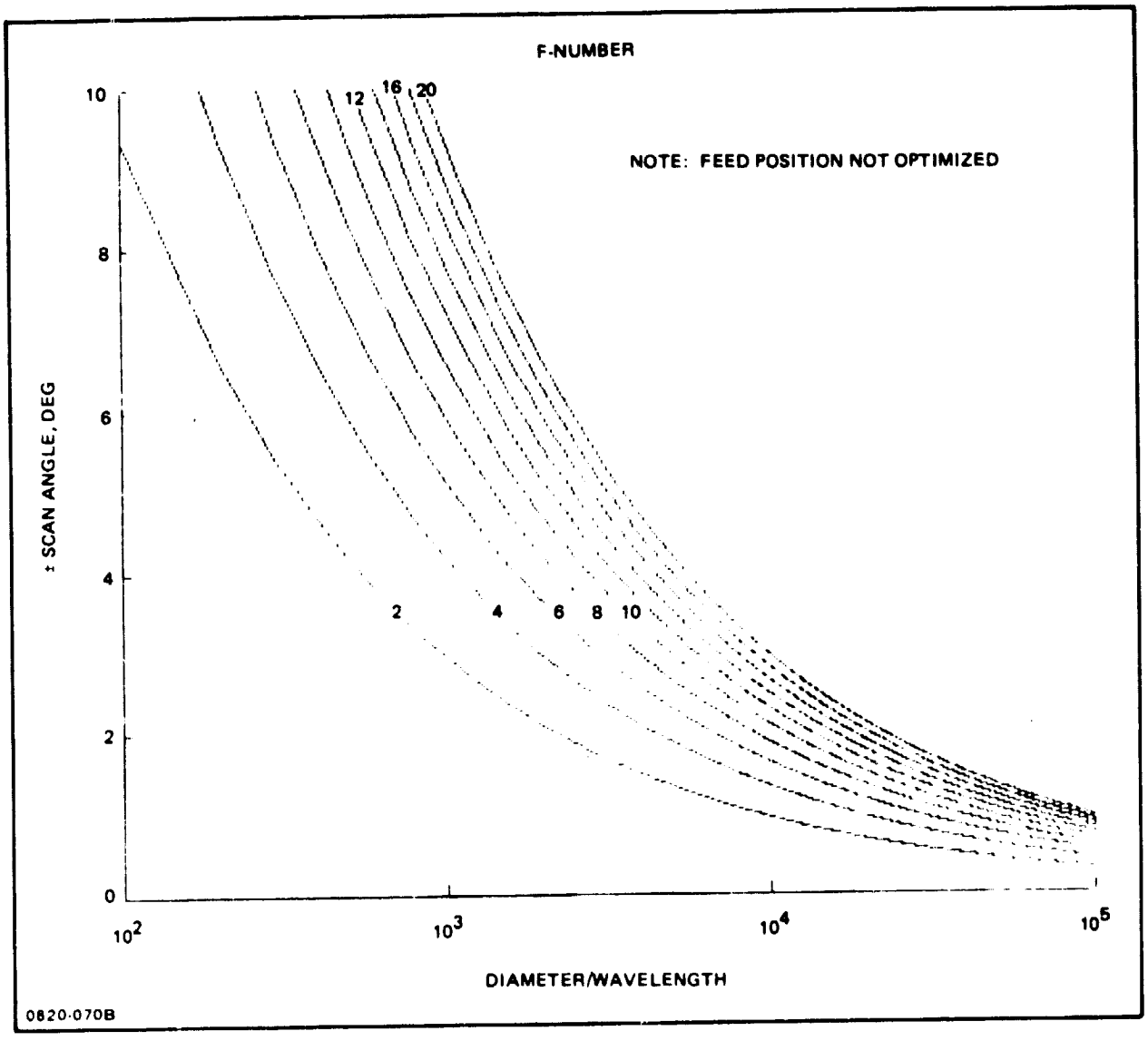

Fig. 3-64 Astigmatism Scan Limits for Displacement Steered Space-Fed Flat-Faced Lens at 1 dB Gain Loss (Uniform Illumination)

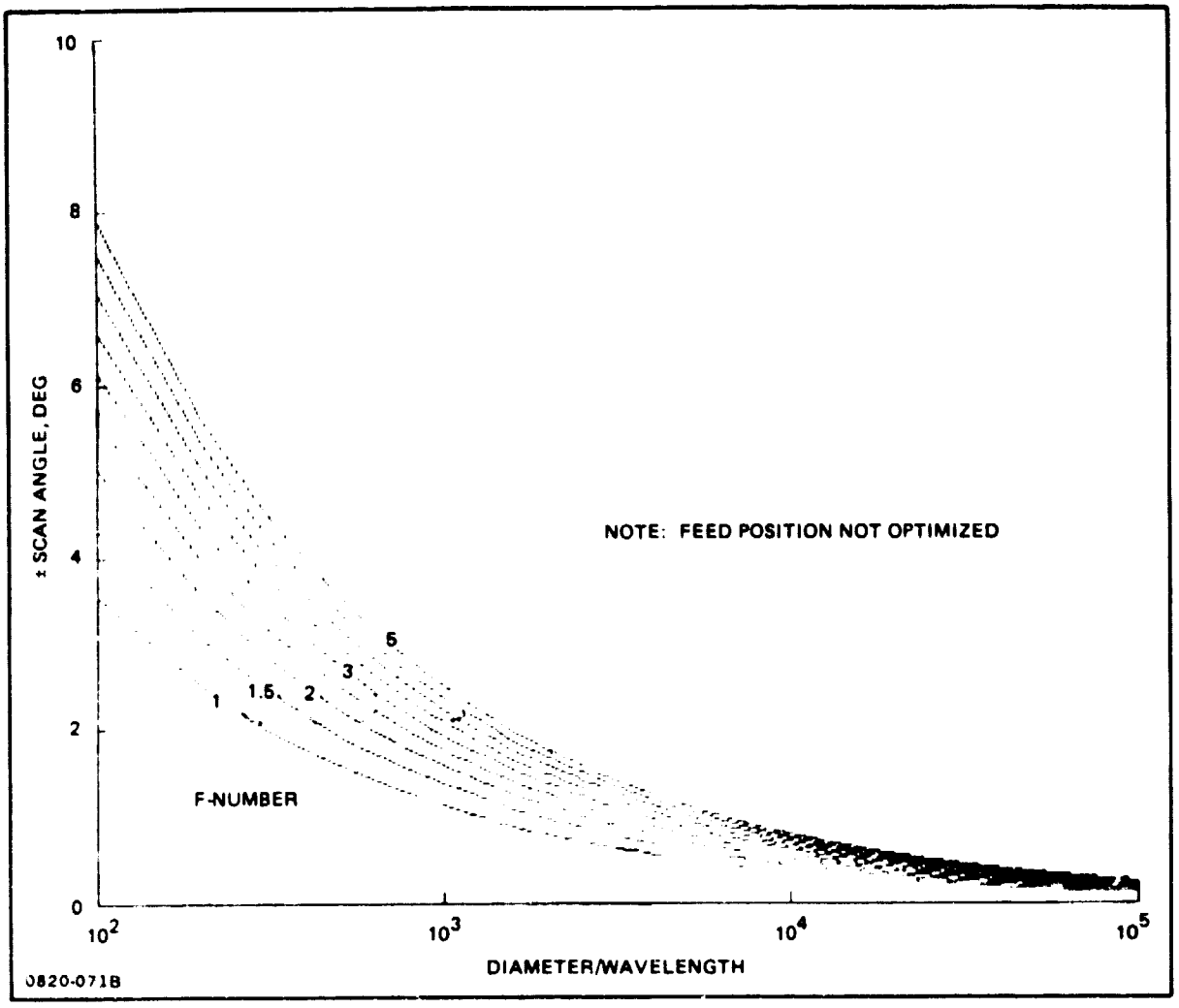

Fig. 3-65 Astigmatism Scan Limits for Displacement Steered Space-Fed Flat-Faced Lens at 0.015 dB Gain Loss (Uniform Illumination)

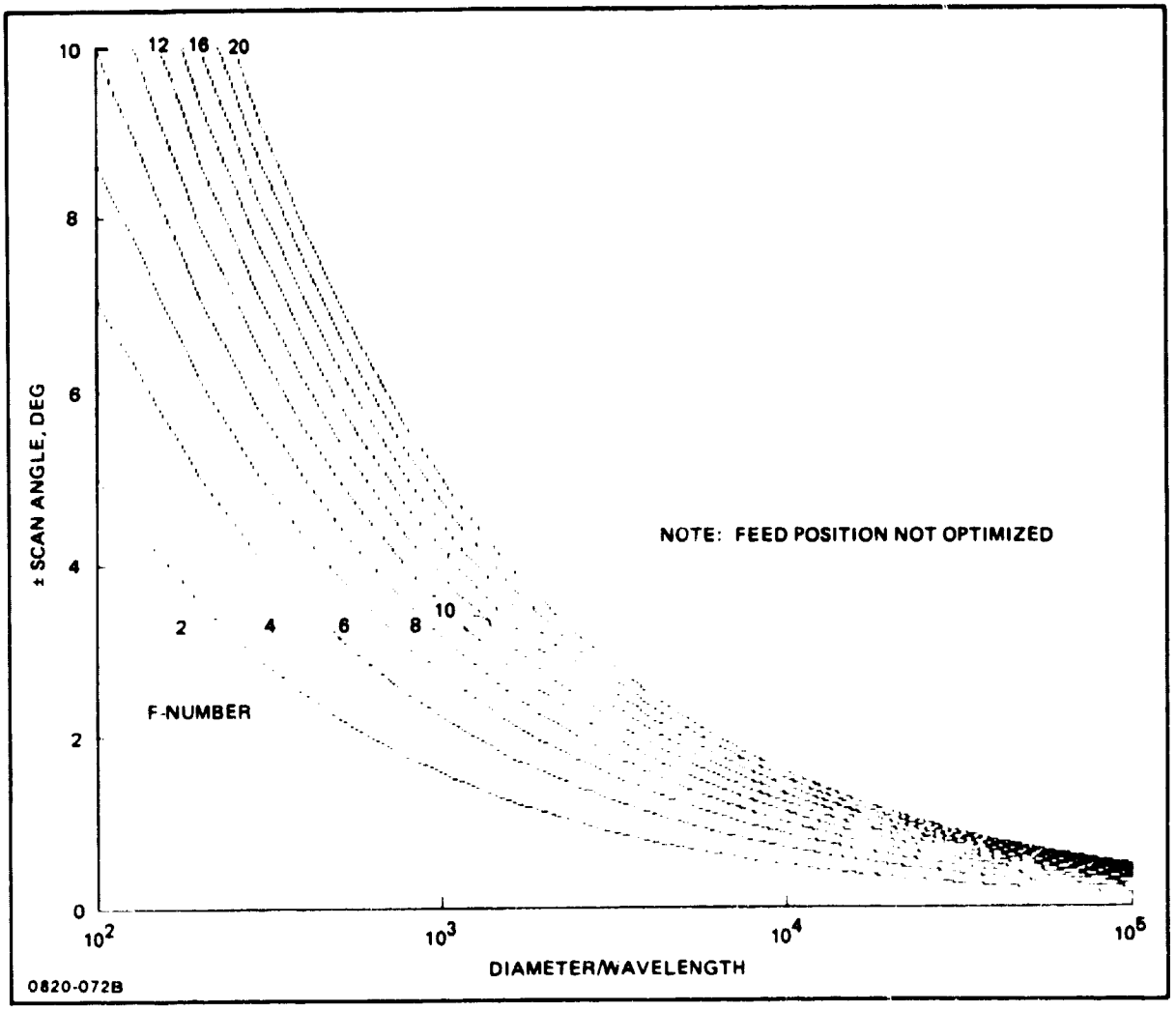

Fig. 3-66 Astigmatism Scan Limits for Displacement Steered Space-Fed Flat-Faced Lens at 0.015 dB Gain Loss (Uniform Illumination)

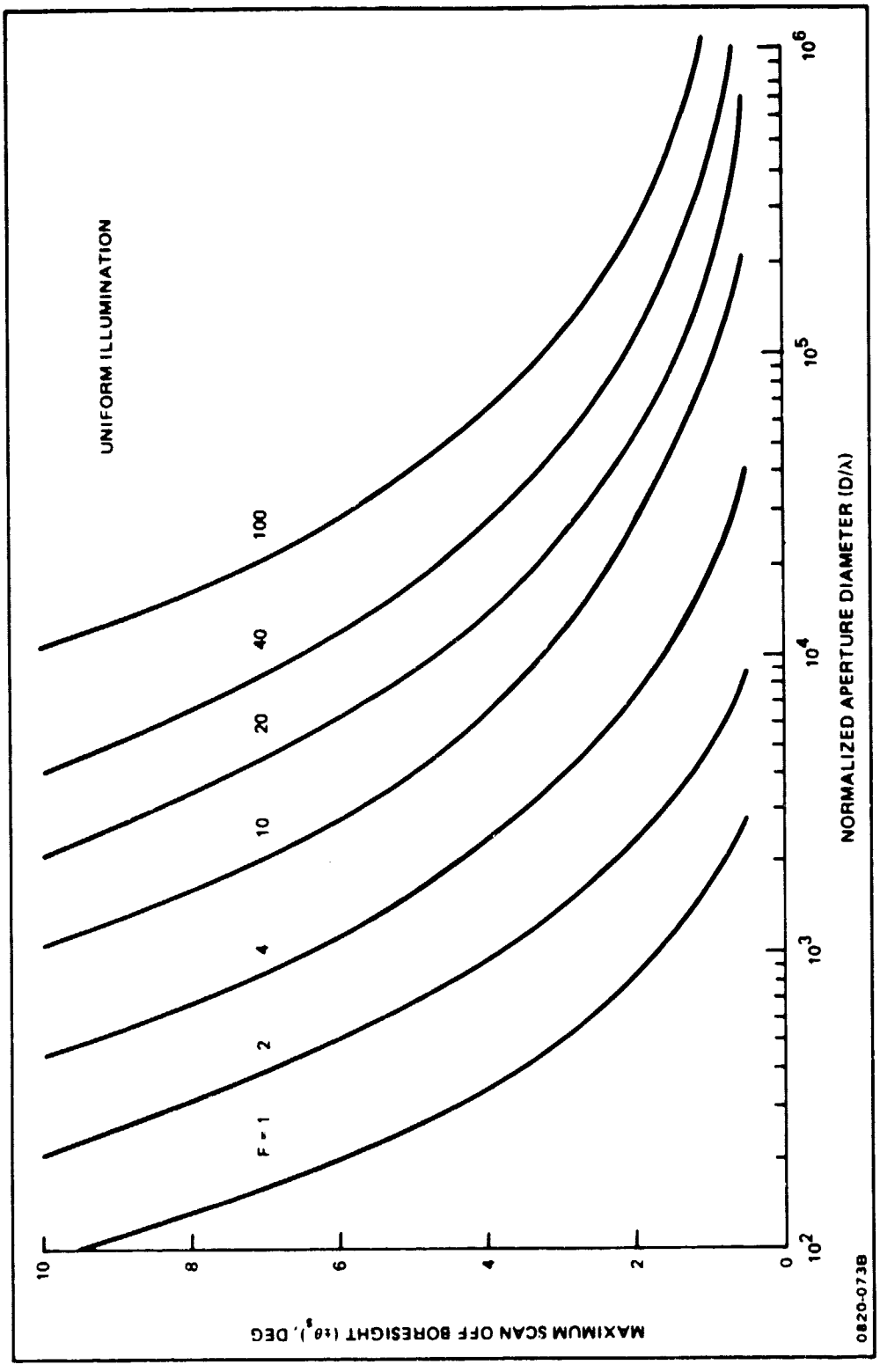

Fig. 3-67 Scan Angle for 1-dB Gain Loss (Paraboloidal Reflectors)

feed locations do not minimize the mean square phase error across the aperture. Secondly, the most easily deployed lens design used flat-faced input and output surfaces. Hence even with an optimally located point source feed, there are not enough degrees of freedom available to drive the mean square error to the same local minimum as in the case of an offset parabola. The only solution in this case is to compensate for the absence of the required degrees of freedom in the lens by introducing additional degrees of freedom at the feed. By making the feed surface curved and introducing real-time delays at the feed, one can asymptotically approach the aberration function of an optimally fed offset reflector.

To achieve the required aperture illumination, one has to synthesize a set of complex coefficients for the nonplanar phased array feed. Hence the procedure is to first find the optimum locus of feed points which minimize the mean squared aberration and then synthesize the feed array coefficients.

3.3.2.9 Three-Dimensional Case

The previous analysis of the flat-faced lens used a two-dimensional formulation. Before we examine the primary aberration terms we consider an unconstrained three-dimensional lens. The three-dimensional case that we consider is limited to a system, that is axially symmetric about the lens axis (Z-axis).

Introduce coordinates for the feed and lens input/output surfaces. Feed: x_f, y_f, z_f; lens input surface x_1, y_1, z_1; lens output surface x_2, y_2, z_2. Next introduce polar coordinates, $x = u \cos \phi$, $y = u \sin \phi$ and define a general point on the lens input surface as $(u_1 \cos \phi, u_1 \sin \phi, z_1)$ and a corresponding general point on the lens outer surface as $(u_2 \cos \phi, u_2 \sin \phi, z_2)$. Note at this point that the axial symmetry is represented by the angular variable ϕ without a subscript. In reference to Fig. 3-47 introduced before, define the lens relative thickness zero at $z = 0$ at (0, 0, 0). Furthermore, with the input/output surfaces flat one can make $z_1 = z_2 = 0$ (since they are not changing). The unconstrained conditions are implicit in the variables u_1 for the input surface and u_2 for the output surface. For example, for bootlace correction of the primary feed this means that the bootlace starting on the input surface at u_1 do not necessarily go to $u_2 = u_1$ on the output surface. Now the previously introduced two-dimensional aberration function can be modified for the three-dimensional case.

$$E(u_1, u_2, \phi, \theta) = u_1^2 \cos^2 \phi + r^2 - 2u_1 r \cos \phi \sin \theta^{1/2} + u_2 \cos \phi \sin \theta - r + n - m. \quad (22)$$

The offset feed location is the same as defined in Fig. 3-47, and

$r = (a^2 + f^2)^{1/2}$, with feed coordinate (a, 0, -f).

To obtain a lens that has good displacement steering performance, we would like to minimize E (u_1, u_2, ϕ , θ) and simultaneously minimize the rate of change (derivative) of E' (u_1, u_2, ϕ , θ) (Ref. 3-16). The minimization of the derivative of E' (u_1, u_2, ϕ , θ) with respect to changes in the feed location should provide the capability of wider scanning. However, one should not expect the minima of E (·) and E' (·) to coincide (Ref. 3-16). That is, the condition for perfect focus is not necessarily a condition for good scanning performance. Hence a weighted minimization criterion may be desirable, minimize W = (1 - ϵ) E + ϵ E', $0 < \epsilon \leq 1$. In either case, we minimize say E (u_1, u_2, ϕ, θ) with u_1, u_2, ϕ , and θ as parameters and the feed coordinates variables. Clearly, for a given feed location there is a corresponding scan angle θ . However, one uses a perturbation solution of the equations (Ref. 3-15) and we minimize the equations with respect to a minimum mean squared error constraint (Ref. 3-16).

3.3.2.10 Perturbation Solution

Assume that the true radiation direction differs from the reference direction θ by an amount β (Ref. 3-15). Hence the path lengths defined in equation (2) must be corrected by an amount ΔE_i. The index i is over all β , θ and ϕ of the lens, i.e., all piercing points with grid spacing adjusted to be greater than a wavelength. It is further assumed that the piercing points are uniformly distributed over the lens. Then we minimize the mean square error about the average. This allows solving for a new set of feed coordinates.

By iterating over the entire surface of the lens, a set of feed coordinates are computed which define as a function of the piercing points a feed surface. The resultant feed surface minimizes the mean square path length error. It should be noted that the lens is assumed to be primary focus compensated. This can be accomplished by either bootlaces or zoning (modulo 2 π phase shifter settings).

To find the extremum of the aberration function subject to side constraints we propose to use the method of Davidon, described by Fletcher and Power (Ref. 3-17). This recursive algorithm uses a descent method for finding a local minimum of a function of several variables. The computer routine is available either on TIME-SHARE or on the BATCH-system in SSPLIB under the SUBROUTINE DFMFP.

An alternative formulation may also be desirable by finding simultaneously the minima of both the aberration function and its derivative. This may be accomplished by a modified Marquardt algorithm for finding the minimum of the sum of square of M functions of N variables (Ref. 3-18). This subroutine is available on the BATCH-system under the name SUBROUTINE ZXMARQ.

3.3.3 RELIABILITY ANALYSIS

A reliability analysis was conducted which included a failure mode and effects analysis (FMEA) and a reliability prediction for the system shown in Fig. 3-3.

The purpose of the FMEA is to identify potential failure modes which could affect antenna performance. Since the design is in the formative stage, the analysis initiated investigations into alternate design approaches for components which were identified as critical to mission performance. In addition the analysis permitted the formulation of several design guidelines which should be utilized as the design progresses.

The results of the FMEA were used to develop a reliability model of the deployable antenna. This model was used to predict the probability of mission success including antenna deployment/retraction, measurement of antenna characteristics, and conducting operational antenna experiments.

3.3.3.1 Summary and Conclusions

Reliability analyses conducted on the present configuration of the Deployable Antenna clearly indicates a potential for launching a successful mission. FMEA and reliability prediction were based upon achieving all mission objectives, i.e. deploying and retracting antenna, obtaining antenna characteristic data, and conducting communications and radar experiments. Based upon this conservative approach, the FMEA identified twenty four single point failures (SPF) and the probability of mission success was calculated to be 0.9958.

The 24 SPF's were assessed and the rationale for acceptability are included in Fig. 3-68. These SPF's will be continually evaluated by reviewing alternate design approaches. Eighteen of the SPFs are associated with the antenna structure/mechanical components while six are related to electronic components. This is due to the fact that redundancy can be more easily implemented with electronic components. With structural/mechanical components the additional complexity of incorporating redundancy is not as advantageous when cost is considered relative to the probability of failure occurrence. Design guidelines were established (Fig. 3-69) in the structural/mechanical area so that the antenna will operate properly in the event of a failure. In most cases, this fail safe approach is achieved by "over design" to compensate for an increase in load due to either dislodgement or increase friction due to binding.

The deployable antenna has the capability to be separated from the shuttle to avoid a hazardous situation in the event that the antenna is extended and cannot retract into the shuttle payload bay. This condition would prevent closing of the payload bay doors if it were not for the separation capability.

CASE NO.	ITEM	FAILURE MODE	CRITICALITY	RATIONALE FOR ACCEPTABILITY
2	STAY REEL CLUTCH	FAILS TO DISENGAGE	I	• DESIGNED FAIL SAFE DISENGAGE (SPRING RETURN) • FAILURE CRITICAL ONLY IF MOTOR FAILS (2 FAILURES)
3	STAY REEL GEAR	BINDING	I	• NO REASONABLE DESIGN ALTERNATIVE • CONTAMINATION PREVENT MINIMIZES PROBABILITY OF FAILURE
4	STAY REEL & LINES	DISLODGEMENT THAT CAUSES BINDING	I	• ALL DRIVES WILL BE DESIGNED TO PREVENT BINDING DUE TO LINES, SPRINGS, ETC, BY PROVIDING SHIELDS OR GUARDS
10	NODE PIVOT JOINT	DISLODGEMENT	I	• SAFETY WIRE FASTENER
10	NODE PIVOT JOINT	BINDING	I	• CONTAMINATION PREVENTION MINIMIZES PROBABILITY OF FAILURE • INVESTIGATE USE OF REDUNDANT BEARING SURFACES
16	GORE SPREADER LINKAGE	BINDING	I	• SAME AS CASE NO. 10 FOR "BINDING"
18	DRUM MOTOR	BINDING	I	• SAME AS CASE NO. 3
19	DRUM RING GEAR & MOTOR INPUT GEARS	BINDING	I	• SAME AS CASE NO. 3
21	DRUM LOCK PIN MOTOR	FAILS TO WITHDRAW	I	• REDUNDANT LEADS & ELECT CIRCUITS • OPERATES ONLY TWICE DURING MISSION
22	ERECT/STOW PIN MOTORS	FAILS TO WITHDRAW PIN	I	• SAME AS ABOVE
22	ERECT/STOW PIN MOTORS	FAILS TO REINSERT	II	• SAME AS ABOVE • CAPABILITY TO SEPARATE ANTENNA FROM SHUTTLE
23	ERECT/STOW PIN GEARS	BINDING	I	• SAME AS CASE NO. 3
24	MAST EXTENSION FLANGE MOTORS	FAILS TO OPEN LATCH	I	• SAME AS CASE NO. 21
24	MAST EXTENSION FLANGE MOTORS	FAILS TO CLOSE LATCH	II	• SAME AS CASE NO. 21 • CAPABILITY TO SEPARATE ANTENNA FROM SHUTTLE
25	MAST EXTENSION FLANGE GEAR	BINDING	I	• SAME AS CASE NO. 3
26	MAST EXTENSION FLANGE MOTOR	BINDING	I	• SAME AS CASE NO. 3
27	MAST EXTENSION ROTATABLE NUT	BINDING	I	• SAME AS CASE NO. 3
28	ANTENNA SEPARATION	PREMATURE SEPARATION	I	• REDUNDANT ARE & FIRE CIRCUITS FOR PIN PULLERS
40	DUPLEXER	ANY FAILURE	III	• LOW PROBABILITY OF FAILURE • CAN STILL ACHIEVE SEVERAL MISSION OBJECTIVES
41	RADAR/COMM TRANSMITTER SELECT SWITCH	SHORT TO GROUND	III	• SAME AS ABOVE
44	FEED ANTENNA	NO OUTPUT	III	• SAME AS ABOVE
48	SIGNAL ANTENNA	NO OUTPUT	III	• SAME AS ABOVE
50	OMNI ANTENNA	NO OUTPUT	III	• SAME AS ABOVE
51	SATELLITE TRANSMITTER SELECT SWITCH	SHORT TO GROUND	III	• SAME AS ABOVE

0820-078B

Fig. 3-68 Single Point Failure Modes Summary

- WHERE REDUNDANT MOTORS ARE USED, CLUTCHES MUST BE DESIGNED FAIL-SAFE OPEN TO THE DISENGAGE POSITION
- GORE EDGE STRIPS MUST BE DESIGNED TO PREVENT DAMAGE TO GORE MATERIAL IN THE EVENT THAT AN ASSOCIATED STAY REEL LINE FAILS
- SPRING FORCE AT RIM NODES AND STAY REEL MOTORS MUST BE SIZED TO OVERCOME INCREASE IN FRICTION CAUSED BY BINDING OF A SINGLE BEARING OF A STAY REEL PULLEY OR BEARING
- ANTENNA MUST DEPLOY AND RETRACT PROPERLY IN THE EVENT OF A SINGLE RIM NODE SPRING OR STAY REEL LINE FAILURE
- ALL BOLTS MUST BE SAFETY WIRED TO PREVENT DISLODGEMENT
- GORE TENSION SPRINGS AND LINES MUST BE REDUNDANT, I.E., A SINGLE FAILURE WILL NOT ADVERSELY AFFECT GORE SURFACE GEOMETRY
- SYSTEM GAIN WILL BE BASED UPON POSSIBLE LOSS OF ONE OF 32 GORES
- GORE SPREADER WILL INCORPORATE REDUNDANT ROTATIONAL BUSHINGS TO PREVENT BINDING FAILURE DUE TO PROXIMITY OF GORE TENSION LINES
- GORES MUST BE DESIGNED TO WITHSTAND INCREASE LOAD DURING DEPLOYMENT AND RETRACTION IN THE EVENT OF BINDING OF A SINGLE DRUM BEARING
- REDUNDANT ELECTRICAL LEADS AND CONTROL CIRCUITS MUST BE USED WHERE NON-REDUNDANT MOTORS ARE USED
- ANTENNA MUST HAVE SHUTTLE SEPARATION CAPABILITY WITH REDUNDANT ARM AND FIRE CIRCUITS

0820 0798

Fig. 3-69 Deployable Antenna Design Guidelines

3.3.3.2 Failure Modes and Effects Analysis (FMEA)

The FMEA analyzed the effect of each potential failure mode during the various operational phases and classified each in accordance with the following criticality definitions:

I - A failure which would result in the inability to deploy the antenna or which does not permit attainment of any major mission objectives.

II - A failure which would prevent the retraction of the antenna but does not affect other major mission objectives.

III - A failure which would cause a major degradation of antenna performance but will permit accomplishment of some mission objectives.

IV - A failure which would cause a minor degradation of antenna performance.

V - Any other failure.

The detailed FMEA worksheets are provided as the last item in Section 3 (see Fig. 3-85).

Failures categorized as I, II and III are considered single point failures (SPF). A summary of all SPF's along with the rationale for their acceptability is shown in Fig. 3-68. Of the 24 failure modes which are classified as SPF's, 18 were associated with the antenna structure while 6 were related to electronic components. This is due to the fact that redundancy can be more easily implemented with the electrical components. Although justification for the retention of these SPF's is included in Fig. 3-68, these areas must be continually elevated by reviewing alternate design approaches.

The vast majority of the antenna structure SPF's are due to binding of gears, joint or line dislodgement, binding of joint or motor bearings and/or failure of meters to activate. Although redundancy was incorporated in all other portions of the antenna structure, redundancy was not deemed necessary and/or practical in these SPF areas.

Gearing binding due to overload can be avoided by gear design and test; however, binding caused by contamination will be prevented by normal contamination control procedures and by designing shields or guards around the gears.

Joint dislodgement will be avoided by safety wiring all fasteners. Joint and motor bearing binding can be minimized by proper bearing selection, contamination control procedures, and the application of appropriate lubricants. Redundant bearing surfaces could also be considered; however, the additional cost and weight does not appear justified considering the low probability of a binding failure.

Although the erect/stow pin motors and mast extension flange motors contain redundant electrical leads and control circuits, the loss of motor output (e.g., due to a short to ground) results in a SPF. Redundant motors were not implemented since these motors are only required to operate twice during the mission.

All electrical components are redundant except for the duplexer, antenna, and transmitter select switches. These components were not made redundant due to the low probability of failure and the fact that several mission objectives could be accomplished if these components should fail. These failures would permit antenna deployment/retraction, measurement of structural/thermal/dynamic antenna characteristics, and for certain failure modes, antenna pattern measurements can be accomplished.

The probability of mission success of the deployable antenna is addressed in subsection 3.3.3.3. The high reliability indices obtained support the justification for acceptability of the SPFs; however, alternate design approaches which would eliminate the SPFs should constantly be evaluated until the design is frozen.

As a result of this FMEA activity, several design guidelines were established and are listed in Fig. 3-69. The guidelines are primarily associated with the antenna structure/mechanical design. Several design criteria were formulated so that the antenna could operate properly in the event of a failure. In most instances this was achieved by "over design" to compensate for an increase in load due to a dislodgement or an increase in friction due to bearing binding.

Reliability Prediction - An estimate was made of the probability of mission success for the deployable antenna. For this analysis mission success was defined as the ability to achieve all the following mission objectives:

- Deploy and retract antenna
- Obtain antenna characteristics, i.e., structural, thermal, dynamic and antenna pattern measurements
- Conduct communications and radar experiments

Utilizing the results of the FMEA, reliability models was generated based upon equipment criticality and redundancy. Figure 3-70, sheet 1 shows the reliability model for the entire deployable antenna system, including the antenna structure; Fig. 3-70, sheet 2 shows the reliability model for the antenna structure only.

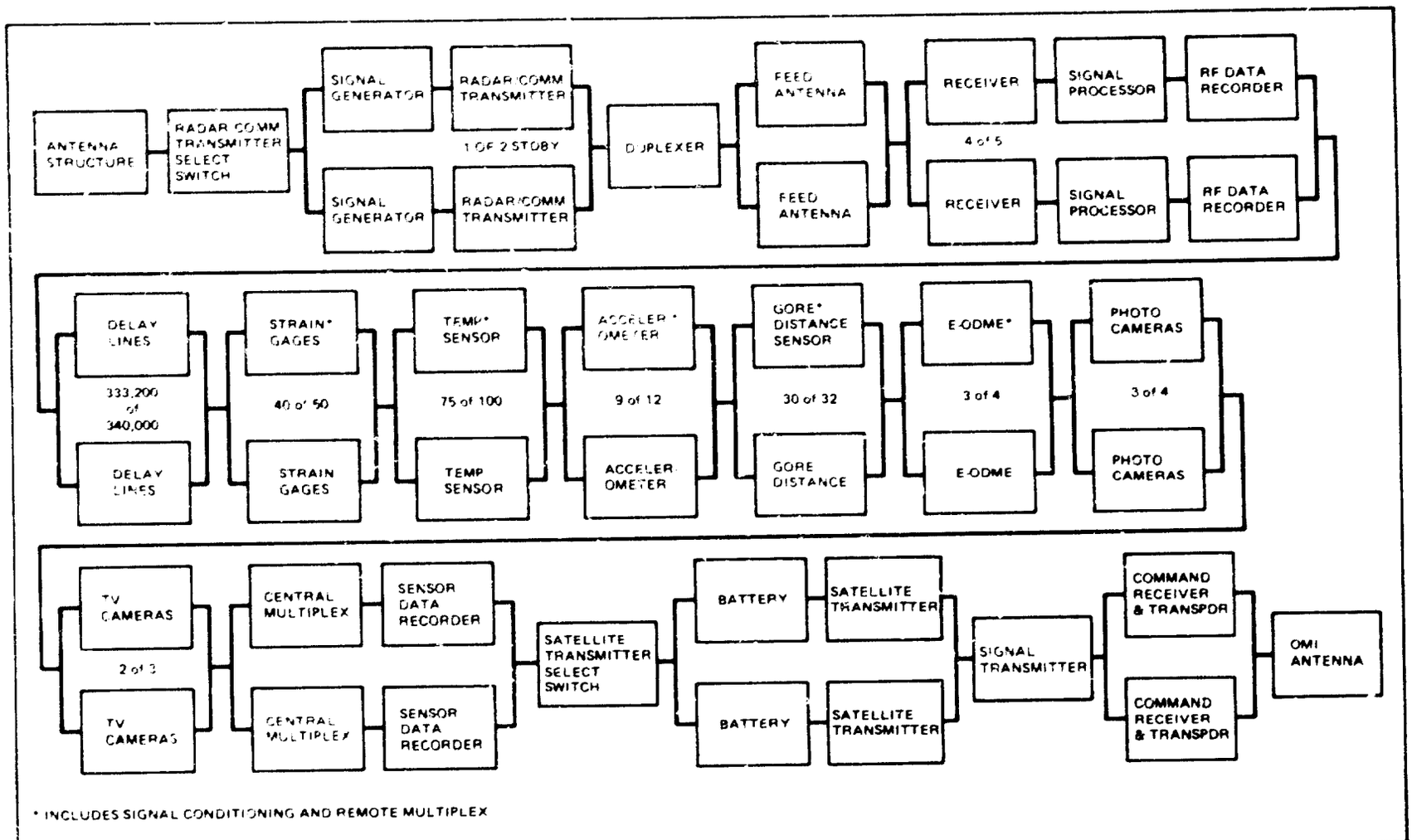

Fig. 3-70 Deployable Antenna System Reliability Model – Complete System (Sheet 1 of 2)

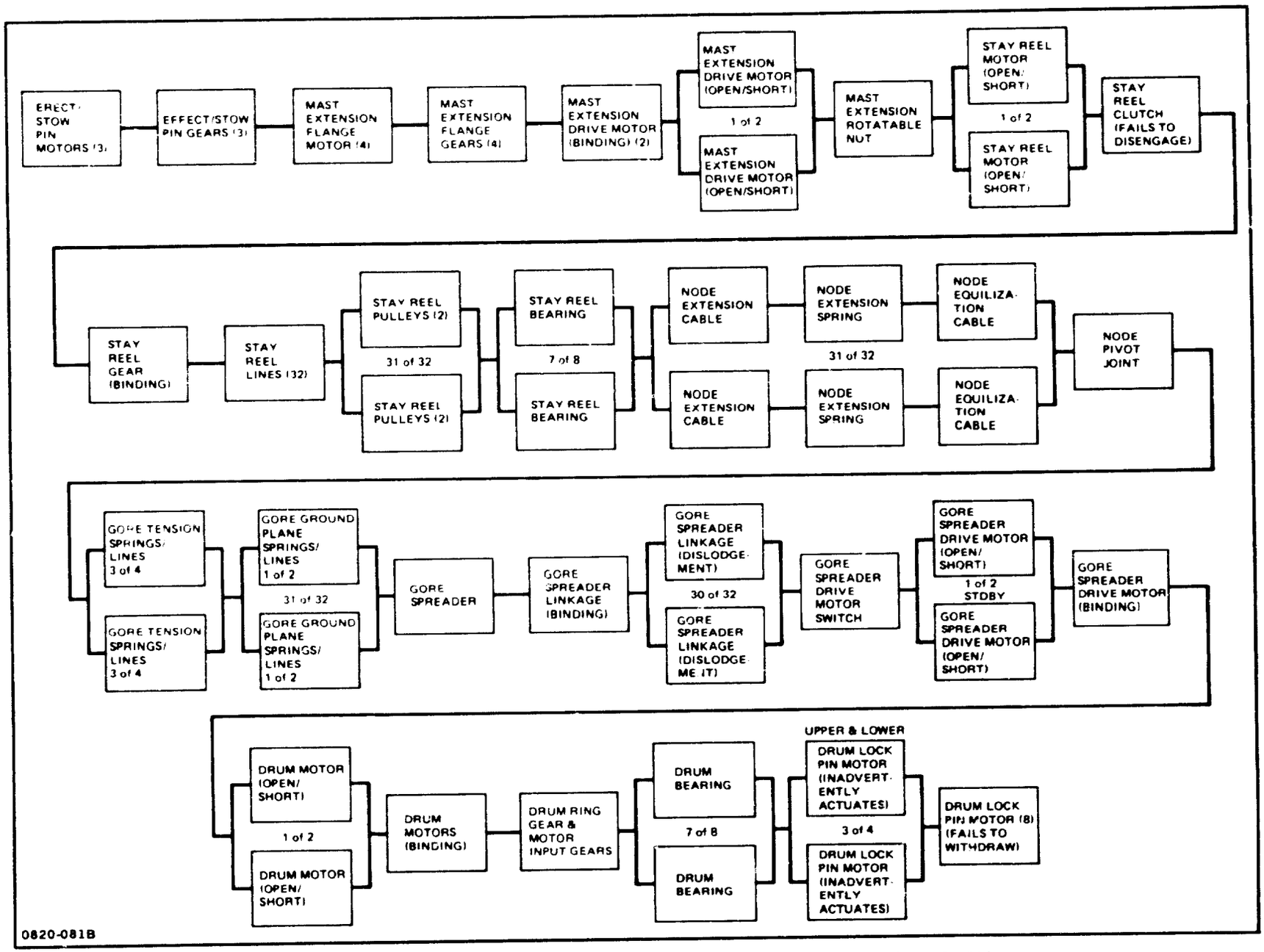

Fig. 3-70 Deployable Antenna System Reliability Model – Structure Only (Sheet 2 of 2)

The operating time for each equipment was obtained using the reference mission profile (Fig. 3-71). Figure 3-72 and 3-73 shows the operating time along with the failure rate for each equipment. The failure rates used are based on SAMSO recommended values and an industry survey performed by Boeing Corporation for SAMSO and published in report TR-76-14, dated October 1975. In addition the failure rate data obtained from PRC System Science Company's evaluation of 310 in-flight spacecrafts for the Naval Space System Activity were used. These data are contained in report PRC D-1864 dated 30 November 1972.

The equipment operating times, failure rates, and reliability models permits the calculation of the probability of mission success as shown in Fig. 3-74. The mission success reliability prediction for the deployable antenna is 0.9958. This represents a high reliability index, particularly since it is based upon obtaining all mission objectives. Reliability estimates were also calculated for a deployable antenna with no redundancy for which a 0.9641 0.9641 probability of success was obtained. Therefore, the use of redundancy resulted in a 9 to 1 improvement, based on a ratio of the unreliabilities. As can be seen in Fig. 3-74, redundancy was used more extensively in the electrical area. Therefore, most of the unreliability is in the structure/mechanical portion of the deployable antenna. As discussed in subsection 3.3.3.2, redundancy applications in the structure/mechanical area cannot be as easily implemented as with electrical components. Each of the single point failures was assessed and it was not deemed advantageous to implement the redundancy based on the low probability of failure.

3.4 MISSION EXPERIMENT PAYLOAD DEFINITIONS

The baseline antenna demonstration will verify many of the mission application test parameters defined in Section 2. For instance, a requirement common to each of the missions, low sidelobe levels, will be demonstrated during antenna pattern measurements. Other parameters which may also be derived from these data include antenna gain (for all missions), beam efficiency (for radiometry) and sidelobe stability (for radar).

Measurement of other mission applications related data will require additional hardware (and operations) which is described below for experiment payloads. As such, they have been defined as typical experiments satisfying the antenna requirements of the reference or generic mission system objectives that were defined in Task 1. Final designs will be tailored, within limits (i.e. compatible with overall antenna demonstration objectives), according to specific experimenter requirements.

The mission application hardware specifications assume that the baseline antenna system, a passive fixed-focus phased array, is used.

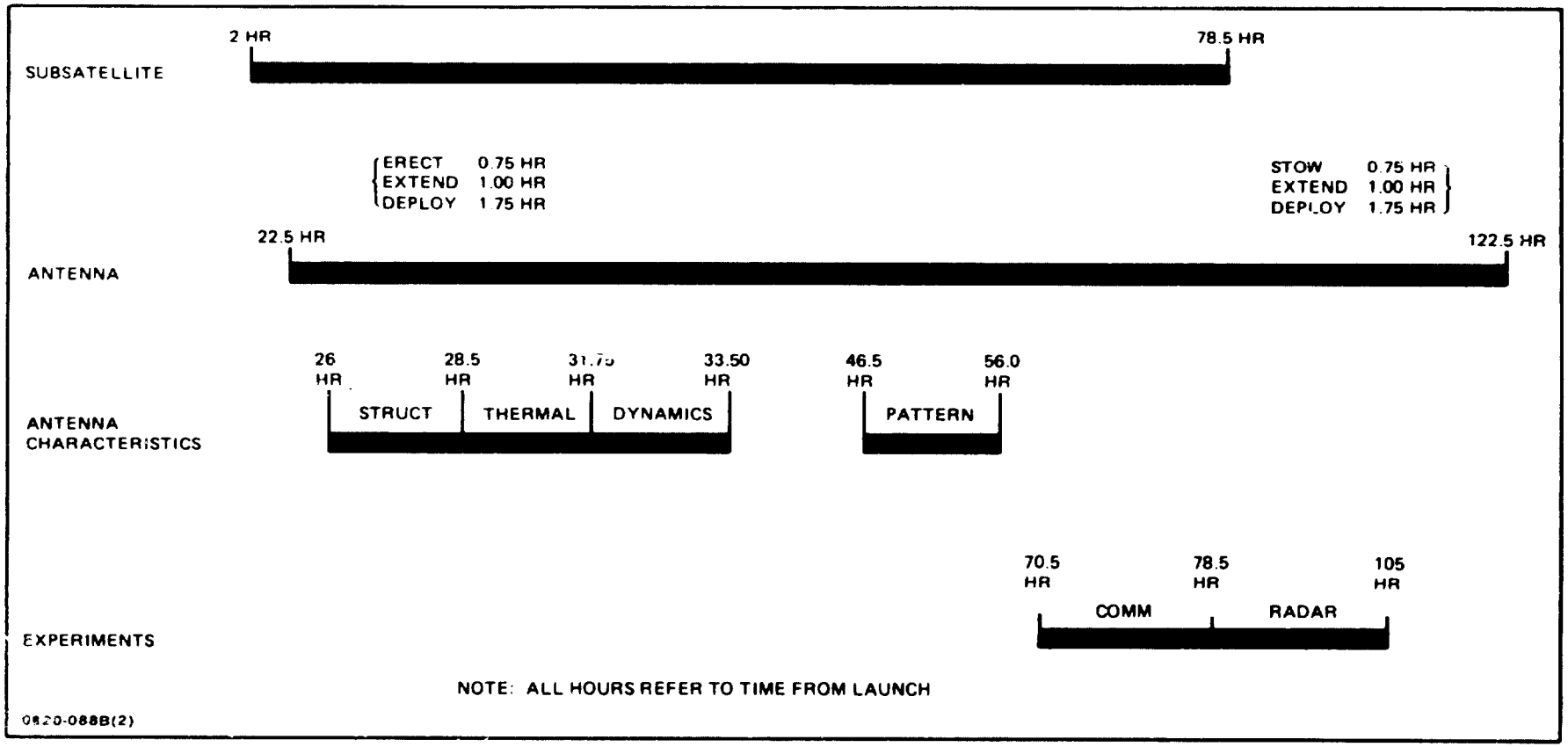

Fig. 3-71 Deployable Antenna Reference Mission Profile

DEPLOYABLE ANTENNA EQUIPMENT	DEPLOYMENT	STRUCTURAL TOLERANCE	THERMAL MEASUREMENTS	DYNAMIC MEASUREMENTS	ANTENNA PATTERN MEAS	COMMUNICATIONS EXPER	RADAR EXPERIMENT	RETRACTION	OPERATING TIME, HR	FAILURE RATE, X 10^6 (NON-REDUNDANT)
ANTENNA STRUCTURE										
ERECT/STOW IN BAY	X							X	1.50	SEE FIG. 3-73
MAST EXTENSION/RETRACTION	X							X	2.00	
DEPLOYMENT/RETRACTION	X							X	3.50	
ANTENNA OPERATION			X	X	X	X	X		93.00	
DELAY LINES	X	X	X	X	X	X	X		82.50	0.10
STRAIN GAGES	X		X	X				X	100.00	0.10
TEMPERATURE SENSORS		X	X	X					11.00	0.14
ACCELEROMETERS	X			X				X	100.00	0.79
GORE DISTANCE SENSORS		X	X	X	X	X	X		82.50	0.05
E-ODME		X	X						9.25	11.72
SIGNAL COND/FILTERS/A-D/REMOTE MULTIPX	X	X	X	X				X	100.00	13.88
PHOTOGRAMMETRIC CAMERAS			X	X					5.00	0.75
SENSOR CENTRAL MULTIPLEXERS	X	X	X	X				X	100.00	1.76
TV CAMERAS	X							X	7.00	7.50
SENSOR DATA RECORDERS	X	X	X	X				X	100.00	35.00
RADAR COMM TRANSMITTER SELECT SWITCH						X	X		1 CYCLE	0.10
RADAR COMM TRANSMITTERS						X	X		34.50	3.00
SIGNAL GENERATORS						X	X		34.50	5.00
DUPLEXER					X	X	X		58.50	0.13
SIGNAL PROCESSORS					X	X	X		58.50	0.39
RF DATA RECORDERS					X	X	X		58.50	35.00
FEED ANTENNAS					X	X	X		58.50	0.09
RECEIVERS					X	X	X		58.50	0.68
SATELLITE TRANSMITTER SELECT SWITCH					X	X			1 CYCLE	0.10
SATELLITE BATTERIES					X	X			32.00	2.20
SATELLITE TRANSMITTERS					X	X			32.00	3.00
SATELLITE SIGNAL ANTENNA					X	X			32.00	0.09
SATELLITE COMD RECEIVER AND TRANSPDR					X	X			32.00	6.98
SATELLITE OMNI ANTENNA					X	X			32.00	0.09

0820.082B

Fig. 3-72 Deployable Antenna Equipment Operating Times and Failure Rates

ANTENNA STRUCTURE COMPONENTS	ERECT/STOW IN BAY	MAST EXTEND/RETRACT	ANTENNA DEPLOY/RETRACT	ANTENNA OPERATION	OPERATING TIME, HR	FAILURE RATE, X 10^6 (NON-REDUNDANT)
ERECT/STOW PIN MOTORS	X				1.50	1.00
ERECT/STOW PIN GEARS	X				1.50	0.10
MAST EXTENSION FLANGE MOTORS		X			2.00	1.00
MAST EXTENSION FLANGE GEARS		X			2.00	0.10
MAST EXTENSION DRIVE MOTORS (BINDING)		X			2.00	0.01
MAST EXTENSION DRIVE MOTORS (OPEN/SHORT)		X			2.00	1.00
MAST EXTENSION ROTATABLE NUT		X			2.00	0.10
STAY REEL MOTORS			X		3.50	1.00
STAY REEL CLUTCH AND GEARS			X		3.50	0.10
STAY REEL LINES			X	X	96.50	1.00
STAY REEL PULLEYS			X	X	96.50	0.01
STAY REEL BEARINGS			X		3.50	0.01
NODE EXTENSION CABLES			X	X	96.50	1.00
NODE EXTENSION SPRINGS			X	X	96.50	0.22
NODE EQUALIZATION CABLES			X	X	96.50	1.00
GORE TENSION SPRINGS/LINES			X	X	96.50	1.22
GORE GROUND PLANE SPRINGS/LINES			X	X	96.50	1.22
GORE SPREADERS			X	X	96.50	0.10
GORE SPREADER LINKAGES (BINDING)			X	X	96.50	0.10
GORE SPREADER LINKAGES (DISLODGEMENT)			X	X	96.50	0.10
GORE SPREADER DRIVE MOTOR SWITCH			X		3.50	0.10
GORE SPREADER DRIVE MOTORS (OPEN/SHORT)			X		3.50	1.00
GORE SPREADER DRIVE MOTORS (BINDING)			X		3.50	0.01
DRUM MOTORS (OPEN/SHORT)			X		3.50	1.00
DRUM MOTORS (BINDING)			X		3.50	0.01
DRUM RING GEAR & MOTOR INPUT GEARS			X		3.50	0.10
DRUM BEARINGS			X		3.50	0.01
DRUM LOCK MOTORS (INADVERTENTLY ACTUATES)	X	X	X	X	100.00	0.10
DRUM LOCK MOTORS (FAILS TO WITHDRAW)			X		3.50	1.00

0820-083B

Fig. 3-73 Antenna Structure Operating Times and Failure Rates

3.4.1 COMMUNICATION EXPERIMENT

As described in subsection 2.2, the objectives of a communication experiment should address the demonstration of a large deployable antenna with narrow beam performance and a scan coverage many beamwidths around boresite. Up to ±4 degrees angular coverage may be provided by a combination of multibeam feed configuration and/or electrical beam steering.

Of particular importance are those performance characteristics which will permit frequency re-use in the multibeam array. Use of the same frequency every second beam requires low sidelobe levels (-30 dB first sidelobe). In addition it is desirable to measure the effect on the sidelobes of beam scan angle off bore site, for comparison of computed values to provide verification of the analysis of the off-boresight performance of antennas that are large in wavelengths (of the order of 500 wavelengths diameter). See subsection 3.3.2.

Sidelobe levels of the antenna (mainbeam) will be measured during pattern tests as the antenna, in a receive mode, is physically scanned past the RF signal transmitted by the subsatellite. Use of additional feeds and receivers, as shown in Fig. 3-75, will provide a measurement of interbeam isolation by comparison of receiver signal levels. Multibeam sidelobe degradation data are derived by comparison of total antenna patterns. Since the configuration only gives look angles a few beamwidths off boresite, the anticipated level of degradation will be small.

The operational sequence described in Section 4 for pattern measurements will provide the data required for multibeam strength calibration measurement at the surface of the array to be used to compensate for short term fluctuations in the signal transmittted from the subsatellite.

The level of intermodulation (IM) products generated in the deployable structure is an important parameter for multibeam communication functions. The measurement of a single two-signal, third-order product is proposed using the experiment configuration shown in Fig. 3-75. As the equal output levels of the two transmitters driving two feeds are increased the spurious IM signals (at -200 dBw/Hz) generated in the mast or antenna structure is measured as it is reflected back to a receiver via a third feed. Variable transmitter outputs up to 200 watts are required to measure the onset of IM levels. The antenna will be pointed at deep space during this test.

	PROBABILITY OF MISSION SUCCESS		IMPROVEMENT DUE TO REDUNDANCY BASED RELIABILITY
	PRESENT CONFIGURATION	NON-REDUNDANT CONFIGURATION	
ELECTRICAL PORTION	.9999	.9899	101:1
STRUCTURE/MECHANICAL	.9959	.9739	6:1
TOTAL DEPLOYABLE ANTENNA	.9958	.9641	9:1

0820-084B

Fig. 3-74 Deployable Antenna Reliability Prediction

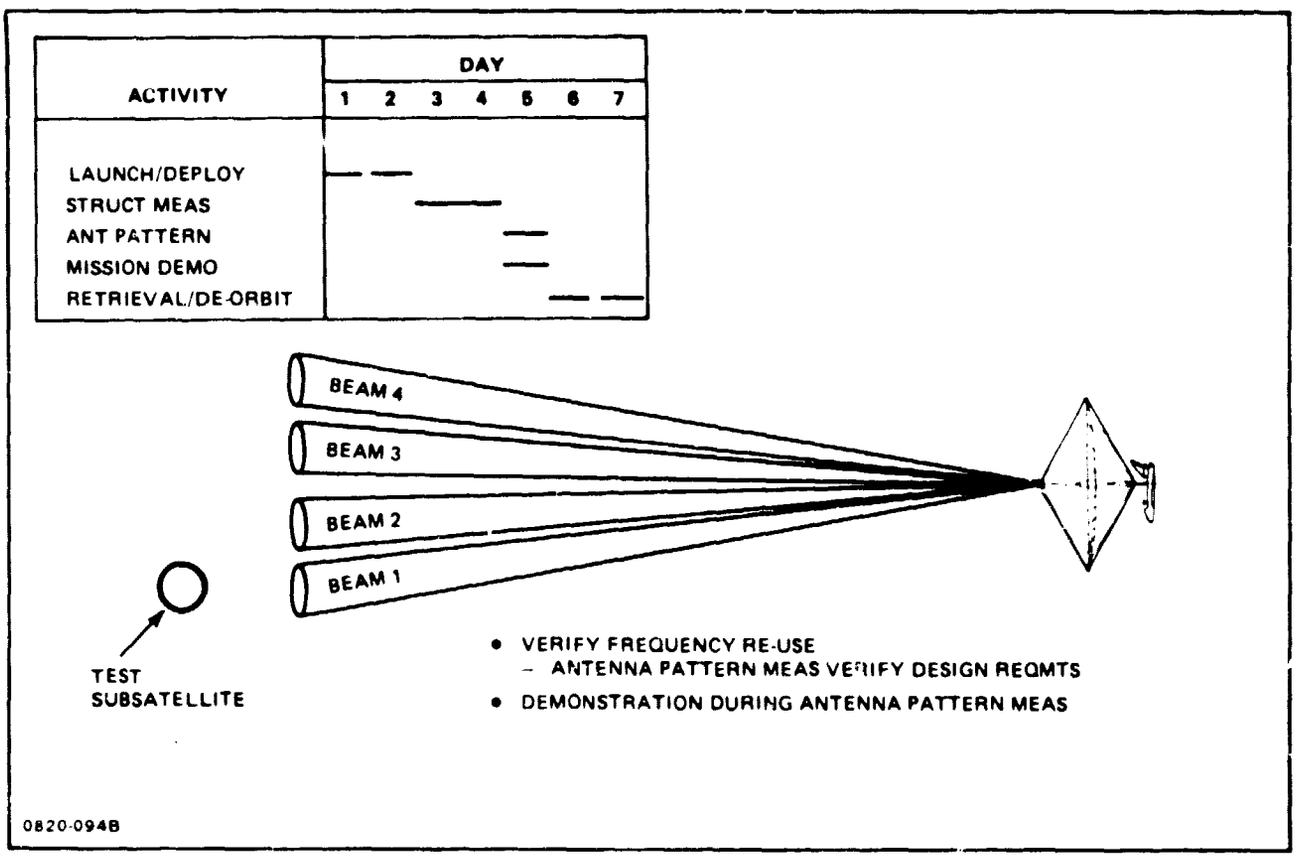

Fig. 3-75 Communications Experiment

3.4.2 RADAR EXPERIMENT

Desired test objectives for a radar experiment include:

- Verification of beam agility
- Measurement of clutter background (amplitude and spectral distribution)
- Detection of a target in the clutter background
- Verification of antenna low loss performance
- Sidelobe cancellation capability.

Direct inflight demonstration of beam agility is not proposed because the low-cost, passive array will form a fixed beam at the angle determined by the settings of the fixed phase shifters (transmission line sections) in the array as manufactured. Electronic beam steering is then verified by ground tests of electronic modules.

The verification of antenna loss parameters can be provided by measurement of the equivalent receiver noise temperatures through the antenna. This measurement is identical to that described for the radiometry experiment in the subsection 3.4.3. Equipment and operational requirements are also identified.

Clutter measurements have the greatest impact on experiment system geometry and antenna configuration parameters. Clutter data from various land, sea and ice background are desired. We anticipate that the maximum orbit inclination possible, 56 degrees (consistent with ETR launch constraints), will be necessary to satisfy these conditions. The magnitude of clutter returned are a function of the projected clutter patch which in turn depends on spot and range bin sizes (see Fig. 3-76) Many radar systems being considered have ground spots of 20 to 30 nautical miles, and range bins of 60 to 150 meters (i.e. clutter patches up to 9×10^6 square meters). Single beam operation at 350 nautical miles (and 150-meter range bins) yields a maximum clutter patch of about 1×10^6 square meter. Therefore in order to better simulate anticipated operational conditions, a multibeam system as shown in Fig. 3-77 has been specified for the experiment. The use of multibeams with separate receivers also provides an enhanced capability for determination of clutter distribution within the clutter patch.

Clutter bandwidth, both intrinsic and that produced by relative sensor/background velocity will be measured. The latter source is a function of beamwidth and grazing angle as shown in Fig. 3-77. Since the antenna being flown has a beamwidth consistent with that of projected operational systems, use of only a single beam system is adequate for this measurement. Antenna pointing, ±1 beamwidth with respect to the local vertical, will be required to provide the desired range of geometry conditions.

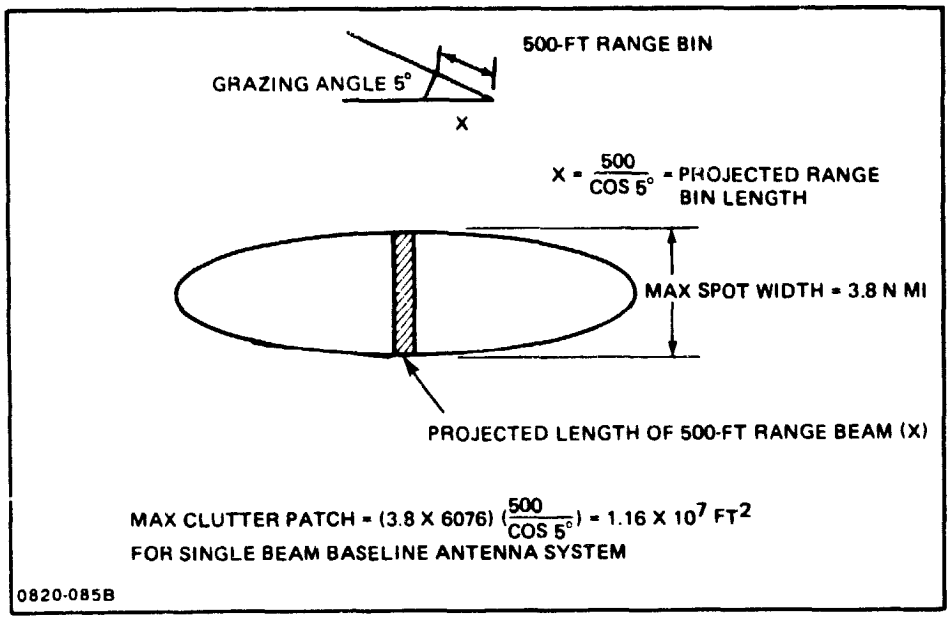

Fig. 3-76 Clutter Patch Geometry

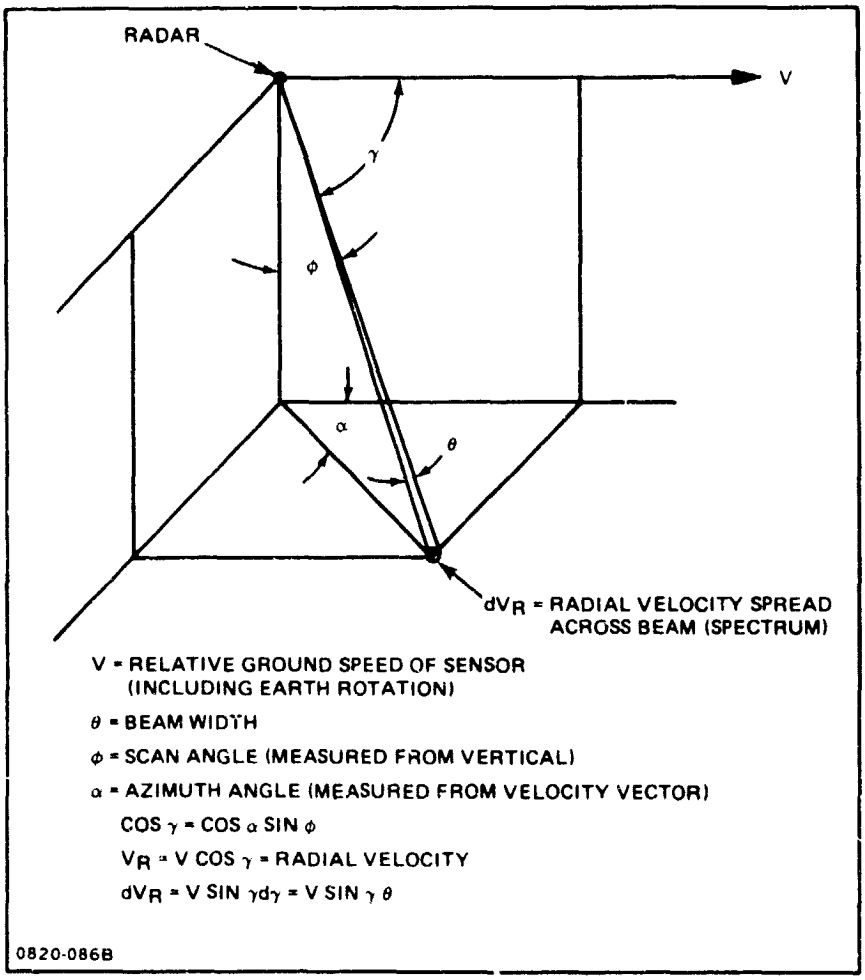

Fig. 3-77 Radar Beam Geometry for Determining Fixed Clutter Spectrum

Experiment RF signal requirements in terms of energy and waveform parameters have been examined. The energy for both clutter measurements and target detection are based on providing a minimum target-to-signal ratio of 6 dB (with a 5 square meter target RCS). A requirement of 21 milliwatt-second was determined from the following relationship:

$$E = \frac{(4\pi)^3 R^4 K T L S/N}{G^2 \lambda^2 \sigma} = 21 \times 10^{-3} \text{ w-sec transmitter energy per pulse}$$

where:

R = 1590 n mi (2.95×10^6 m) at zero-degree grazing angle

$K = 1.38 \times 10^{-23}$

T = 600°K

L = 6 dB (4 ratio)

S/N = 6 dB (4 ratio)

λ = .22 m for 1350 MHz frequency

σ = 5 m^2 (assumed aircraft target RCS)

$G = \left(\frac{D}{\lambda}\right)^2$ = 63 dB for 1 beam, D = 100 m

Definition of signal waveform parameters is based on a number of factors. Integration time constraints are dependent on time on target (clutter patch), look geometry and range-walk compensation considerations. The speed of the beam spot on the ground (due to antenna orbital motion) is 3.7 n mi/sec. If no range walk compensation techniques are used, the integration time is limited to the time the range bin stays on target (i.e., 0.022 seconds for a 500-foot range bin). With range walk compensation (applied in the post flight data processing), spot time on target limits the maximum integration time. At 5-degree grazing angle, the footprint is projected 44 nautical miles in the range direction and integration in excess of 10 seconds is theoretically possible. With range walk compensation, a simple two-pulse MTI system can be used for target detection.

Waveform PRF for clutter measurements is determined primarily by the two-way transmission time geometry. At maximum range (1590 nautical miles for zero-degree grazing angle) the two-way transmission time is 20 milliseconds. Two waveform approaches considered were: (1) place all the energy in a single pulse, or (2) split the energy between a number of pulses and integrate the return signals. The first approach was selected in this study for system sizing. A typical waveform was defined assuming a 0.5 microseconds transmitter pulse at 50 Hz PRF. The peak transmitter power is 42 kilowatts and the average transmitter power is 1 watt.

For ground clutter spectrum analysis, a higher PRF must be used to avoid Doppler ambiguity. The waveform definition for this function, a considerably more complicated problem, was not considered as part of this study.

Performance parameters of our postulated radar experiment are summarized in Fig. 3-78. Also shown is a functional block diagram of the hardware required. The signal generator is assumed to be commandable inflight to permit flexibility in waveform selection during clutter measurement and target detection sequences. Data will be recorded and/or transmitted to the ground for post-flight data reduction. Therefore a minimum of on-board signal conditioning has been assumed.

Integration of the experiment with a 50-meter antenna (instead of 100 meters) would primarily impact power requirements. The two way antenna gain is reduced by 12 dB. Therefore, some combination of waveform modification (i.e. integrating more pulses) and/or increasing transmitter output (peak and average power) must be provided to maintain the desired energy.

3.4.3 RADIOMETRY EXPERIMENT

Test objectives identified for this experiment include:

- Verification of scan angle performance
- Measurement of temperature sensitivity
- Soil moisture measurement.

Scan angle performance will be measured during antenna pattern tests using a multibeam feed/receiver system. These measurements have been described for the communication experiment (multibeam performance measurements in subsection 3.4.1). The experiments to satisfy the remaining test objectives are described below.

The temperature sensitivity (ΔT) of a radiometry system is given by:

$$\Delta T = \frac{2}{\sqrt{B\tau}} (T_A + T_{REC})$$

where:

B = RF Bandwidth

τ = Integration Time

T_A = Antenna Temperature

T_{REC} = Equivalent Receiver Noise Temperature

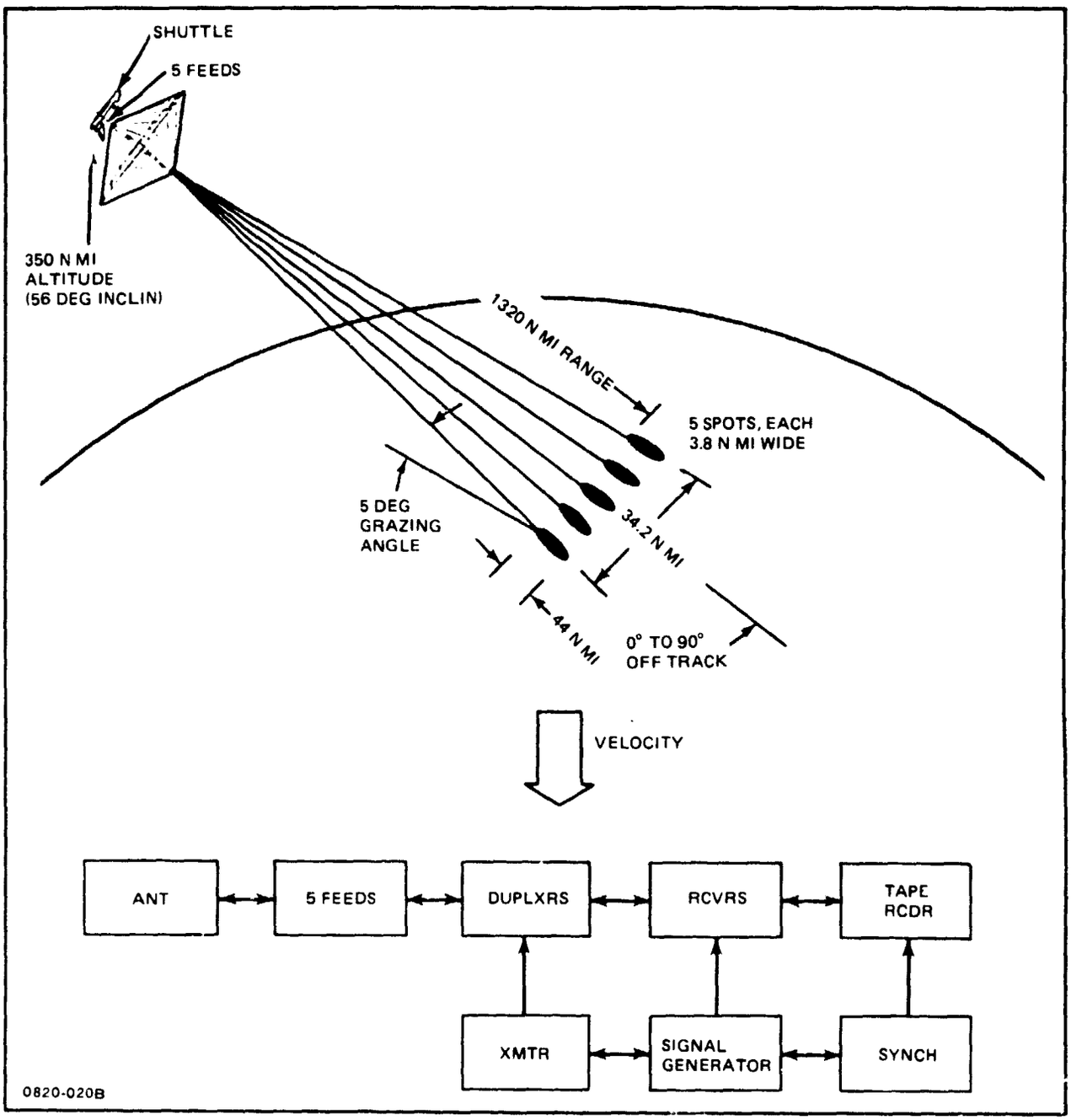

Fig. 3-78 Radar Experiment

Of these parameters, the first two, B and τ, are under control of the experiment designer and therefore considered known. Antenna temperature, T_A, is a function of where the system is looking. By pointing the antenna to a cold location in the sky (deep space) with a known temperature, T_{REC} can be measured and the ΔT of the system can be computed for any combination of the other variables. A calculation of the expected T_{REC} for the demonstration antenna-feed-radiometer receiver combination is shown in Fig. 3-79.

The addition of feeds in a row gives a limited push broom radiometer configuration, which, when pointed to the earth, provides soil-moisture measurements (see Fig. 3-80). Each feed requires an electronic module containing a radiometer receiver, typified by the Dickie receiver shown, and a sampling device to interface with the orbiter DMS. The major demand on the orbiter for support is the pointing requirement. In order to determine how well the system works, flight data will be compared to selected ground-truth data in post-flight analysis. A valid comparison will require accurate time/location data correlation. To reduce errors due to pointing, a requirement of ±1 beamwidth with respect to a local vertical reference has been specified.

Operating from a 350-nautical mile orbit, a 100-meter diameter system will provide ground resolution (spot size) of approximately one nautical mile with a spot ground speed of 3.7 n mi/sec. This in turn dictates a maximum integration time of 1/3.7 or .27 seconds. The anticipated ΔT of the system is given by:

$$\Delta T = \frac{2}{|(12\text{MHz})(.27\text{ sec})|^{1/2}} \quad (280^\circ\text{ K} + 397.7^\circ\text{ K}) = .75^\circ\text{ K}$$

where the bandwidth is limited to 12 MHz by the antenna configuration and $T_A = 280^\circ$ K when the antenna is looking down at the earth.

Should a 50-meter antenna be flown, the ground resolution is degraded to approximately 2 nautical miles, but the integration time can be doubled. In addition the bandwidth can also be doubled to 24 MHz resulting in a system ΔT of 0.38° K. There is no impact on the experiment payload requirements, but the antenna pointing requirements can be relaxed since the beamwidth has doubled.

BLOCK DIAGRAM FOR SYSTEM NOISE TEMPERATURE (PASSIVE ZONED LENS)

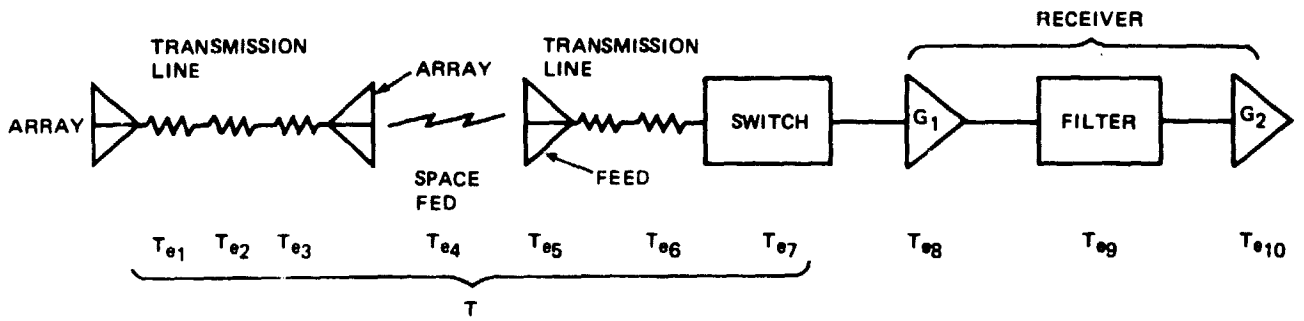

$$T_{rec} = T + \frac{Te8}{G} + \frac{Te9}{GG_8} + \frac{Te10}{GG_8G_g}$$

(1) T

AVG ARRAY BOOTLACE TRANSMISSION LINE LENGTH = $\frac{\lambda}{2}$

SUBARRAY LOSS (4 X 4 SUBARRAY) = (3.25 λ) ($\frac{.1dB}{\lambda}$) = 0.325 dB

$L_1 + L_2 + L_3 = 0.325 + (\frac{}{2})\ (\frac{.1dB}{\lambda}) + .325 = 0.7dB$

L_4 = 0.088 dB (987. TRANSMISSION EFFICIENCY)

$L_5 + L_6 + L_7$ = 1dB

L = .7 + .088 + 1 = 1.79 dB (1.51 RATIO) jG = 0.676

T = (L - 1) 290 = (1.51 - 1)(290) = 148° K

(2) T_{eg} = 168.2° K; G_8 = 316

(3) T_{eg} = 17.4° K; G_g = 0.944

(4) T_{e10} = 168.2° K; G_{10} = 316

$$T_{rec} = 148 + \frac{168.2}{0.676} + \frac{17.4}{(0.676)(316)} + \frac{168.2}{(0.676)(316)(.944)} = 397.7$$

0820-087B

Fig. 3-79 Passive Zoned Lens Noise Temperature Estimate

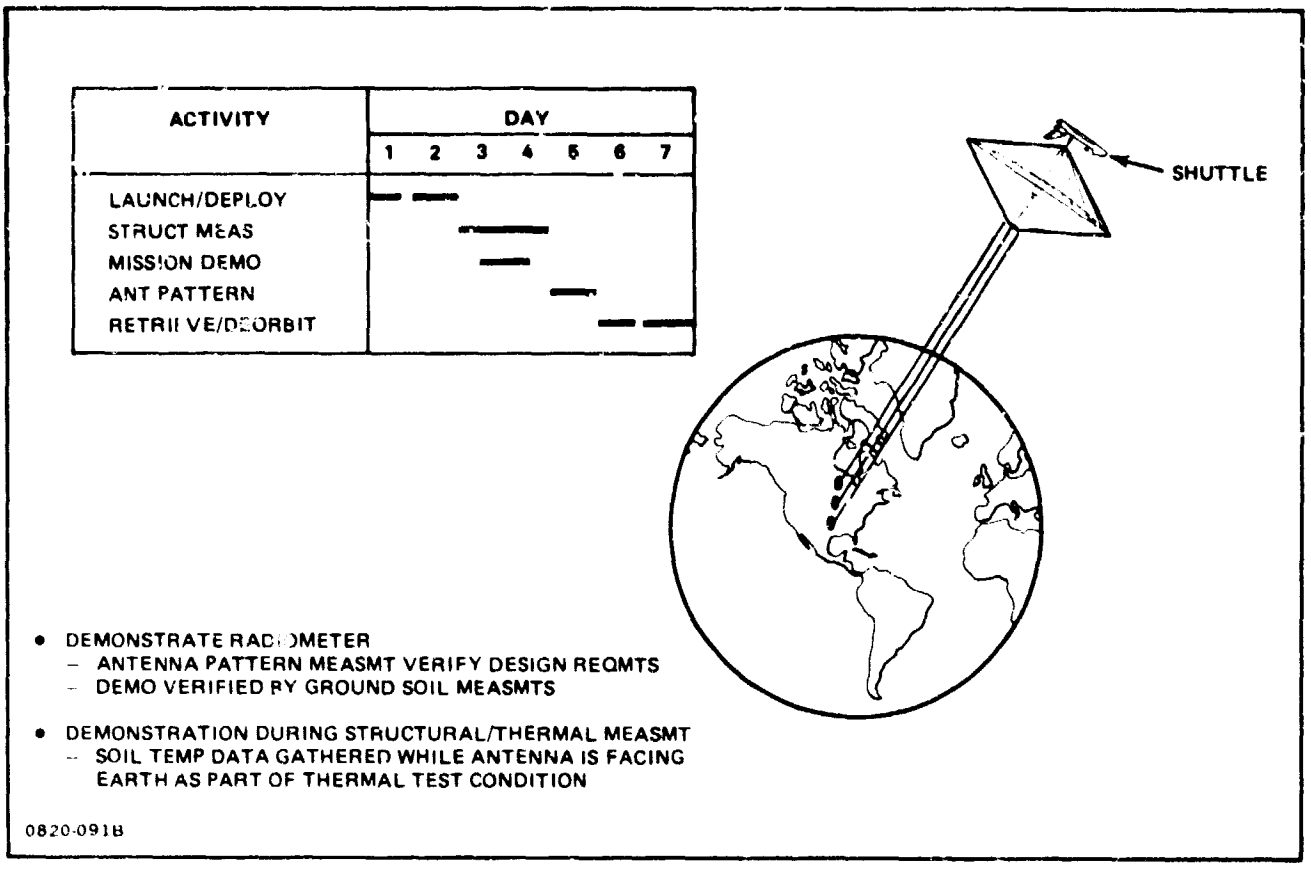

Fig. 3-80 Radiometry Experiment

3.5 FLIGHT SUPPORT EQUIPMENT

3.5.1 ORBITER INTERFACE/INTEGRATION EQUIPMENT

3.5.1.1 Support Structure

The antenna, mast canister and separation base are stowed in the shuttle payload bay as one unit. This unit is supported at the forward aft ends by tubular truss structures. (Fig. 3-81) These trusses are fabricated from square aluminum extruded tubes bolted together. The forward truss supports two actuator driven pins which engage fittings attached to the forward stay platform. These pins are retracted to allow the unit to rotate, and be extended for final stowage. The pins take Y and Z loads only. The forward truss is attached to the shuttle at the longerons and keel member. The primary load path is in the Z direction into the longerons with loads in the Y direction resisted by the keel attachment. The aft truss structure transmits loads from the separation base at the pivot fittings to the longerons in the X and Z direction and to the keel fitting in the Y direction. Where the trusses interface with the shuttle structure the current interface design is incorporated as dictated by Ref. 3-19.

When the unit is erected all loads will be transmitted to the shuttle through the aft truss structure. After the RMS have rotated the unit from the stowed position to the 90-degree erected position, an actuator driven pin will engage the separation base to provide a three point support for the deployed antenna. The actuator is mounted on a member of the aft truss. After antenna testing is completed the reverse procedure is initiated and the unit will be restowed in the shuttle payload bay.

3.5.1.2 The Mast

The deployable mast is attached at one end to the hub and is stowed within the hub. The other end is secured to the separation base. The canister which contains the deployment mechanism and transition region is bolted at the antenna end to the hub and is clamped at the shuttle end to a ring mounted on the separation base. When the clamps are released and the motors on the canister are energized, the mast will deploy raising the antenna to its 100-meter position outside the shuttle.

The principle structural components of the mast are the longerons, battens and the diagonals (see Fig. 3-82). These members are made of graphite epoxy. Typically, the longerons are segments of tubing, of 0.092 $in.^2$ cross sectional area, which are articulated

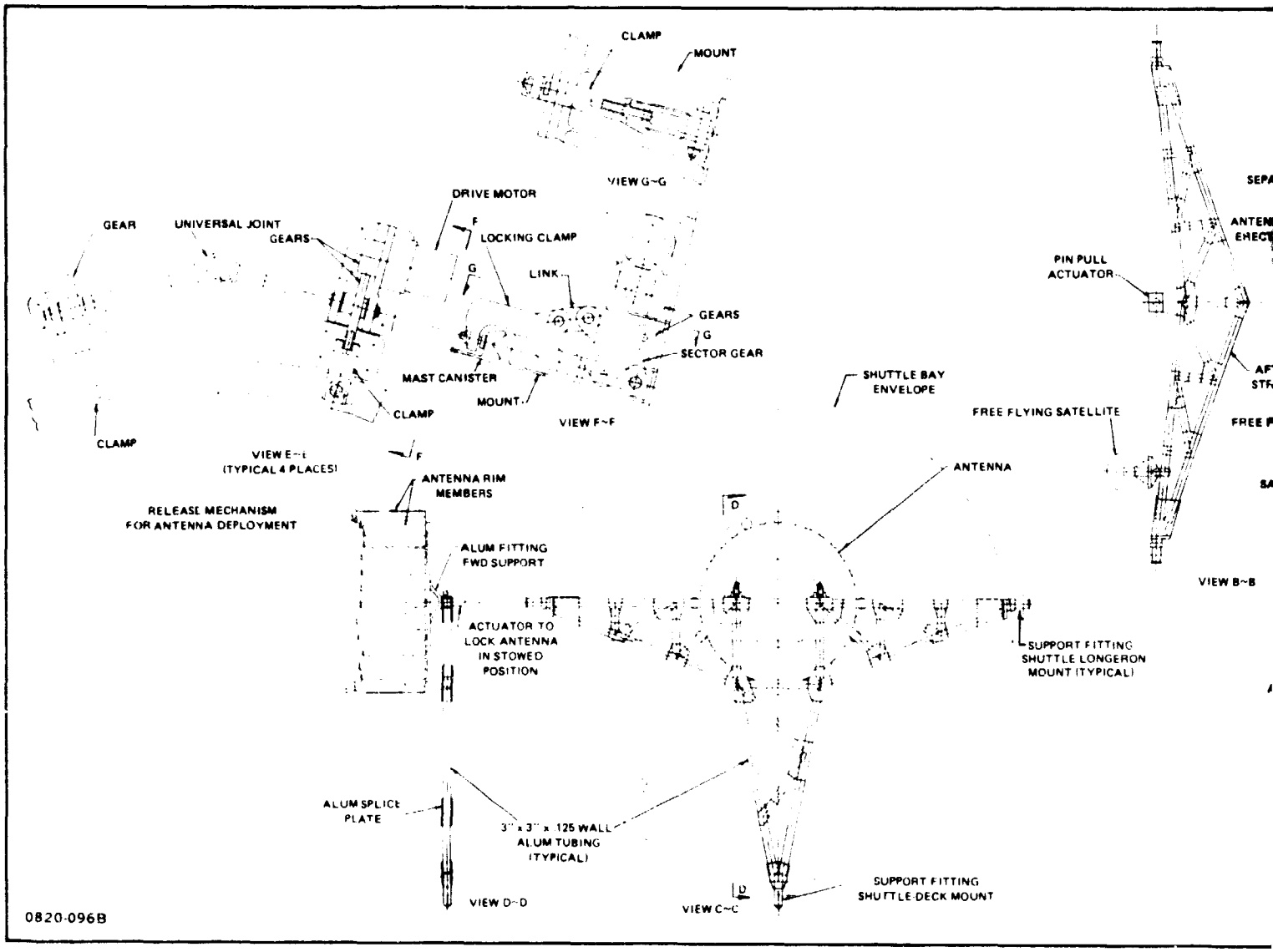

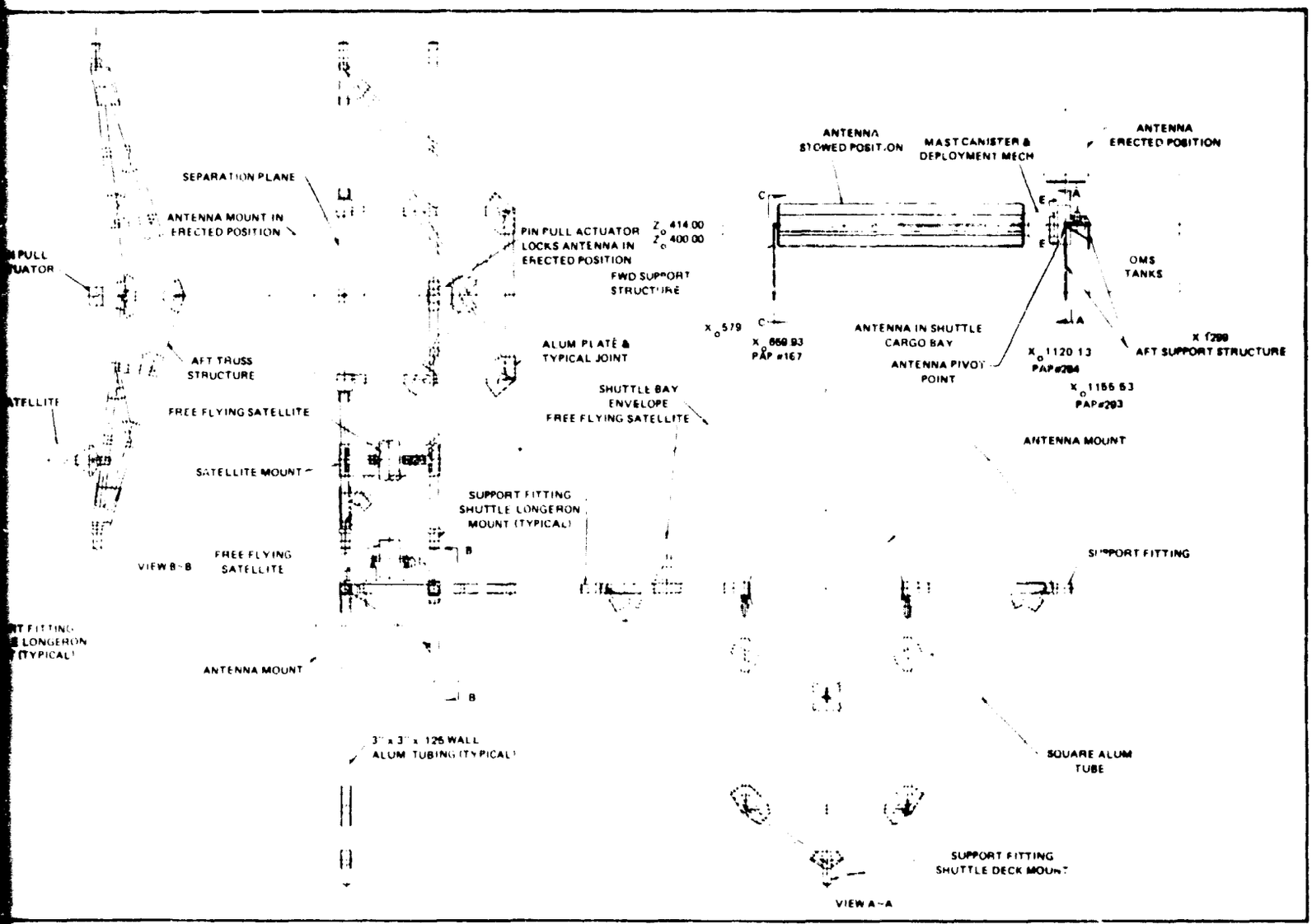

Fig. 3-81 Payload Support Structure

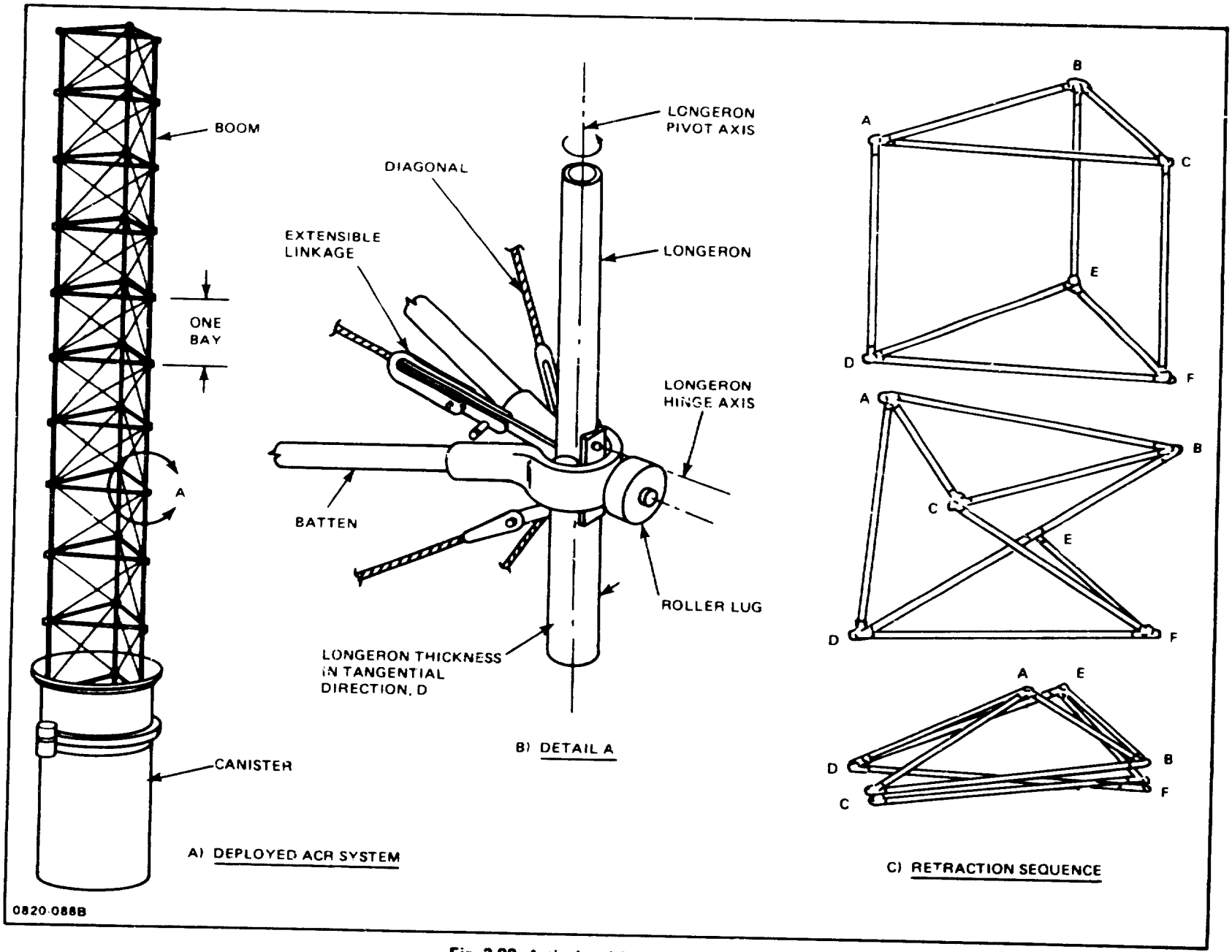

Fig. 3-82 Articulated Boom and Canister

to the batten frames with universal hinge fittings. Six diagonal cables provide shearing stiffness and strength for each section of the mast. Three of extendible diagonals and hinged linkages which extend when unlatched. This combination of extendable diagonals and hinged longerons permits adjacent batten frames to be rotated differentially about the mast axis thus collapsing the section into a compact retracted configuration. Retraction and deployment of each section proceeds independently of the extent to which adjacent sections are deployed. The canister section consists of a large motor-driven, three-threaded nut and three pairs of stationary, vertical guide rails. Round roller lugs which protrude from the mast at each batten corner are engaged between the stationary guides and the threads of the nut. When the nut is rotated by a drive motor, the mast is forced to deploy from or retract into the canister and hub. The deployed part of the mast does not rotate as it deploys. As the mast is so deployed or retracted, cams located in the top of the transition region automatically latch or unlatch the mast diagonal linkages. Since one level of roller lugs is always engaged by the canister, the deployed portion of the mast is always supported. Since the mast must be twisted to retract and since the deployed part of the mast does not rotate in the canister, the retracted part within the stowage region of the hub must rotate. To accommodate this rotation, the end of the mast is mounted on a rotatable plate within the hub.

3.5.1.3 Separation Base

The separation base is an aluminum structure mounted on the support truss which interfaces with the shuttle payload bay. It supports the antenna and contains the pivot about which the antenna rotates 90 degrees from shuttle stowage to erected position (see Fig. 3-81). This base also provides the mount for the mast canister release clamps and actuators. Springs and clamps within the base allow the portion above the pivot mount to be ejected to remove the deployed antenna and mast from the payload bay.

3.5.2 SUBSATELLITE DESIGN

The use of a small spin-stabilized satellite as a RF signal source for antenna pattern measurements is described in Ref. 1-1. The subsatellite system consist of those elements shown in Fig. 3-3 plus the necessary equipment to interface with the orbiter (including spinup and release mechanism). Prior to deployment these equipments are installed on the antenna aft support structure in the orbiter payload bay (see Fig. 3-81). The satellite is a drum (14.94-inches in diameter by 7.65-inches high) housing two each of the following: RF generator, TT&C, and batteries. These items are connected by two individual harnesses to achieve redundancy. The above equipment is mounted on aluminum brackets which in turn are attached to a central shaft and to each end cover. The end covers are fabricated from

aluminum sheet and are fastened to the rolled aluminum sheet which forms the drum. The sides of the drum contain eight equally spaced slots and each end cover contains two slots (see Fig. 3-83). A fitting is secured to each end of the central shaft and provides the mount for the spin up bearings. Standard aircraft hardware and fabrication procedures are employed in the satellite's construction.

The support brackets holding the spin up motor and satellite release mechanism (see Fig. 3-84) are mounted on an aluminum honeycomb base. The two bearings on the satellite shaft are gripped by aluminum scissor fittings, two fittings at each end. Prior to release, the motor brings the satellite to a 60-rpm rotation speed. A slot on the satellite's shaft engages a mating tang on the motor shaft for torque transmission. Positive engagement of the slot and tang is ensured by the compression spring. Energizing the solenoid overcomes the spring's force and withdraws the tang from the slot. The satellite is held by the scissor fittings while it is spinning. When the screw jack actuator opens the scissors the satellite is free of all restraints. The shuttle may then be backed away from the satellite the required distance for test purposes.

The total subsatellite system weight is estimated to be 180 pounds (110 pounds for the subsatellite and 70 pounds for the spin-up and release mechanism).

3.6 GROUND SUPPORT EQUIPMENT (GSE)

Several items of GSE have been identified to the deployable antenna demonstration flight system. These can be grouped basically under mechanical and electrical GSE. Preliminary specifications defining requirements, capabilities and usage are presented below for each item.

3.6.1 MECHANICAL GSE

3.6.1.1 Antenna Shipping Container

- Requirements
  - Provide suitable protection from physical damage and contamination for the antenna during transportation and storage
  - Provide hoisting and fork lift provisions for the fully loaded unit
  - Provide a means of mounting a dry nitrogen supply and control unit
  - Provide a means of detecting and recording acceleration loads during transportation and handling.

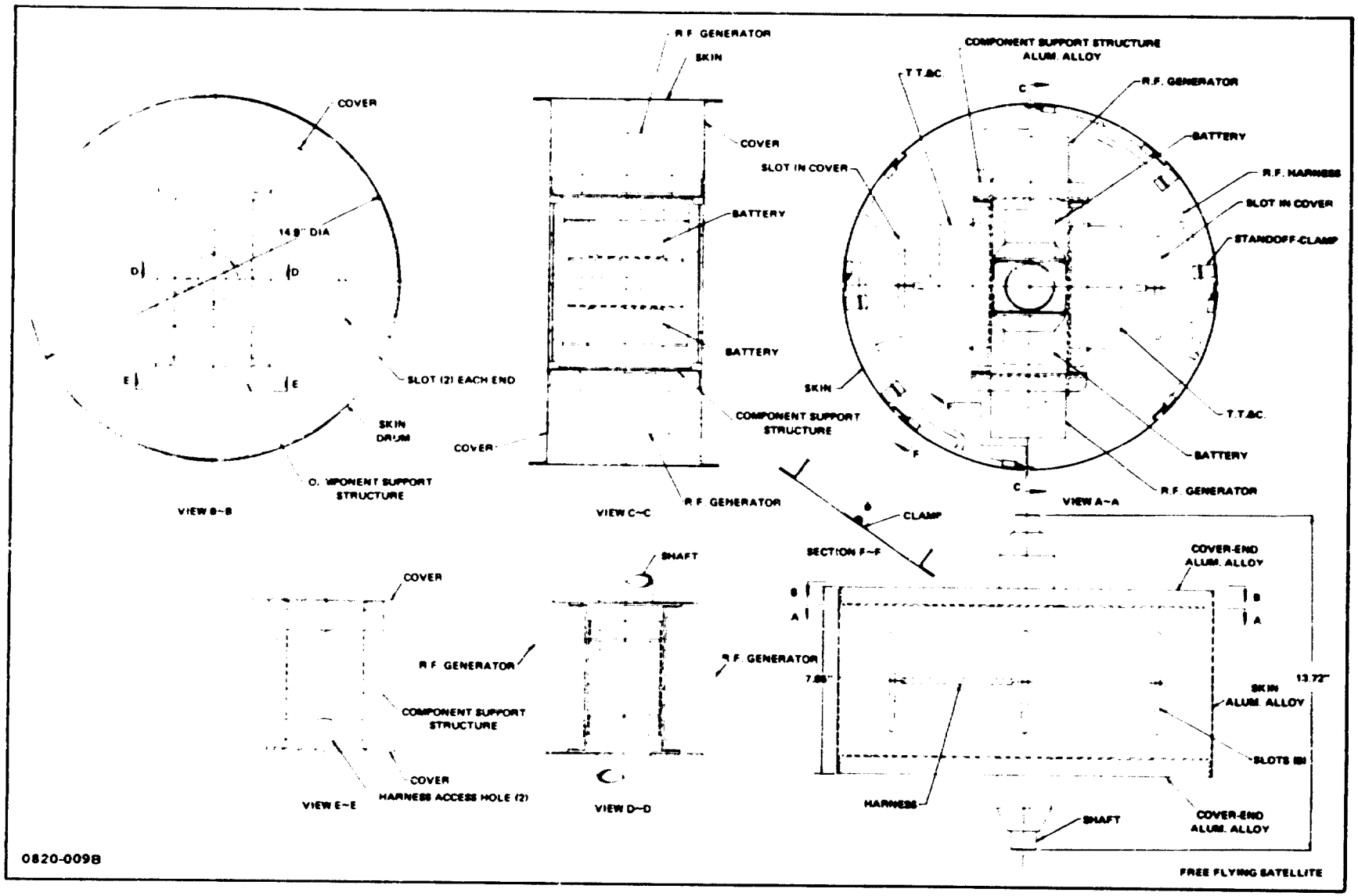

Fig. 3-83 Subsatellite Design

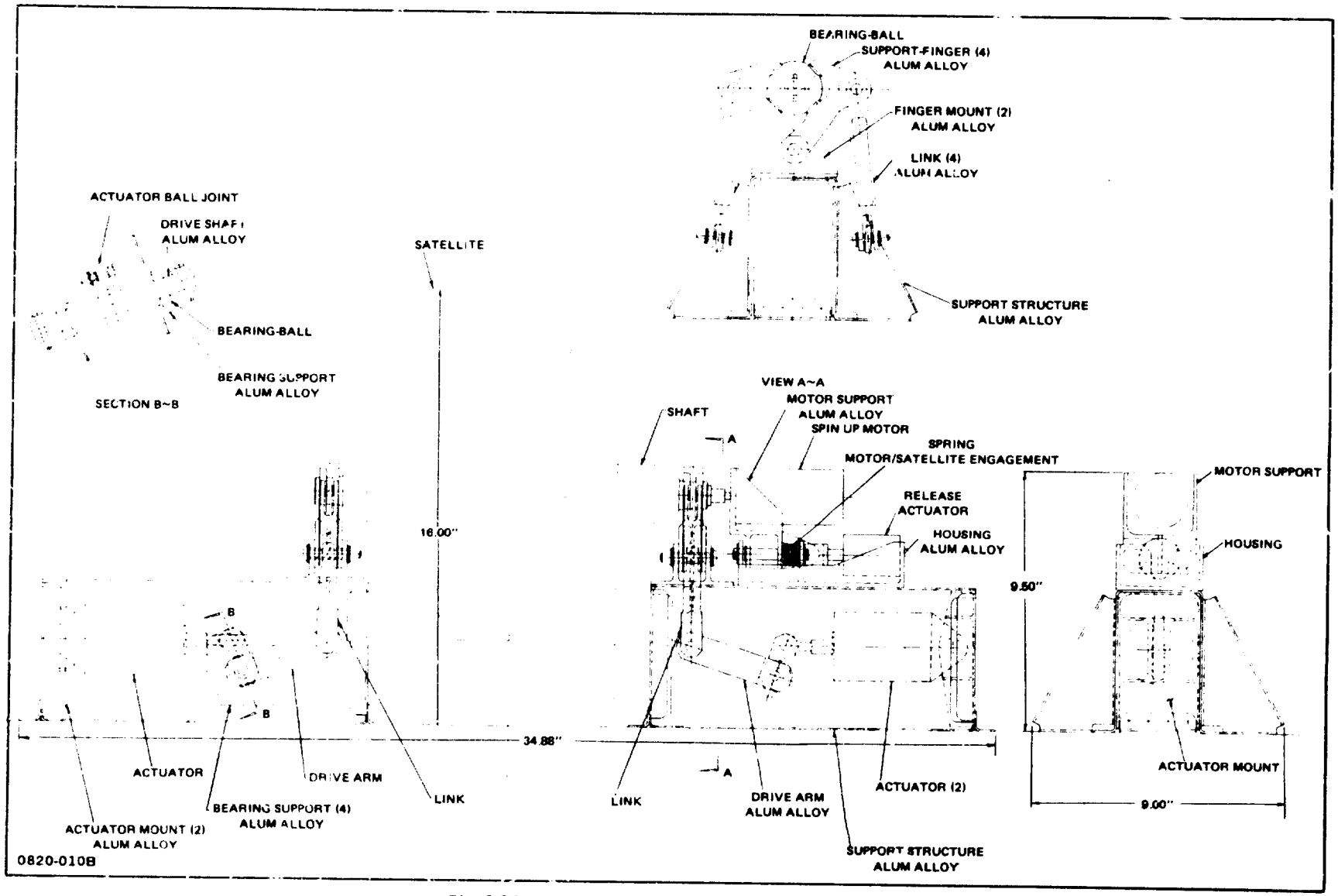

Fig. 3-84 Subsatellite Support & Release Mechanism

- Capabilities
  - The antenna shipping container is capable of providing suitable protection from mechanical damage and foreign particle contamination for the antenna while mounted on the handling dolly.
  - The shipping container is a two-part enclosure consisting of a base section, formed by the handling dolly with casters removed, and a cover section. The complete container will be approximately 40 feet long, 8 feet wide, and 8 feet high. It will incorporate hoisting and tie-down points, provisions for attachment of instrumentation, and provisions for incorporating a nitrogen purge system.
  - The cover will consist of an aluminum welded frame enclosed with armorply panels, which will in turn bolt to the base section.
- Usage
  - Transportation between factory and test or launch sites
  - Storage at factory, test, or launch sites.

3.6.1.2 Antenna Handling Dolly

- Requirements
  - Support antenna in horizontal attitude by means of fore-and-aft fittings during final assembly and integration
  - Provide means to safely move antenna within a manufacturing plant or test facility
  - Provide pivot points for rotation of antenna to vertical attitude for checkout and test.
- Capabilities
  - The antenna handling dolly will consist of a structural metal frame approximately 40 feet long and 7-1/2 feet wide. Shock mounted casters, removable for shipping, will be secured to mounting flanges on the dolly frame to enable local movement of dolly.
  - Support points will be provided for the antenna, with the rear supports acting as pivot points for rotation of the antenna to the vertical position. Locking devices will hold the antenna in either the horizontal or vertical attitude
  - An armorply (plywood faced with aluminum) deck will be placed over the dolly frame to provide walking room adjacent to the antenna. This will also enable the dolly to serve as the base of the shipping container during the transportation mode.

- Usage
  - Assembly fixture during factory final assembly and integration
  - Dolly for intra-plant movement of antenna between various work and test areas
  - Test fixture during final checkout and test in either horizontal or vertical attitudes
  - Base of shipping container during transportation of antenna to test or launch sites.

3.6.1.3 Transporter Pressurization Unit

- Requirements
  - Supply dry gaseous nitrogen to the shipping container to preclude entry of particulate contamination and to control humidity levels
  - Maintain pressure of 3 inches of water nominal in container
  - Provide sufficient storage of nitrogen for a 30-day supply
  - Provide means of controlling and monitoring container pressure.
- Capabilities
  - The transporter pressurization unit is lightweight, frame and panel construction, designed to be mounted to the shipping container. The unit contains the necessary cylinders, regulators, filters, valves, monitoring, warning, and safety devices to ensure an uninterrupted flow of dry gaseous nitrogen to the unit. The unit may be recharged from an external nitrogen supply. The nitrogen supply will be routed via hoses to the environmental cover. It will bleed from these to the hard container and thence to atmosphere.
- Usage
  - The pressurization unit will be used during transportation of the antenna and during storage periods in an uncontrolled environment.

3.6.1.4 Environmental Cover

- Requirements
  - Provide suitable protection for the antenna from particulate contamination and excessive humidity during transportation and storage periods.
- Capabilities
  - The cover will consist of a soft fiberglass reinforced vinyl material, fabricated to fit around the outer contours of the antenna. It will be made in two sections which will lock together by means of interlocking plastic "zippers." Sealable openings will be provided at the antenna support joints and at inlet and outlet purge ports.

- Usage
  - The environmental cover will be used during the transportation mode and during long term storage periods. It also may be used during local movement in non-clear or high humidity areas.

3.6.1.5 Portable Work Stands

- Requirements
  - Provide complete access to all areas of the antenna while installed in the antenna dolly. Access is required for the installation and checkout of subsystems and components.
- Capabilities
  - The work stand will consist of commercially available tubular scaffolding materials, joined together to form a custom designed work platform which provides maximum accessibility to the antenna. Wide work areas, convenient stair locations and wrap around design facilitate operations. Other features include hand rails, kick plates, and bumpers of soft material to protect personnel and equipment.
- Usage
  - The work stand will be used to provide access to the antenna during installation and check-out of components and subassemblies at the factory, at test sites, and at the launch site.

3.6.1.6 Antenna Sling Set

- Requirements
  - Assist in lifting deployable antenna assembly, using conventional overhead hoists, for installation/removal from the work stand, dolly, shipping container, CITE, test fixture, or shuttle payload cannister
  - Install/remove flight support structure in factory, from shipping container, CITE, or shuttle payload cannister
  - Hoist fully loaded shipping container.

- Capabilities
  - The sling set will consist of a tee-shaped spreader bar, steel cables, and hoist fittings for attachment of cables to antenna or major sub-assemblies. Suitable shackles and lifting rings will also be included in the sling set. Provisions will be made on the spreader bar for multiple pickup point capability to be compatible with a variable center of gravity of the antenna assembly and sub-assemblies
  - A sling to hoist a fully loaded shipping container onto truck or other transportation vehicle will also be part of this set.
- Usage
  - Hoisting of antenna assembly for removal/installation from work fixtures, dolly, test stands, and shuttle payload cannister
  - Hoisting of flight support structure from work stands, shipping container, and removal/installation in the shuttle payload cannister prior to antenna installation.

3.6.1.7 Transportation Tiedown Set

- Requirements
  - Provide interface between shipping container and "Guppy" aircraft
  - Provide means to secure the shipping container to the transportation vehicle pallet.
- Capabilities
  - The tiedown set will consist of the following items:
    - o An interface structure to adapt the shipping container/dolly assembly to the Guppy pallet
    - o Chain binders, shackles, and fittings to secure the shipping container to the pallet and aircraft.
- Usage
  - The tiedown set will be used during transportation of the deployable antenna.

3.6.2 ELECTRICAL GSE

3.6.2.1 Instrumentation Stimuli Generator

- Requirements
  - Simulate the output signals of all operational sensors and transducers used in the flight article

- Random selection of any analog channel and the application of a precision input to these channels for the purpose of verifying channel accuracy and crosstalk
- Random selection of any discrete channel and the application to these channels of the proper inputs to yield a "one or a zero" for the purpose of verifying discrete channel operation
- Provide a means for manually implementing the operations of the above three requirements.

- Capabilities
  - The instrumentation stimuli generator will be capable of supplying the signal sources, switching facility and the controls functions necessary to implement the testing of the instrumentation system on the flight article. This stimuli generator will be housed in a console containing several removable panels.

- Usage
  - Factory check-out of the instrumentation subsystem
  - Pre-launch check-out of the instrumentation subsystem.

3.6.2.2 Display and Control Panel Used in PSS

- Requirements
  - Provide manual commands to the flight article
  - Display information on the deployment of the antenna, status of the motors, and the relays
  - Provide alarm and status lights for the caution and warning electronic assembly.

- Capabilities
  - The display and control panel located in the payload specialist station (PSS) will be capable of controlling the deployment of the antenna by manual controls which will allow the antenna to deploy at a given rate. A pictorial display will be monitored to evaluate the performance of the antenna as it deploys. There will be a master warning light (light and audible tone) that will indicate a serious malfunction during deployment that requires immediate attention. There will be other status lights that will indicate open or closed positions for a number of functions on the flight article. Additionally, there will be a test mode to check the lighting of all status and warning lights.

- Usage
  - For the horizontal cargo interface test equipment (CITE) check-out at KSC
  - During the shuttle mission operation for antenna deployment.

3.6.2.3 Caution and Warning Electronic Assembly Stimuli Generator

- Requirements
  - Supply stimuli to exercise the caution and warning electronics assembly (C&WEA) in order to checkout its operation after installation in the shuttle vehicle.
- Capabilities
  - The C&SEA stimuli generato. ill be capable of supplying several 0-5 VDC signals to the C&WEA via GSE connectors on the display and control panel. Each 0-5 vdc stimuli signal will be independently adjustable in order to check C&WEA threshold levels, and the capability for external monitoring of each stimulus will be provided. The equipment will consist of a rotary switch for selecting an individual signal path, while toggle switches will be used to connect a signal. The signal will be adjustable by using a potentiometer, and an output jack to a digital voltmeter will monitor any signal line.
- Usage
  - Factory check-out of the display and control panel
  - CITE check-out of the panel at KSC.

3.6.2.4 Sub-Satellite Electronics Test & Maintenance Station

- Requirements
  - Test and troubleshoot the sub-satellite's command receiver and S-band transmitter
  - Supply the necessary RF stimuli to the receiver to obtain an output from the transmitter
  - Display the waveforms of the receiver and transmitter to facilitate periodic maintenance overhaul and calibration.
- Capabilities
  - The test and maintenance station will be capable of energizing, stimulating and monitoring the inputs and outputs of the sub-satellite electronics. In this way, it can be determined that the transmitter is operating within its specified limits. Test and maintenance procedures will be followed in accordance with written instructions. This Test and Maintenance Station will consist of a rack of special and commercial test equipment.

- Usage
  - Factory check-out of the subsatellite electronics
  - Pre-launch check-out of the subsatellite electronics.

3.6.2.5 Electrical Load Simulator

- Requirements
  - Apply loads to the flight article in 50 watt steps with changes up to 1000 watts
  - Make step increases or decreases in any increment that is divisible by 50, at any power level so that the step change and the power level do not exceed 1000 watts
  - Be able to operate to a maximum of 32 volts, and a nominal of 28 volts.
- Capabilities
  - The electrical load simulator will apply loads to the flight article in 50 watts steps with changes up to 1000 watts. When the various loads are applied, the voltage and the current will be remotely monitored. Also, all loads that are applied will be controlled remotely. The electrical load simulator will have the capability of incorporating external inductive and capacitive loads.
- Usage
  - Factory check-out of the flight article
  - Pre-launch checks of the flight article before installation in the shuttle bay.

3.6.2.6 Constant Current Battery Charger

- Requirements
  - The secondary batteries will be received in a dry-uncharged condition. After activation with electrolyte, the batteries must be charged. The constant current battery charger is also required to recharge the secondary batteries when the charge on the batteries is dissipated in tests.
- Capabilities
  - The constant current charger will be capable of simultaneously charging several silver-zinc batteries with a two-stage constant current supply. In the first stage, it will be automatically programmed to furnish 20 amps for about 10 hours. For the second stage, the charge current will be reduced to 5 amps until the battery voltage reaches 32 volts. This unit will consist of a rack containing several identical battery chargers with integral volt-meters and ammeters. A blower will be used to maintain safe operating temperatures for the charges.

- Usage
  - Factory check-out of the flight article
  - Pre-launch checks of the flight article before installation in the shuttle bay.

3.6.2.7 Flight Article Ground Power Supply

- Requirements
  - To supply the flight article with prime power during the ground test program.
- Capabilities
  - The flight article ground power supply will be capable of supplying a regulated dc voltage within an adjustable range. The adjustable output voltage settings will be from 20 to 32 vdc measured at the flight article bus. For the peak steady state power, the power supply will deliver 1000 watts throughout the adjustable voltage range with the output ground isolated. There will be front panel meters for measuring output current, and voltage. In addition, there will be a "Power ON" indicator and a "Blown Fuse" Indicator. The unit will also protect the flight article against over-load and reverse current conditions.
- Usage
  - Factory check-out of the flight article
  - Pre-launch check-out of the flight article.

3.6.2.8 Display and Control Maintenance Test Station

- Requirements
  - Perform maintenance and acceptance testing on the display and control panel used in the payload specialist station (PSS) in the shuttle
  - Test the entire panel and functionally verify its operation.
- Capabilities
  - The display and control (D&C) maintenance test station will be capable of supplying the necessary power and loads to the PSS panel. It will provide stimuli with a given tolerance and accuracy to check the status lights for a number of functions on the flight article. The D&C maintenance test station will isolate a malfunction on the PSS panel to the lowest replaceable level. A simulated signal will be sent to the pictorial display that viewed the deployment of the antenna to verify its correct operation. The master warning light will be exercised to make certain that it lights and an audible tone is heard. In addition, all status and warning lights will be lit to verify their correct operation.

- Usage
  - Factory check-out of PSS Panel
  - Pre-launch check-out before CITE and installation in the shuttle bay.

3.6.2.9 DC Transient Voltage Power Supply

- Requirements
  - Provide a means to introduce into the dc power line of the flight article, ripple, timed transients and steady state variations.
- Capabilities
  - The dc transient supply will provide the ripple, timed transient and steady state output voltage variations. In addition, provisions will be incorporated for monitoring both the steady state and transient power applied to any subsystem under test. The variations that will be applied to a subsystem under test will be specified by the NASA electrical specifications that the flight article is designed to. As an example, the steady state voltage could be varied between 24 to 32 vdc. Also, the transient voltage limit could be plus or minus 100 volts for 10 microseconds at a 10 pps repetition rate for a period of five minutes. The output ripple using MIL-STD-704 would be supplied by two audio oscillator signals, which are added and transformer coupled to the dc output terminals. The transient voltage limits will be transformer coupled to the dc output terminals from a high power pulse generator. Several panels mounted in a roll-about with a rack configuration will consist of the dc transient supply.
- Usage
  - Factory [illegible] of each individual subsystem
  - Electronic integration of the flight article with all the subsystems present.

3.6.2.10 Battery Maintenance Test Station

- Requirements
  - Monitor and record the battery voltage and current output
  - Monitor, record and control the battery charge rate and terminal voltage
  - Control the battery output current by providing resistive loads.

- Capabilities
  - The battery maintenance test station will primarily be manually operated through a series of control switches and indicating lights. It will monitor and record the battery voltage, current and power output from 0 to 32 vdc, 0 to 50 amps dc and 0 to 1000 watts respectively. Also, it will control the battery current output by providing resistive loads so that the power output goes from 0 to 1 kw in 100 watt steps. Independently, it will monitor charge time, discharge time, and total operating time for the batteries. The battery test station will also monitor record, and control the constant current charge rate from 0 to 10 amps dc with an automatic cut-off at a pre-selected voltage from 0 to 32 vdc.
- Usage
  - Factory check-out of the flight article
  - Pre-launch check-out before installation in the shuttle bay.

3.7 REFERENCES AND BIBLIOGRAPHY

3-1 T. Balderes, "Structural Analysis of the 100-m Dia Deployable Antenna", Grumman Aerospace Corporation Memorandum, May 31, 1978.

3-2 F. Austin, G. R. Isakson, "Dynamic Structural Analysis of the 100-m Diameter Deployable Antenna", Grumman Aerospace Corporation Memorandum, August 28, 1978.

3-3 Oman, R. A., "Numerical Calculations of Gas-Surface Interactions", AIAA Journal Vol. 5, No. 7, July 1967, pp. 1280-1287.

3-4 Oman, R. A. and Calia, V. S., "Gas Surface Interaction Research", Grumman Research Department Report RE-365, June 1969.

3-5 National Oceanic and Atmospheric Administration, NASA, and United States Air Force, "U. S. Standard Atmosphere, 1976", October 1976.

3-6 Evans, W. J., "Aerodynamic and Radiation Disturbance Torques on Satellites Having Complex Geometry", J. Astronautical Sci, V. IX, No. IV, Winter 1962.

3-7 Austin, F., "Introduction of Gravity-Gradient and Rotation Into V7", informal notes, October 1978.

3-8 Lowe, E. J., and Austin, F., "A Study of the Dynamics of Rotating Space Stations with Elastically Connected Counterweight and Attached Flexible Appendages," Volume II, Computer Program User's Manual, NASA CR-112244, March 1973.

3-9 J. F. Kauffman, W. F. Croswell and L. J. Powers, "Analysis of the Radiation Patterns of Reflector Antennas", IEEE Trans Antennas and Propagation, January 1976.

3-10 P. K. Agrawal, "A Computer Program to Calculate Radiation Properties of Reflector Antennas", NASA Technical Memorandum 78721, May 1978.

3-11 R. Miezis, "Single Reflector Antenna Radiation Pattern Analysis", SR (E 00021), GSFC, Contract No. NAS5-117222, July 1970.

3-12 R. Miezis, "Dual Reflector Antenna System Radiation Calculation Program", FFD (E 00026), GSFC, Contract No. NAS5-11722, July 1970.

3-13 R. E. Collin and F. J. Zucker, Antenna Theory, Part II, McGraw-Hill 1969.

3-14 M. Born and E. Wolf, Principles of Optics, Fifth Edition, Pergamon Press, 1975.

3-15 A. V. Mrstik, "Scan Limits of Point-Fed Parabolas and Paraboloids, " General Research Corporation, March 1978.

3-16 N. Amitay and H. Zucker, "Compensation of Spherical Reflector Aberrations by Planar Array Feeds", IEEE Trans Antennas and Propagation, Vol AP-20, No. 1, January 1972.

3-17 R. Fletcher and M. J. D Powell, "A Rapidly Convergent Descent Method for Minimization", Computer Journal, Vol 6, No. 2, 1963.

3-18 K. M. Brown, "Derivative Free Analogues of the Levenberg-Marquardt and Gauss Algorithms for Nonlinear Least Squares Approximations", IBM Philadelphia Scientific Center Technical Report, No. 320-2994, 1970.

3-19 Space Shuttle System Payload Accommodations JCS 07700, Volume XIV Revision F.

GRUMMAN AEROSPACE CORPORATION

FAILURE MODE AND EFFECTS ANALYSIS

Check one: ☒ VEHICLE ☐ GSE ☐ TRAINER

Subsystem Equipment | Program | Drawing Number | Prepared By | Approved By | Date | Rev | Page of

ITEM NUMBER	ITEM/PART	FUNCTION	FAILURE MODE	MISSION OR OPERATIONAL PHASE	FAILURE EFFECT	FAILURE DETECTION	REDUNDANCY OR COMPENSATING PROVISIONS	CRITICALITY
1	STAY REEL MOTOR (UPPER OR LOWER)	PROVIDES POWER TO DRIVE STAY REEL	A) NO OUTPUT OR BINDING	ALL	DURING DEPLOYMENT OR RETRACTION THE LOSS OF OUTPUT FROM ONE OF THE TWO REDUNDANT MOTORS WILL NOT AFFECT ANTENNA OPERATION SINCE EITHER MOTOR CAN DRIVE THE STAY REEL. FAILED MOTOR IS DE CLUTCHED AND CLUTCH IS ENGAGED WITH OPERABLE MOTOR	NO STAY REEL DISPLACEMENT	• REDUNDANT STAY REEL MOTORS FOR DEPLOYMENT AND EXTENSION	V
			B) SHORTED MOTOR	ALL	EACH REDUNDANT STAY REEL MOTOR IS INDIVIDUALLY FUSED TO ISOLATE SHORT TO AFFECTED MOTOR. SAME AS CASE NO. 1 A	NO STAY REEL DISPLACEMENT	• INDIVIDUALLY FUSED STAY REEL MOTORS AND CLUTCHES	V
2	STAY REEL CLUTCH (UPPER OR LOWER)	ENGAGES AND DISENGAGES MOTOR POWER TO STAY REEL	A) FAILS TO ENGAGE	ALL	DURING DEPLOYMENT OR RETRACTION FAILURE TO ENGAGE ONE OF THE TWO CLUTCHES WILL NOT AFFECT ANTENNA OPERATION SINCE EITHER CLUTCH ENGAGEMENT WILL PERMIT ONE OF THE REDUNDANT MOTORS TO DRIVE THE STAY REEL	NO STAY REEL DISPLACEMENT	• REDUNDANT STAY REEL MOTORS AND CLUTCHES	V
			B) FAILS TO DISENGAGE	ALL	DURING DEPLOYMENT OR RETRACTION IF A MOTOR FAILS AND ASSOCIATED CLUTCH DOES NOT DISENGAGE THIS CAUSES THE OPERATIVE MOTOR TO DRIVE THRU STAY REEL GEAR AND THRU THE FAILED MOTOR WHICH COULD CAUSE THE "GOOD" MOTOR TO STALL. THIS WOULD RESULT IN THE INABILITY TO EXTEND OR RETRACT THE ANTENNA SINCE THE STAY LINE REMAINS FIXED. THIS IS A DOUBLE FAILURE CONDITION (MOTOR AND ASSOCIATED CLUTCH) WHICH IS REMOTE SINCE CLUTCH IS DESIGNED FAIL SAFE OPEN, I.E. ENERGIZED CLOSED AND SPRING LOADED OPEN WHEN DE ENERGIZED	NO STAY REEL DISPLACEMENT	• CLUTCH DESIGNED FAIL SAFE OPEN • CLUTCH DISENGAGEMENT REQUIRED ONLY IN THE EVENT MOTOR FAILURE	I
			C) SHORTED CLUTCH	ALL	EACH CLUTCH IS INDIVIDUALLY FUSED TO ISOLATE SHORT TO AFFECT CLUTCH SAME AS CASE NO. 2 A	NO STAY REEL DISPLACEMENT	• SAME AS CASE NO. 1 B	V
3	STAY REEL LINES (UPPER OR LOWER)	PERMITS REEL DISPLACEMENT TO EXTEND OR RETRACT STAYS	BINDING	ALL	INABILITY TO EXTEND OR RETRACT THE ANTENNA SINCE STAY LINE REMAINS FIXED IN LENGTH	NO STAY REEL DISPLACEMENT	• NONE	I
4	STAY REEL LINES (UPPER OR LOWER)	CONTROLS ANTENNA DEPLOYMENT BY RESTRAINING RIM MODE DISPLACEMENT VIA REEL ROTATION	DISLODGEMENT DUE TO EITHER LINE BREAKAGE OR DETACHED HARDWARE	LAUNCH	NONE SINCE DRUM LOCK PINS WILL PREVENT PREMATURE ANTENNA DEPLOYMENT IN SHUTTLE BAY	NONE	• DRUM LOCK PINS WILL PREVENTS DEPLOYMENT IN SHUTTLE BAY	V
				DEPLOYMENT OPERATION & RETRACTION	ASSOCIATED RIM MODE IS NOT RESTRAINED BY STAY. EDGE STRIPS ON GORE WILL PREVENT RIPPING OF GORE MATERIAL. A LOOSE STAY REEL LINE COULD CAUSE BINDING OF REEL DRIVE MECHANISM IF THE LINE MIGRATES NEAR THE GEARS.	NONE	• EDGE STRIPS DESIGNED TO WITH STAND LOAD OF STAY (APPROX 5 POUNDS)	I

Fig. 3-85 Deployable Antenna Failure Mode and Effects Analysis (Sheet 1 of 9)

GRUMMAN AEROSPACE CORPORATION

FAILURE MODE AND EFFECTS ANALYSIS

SYSTEM EQUIPMENT ☒ VEHICLE ☐ GSE ☐ TRAINER

ITEM NUMBER	ITEM/PART	FUNCTION	FAILURE MODE	MISSION OR OPERATIONAL PHASE	FAILURE EFFECT	FAILURE DETECTION	REDUNDANCY OR COMPENSATIONS PROVISIONS	CRITICALITY
					CLUTCHES OR MOTOR IN ADDITION AN UNATTACHED LINE CAN INTERTWINE WITH ATTACHED LINES AND CAUSE IMPROPER DEPLOYMENT OR RETRACTION			
5	STAY REEL PULLEY (2) (UPPER AND LOWER)	PROVIDES A GUIDE FOR STAY REEL LINES DURING DEPLOYMENT OR RETRACTION	BINDING	ALL	DURING DEPLOYMENT OR RETRACTION BINDING WILL CAUSE AN INCREASE IN THE FRICTION FORCE ON THE ASSOCIATED STAY REEL LINE. THIS WILL CAUSE A SLIGHT RETARDATION OF THE ASSOCIATED RIM NODE. HOWEVER ANTENNA EXTENSION AND RETRACTION WILL BE NORMAL	NONE	• SPRING FORCE AT RIM NODES AND STAY REEL MOTOR ARE SIZED TO OVERCOME PULLEY AND BEARING FRICTION IN THE EVENT OF BINDING DUE TO FAILURE OF ANY ONE COMPONENT	V
6	STAY REEL BEARINGS (UPPER AND LOWER)	PROVIDES ROLLING SURFACE FOR STAY REEL & LOAD PATH DURING LAUNCH	BINDING	ALL	DURING DEPLOYMENT OR RETRACTION A BINDING OF THE BEARING WILL INCREASE THE FRICTION FORCE ON THE STAY REEL BOTH ANTENNA RETRACTION AND EXTENSION WILL TAKE LONGER HOWEVER NO OTHER DEGRADATION WILL OCCUR	NONE	• SAME AS ABOVE	V
7	NODE EXTENSION CABLE	TRANSMIT STORED SPRING ENERGY TO ERECT RIM STRUCTURE ACROSS RIM NODE	DISLODGEMENT DUE TO EITHER LINE BREAKAGE OR DETACHED HARDWARE	LAUNCH	NONE	NONE	• NONE	V
				DEPLOYMENT	LOSS OF EXTENSION LOAD AT ONE RIM NODE. ANTENNA WILL EXTEND BY VIRTUE OF THE EXTENSION FORCES ON THE ADJACENT NODES	NONE	• ANTENNA CAN BE DEPLOYED, RETRACTED & HELD FIXED WITH THE LOSS OF ONE NODE EXTENSION CABLE OR SPRING	V
				OPERATIONAL	LOSS OF EXTENSION LOAD AT ONE RIM NODE ADJACENT NODE FORCES WILL MAINTAIN ANTENNA GEOMETRY	NONE	• SAME AS ABOVE	V
				RETRACTION	LOSS OF EXTENSION LOAD AT ONE RIM NODE, ANTENNA WILL RETRACT NORMALLY SINCE ALL STAY DISPLACEMENTS ARE THE SAME	NONE	• SAME AS ABOVE	V
8	NODE EXTENSION SPRING	STORE ENERGY TO ERECT ANTENNA ACROSS RIM NODE	LOSS OF SPRING FORCE DUE TO EITHER A BROKEN SPRING OR DETACHED HARDWARE	ALL	SAME AS CASE NO. 7 ABOVE			V
9	NODE EQUALIZATION CABLE	ASSURES EQUAL DISPLACEMENT OF ADJACENT RIM TUBES DURING DEPLOYMENT AND RETRACTION	DISLODGEMENT DUE TO EITHER CABLE BREAKAGE OR DETACHED HARDWARE	ALL	IN THE EVENT THAT THE RIM TUBE ROTATION JOINT FRICTION IS UNEQUAL ON OPPOSITE SIDES OF THE NODE, THE RIM TUBE ANGULAR DISPLACEMENT COULD ALSO DIFFER DURING DEPLOYMENT OR RETRACTION THE DISPLACEMENT DIFFERENCE IS LIMITED BY THE ADJACENT NODE GEOMETRY AND THEREFORE WILL NOT AFFECT ANTENNA DEPLOYMENT AND RETRACTION	NONE	• DEPLOYMENT & RETRACTION OF ANTENNA WILL NOT BE ADVERSELY AFFECTED BY LOSS OF A SINGLE EQUALIZATION CABLE	V

Fig. 3-85 Deployable Antenna Failure Mode and Effects Analysis (Sheet 2 of 9)

GRUMMAN AEROSPACE CORPORATION

FAILURE MODE AND EFFECTS ANALYSIS

Check one: ☒ VEHICLE ☐ GSE ☐ TRAINER

SUBSYSTEM/EQUIPMENT	PROGRAM	DRAWING NUMBER	PREPARED BY	APPROVED BY	DATE	REV.	PAGE OF

CASE NUMBER	ITEM/PART	FUNCTION	FAILURE MODE	MISSION OR CHECKOUT PHASE	FAILURE EFFECT	FAILURE DETECTION	REDUNDANCY OR COMPENSATING PROVISIONS	CRITICALITY
10	NODE PIVOT JOINT	PROVIDES JOINT CONTINUITY & COLLAPSIBILITY FOR RIM TUBE STRUCTURE	A) DISLODGEMENT DUE TO ATTACHMENT HARDWARE	ALL	LOSS OF JOINT CONTINUITY FOR RIM TUBE STRUCTURE. ANTENNA WILL NOT DEPLOY TO PROPER GEOMETRY. ATTACHMENT HARDWARE USES SELF LOCKING NUTS TO MINIMIZE PROBABILITY OF FAILURE.	ANTENNA PERFORMANCE	• SELF LOCKING NUTS MINIMIZE POSSIBILITY OF DISLODGEMENT.	V
			B) BINDING	ALL	BINDING OF ANY ONE OF 32 NODE PIVOT JOINTS COULD CAUSE THE FAILURE OF THE ANTENNA TO DEPLOY OR RETRACT	ANTENNA FAILS TO DEPLOY	• NONE	I
11	GORE TENSION SPRINGS (UPPER OR LOWER)	MAINTAIN EXTERIOR GORE SURFACE TAUT TO COMPENSATE FOR THERMAL EXPANSION DURING VARIOUS ANTENNA OPERATIONAL MODES (EARTH SHADOW AND SUN NORMAL)	LOSS OF SPRING FORCE DUE TO EITHER A BROKEN SPRING OR DETACHMENT HARDWARE	ALL	DURING DEPLOYMENT, OPERATION, OR RETRACTION THE LOSS OF ANY ONE OF THE FOUR GORE TENSION SPRINGS OR LINES WILL NOT AFFECT ANTENNA PERFORMANCE. GORE EXTERIOR SURFACE WILL REMAIN TAUT DURING VARIOUS TEMPERATURE CONDITIONS DUE TO TENSION EXERTED BY REMAINING THREE LINES ON THE GORE SPREADER.	NONE	• REDUNDANT GORE TENSION SPRINGS/LINES • SYSTEM GAIN IS BASED ON POSSIBLE LOSS OF ONE OF 32 GORES	V
12	GORE TENSION LINES (UPPER OR LOWER)	TRANSMIT SPRING TENSION TO GORE SPREADER TO MAINTAIN GORE EXTERIOR SURFACE TAUT DURING VARIOUS TEMPERATURE EXTREMES	DISLODGEMENT DUE TO EITHER LINE BREAKAGE OR DETACHMENT HARDWARE	ALL	SAME AS ABOVE	NONE	• SAME AS ABOVE	V
13	GROUND PLANE SPRINGS	MAINTAIN INTERIOR GORE SURFACE TAUT DURING VARIOUS TEMPERATURE EXTREMES BY SPRING TENSION	LOSS OF SPRING FORCE DUE TO EITHER A BROKEN SPRING OR ATTACHMENT HARDWARE	ALL	DURING DEPLOYMENT, OPERATION, OR RETRACTION THE LOSS OF ONE OF THE TWO GROUND PLANE SPRINGS OR LINES WILL CAUSE THE INTERIOR GORE SURFACE TO DISPLACE SLIGHTLY. THIS WILL NOT DEGRADE ANTENNA PERFORMANCE	NONE	• REDUNDANT GROUND PLANE SPRINGS/LINES • SYS GAIN IS BASED ON POSSIBLE LOSS OF ONE OF 32 GORES	V
14	GROUND PLANE LINES	TRANSMIT SPRING TENSION TO MAINTAIN INTERIOR GORE SURFACE TAUT DURING VARIOUS TEMPERATURES	DISLODGEMENT DUE TO EITHER LINE BREAKAGE OR DETACHMENT HARDWARE.	ALL	SAME AS ABOVE	NONE	• SAME AS ABOVE	V
15	GORE SPREADER	ROTATES GORE ATTACHMENT TO DRUM THRU 90° AFTER GORES ARE UNFURLED FROM DRUM	BINDING	LAUNCH	NONE	NONE	• NONE	V
				DEPLOYMENT	BINDING OF ANY ONE OF 32 GORE SPREADERS OR LINKAGES WILL PREVENT 90° ROTATION OF GORE ATTACHMENT TO DRUM. GORE PLANE WILL BE TWISTED CAUSING MAJOR DEGRADATION OF ANTENNA PERFORMANCE. DESIGN INCORPORATES REDUNDANT ROTATION BUSHINGS WHICH PREVENTS THE POSSIBILITY OF BINDING	ANTENNA PERFORMANCE	• REDUNDANT ROTATION BUSHINGS	
				OPERATION	NONE DURING THIS PHASE	NONE	• NONE	V

GAC 3701 REV. D 8-76

Fig. 3-85 Deployable Antenna Failure Mode and Effects Analysis (Sheet 3 of 9)

GRUMMAN AEROSPACE CORPORATION

FAILURE MODE AND EFFECTS ANALYSIS

Check one: ☒ VEHICLE ☐ GSE ☐ TRAINER

SUBSYSTEM/EQUIPMENT	PROGRAM	DRAWING NUMBER	PREPARED BY	APPROVED BY	DATE	REV.	PAGE OF

CASE NUMBER	ITEM/PART	FUNCTION	FAILURE MODE	MISSION OR CHECKOUT PHASE	FAILURE EFFECT	FAILURE DETECTION	REDUNDANCY OR COMPENSATING PROVISIONS	CRITICALITY
				RETRACTION	BINDING OF ANY ONE OF 32 GORE SPREADERS OR LINKAGES WILL PREVENT 90° ROTATION OF DRUM GORE ATTACHMENTS. THIS WOULD PREVENT THE PROPER FURLING OF THE GORES ON THE DRUM. ALTHOUGH THE ANTENNA COULD PROBABLY BE RETRACTED, ALL THE GORES WOULD BE RUINED IN THE PROCESS. DESIGN INCORPORATES REDUNDANT ROTATION BUSHINGS WHICH PREVENTS THE POSSIBILITY OF BINDING.	NONE	• REDUNDANT ROTATION BUSHINGS	V
16	GORE SPREADER LINKAGE	TRANSMITS MOTOR POWER TO GORE SPREADERS	A) BINDING OF ANY LINKAGE	ALL	SAME AS CASE NO. 15 EXCEPT NO REDUNDANT BUSHINGS	SAME AS CASE NO. 15	• NONE	I
			B) DISLODGEMENT OF ANY LINKAGE EXCEPT INPUT, SLAVE, OR DRIVE CRANK LINKS	ALL	DURING DEPLOYMENT OR RETRACTION GORE SPREADER CAN ROTATE NORMALLY IN THE EVENT OF A SINGLE LINK DISCONTINUITY. LINKAGE FORMS A LOOP WITH DUAL UNIVERSAL JOINTS ON THE DRIVE CRANK. INPUT TO EITHER DRIVE CRANK UNIVERSAL JOINT ASSURES ROTATION OF GORE SPREADER	NONE	• DUAL UNIVERSAL INPUT JOINTS TO CRANK PERMITS DISCONTINUITY OF ONE LINKAGE • SYS GAIN IS BASED ON POSSIBLE LOSS OF ONE OF 32 GORES.	V
17	GORE SPREADER DRIVE MOTOR	PROVIDES POWER TO DRIVE GORE SPREADERS	A) NO OUTPUT	ALL	DURING DEPLOYMENT OR RETRACTION THE LOSS OF OUTPUT OF ONE MOTOR WILL HAVE NO EFFECT SINCE A STAND BY REDUNDANT MOTOR CAN BE ACTIVATED.	NO ROTATION OF GORE-DRUM ATTACHMENTS	• STANDBY REDUNDANT GORE SPREADER MOTORS	V
			B) SHORTED MOTOR	ALL	EACH REDUNDANT GORE SPREADER MOTOR IS INDIVIDUALLY FUSED TO ISOLATE SHORT TO AFFECTED MOTOR SAME AS CASE NO. 17 A	NO ROTATION OF GORE-DRUM ATTACHMENTS	• INDIVIDUALLY FUSED GORE SPREADER MOTORS	V
			C) BINDING	ALL	SAME AS CASE NO 15 EXCEPT NO REDUNDANT BUSHINGS	SAME AS CASE NO. 15	• NONE	I
18	DRUM MOTOR (UPPER ONLY)	PROVIDES POWER TO RESTRAIN DRUM ROTATION DURING ANTENNA DEPLOYMENT TO MAINTAIN GORES TAUT. DURING ANTENNA RETRACTION MOTOR DRIVES DRUM TO FURL GORES	A) NO OUTPUT	ALL	DURING DEPLOYMENT OR RETRACTION THE LOSS OF OUTPUT FROM ONE OF TWO REDUNDANT MOTORS WILL NOT AFFECT THE UNFURLING/FURLING OF GORES AROUND THE DRUM.	NONE	• REDUNDANT DRUM MOTORS FOR DEPLOYMENT AND EXTENSION	V
			B) SHORTED MOTOR	ALL	EACH REDUNDANT DRUM MOTOR IS INDIVIDUALLY FUSED TO ISOLATE SHORT TO AFFECTED MOTOR. SAME AS CASE NO. 18 A	NONE	• INDIVIDUALLY FUSED DRUM MOTORS	V
			C) BINDING	ALL	INABILITY TO EXTEND ANTENNA SINCE DRUM WILL NOT ROTATE RELATIVE TO MAST SUPPORT STRUCTURE PREVENTING UNFURLING OF GORES. THIS RESTRAINS MOVEMENT OF RIM TUBES IF FAILURE OCCURS AFTER DEPLOYMENT, ANTENNA RETRACTION WOULD RESULT IN DEMOLISHMENT OF ALL	NONE	• NONE	I

GAC 2707 REV. B 9-76

Fig. 3-85 Deployable Antenna Failure Mode and Effects Analysis (Sheet 4 of 9)

GRUMMAN AEROSPACE CORPORATION

FAILURE MODE AND EFFECTS ANALYSIS

Check one: ☒ VEHICLE ☐ GSE ☐ TRAINER

SUBSYSTEM/EQUIPMENT | PROGRAM | DRAWING NUMBER | PREPARED BY | APPROVED BY | DATE | REV | PAGE OF

CASE NUMBER	ITEM/PART	FUNCTION	FAILURE MODE	MISSION OR CHECKOUT PHASE	FAILURE EFFECT	FAILURE DETECTION	REDUNDANCY OR COMPENSATING PROVISIONS	CRITICALITY
					GORES AND WOULD NECESSITATE SEPARATION OF THE ANTENNA FROM THE SHUTTLE			
19	DRUM RING GEAR & MOTOR INPUT GEARS	TRANSMITS MOTOR POWER TO RESTRAIN DRUM ROTATION DURING ANTENNA DEPLOYMENT. DURING RETRACTION DRIVES DRUM TO UNFURL GORES	BINDING	ALL	SAME AS CASE NO. 18 C	NONE	• NONE	I
20	DRUM BEARINGS (UPPER OR LOWER)	PROVIDES ROLLING SURFACE FOR DRUM & LOAD PATH DURING LAUNCH	BINDING	ALL	DURING ANTENNA DEPLOYMENT BINDING OF A SINGLE BEARING WILL INCREASE THE FRICTION FORCE WHICH WILL INCREASE THE TENSION IN THE GORES WITHIN ACCEPTABLE LIMITS. DURING RETRACTION THE INCREASED FICTION ACTS COUNTER TO THE DRUM ROTATION, WITH BOTH MOTORS OPERATING ANTENNA RETRACTION WILL BE NORMAL	NONE	• GORES DESIGNED TO WITHSTAND TORQUING OF BOTH DRUM MOTOR AND A SINGLE DRUM BEARING BINDING DURING DEPLOYMENT • DRUM DRIVE DESIGNED TO OPERATE WITH A SINGLE BEARING BINDING WITH BOTH MOTORS OPERATING DURING RETRACTION	V
21	DRUM LOCK PIN MOTOR (UPPER OR LOWER)	PREVENTS MOVEMENT OF DRUM RELATIVE TO MAST STRUCTURE	A) INADVERTEANTLY ACTUATES CAUSING PIN TO WITHDRAW	ALL	DURING LAUNCH/LANDING IF ONE PIN IS INADVERTENTLY RETRACTED THE REMAINING THREE PINS CAN SUSTAIN LAUNCH/LANDING LOADS	NONE	• 3 OF 4 PINS REQUIRED FOR LAUNCH LOADS • REDUNDANT POWER & ELEC MOTOR CIRCUITS	V
			B) FAILS TO WITHDRAW PIN	ALL	UNABLE TO DEPLOY ANTENNA SINCE DRUM CAN NOT ROTATE TO UNFURL GORES. FAILURE MODE IS MINIMIZED SINCE MOTOR HAS REDUNDANT LEADS & CIRCUITS	• NO ANTENNA DEPLOYMENT • PIN POSITION INDICATORS	• REDUNDANT ELEC CIRCUITS & LEADS	I
			C) FAILS TO INSERT PIN	ALL	AFTER ANTENNA MISSION IS COMPLETED & DRUM WAS ROTATED TO FURL GORES, DRUM LOCK CANNOT BE ACTUATED TO PREVENT DRUM ROTATION DURING LANDING. THIS COULD RESULT IN DAMAGE TO THE GORES	• PIN POSITION INDICATORS	• NONE	IV
22	ERECT/STOW PIN MOTORS	PINS TRANSMIT ANTENNA LAUNCH LOADS TO SHUTTLE STRUCTURE MOTORS WITHDRAW PINS SO THAT SHUTTLE MANIPULATOR CAN ROTATE ANTENNA OUT OF PAYLOAD BAY	A) INADVERTENTLY ACTUATES, CAUSING PIN TO WITHDRAW	ALL	PREMATURE MOTOR ACTUATION IS PREVENTED BY REDUNDANCY IN THE ELECTRICAL POWER CIRCUITS REQUIRING MORE THAN ONE FAILURE	NONE	• REDUNDANCY IN ELECTRICAL POWER CIRCUITS	V
			B) FAILS TO WITHDRAW PIN	ALL	UNABLE TO ROTATE ANTENNA OUT OF PAYLOAD BAY IF PINS CANNOT BE RETRACTED. FAILURE MODE IS MINIMIZED SINCE MOTOR WILL HAVE REDUNDANT ELEC LEADS & CIRCUITS	• NO ANTENNA ROTATION • PIN POSITION INDICATORS	• REDUNDANT ELECT LEADS AND CIRCUITS	I

Fig. 3-85 Deployable Antenna Failure Mode and Effects Analysis (Sheet 5 of 9)

GRUMMAN AEROSPACE CORPORATION

FAILURE MODE AND EFFECTS ANALYSIS

Check one: ☒ VEHICLE ☐ GSE ☐ TRAINER

SUBSYSTEM/EQUIPMENT | PROGRAM | DRAWING NUMBER | PREPARED BY | APPROVED BY | DATE | REV | PAGE OF

CASE NUMBER	ITEM/PART	FUNCTION	FAILURE MODE	MISSION OR CRITICAL PHASE	FAILURE EFFECT	FAILURE DETECTION	REDUNDANCY OR COMPENSATIONS PROVISIONS	CRITICALITY
			C) FAILS TO RE-INSERT PIN	ALL	THE INABILITY TO RE-INSERT A PIN WILL ELIMINATE A LOAD PATH DURING LAUNCH AND LANDING. IF THIS FAILURE OCCURS AFTER ANTENNA EXTENSION, THE ANTENNA WILL HAVE TO BE SEPARATED FROM THE SHUTTLE AND LEFT IN SPACE	PIN POSITION INDICATORS	• REDUNDANT ELEC LEADS AND CIRCUITS • CAPABILITY TO SEPARATE ANTENNA FROM SHUTTLE	II
23	ERECT/STOW PIN GEARS	TRANSMITS MOTOR POWER TO ERECT/STOW MOTORS	BINDING	ALL	SAME AS CASE NO. 22 B & 22 C	PIN POSITION INDICATORS	• NONE	I
24	MAST EXTENSION FLANGE MOTORS	FLANGE PROVIDES LOAD PATH DURING LAUNCH & LANDING ACROSS PIVOT STRUCTURE & MAST CANISTER. FLANGE MOTOR/GEAR ACTUATES OVER-CENTER FLANGE ATTACHMENTS	A) INADVERTENTLY ACTUATES	ALL	SAME AS CASE NO. 22 A	FLANGE TELEMETRY	• REDUNDANCY IN ELECT POWER CIRCUITS	V
			B) FAILS TO OPEN FLANGE LATCH	ALL	FLANGE CANNOT BE SEPARATED THEREFORE, ANTENNA CANNOT BE DEPLOYED RESULTING IN A MISSION FAILURE	FLANGE TELEMETRY	• SAME AS ABOVE	I
			C) FAILS TO CLOSE FLANGE LATCH	ALL	SAME AS CASE NO. 22 C	FLANGE TELEMETRY	• SAME AS CASE 22 C	II
25	MAST EXTENSION FLANGE GEAR	SAME AS ABOVE	BINDING	ALL	SAME AS CASE NO. 22 B & 22 C	FLANGE TELEMETRY	• NONE	I
26	MAST EXTENSION DRIVE MOTOR	PROVIDES POWER TO DRIVE MAST DURING EXTENSION & RETRACTION	A) BINDING	ALL	UNABLE TO EXTEND MAST OF ANTENNA SINCE MOTOR CANNOT TURN ROTATABLE NUT.	MAST DOES NOT MOVE	• NONE	I
			B) NO OUTPUT OR SHORTED	ALL	EACH MOTOR IS INDIVIDUALLY FUSED TO ISOLATE SHORT TO AFFECTED MOTOR. A SINGLE MOTOR FAILURE (NO OUTPUT OR SHORT) WILL NOT PREVENT MAST EXTENSION OR RETRACTION.	NONE	• REDUNDANT MAST EXTENSION MOTORS	V
27	MAST EXTENSION ROTATABLE NUT	NUT ROTATES TO PERMIT EXTENSION OR RETRACTION OF MAST	A) BINDING	ALL	SAME AS CASE NO. 26 A	UNABLE TO MOVE MAST	• NONE	I
28	ANTENNA SEPARATION	PERMITS SEPARATION OF ANTENNA STRUCTURE FROM SHUTTLE IN THE EVENT THE ANTENNA CANNOT BE PROPERLY STOWED IN SHUTTLE BAY	A) FAILS TO SEPARATE	ALL	THIS IS A DOUBLE FAILURE MODE CONDITION I.E., ANTENNA DOES RETRACT OR SEPARATE. THIS COULD CAUSE A SAFETY HAZARD TO SHUTTLE CREW REQUIRING A RESCUE MISSION IF ANTENNA CAN NOT PHYSICALLY SEPARATE FROM SHUTTLE. SEPARATION SYSTEM UTILIZES PIN PULLERS WITH REDUNDANT ELEC LEADS & CIRCUITS.	UNABLE TO SEPARATE ANTENNA FROM SHUTTLE	• REQD ONLY IF ANTENNA DOES NOT RETRACT PROPERLY • PIN PULLERS USE REDUNDANT ELEC LEADS & CIRCUITS	V
			B) PREMATURE SEPARATION	ALL	SEPARATION OF ANTENNA FROM THE SHUTTLE WOULD RESULT IN LOSS OF MISSION CAPABILITY. THIS FAILURE MODE IS MINIMIZED SINCE PIN PULLER ELEC POWER MUST FIRST BE ARMED BEFORE THEY ARE FIRED, PREVENTING PREMATURE ACTUATION	SEPARATION OF ANTENNA FROM SHUTTLE	• REDUNDANT ARM & FIRE CIRCUIT FOR PIN PULLERS	I

Fig. 3-85 Deployable Antenna Failure Mode and Effects Analysis (Sheet 6 of 9)

GRUMMAN AEROSPACE CORPORATION

FAILURE MODE AND EFFECTS ANALYSIS

Check one: ☒ VEHICLE ☐ GSE ☐ TRAINER

SUBSYSTEM/EQUIPMENT	PROGRAM	DRAWING NUMBER	PREPARED BY	APPROVED BY	DATE	REV.	PAGE OF

CAM NUMBER	ITEM/PART	FUNCTION	FAILURE MODE	MISSION OR CHECKOUT PHASE	FAILURE EFFECT	FAILURE DETECTION	REDUNDANCY OR COMPENSATING PROVISIONS	CRITICALITY
29	TEMPERATURE SENSORS	MEASURE ANTENNA COMPONENT TEMPERATURES	OPEN, SHORT OR INACCURATE	ALL	SAME AS CASE NO. 28 A	NONE	• MULTIPLE SENSORS	IV
30	ACCELEROMETERS	MEASURE ANTENNA COMPONENT ACCELERATIONS	OPEN, SHORT OR INACCURATE	ALL	SAME AS CASE NO. 28 A	NONE	• MULTIPLE SENSORS	IV
31	GORE DISTANCE SENSORS	MEASURE GORE DISPLACEMENT AT DRUM ATTACHMENT FOR VARIOUS THERMAL CONDITIONS	OPEN, SHORT OR INACCURATE	ALL	SAME AS CASE NO. 28 A	NONE	• MULTIPLE SENSORS	IV
32	E-ODME ELECTRO-OPTIC DISTANCE MEASURING EQUIPMENT	DETERMINE THE ANTENNA SURFACE GEOMETRY BY ELECTRO-OPTIC TRIANGULATION USING "TARGETS" ON THE GORE & RIM SURFACE	OPEN, SHORT OR INACCURATE	ALL	ANTENNA SURFACE GEOMETRY CAN BE DETERMINED WITH THREE E-ODME'S; THEREFORE, A SINGLE E-DOME FAILURE WILL HAVE NO CONSEQUENCE SINCE FOUR E-ODME'S ARE AVAILABLE	NONE	• ONLY THREE OF FOUR E-ODME REQ'D • EACH E-ODME IS INDIVIDUALLY FUSED	V
33	SIGNAL CONDITIONERS, FILTER CARDS, REMOTE MULTIPLEXER & A/D CONVERTER	CONDITION & MULTIPLEX SENSOR DATA PRIOR TO RECEIPT AT SHUTTLE CENTRAL MULTIPLEXER	OPEN OR SHORT	ALL	SINCE INPUT SENSOR DATA IS FROM MULTIPLE SENSOR & REDUNDANCY IS USED IN THE REMOTE MULTIPLEXERS & A/D CONVERTERS, NO SINGLE FAILURE WILL CAUSE SYSTEM DEGRADATION	NONE	• MULTIPLE SENSORS • REDUNDANCY IN MULTIPLEXERS & A/D CONVERTERS	IV
34	PHOTOGRAMMETRIC CAMERAS	PHOTOGRAPHS FROM SEVERAL CAMERAS ARE USED TO PRODUCE A CONTOUR MAP OF THE ANTENNA STRUCTURE DURING VARIOUS DYNAMIC CONDITIONS	OPEN, SHORT, OR FAILS TO OPERATE	ALL	ONLY THREE OF FOUR OF THE AVAILABLE CAMERAS MUST OPERATE IN ORDER TO OBTAIN A CONTOUR MAP OF THE ANTENNA.	NONE	• ONLY THREE OF FOUR CAMERAS REQD • EACH CAMERA IS INDIVIDUALLY FUSED	V
35	SENSOR CENTRAL MULTIPLEXER	SERIALIZES SENSOR DATA FOR TRANSMISSION AND/OR STORAGE	OPEN OR SHORT	ALL	FAILURE OF ONE OF TWO MULTIPLEXERS WILL HAVE NO EFFECT ON DATA COLLECTION CAPABILITY.	• NO DATA FROM ONE MULTIPLEXER	• REDUNDANT MILTIPLEXERS • EACH MULTIPLEXER FUSED	V
36	SENSOR DATA RECORDER	STORES SENSOR DATA ON TAPE	ANY FAILURE	ALL	NO EFFECT DUE TO REDUNDANT RECORDERS	NO DATA ON ONE RECORDER	• REDUNDANT RECORDERS	V
37	RECEIVERS	RECEIVES SUBSATELLITE TRANSMITTED RF SIGNAL VIA ANTENNA FOR PATTERN MEASUREMENTS	ANY FAILURE	ALL	FAILURE OF ONE OF TWO RECEIVERS WILL HAVE NO EFFECT ON DATA COLLECTION CAPABILITY	LOSS OF DATA FROM ONE RECEIVER	• REDUNDANT RECEIVERS	V
38	RADAR/COMM TRANSMITTER	TRANSMITS RF FOR RADAR & COMMUNICATION EXPMTS & PATTERN MEASUREMENTS	ANY FAILURE	ALL	NO EFFECT DUE TO TRANSMITTER REDUNDANCY	LOSS OF TRANSMISSION FROM ONE TRANSMITTER	• REDUNDANT TRANSMITTERS	V
39	SIGNAL GENERATOR	PROVIDES RADAR & COMM SIGNAL MODULATION	ANY FAILURE	ALL	NO EFFECT DUE TO SIGNAL GENERATOR REDUNDANCY	NONE	• REDUNDANT SIGNAL GENERATORS	V

Page 9701 REV. B 5-70

Fig. 3-85 Deployable Antenna Failure Mode and Effects Analysis (Sheet 7 of 9)

FAILURE MODE AND EFFECTS ANALYSIS

CASE NUMBER	ITEM/PART	FUNCTION	FAILURE MODE	MISSION PHASE	FAILURE EFFECT	FAILURE DETECTION	REDUNDANCY OR COMPENSATING PROVISIONS	CRITICALITY
40	DUPLEXER	PERMITS SIMULTANEOUS TRANS/RECEPT VIA ANTENNA	A) FAILS TO TRANSMIT	ALL	UNABLE TO CONDUCT EITHER RADAR OR COMMUNICATIONS EXPERIMENTS SOME MAJOR MISSION OBJECTIVES CAN BE ACCOMPLISHED I.E., ANTENNA DEPLOYMT/RETRACTION, PATTERN MEASUREMENTS, ETC	NO TRANSMISSION	• NONE	III
			B) FAILS TO RECEIVE	ALL	SAME AS CASE NO. 40 A EXCEPT UNABLE TO PERFORM PATTERN MEASUREMENTS	NO RF DATA	• NONE	III
			C) FAILS TO TRANSMIT OR RECEIVE	ALL	SAME AS CASE NO. 40 B	NO RF DATA RECEIVED OR TRANSMITTED	• NONE	III
41	RADAR/COMM TRANSMITTER SELECT SWITCH	PERMITS SELECTION OF EITHER TRANSMITTER TO BE PUT ON LINE	A) SHORT TO GROUND	ALL	SAME AS CASE NO 40 A LOSS OF BOTH TRANSMITTERS	NO RF DATA	• NONE	III
			B) OPEN CONTACT OR COIL	ALL	NO EFFECT SINCE REDUNDANT CONTACTS & COILS WILL BE USED	NONE	• REDUNDANT CONTACTS & COILS	V
42	SIGNAL PROCESSORS	PROCESSES RF DATA FOR TAPE STORAGE	A) ANY FAILURE	ALL	NO EFFECT DUE TO REDUNDANT SIGNAL PROCESSORS	LOSS OF RF DATA TO ONE RECORDER	• REDUNDANT SIGNAL PROCESSORS	V
43	RF DATA RECORDERS	STORE RF DATA	A) ANY FAILURE	ALL	NO EFFECT DUE TO REDUNDANT RECORDERS	LOSS OF DATA STORAGE WITH ONE RECORDER	• REDUNDANT RECORDERS	V
44	FEED ANTENNAS	FEED ANTENNAS RECEIVE & TRANSMIT REFLECT RF SIGNALS FROM DEPLOYABLE ANTENNA	A) NO OUTPUT	ALL	LOSS OF ONE OF FIVE FEED ANTENNAS WILL CAUSE DEGRADATION OF PATTERN MEASUREMENTS AS WELL AS AFFECTING THE PERFORMANCE OF RADAR AND COMMUNICATIONS EXPERIMENTS	NONE	• MULTIPLE FEED ANTENNAS	III
46	TV CAMERAS	RECORD ANTENNA EXTENSION & RETRACTION ON VIDEO FOR FUTURE DIAGNOSTICS	A) ANY FAILURE	ALL	LOSS OF ONE OF MULTIPLE TV CAMERAS WILL ONLY AFFECT DIAGNOSTICS IN THE EVENT OF ANOTHER FAILURE, BUT BY ITSELF WOULD NOT AFFECT MISSION PERFORMANCE	LOSS OF VIDEO FROM ONE CAMERA	• MULTIPLE TV CAMERAS	V
46	BATTERY	SOURCE OF SUBSATELLITE ELEC POWER	A) ANY FAILURE	ALL	NO EFFECT DUE TO REDUNDANT BATTERIES	POWER OUTPUT TELEMETRY	• REDUNDANT BATTERIES	V
47	SATELLITE TRANSMITTER	RETRANSMITS RF SIGNAL FROM SATELLITE TO ANTENNA FOR COMMUNICATION EXPERIMENT AND ALSO TRANSMITS RF SIGNAL FOR PATTERN MEASUREMENTS	A) ANY FAILURE	ALL	NO EFFECT DUE TO REDUNDANT TRANSMITTERS	RF TRANSMITTER OUTPUT TELEMETRY	• REDUNDANT TRANSMITTERS	V
48	SIGNAL ANTENNA	SAME AS ABOVE	A) NO OUTPUT	ALL	LOSS OF RF SIGNAL FROM SUBSATELLITE TO DEPLOYABLE ANTENNA, RESULTING IN LOSS OF PATTERN MEASUREMENT CAPABILITY & COMMUNICATION EXPERIMENT. ALL OTHER MISSION OBJECTIVES CAN BE ACCOMPLISHED.	NO RF SIGNAL RECEIVED	• NONE	III
49	COMMAND RECEIVER & TRANSPONDER	RECEIVES SUBSATELLITE COMMANDS & TRANSMITS TELEMETRY DATA & TRACKING SIGNAL	A) ANY FAILURE	ALL	NO EFFECT DUE TO REDUNDANT COMPONENTS	NONE	• COMPONENT REDUNDANCY	V

Fig. 3-85 Deployable Antenna Failure Mode and Effects Analysis (Sheet 8 of 9)

SPACE SHUTTLE AEROSPACE CORPORATION

FAILURE MODE AND EFFECTS ANALYSIS

Check one: X VEHICLE ___ GSE ___ TRAINER

SUBSYSTEM OR EQUIPMENT | PROGRAM | DRAWING NUMBER | PREPARED BY | APPROVED BY | DATE | REV | PAGE OF

CASE NUMBER	ITEM/PART	FUNCTION	FAILURE MODE	MISSION OR CRITICAL PHASE	FAILURE EFFECT	FAILURE DETECTION	REDUNDANCY OR COMPENSATING PROVISIONS	CRITICALITY
50	OMNI ANTENNA	SAME AS CASE NO 49 A	NO OUTPUT	ALL	UNABLE TO RECEIVE SATELLITE COMMANDS, E.G., SWITCHING TRANSMITTERS IN THE EVENT OF A FAILURE FAILURE ALSO PREVENTS TRANSMISSION OF SATELLITE TELEMETRY DATA & TRACKING SIGNAL. THE LOSS OF THE ABILITY TO LOCATE SATELLITE (VIA SHUTTLE RADAR) INVALIDATES THE PATTERN MEASUREMENT CAPABILITY AND COULD DEGRADE THE COMMUNICATION EXPERIMENT ALL OTHER MISSION OBJECTIVES CAN BE ACCOMPLISHED.	NO TELEMETRY OR TRACKING DATA	• NONE	III
51	SATELLITE TRANSMITTER SELECT	PERMITS SELECTION OF EITHER TRANSMITTER TO BE BROADCASTING	A) SHORT TO GROUND	ALL	LOSS OF BOTH TRANSMITTERS SAME AS CASE NO 48	NO TRANSMISSION OF RF SIGNAL	• NONE	III
			B) OPEN CONTACTS OR COILS	ALL	NO EFFECT DUE TO REDUNDANT CONTACTS OR COILS	NONE	• REDUNDANT CONTACTS & COILS	
52	ANTENNA DELAY LINES	PERMITS TRANSMISSION OF PLANER RF WAVE FROM ANTENNA	A) ANY FAILURE	ALL	NO EFFECT DUE TO SYSTEM TOLERANCE TO MULTIPLE FAILURE OF DELAY LINES (ASSUMES RANDOM DISTRIBUTION ALONG ANTENNA SURFACE)	NONE	• MULTIPLE FAILURE TOLERANT DESIGN	V
53	STRAIN GAGES	MEASURE ANTENNA COMPONENT STRUCTURAL DEFORMATION	OPEN, SHORT IR INACCURATE	ALL	THE FAILURE OF ONE OR MORE SENSORS WILL NOT SIGNIFICANTLY DEGRADE THE OVERALL DATA AVAILABLE SINCE MULTIPLE SENSORS ARE USED.	NONE	• MULTIPLE SENSORS	IV

Fig. 3-85 Deployable Antenna Failure Mode and Effects Analysis (Sheet 9 of 9)

4 - ORBITAL OPERATIONS ANALYSIS (TASK 3)

4.1 FLIGHT OPTIONS

Our thinking on flight options has been modified from the prior study results based on a further definition of equipment and orbital operational requirements.

Four flight options had been defined as part of the FY-77 study.

- Antenna development flight only
  - (mesh deployable reflector)
- Antenna development flight only
  - (passive bootlace array)
- Multibeam communication antenna configuration - using array in shuttle-attached or free-flying mode.
  - (mission application experiment only).
- Earth-looking radiometer test using deployable reflector
  - (mission application experiment only).

Each of these options was considered an individual flight, with the antenna retrieved and reconfigured between flights as required.

It is now believed that additional objectives can be accomplished on a single flight with the participation of guest experimenters, (e.g., mission application experiments can be flown on the same flight with a basic antenna development configuration). Therefore, while retaining the capability for multiple flights and different antenna configurations, emphasis in this study has been towards definition of how much can be done on a single flight. Options include the demonstration of a passive array with some combination of mission experiments (radiometry, radar or communication). A phased array has been selected for first flight because it is most applicable to priority users (communications and radar). For the same reason, these missions are leading candidates for experiments on the first flight. Based on the orbital operations analysis summarized below, the experiments and the basic antenna development tests can be completed within a 7-day mission timeline.

4.2 DEMONSTRATION TEST OBJECTIVES

Test objectives associated with the baseline antenna system (Fig. 4-1) were identified in Ref. 1-1. Upon review, we have determined that they are still consistent with the

PRIMARY OBJECTIVE	TEST ACTIVITY
• DEMONSTRATE DEPLOYMENT	• SEQUENTIAL DEPLOYMENT • VISUAL & PHOTO COVERAGE • STRUCTURAL & MECH MEASUREMENTS
• STRUCTURAL TOLERANCES MEASUREMENTS	• DISCRETE ELECTRO-OPTICAL DISTANCE MEASURING EQUIPMENT MEASUREMENTS • PHOTOGRAMMETRIC SURFACE CONFORMITY MEASUREMENTS FOR VARIOUS DYNAMIC AND THERMAL CONDITIONS
• DETERMINE DYNAMIC CHARACTERISTICS	• SPECIFIC SHUTTLE INDUCED DISTURBANCES • STRAIN MEASUREMENTS • PHOTOGRAMMETRIC MEASUREMENTS
• DETERMINE THERMAL CHARACTERISTICS	• ADJUST ANTENNA ORIENTATION FOR DIFFERENT THERMAL CONDITIONS • TEMPERATURE MEASUREMENTS • ELECTRO-OPTICAL DISTANCE MEASUREMENTS
• DETERMINE ANTENNA FAR FIELD PATTERN	• FREE-FLYING RF TEST GENERATOR DEPLOYED PRIOR TO ANTENNA DEPLOYMENT • ADJUST ORBIT SO THAT RF GENERATOR CROSSES ANTENNA ORBIT TWICE A DAY • MEASURE MAIN BEAM AND SIDE LOBES
• VERIFICATION OF ANALYSIS TOOLS	• COMPARISON OF TEST RESULTS WITH PREDICTIONS (POST FLIGHT)

0820-049B

Fig. 4-1 Orbital Demonstration Program Objectives

overall objectives of the demonstration system. During this study, our definition of mission related experiment objectives has been expanded as follows:

- Communications Experiment
  - measurement of interbeam isolation
  - measurement of passively generated intermodulation products.
- Radar Experiment
  - Verification of antenna loss parameters
  - Measurement of clutter backgrounds for various geometry conditions
  - Demonstration of target detection in a clutter background.
- Radiometry Experiment
  - Measurement of equivalent receiver noise temperatures through the antenna (from which system temperature sensitivity can be computed)
  - Demonstration of soil moisture measurements.

4.3 DEMONSTRATION DESIGN REFERENCE MISSION

A design reference mission (DRM) has been developed for a 100-meter diameter antenna demonstration mission. This mission will demonstrate:

- Antenna deployment
- Structural tolerance attainment
- Antenna pattern
- Communication frequency reuse
- Radar utilization
- Antenna furling and stowage.

Figure 4-2 presents this DRM timeline. A mission summary is illustrated in Fig. 4-3 while Fig. 4-4 identifies the assumptions, groundrules and orbital parameters used to define the DRM. The 350-nautical mile altitude will provide acceptably low atmospheric drag and can be obtained with a single OMS package. The 56.5-degree inclination is also the highest inclination that can be obtained at 350 nautical miles with a single OMS package. A high inclination is required to obtain radar clutter data.

After launch and into the proper orbit, the first day's activities will be primarily a period of space acclimination to allow the crew to adjust to the space environment and motion so that they will be able to perform subsequent tasks efficiently. It will be necessary however, to launch the test subsatellite on the first day so that the proper separation between the orbiter and the subsatellite can be achieved by the third mission day. After the subsatellite is launched the orbiter will begin to separate slowly from the subsatellite.

EVENT	GRD ELAPSED TIME HR:MIN	ΔT HR:MIN	ORBITER ATTITUDE	REMARKS
LIFT-OFF	00:00			
STAGE SRBs	00:02			
MECO	00:08			
OMS-1	00:09			
OMS-2	00:52			
ORBITER & PAYLOAD C/O	01:40	00:15		
OPEN PAYLOAD DOORS	01:55	00:05		
SUBSAT TURN ON & C/O	02:00	00:10		
ESTABLISH SUBSAT DEPLOY ATT	02:10	00:05	Y-POP; −X VERT	
SUBSAT SPIN UP & DEPLOY	02:15	00:10	Y-POP; −X VERT	ORBITER BACKS AWAY FROM SUBSAT
ESTABLISH SUBSAT TRACK	02:25	00:05		
MEAL	02:30	01:00		
SPACE ACCLIMATION	03:30	05:30		
MEAL	09:00	01:00		
FREE TIME	10:00	02:15		
PRE SLEEP ACTIVITIES	12:15	00:45		
SLEEP	13:00	08:00		
POST SLEEP ACTIVITIES	21:00	00:45		
MEAL	21:45	00:45		
ESTABLISH ORBITER ANT ERECTION ATTITUDE	22:30	00:05	Y-POP; −X VERT	
DEPLOY RM-1 WITH TV CAMERA	22:35	00:10	Y-POP; −X VERT	
C/O & START ANT. STRUCT/THERMAL DATA ACQ	22:45	00:10+	Y-POP; −X VERT	DATA ACQUISITION CONTINUOUS FOR MISSION DURATION
ERECT ANT. PACKAGE IN PAYLOAD BAY & VERIFY	22:55	00:20	Y-POP; −X VERT	RM-2 ERECTS ANT.; ANT. SENSORS VERIFY ANT. PACKAGE IS PROPERLY ERECTED AND LOCKED IN POSITION FOR REMAINDER OF DEPLOYMENT SEQUENCE
DEPLOY RM-2 WITH TV CAMERA	23:15	00:10	Y-POP; −X VERT	RM-1 & -2 ARE POSITIONED FOR OPTIMUM VIEWING.
HOLD ACTIVITIES FOR SUNLIGHT	23:25	00:35	Y-POP; −X VERT	SUNLIGHT REQD FOR DEPLOYMENT VIEWING
DEPLOY ANTENNA MAST	24:00	00:30	Y-POP; −X VERT	
VERIFY MAST DEPLOYMENT	24:30	00:20	Y-POP; −X VERT	SENSOR DATA REVIEWED TO ASCERTAIN PROPER MAST DEPLOYMENT
HOLD ACTIVITIES FOR SUNLIGHT	24:50	00:40	Y-POP; −X VERT	SUNLIGHT REQD FOR DEPLOYMENT VIEWING
DEPLOY ANTENNA	25:30	00:40	Y-POP; −X VERT	
VERIFY DEPLOYMENT	26:10	00:45	Y-POP; −X VERT	
ESTABLISH MINIMUM DISTURBANCE ATTITUDE	26:55	00:05	Y-POP; −X VERT	
ACTIVATE E-ODME & START MEASUREMENT SEQUENCE	27:00	00:45		
EXPOSE PHOTOGRAMMETRIC PLATES	27:15			
EXPOSE PHOTOGRAMMETRIC PLATES	27:30	00:30		
EXPOSE PHOTOGRAMMETRIC PLATES	27:45			
MEAL	27:50	00:40		

0820-050B(1)

Fig. 4-2 Deployable Antenna Demo DRM Timeline (Sheet 1 of 4)

EVENT	GRD ELAPSED TIME HR:MIN	ΔT HR:MIN	ORBITER ATTITUDE	REMARKS
ESTABLISH FULL SUN ATTITUDE	28:30	00:05		
CONTINUE E-ODME MEASUREMENT SEQUENCE	28:35	00:45		FULL SUN STRUCT/THERMAL MEASUREMENTS
EXPOSE PHOTOGRAMMETRIC PLATES	28:40			
EXPOSE PHOTOGRAMMETRIC PLATES	29:00	00:35		
EXPOSE PHOTOGRAMMETRIC PLATES	29:10			
ESTABLISH EDGE SUN ATTITUDE	29:15	00:05		
CONTINUE E-ODME MEASUREMENT SEQUENCE	29:20	01:10		
EXPOSE PHOTOGRAMMETRIC PLATES	29:25			EDGE SUN STRUCT/THERMAL MEASUREMENTS
EXPOSE PHOTOGRAMMETRIC PLATES	30:00	01:10		
EXPOSE PHOTOGRAMMETRIC PLATES	30:30			
ESTABLISH 45° SUN ATTITUDE	30:35	00:05		
CONTINUE E-ODME MEASUREMENT SEQUENCE	30:40	01:05		
EXPOSE PHOTOGRAMMETRIC PLATES	30:45			45° SUN STRUCT/THERMAL MEASUREMENTS
EXPOSE PHOTOGRAMMETRIC PLATES	31:00			
EXPOSE PHOTOGRAMMETRIC PLATES	31:15	01:00		
EXPOSE PHOTOGRAMMETRIC PLATES	31:30			
EXPOSE PHOTOGRAMMETRIC PLATES	31:45			
ESTABLISH DYNAMIC DISTURBANCE ATTITUDE	31:50	00:05		
CONTINUE E-ODME MEASUREMENT SEQUENCE	31:55			DYNAMIC MEASUREMENTS
FIRE - Z THRUSTERS	32:00 32:30 33:00	01:00		
EXPOSE PHOTOGRAMMETRIC PLATES	32:00 32:30 33:00	01:00		
MEAL	33:30	01:00		
FREE TIME	34:30	02:00		
PRE-SLEEP ACTIVITIES	36:30	00:30		
SLEEP	37:00	08:00		
POST-SLEEP ACTIVITIES	45:00	00:30		
MEAL	45:30	00:45		
ESTABLISH PATTERN MEASUREMENT ATTITUDE	46:15	00:15	X-POP	
ESTABLISH & VERIFY SUBSAT/ORBITER PATTERN MEASURING EQUIP INTERFACE	46:30	01:30		X-POP PATTERN MEASUREMENTS
PATTERN DATA ACQUISITION	48:00	03:30		
MEAL	51:30	01:00		
ESTABLISH PATTERN MEASUREMENT ATTITUDE	52:30	00:15	Y-POP	
VERIFY SUBSAT/ORBITER PATTERN MEASURING EQUIP INTERFACE	52:45	00:15		Y-POP PATTERN MEASUREMENTS
PATTERN DATA ACQUISITION	53:00	03:00		
FREE TIME	56:00	01:00		
MEAL	57:00	01:00		
FREE TIME	58:00	02:30		
PRE-SLEEP ACTIVITIES	60:30	00:30		

0820-050B(2)

Fig. 4-2 Deployable Antenna Demo DRM Timeline (Sheet 2 of 4)

EVENT	GRD ELAPSED TIME HR:MIN	ΔT HR:MIN	ORBITER ATTITUDE	REMARKS
SLEEP	61:00	00:00		
POST-SLEEP ACTIVITIES	69:00	00:30		
MEAL	69:30	00:45		
ESTABLISH COMM EXP ATTITUDE	70:15	00:15	Y-POP; –X VERT	
ESTABLISH & VERIFY SUBSAT/ORBITER COMM EXP MEASURING EQUIP INTERFACE	70:30	01:15	Y-POP; –X VERT	
COMMUNICATIONS EXP DATA ACQUISITION	71:45	03:45	Y-POP; –X VERT	
MEAL	75:30	01:00		
COMMUNICATIONS EXP DATA ACQUISITION	76:30	02:00	Y-POP; –X VERT	
RECONFIGURE ANTENNA ELECTRONIC CONFIG FOR RADAR EXP	78:30	01:30		
FREE TIME	80:00	01:00		
MEAL	81:00	01:00		
FREE TIME	82:00	02:30		
PRE-SLEEP ACTIVITIES	84:30	00:30		
SLEEP	85:00	08:00		
POST-SLEEP ACTIVITIES	93:00	00:30		
MEAL	93:30	00:45		
ESTABLISH RADAR EXP ATTITUDE	94:15	00:15		
VERIFY RADAR ELECT EQUIP	94:30	00:30		
RADAR CLUTTER EXP DATA ACQUISITION	95:00	04:00		
QUICK LOOK CLUTTER DATA EVALUATION	96:00	03:00		
MEAL	99:00	01:00		
RADAR COOPERATIVE TARGET EXP DATA ACQUISITION	100:00	05:00		
QUICK LOOK CO-OP TARGET DATA EVALUATION	101:00	04:00		
MEAL	105:00	01:00		
FREE TIME	106:00	02:30		
PRE-SLEEP ACTIVITIES	108:30	00:30		
SLEEP	109:00	08:00		
POST-SLEEP ACTIVITIES	117:00	00:45		
MEAL	117:45	00:45		
ESTABLISH ATTITUDE FOR ANTENNA RETRACTION	118:30	00:10	Y-POP; –X VERT	
POSITION RMs WITH TV CAMERAS FOR OPTIMUM VIEWING	118:40	00:20	Y-POP; –X VERT	
ACQUIRE E-ODME RIM MEMBER TARGET	119:00	00:10	Y-POP; –X VERT	
HOLD FOR SUNLIGHT	119:10	00:50	Y-POP; –X VERT	SUNLIGHT REQD FOR VIEWING
RETRACT ANTENNA	120:00	00:40	Y POP; –X VERT	
VERIFY RETRACTION	120:40	00:10	Y-POP; –X VERT	
HOLD FOR SUNLIGHT	120:50	00:40	Y-POP; –X VERT	SUNLIGHT REQD FOR VIEWING
RETRACT MAST	121:30	00:30	Y-POP; –X VERT	
VERIFY RETRACTION	122:00	00:10	Y-POP; –X VERT	
STOW ONE RM TV CAMERA	122:10	00:10	Y-POP; –X VERT	

0820-050B(3)

Fig. 4-2 Deployable Antenna Demo DRM Timeline (Sheet 3 of 4)

EVENT	GRD ELAPSED TIME HR:MIN	ΔT HR:MIN	ORBITER ATTITUDE	REMARKS
HOLD FOR SUNLIGHT	122:20	00:40	Y-POP; –X VERT	SUNLIGHT REQD FOR VIEWING
LOWER ANTENNA PACKAGE INTO PAYLOAD BAY & SECURE	123:00	00:20	Y-POP; –X VERT	
VERIFY ANTENNA PACKAGE STOWAGE	123:20	00:30	Y-POP; –X VERT	
STOW RMs & TV CAMERA	123:50	00:10	Y-POP; –X VERT	
MEAL	124:00	01:00		
CLOSE OUT ANTENNA EXP & ORBITER	125:00	04:00		
MEAL	129:00	01:00		
FREE TIME	130:00	02:30		
PRE-SLEEP ACTIVITIES	132:30	00:30		
SLEEP	133:00	08:00		
POST-SLEEP ACTIVITIES	141:00	00:45		
MEAL	141:45	00:45		
DE-ORBIT & LAND	142:30			

0820-050B(4)

Fig. 4-2 Deployable Antenna Demo DRM Timeline (Sheet 4 of 4)

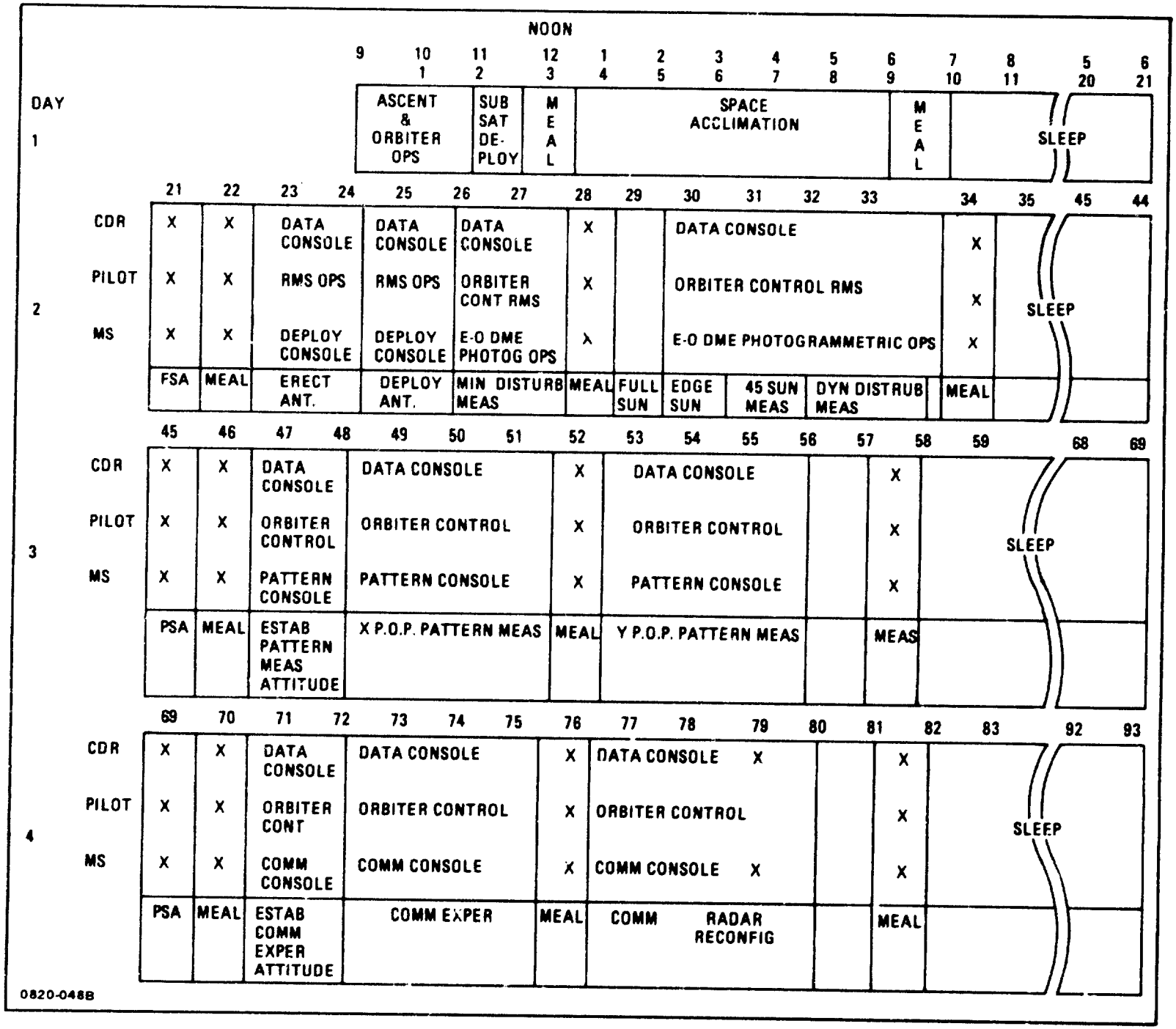

Fig. 4-3 Deployable Antenna Demo DRM Summary (Sheet 1 of 2)

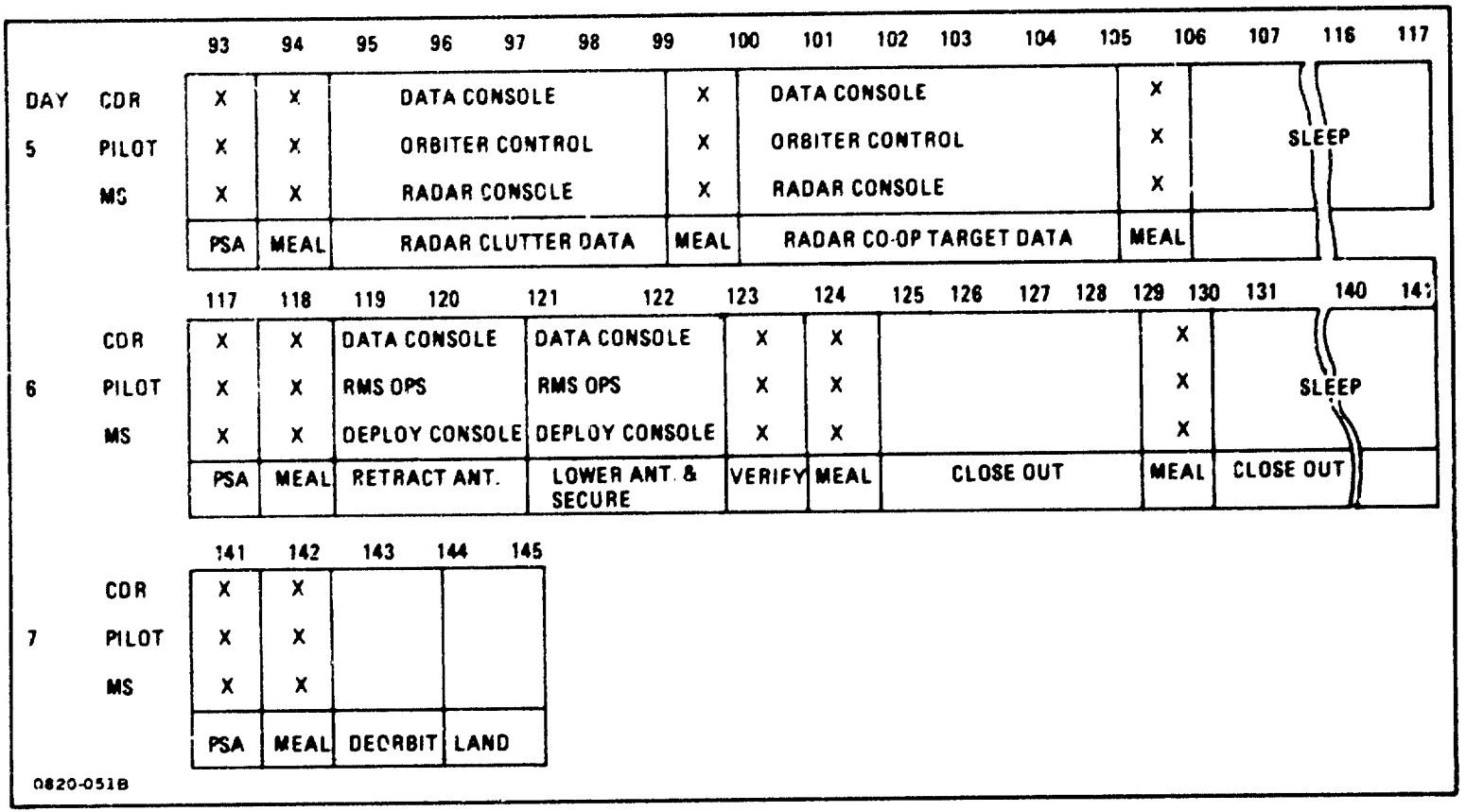

Fig. 4-3 Deployable Antenna Demo DRM Summary (Sheet 2 of 2)

- ALTITUDE – 350 N MI
- INCLINATION – 56.5°
- MISSION DURATION – 7 DAYS
- CREW – 3 MEMBERS
  - COMMANDER
  - PILOT
  - MISSION SPECIALIST
- ONE OMS PACKAGE REQUIRED
- IT HAS BEEN ASSUMED FOR THE PURPOSES OF GENERATING THIS DRM THAT THE DEPLOYABLE ANTENNA IS THE ONLY MISSION ACTIVITY ON THE SHUTTLE FLIGHT
- NO EVAs ARE PLANNED
- ALL DEPLOYMENT ACTIVITIES ARE PLANNED TO OCCUR IN SUNLIGHT SO THAT THESE ACTIVITIES CAN BE VIEWED AND PHOTOGRAPHED
- THE DRM TIMELINE IS BASED ON A NOMINAL 8-HOUR CREW EXPERIMENT WORK DAY.

0820-052B

Fig. 4-4 Deployable Antenna Demonstration DRM Groundrules and Orbital Parameters

Antenna deployment will be accomplished on the second day. The orbiter will be placed in a Y axis POP attitude with the +Z axis facing away from the direction of orbital travel. This attitude will produce a uniform disturbance across the antenna during deployment. All deployments will be performed during sunlight to permit visual monitoring. Deployment will be accomplished in three steps:

Step 1 - The RMS will be used to erect the antenna package in the payload bay.

Step 2 - The antenna mast will be extended. TV cameras, held by the two RMS, will record mast extension. Structural, mechanical and thermal data will be acquired.

Step 3 - The wire wheel antenna will be deployed. The TV cameras will record deployment. Structural, mechanical and thermal data from antenna-mounted transducers will be acquired by the antenna experiment data acquisition console. Data from these sensors will be recorded continuously during the entire mission.

After antenna deployment, both the electro-optical distance measuring equipment, (E-ODME) and the photogrammetric measurements will be made, to verify the structural tolerance of the deployed antenna. The E-ODME will acquire data automatically, stepping from one target to another.

A series of thermal and dynamic test conditions will be established using the orbiter to orient the antenna with respect to the sun and to provide mechanical disturbances from thruster firing. Photogrammetric, E-ODME and standard instrumentation data will be acquired for each of these conditions. These data will be used to verify antenna structural performance and tolerance.

Antenna patterns will be measured on day 3. Boresight equipment mounted atop the antenna will be used to determine the position of the subsatellite with respect to antenna axes. The orbiter will rotate the antenna through successive 180-degree arcs. During each rotation or cut, pattern data will be obtained by coordinating the strength of the subsatellite signal received by the antenna to the attitude of the antenna relative to the subsatellite. Patterns will be obtained for X-POP and Y-POP orbiter attitudes.

Antenna-use experiments will be conducted on days 4 and 5. On day 4, a frequency-re-use communications experiment will be performed. The subsatellite will be used as a communications test station to evaluate multibeam isolation and intermodulation products. Subsection 3.4.1 describes the communications experiment.

A radar experiment, conducted on day 5, will verify:

- Beam agility
- Detection of a target in the clutter background
- Antenna low loss performance
- Sidelobe cancellation capability.

Also measurements will be made of the clutter background (amplitude and spectral distribution). The high 56-degree orbit inclination was chosen to permit clutter measurement. A complete description of the radar experiment is contained in subsection 3.4.2.

Antenna retraction and stowage in the payload bay will be accomplished on day 6. After the close out of the antenna experiment the orbiter will be made ready for deorbit and landing which will be accomplished on mission day 7.

5 - PROGRAMMATICS ANALYSIS (TASK 4)

Preliminary design results from Task 2 and the demonstration flight program defined in Task 3 form the basis for programmatic data developed in Task 4. Results of this task, presented in this section, include:

- Work Breakdown Structure and Dictionary
- Program Planning (schedule)
- Development Activities

5.1 WORK BREAKDOWN STRUCTURE (WBS)

The Deployable Antenna Demonstration Program WBS contains all labor and material required for the DDT&E, manufacturing and operation phases for all program elements. These phases are defined in the subsection below.

5.1.1 DDT&E

This item includes all labor, materials, tooling, facilities, studies, analyses, etc., which are required to determine specification requirements and the subsequent analysis, design, development, evaluation and redesign for the subsystems. Specifically included are the preparation of specifications, drawings, parts lists, wiring diagrams, technical coordination between engineering and manufacturing, vendor coordination, component and subsystem hardware development and testing, data reduction, report preparation, determination and specification of requirements for reliability, maintainability, and quality assurance. In addition, efforts are included to complete the planning, design, fabrication, assembly, inspection, installation and modification of initial tooling, jigs, fixtures, and special test equipment/GSE. Also included in this item is the effort expended in conducting system design reviews, evaluating the results of those reviews, and performing engineering cost analysis and materials analysis. This includes subsystem management and engineering which is directly a part of a particular subsystem or component. DDT&E also includes developmental test articles, major ground test articles and development testing. It includes engineering models, breadboards, and engineering mockups as required in the development of individual subsystems and components.

5.1.2 MANUFACTURING

This item includes all labor and materials required for the production of space hardware through the acceptance of this hardware by the Government. Space hardware includes all hardware produced for deployment in space. Specifically included in this item are the following:

- Procurement, fabrication, assembly and checkout of space hardware
- Ground test and factory checkout of space hardware
- Initial spares
- Maintenance of tooling and factory test equipment/GSE
- Sustaining engineering for liaison support of space hardware manufacturing.

5.1.3 OPERATIONS

This item includes all ground and flight operations and the support of these operations as follows:

- Ground operations - receipt, assembly, checkout, servicing, launching, post-launch support, and maintenance/refurbishment of the reusable space hardware as required at the launch site
- Flight operations - mission planning, in-orbit mission execution and ground mission control support
- Support operations - transportation and handling of Deployable Antenna System hardware requiring special consideration, training equipment, training programs and space hardware/GSE operational spares.

5.1.4 WBS DEFINITION

The program elements are grouped into seven categories as shown in Fig. 5-1:

(1) Program Management
(2) System Engineering and Integration
(3) Design and Development
(4) Manufacturing, Checkout and Assembly
(5) System Test
(6) Logistics
(7) Operations

The WBS definition, as detailed in Appendix A, is intended to apply, as appropriate to the DDT&E, manufacturing and operational phases of the program.

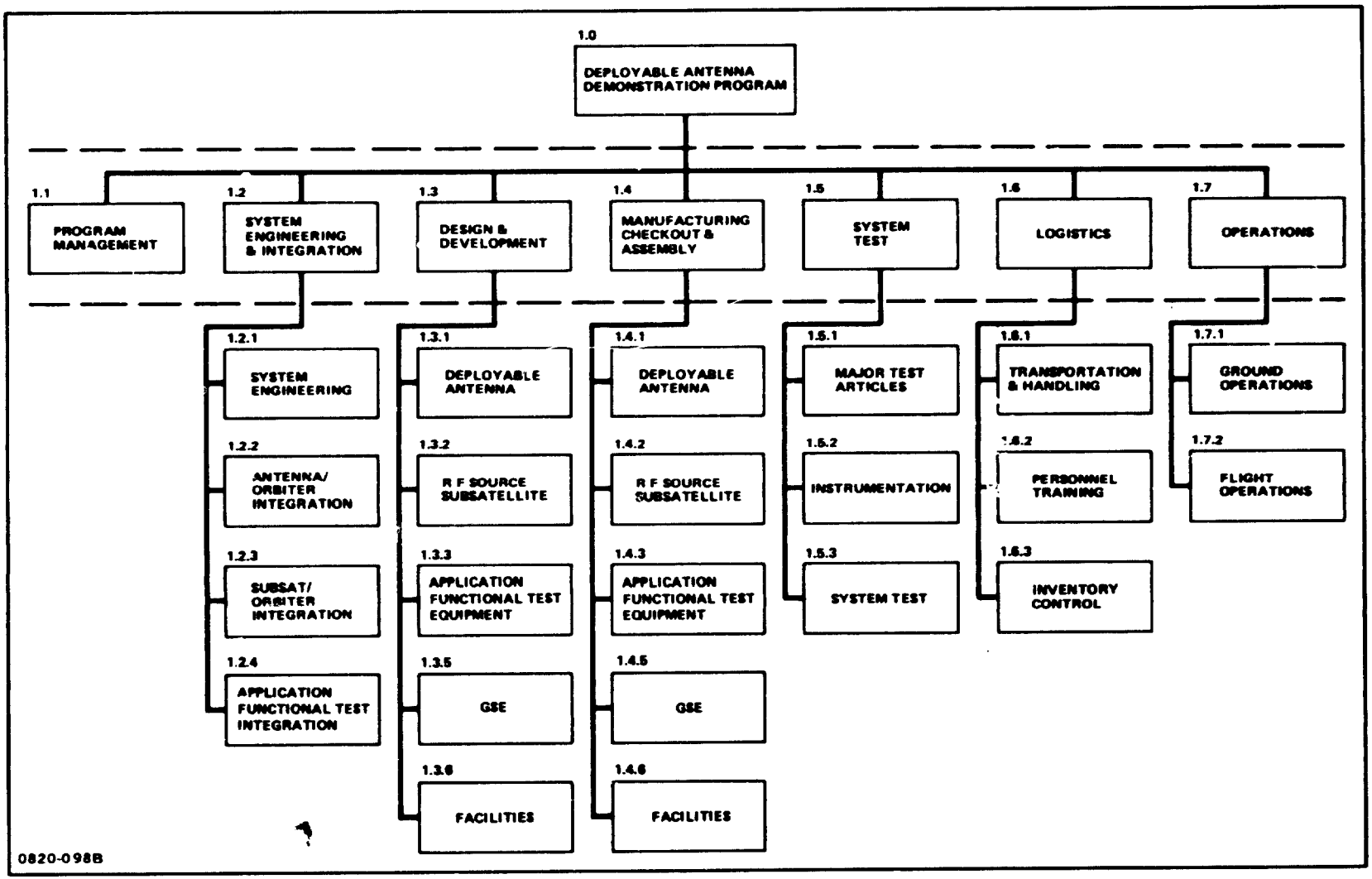

Fig. 5-1 Work Breakdown Structure

5.2 PROGRAM SCHEDULE

A schedule of required activites leading to a deployable antenna demonstration flight in early CY-84 is shown in Fig. 5-2. The schedule is based on assumed continued preliminary design activity in FY-80 leading to a program go-ahead in FY-81. User participation to further identify requirements is shown in parallel with the preliminary design effort to ensure that the baseline antenna demonstration can support functional tests. Although a single demonstration flight is shown in the schedule, the antenna has been designed to be retrieved and therefore can be reconfigured for additional testing (antenna development and/or mission functional tests) in later flights. Such testing in a second flight could occur a year later if activities leading to it are started with appropriate lead time (i.e., starting before the first launch).

5.3 DEVELOPMENT ACTIVITIES

The ground validation activity in the schedule has been further subdivided into the development tests shown in Fig. 5-3. These tests, identified and described in Ref. 1-1 include:

- Rim hinge - a preproduction unit will be used to determine torques, friction, and locking characteristics
- Rim members - representative rim members will be tested to determine the rim member's mechanical and thermal properties
- Stay - representative stays will be tested to determine the stay's mechanical and thermal properties
- Gore wrap - demonstration of lens and reflector gore wrap and unwrap
- Stay reel - a preproduction unit will be used to determine torque and friction forces
- Measurement system - an electro-optical distance measurement equipment test set up representative of the flight system geometry will be tested to verify measurement errors
- Membrane characteristics - representative lens and/or reflector gore segments will be tested to determine thermal and mechanical characteristics
- Bootlace lens patterns - a test array of approximately 200 subarrays will be tested to obtain pattern, gain, beamwidth, sidelobes, and impedance data

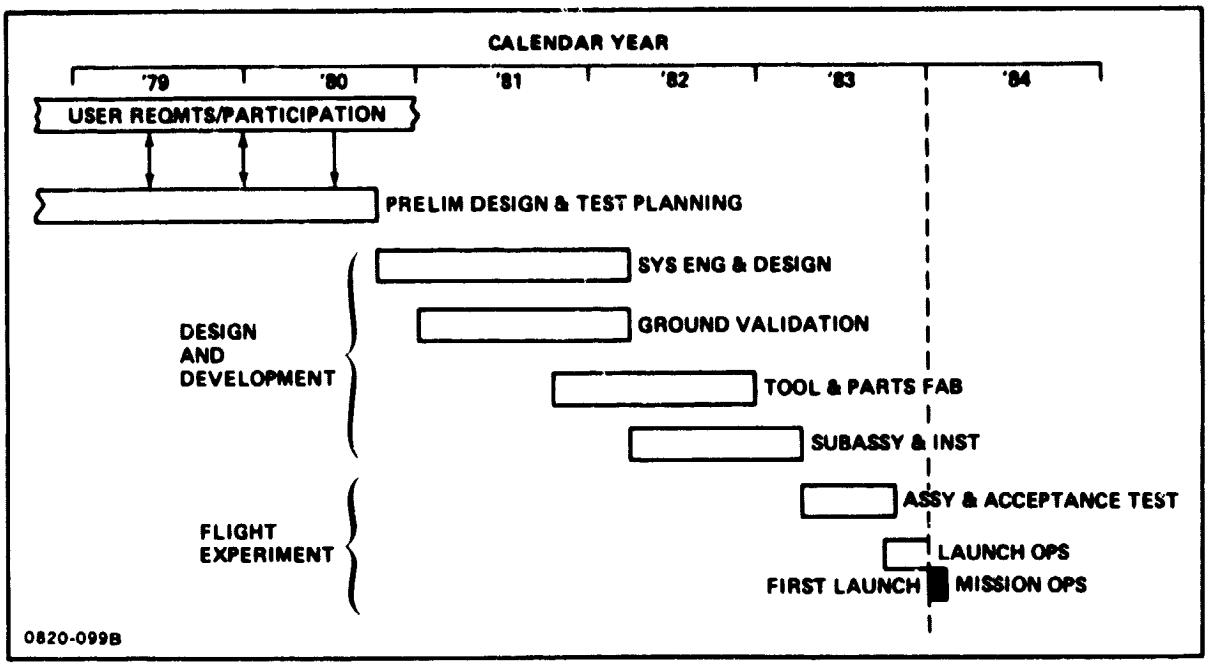

Fig. 5-2 Schedule

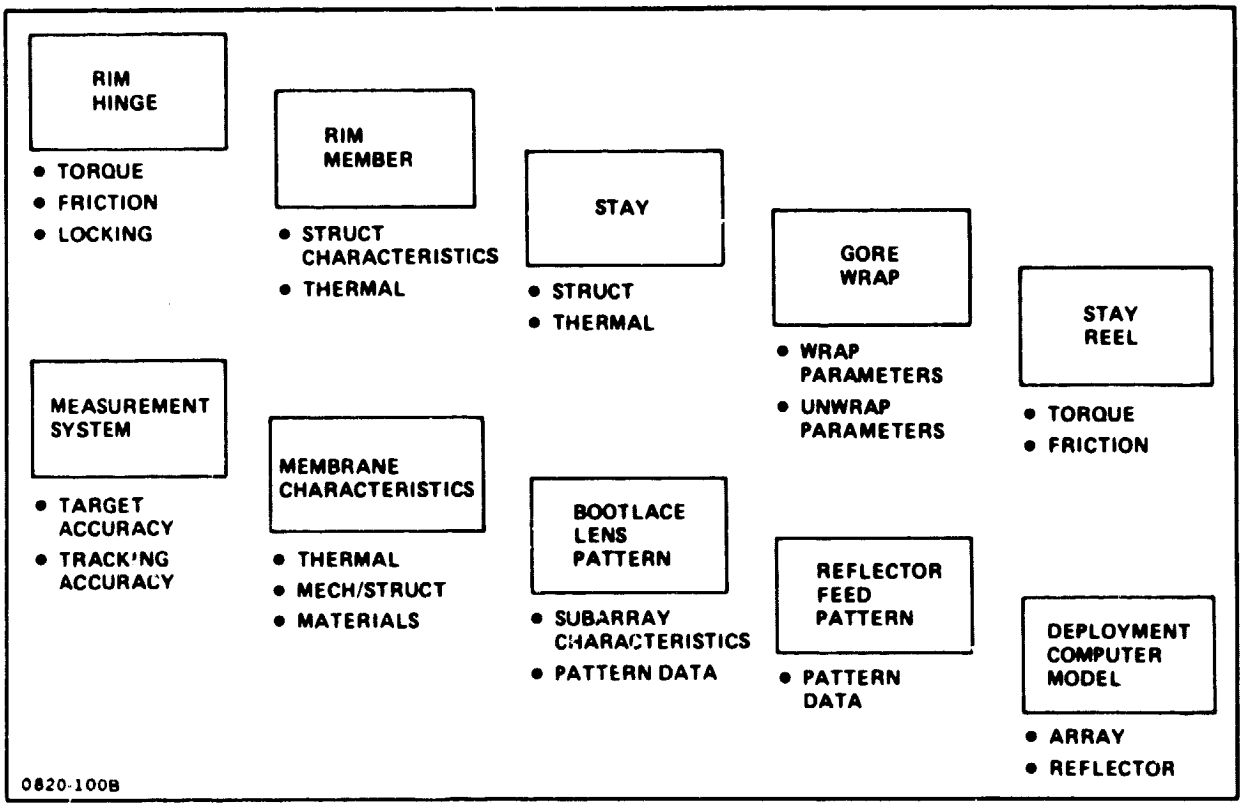

Fig. 5-3 Ground Development

- Reflector feed pattern - full-scale reflector feed pattern data
- Computer model - computer deployment models of the lens and reflector configurations will be updated with the results of the above identified development tests.

Final definition of these validation activities will reflect results of development work in progress (and planned for the Phased Array Radiating Membrane Development Program sponsored by DARPA). In this program 10 by 9 foot phased array test articles are being designed, fabricated and tested. Results defining membrane characteristics will be directly applicable to the Deployable Antenna Demonstration Program. Limited gore wrap and pattern tests will also provide inputs, but to a lesser extent.

Appendix A

WBS DICTIONARY

Appendix A

WBS DICTIONARY

1.0 DEPLOYABLE ANTENNA DEMONSTRATION PROGRAM

This element summarizes the effort to provide hardware, software, services and facilities that are required to develop, manufacture, operate and maintain the deployable antenna system. It also includes the DAS/shuttle integration activities.

1.1 PROGRAM MANAGEMENT

This element summarizes the management activities of planning, organizing, directing, coordinating, controlling, and approving actions required to accomplish overall DAS objectives. It excludes management activities associated with specific DAS hardware elements but includes the management activities required for DAS integration with other categories. The management activities associated with specific DAS hardware elements will be included as part of those particular elements. Functions costed herein include Program Manager, Administrative Staff, Cost/Performance Management, Information Management, Contract Administration, and Material Procurement.

1.2 SYSTEM ENGINEERING AND INTEGRATION

This element summarizes the effort required for systems engineering and integration of the DAS. The systems engineering effort includes directing and controlling requirements analysis and integration, system definition, system test definition, interface, safety, reliability, maintainability, configuration management, quality engineering and technology utilization. The integration effort includes DAS/shuttle integration.

This element is subdivided as follows:

WBS	TITLE
1.2.1	Systems Engineering
1.2.2	DAS/Orbiter Integration

1.2.1 SYSTEMS ENGINEERING

This element pertains to the systems engineering effort associated with the design, development, production and test of the DAS. Included are analyses required to verify compatibility of designs with requirements; to control and direct the engineering activities,

and to make cost/performance tradeoffs. Also included are engineering planning studies, technology utilization, technical risk assessment, reliability engineering, safety engineering, quality engineering, configuration requirements analysis, and associated support required to perform the DAS systems engineering task.

1.2.2 DAS/SHUTTLE INTEGRATION

This element includes all systems engineering and integration effort associated with the combined functioning of the DAS and shuttle. Included are system analysis, test and evaluation required to ensure the efficient accomplishment of this task; analysis and identification of DAS test and checkout operations affecting the interface; evaluation/coordination of recommended changes to this interface; and preparation, submittal, and maintenance of Interface Control Documents. DAS integration in this context includes the deployable antenna in each of two antenna development configurations and the functional test equipment. Integration of the subsatellite and instrumentation with the orbiter is also included as appropriate for the different configurations.

1.3 DESIGN AND DEVELOPMENT

This item includes all labor, materials, tooling, facilities, studies, analyses, etc., which are required to determine specification requirements and the subsequent analysis, design, development, evaluation and redesign for the subsystems. Specifically included are the preparation of specifications, drawings, parts lists, wiring diagrams, technical coordination between engineering and manufacturing, vendor coordination, component and subsystem hardware development and testing, data reduction, report preparation, determination and specification of requirements for reliability, maintainability, and quality assurance. In addition, costs are included for efforts to complete the planning and design of tooling, jigs, fixtures, and special test equipment/GSE. Also included in this item is the effort expended in conducting system design reviews, evaluating the results of those reviews, and performing engineering cost analysis and materials analysis. This includes subsystem management and engineering which is directly charged to a particular subsystem or component. Design and development also includes costs associated with developmental test articles hardware such as engineering models, breadboards, engineering mockups and such other hardware as required in the development of individual subsystems and components.

This element is subdivided into the following systems.

WBS	TITLE
1.3.1	Deployable Antenna
1.3.2	RF Source Subsatellite

WBS	TITLE
1.3.3	Application Functional Test Equipment
1.3.4	(Reserved)
1.3.5	GSE
1.3.6	Facilities

1.3.1 DEPLOYABLE ANTENNA

This element contains the costs associated with design and development of all the subsystems required to provide the flight hardware for the two antenna development configurations; a bootlace array and a parabolic reflector. The RF source subsatellite, also required with these configurations is included in WBS 1.3.2.

The deployable antenna is divided into the following elements:

WBS	TITLE
1.3.1.1	Basic Structure
1.3.1.2	Bootlace Array Configuration Kit
1.3.1.3	Reflector Configuration Kit
1.3.1.4	Instrumentation
1.3.1.5	Payload/Orbiter Interface Structure
1.3.1.6	Integration and Assembly

Each of the subdivisions - 1.3.1.1 through 1.3.1.5 are subsystems and contain labor and materials necessary to design and develop that particular subsystem.

1.3.1.1 Basic Structure

This element includes the design and development of hardware which makes up the wire wheel structure that is common to both flight configurations. It consists of the hub, rims, stays, stay platforms/reels and interconnecting umbilicals.

1.3.1.2 Bootlace Array Configuration Kit

This element includes the design and development of hardware which when integrated with the Basic Structure (WBS 1.3.1.1) results in a bootlace array antenna system. It consists of a rotating gore drum, three gore planes and interconnecting delay lines, gore mounting/tensioning hardware and the feed structure and electronics.

1.3.1.3 Reflector Configuration Kit

This element includes design and development of hardware which when integrated with the Basic Structure (WBS 1.3.1.1) results in a parabolic reflector system. It consists of

three extendible masts and associated canisters, mesh reflecting surface, axial control system and feed structure. Feed electronics in WBS 1.3.1.2 are common to this element.

1.3.1.4 Instrumentation

This element includes design and development of hardware required to perform structural measurements during shuttle attached flights. It consists of the electro-optical distance measurement system, the analytical photogrammetry system, TV, instrumentation and signal conditioning modems.

1.3.1.5 Payload/Orbiter Interface Structure

This element includes design and development of hardware which provides the physical interface between the deployable antenna and the orbiter during the three shuttle-attached flights as identified above. It consists of an orbiter separation mast and canister, pivot structure support, pivot structure and forward support structure.

1.3.1.6 Integration, Assembly and Checkout

This element contains all labor required to perform an integration analysis for the combining of the various subsystems into the two antenna development configurations.

1.3.2 RF SOURCE SUBSATELLITE

This element contains the costs associated with the design and development of all the subsystems required as part of the expendable subsatellite which provides RF signals for beam pattern measurements on antenna development flights. The RF source subsatellite is subdivided into the following elements:

WBS	TITLE
1.3.2.1	Structure
1.3.2.2	RF Electronics
1.3.2.3	EPS
1.3.2.4	TT&C
1.3.2.5	Subsatellite/Orbiter Interface Structure
1.3.2.6	Integration and Assembly

Each of the subdivisions 1.3.2.1 through 1.3.2.5 are subsystems and contain labor and materials necessary to design and develop that particular subsystem.

1.3.2.1 Structure

This element includes design and development of structural stringers, hardware mounting brackets and external skin.

1.3.2.2 RF Electronics

This element includes design and development of the RF transmitter (signal source) and omni antenna network including harness, dummy load and hybrid.

1.3.2.3 EPS

This element includes design and development of primary batteries and interconnecting wiring.

1.3.2.4 TT&C

This element includes design and development of command receivers, baseband/ transponder, electronics and omni-antennas.

1.3.2.5 Subsatellite/Orbiter Interface Structure

This element includes design and development of a spin-up table and associated subsatellite mounting/release mechanism.

1.3.2.6 Integration and Assembly

This element contains all labor required to perform an integration analysis for the combining of the various subsystems into the subsatellite.

1.3.3 APPLICATION FUNCTIONAL TEST EQUIPMENT

This element contains the costs associated with design and development of hardware which, when integrated with the deployable antenna (1.3.1), results in a shuttle attached test configuration for one or more applications.

The application functional test equipment is divided into the following elements.

WBS	TITLE
1.3.3.1	Radar Test Equipment
1.3.3.2	Communications Test Equipment
1.3.3.3	Radiometry Test Equipment

Each of the subdivisions 1.3.3.1 through 1.3.3.3 is a subsystem and contains labor and materials necessary to design and develop that particular subsystem. Also included is all labor required to perform an integration analysis for combining the subsystem with the deployable antenna (1.3.1).

1.3.3.1 Radar Test Equipment

This element includes design and development of hardware which when integrated with the shuttle attached deployable antenna will provide radar functional tests. Hardware in this element includes a signal generator, transmitter, feeds, receivers and tape recorders as required to satisfy test objectives.

1.3.3.2 Communication Test Equipment

This element includes design and development of hardware which when integrated with the shuttle attached deployable antenna will provide communication functional tests. Hardware in this element includes transmitters, multibeam feeds and receivers as required to satisfy test objectives.

1.3.3.3 Radiometry Test Equipment

This element includes design and development of hardware which when integrated with the shuttle attached deployable antenna will provide radiometry functional tests. Hardware in this element includes a multichannel radiometer receiver, multi-beam feeds and a data sampling device as required to satisfy test objectives.

1.3.4 (RESERVED)

1.3.5 GROUND SUPPORT EQUIPMENT (GSE)

This element summarizes the labor and material required to design and develop the GSE hardware required for DAS systems level in-process and final assembly/checkout, development/verification test site operation, ground operations, and flight operations mission support. The GSE requirements include the electrical/mechanical/hydraulic equipment needed for DAS test/checkout, fault isolation, handling, transportation, servicing and repair. It also includes DAS GSE software requirements.

This element is subdivided as follows:

WBS	TITLE
1.3.5.1	Mechanical GSE
1.3.5.2	Electrical GSE
1.3.5.3	Fluid GSE

1.3.5.1 Mechanical GSE

This element includes design and development of a factory stand and local transportation dolly, sling assembly, access and work stand, antenna handling equipment and spacecraft shipping container.

1.3.5.2 Electrical GSE

This element includes design and development of a console to support the assembly and checkout testing of the payload.

1.3.5.3 Fluid GSE

This element includes design and development of a propellant checkout and servicing unit to support checkout testing of the RCS.

1.3.6 FACILITIES

This element includes the planning, design and development associated with the construction/major modification of required facilities for the DAS manufacture, test, maintenance/refurbishment and ground/flight operations support. At this time, the program is assumed to be performed in existing facilities; no requirements for additional facilities or major modifications have been identified. In future WBS updates, this element will be subdivided to include facilities associated with manufacture/acceptance test, development/verification test, ground operations and flight operations as appropriate.

1.4 MANUFACTURING, CHECKOUT AND ASSEMBLY

This item includes all labor and materials required for the manufacturing, checkout and assembly of space hardware through the acceptance of this hardware by the Government. Specifically included in this item are all costs associated with the following:

- Procurement, fabrication, assembly and checkout of space hardware
- Ground test and factory checkout of space hardware
- Initial spares
- Maintenance of tooling and factory test equipment/GSE.

This element is subdivided into systems which have a one-to-one correspondence to those defined under WBS 1.3; i.e., 1.4.1 includes costs associated with manufacture of the deployable antenna which was designed/developed under 1.3.1. This one-to-one correspondence is further extended down to the next level for definitions of subsystem and components included in this system. The resulting subdivision is as follows:

WBS	TITLE
1.4.1	Deployable Antenna
1.4.1.1	Basic Structure
1.4.1.2	Bootlace Array Configuration Kit
1.4.1.3	Reflector Configuration Kit
1.4.1.4	Instrumentation
1.4.1.5	Payload/Orbiter Interface Structure
1.4.1.6	Integration, Assembly and Checkout
1.4.2	RF Source Subsatellite
1.4.2.1	Structure
1.4.2.2	RF Electronics
1.4.2.3	EPS
1.4.2.4	TT&C
1.4.2.5	Subsatellite/Orbiter Interface Structure
1.4.2.6	Integration and Assembly
1.4.3	Application Functional Test Equipment
1.4.3.1	Radar Test Equipment
1.4.3.2	Communications Test Equipment
1.4.3.3	Radiometry Test Equipment
1.4.4	(Reserved)
1.4.5	Ground Support Equipment

WBS	TITLE
1.4.5.1	Mechanical GSE
1.4.5.2	Electrical GSE
1.4.5.3	Fluid GSE
1.4.6	Facilities

1.5 SYSTEMS TEST AND EVALUATION

This element summarizes the effort required to plan and perform the integrated system and vehicle level tests for DAS ground testing that are necessary to evaluate and verify hardware integrity/performance. It includes major test article and instrumentation costs in addition to test program costs, subdivided as follows:

WBS	TITLE
1.5.1	Major Test Articles
1.5.2	Instrumentation
1.5.3	System Test

1.5.1 MAJOR TEST ARTICLES

This element includes the labor and material required for all DAS test articles that provide design development information necessary to verify design concepts. It includes the design, tooling, fabrication, assembly, installation, quality assurance and checkout of test articles such as the gore wrap/unwrap test article, bootlace lens pattern measurement test article, etc. The installation of subsystem hardware on the test article and test fixture design/fabrication/assembly are also included. Test specimens for component and subsystem development/qualification test are excluded. They are included in the respective subsystem elements.

1.5.2 INSTRUMENTATION

This element includes the labor and material required for the instrumentation of DAS major test articles. It includes the design, procurement, installation, checkout and operation of required instrumentation systems.

1.5.3 SYSTEM TEST

This element includes the planning, coordination, design, set-up, conduct, data reduction and evaluation of DAS system level ground development and verification tests. Consumables for system level development/verification tests are also included. It excludes systems or vehicle level flight testing.

1.6 LOGISTICS

This element summarizes all labor and material required to implement, operate and maintain an integrated logistics system for the DAS and its related GSE. It includes transportation and handling of DAS hardware requiring special consideration; provision of training equipment; planning and implementation of training programs; and the provisioning for and control of flight hardware/GSE spares.

This element is subdivided as follows:

WBS	TITLE
1.6.1	Transportation and Handling
1.6.2	Personnel Training
1.6.3	Inventory Control

1.6.1 TRANSPORTATION AND HANDLING

This element contains the cost of preparation for and transportation of major items of DAS hardware which have special requirements due to their size, weight, shape or controlled environment. Transportation of DAS modules from the factory to test sites is included in this element. Transportation of hardware items not requiring special consideration is excluded from this element since these charges are indirect.

1.6.2 PERSONNEL TRAINING

This element contains the cost of instruction as well as training aids such as manuals, audio-visual aids and accessories required for the training of DAS ground and flight crews.

1.6.3 INVENTORY CONTROL

This element contains the effort required for provisioning, warehousing and maintaining a supply of DAS flight hardware and GSE spares.

1.7 OPERATIONS

This element summarizes all efforts associated with planning, coordination and implementation of DAS operations, subdivided as follows:

WBS	TITLE
1.7.1	Ground Operations
1.7.2	Flight Operations

1.7.1 GROUND OPERATIONS

This element summarizes all efforts associated with the planning, coordination and implementation of DAS launch activities and maintenance/refurbishment of DAS modules.

This element is subdivided as follows:

WBS	TITLE
1.7.1.1	Launch Operations
1.7.1.2	Maintenance/Refurbishment

1.7.1.1 Launch Operations

This element contains the planning for DAS launch site operations including initial launch site checkout of DAS subsequent to factory acceptance test, integration of the DAS with the launch system, and launch countdown support. It includes such tasks as requirements development, test planning, coordination of schedules, preparation of checkout/countdown procedures, liaison between launch site and home plant, module checkout and support of integrated check-out countdown activities.

1.7.1.2 Maintenance/Refurbishment

This element contains the maintenance and refurbishment activity required to restore DAS after each mission to a readiness condition for subsequent missions. It includes the home plant planning for this function, development of requirements, procedure preparation, liaison maintenance/refurbishment site and home plant, post-flight safing and inspection, conduct of the maintenance/refurbishment tasks, and revalidation/functional checkout of DAS.

1.7.2 FLIGHT OPERATIONS

This element summarizes all efforts associated with DAS mission planning, in-orbit execution of the mission, and ground support of the mission. It includes all mission activity required to certify the readiness of the DAS as well as support of operational missions.

This element is subdivided as follows:

WBS	TITLE
1.7.2.1	Mission Planning
1.7.2.2	Mission Implementation
1.7.2.3	Mission Ground Support

1.7.2.1 Mission Planning

This element contains the mission planning to certify the readiness of the DAS for mission operations and the mission planning required to establish DAS/mission compatibility. It includes definition of objectives, establishment of requirements, formulation of plans, preparation of in-orbit procedures, coordination of communication and data requirements, preparation of crew timelines, and participation in mission planning working groups.

1.7.2.2 Mission Implementation

This element includes all in-orbit activities performed by flight crews to certify DAS operational readiness and to provide DAS support of operational missions.

1.7.2.3 Mission Ground Support

This element contains the effort associated with real-time ground support of DAS operational missions and post-flight data processing, analyses and report preparation relative to DAS performance.